NASA TECHNICAL TRANSLATION

NASA TT F-183

INTENSITY VARIATIONS OF COSMIC RAYS

A. I. Kuz'min, Editor

USSR Academy of Sciences, Siberian Department,
Transactions of the Yakutsk Section,
Physics Series, No. 4, 1962

NATIONAL AERONAUTICS AND SPACE ADMINISTRATION - WASHINGTON, D. C. - FEBRUARY 1966

INTENSITY VARIATIONS OF COSMIC RAYS

A. I. Kuz'min, Editor

Scripta-Technica, Inc. translated and prepared the reproducible copy for this publication and is responsible for the accuracy and fidelity of the translation and editorial quality of the contents.

Translation of "Variatsii intensivnosti kosmicheskikh luchey."
Akademiya Nauk SSSR, Sibirskoye Otdeleniye,
Trudy Yakutskogo Filiala, Seriya Fizicheskaya, Vypusk 4,
Moscow-Leningrad, 1962.

NATIONAL AERONAUTICS AND SPACE ADMINISTRATION

For sale by the Clearinghouse for Federal Scientific and Technical Information
Springfield, Virginia 22151 – Price $6.00

TABLE OF CONTENTS

Page

Page

PREFACE

This collection of papers from the Yakutsk Branch of the Siberian Division of the Academy of Sciences USSR reports some of the results of studies which were carried out in 1959 at the Laboratory of Physical Problems.

The first part of this collection is devoted to neutron measurements in the upper atmosphere, the recording of auroras and telluric currents and studies of certain general properties of secondary cosmic rays. In particular, results are reported of experimental studies of the frequency of extensive air showers (EAS) as a function of depth and the distance between the detectors, and also the dependence of the angular distribution of μ-mesons on the depth at which the measurements are performed.

The second part reports experimental and theoretical work on the meteorological effects of the μ-meson component of cosmic rays, variations in the temperature of the upper atmosphere, and estimates of geometrical factors in the meteorological effects of EAS frequency.

The third part describes investigations of extra-atmospheric variations in cosmic rays, which were based on composite cosmic-ray measurements in a wide energy range in 1957-1959. Most of this work was concerned with variations in cosmic rays at different depths below sea level. Part 3 also includes a paper on the theory of probability.

All the papers included in this collection were discussed at a seminar at the Yakutsk Branch and at a conference of young specialists working at the Yakutsk Branch, which took place in March-April 1960.

The papers included in this collection are devoted mainly to the analysis of cosmic-ray measurements during the IGY and IGC and, although it does include a number of papers which are not directly concerned with cosmic rays, we have decided to publish this collection as a continuation of the series "Variations in the Intensity of Cosmic Rays".

The contributors wish to express their gratitude to the Corresponding Member AS USSR, Professor S.I. Vernov, Doctor of Physicomathematical Sciences, Professor N. L. Grigorov, Candidate of Physicomathematical Sciences L.I. Dorman, Candidate of Physicomathematical Sciences S.I. Nikol'skiy, and the members of the staff of the above laboratory for their active participation and constant and generous assistance during the development of the scientific program.

PART ONE

EXPERIMENTAL METHODS AND TECHNIQUES

N. L. Grigorov, V. D. Sokolov and V. F. Lyutenko

AIRPLANE MEASUREMENTS OF SLOW COSMIC-RAY NEUTRONS

1. Boron trifluoride filled proportional counters are widely used for measurements of cosmic-ray neutrons both at ground level and in the atmosphere. Such counters have a low neutron recording efficiency. This reduces the accuracy of the measurements, particularly in balloon work when the time spent at high altitudes and the weight of the instrument must necessarily be limited. It is therefore important to increase the efficiency of the counters without any great increase in their weight.

A considerable increase in the slow-neutron recording efficiency may be achieved if an ionization chamber is used as the neutron detector. The neutron recording efficiency of a detector filled with boron trifluoride gas is proportional to the cross-section for the reaction B^{10} (n, α) Li^7, the working dimensions of the detector, and the number of boron atoms per unit volume of the gas. Since in proportional counters the gas pressure cannot be increased beyond a certain limit, it follows that their efficiency is also limited and does not in fact exceed more than a few percent. In ionization chambers, the pressure can be increased to any reasonable value. Tobey and Montgomery [1] have used a BF_3-filled ionization chamber, but this method has not been widely adopted.

2. In this paper, we report the development of an instrument for measurements of slow cosmic-ray neutrons, which is based on an integrating ionization chamber, and the first results which have been obtained with this apparatus.

The chamber was filled with BF_3 gas. In this type of chamber, the total ionization current consists largely of two components, namely, the current due to the decay products of B^{10} resulting from the B^{10} (n, α) Li^7 reaction, and the current due to all the other ionization agents. A second ionization chamber was used to

compensate the latter current so that the ionization current due to the B^{10} (n, α) Li^{7} reaction products alone could be determined.

Both chambers are spherical in form and have an internal diameter of 20 cm. The walls of the chambers are made of 1 mm thick steel. The collecting electrodes are joined to form a single electrical system. The electrical capacitance of these chambers with the single system of collecting electrodes is about 12 pF. The spheres are electrically insulated from each other and potentials of different sign are applied to them. One of the chambers is filled with BF_3 enriched with B^{10} to about 83 percent. The pressure in the chamber is 76.5 cm Hg. The second chamber is filled with nitrogen which has ionization properties resembling BF_3 more closely than any other gas. The pressure in the second chamber was chosen so as to ensure equal ionization currents in the two chambers when irradiated with ionizing radiations of equal intensity.

The correct pressure was found with the aid of a Co^{60} γ-ray source. After the ionization currents through the two chambers were made equal, a check was made of the dependence of the ionization currents on the energy of the radiation. Measurements using a radium γ-ray source showed no evidence of a departure from the equality of the currents in the two chambers. The ionization currents were equal when the pressure in the nitrogen-filled chamber was about 2.33 atm.

3. Under the working conditions, when different potentials are applied to the spheres, the charge accumulated on the collecting electrodes due to the neutron component of the ionization current in a time Δt is proportional to the neutron intensity. The charge was measured by the method described by Grigorov [2], which is based on the conversion of a fraction of the charge on the collecting electrode into a voltage pulse of given magnitude. Voltage pulses produced in this way are fed into the input of the electronic circuit shown in Fig. 1, which is based on directly-heated tubes. The negative going voltage pulse from the central electrodes is fed to the grid of the first tube which functions as a cathode follower. The length of the input pulse is about 850 μsec. The output of the cathode follower is fed into the first grid of the amplifier T_2 and the resulting positive pulse is received by the first grid of the pulse stretcher T_3 which operates without a negative bias. As soon as the pulse arrives, the capacitor (450 pF) is rapidly charged by the grid current and as soon as the cut off pulse is over, it begins to discharge slowly through the large resistance (100 MΩ). As a result, a positive pulse having a length of about 40 μsec is produced at the anode of T_3 whose amplitude is proportional to the amplitude of the input pulse. This pulse is then applied to the tone manipulator T_4 whose threshold sensitivity is about 1 V. When the pulse amplitude reaches 2 V, further increase in the amplitude of the signal results in the limitation of its amplitude

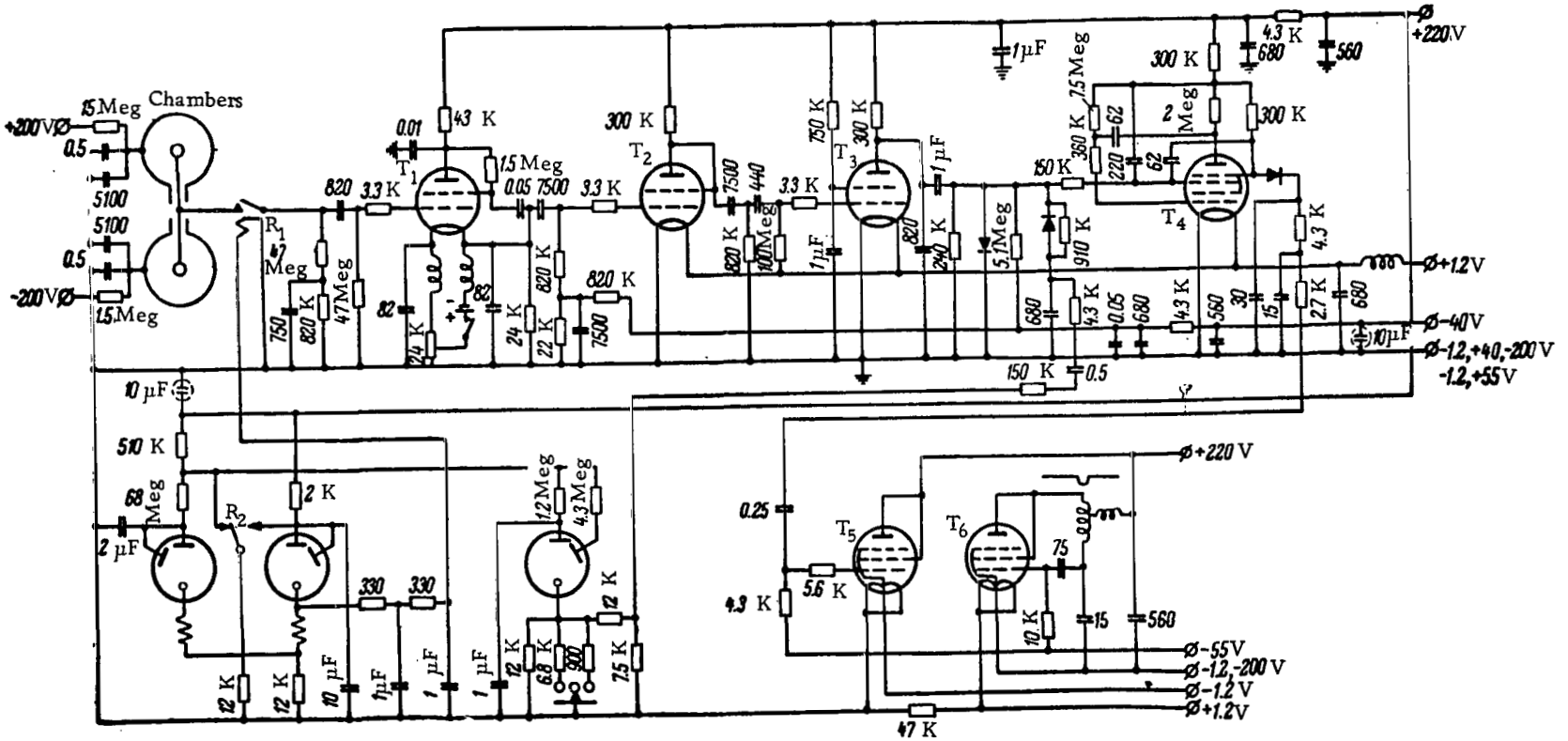

Fig. 1. Basic circuit of the device.

to 2 V (i.e., zero voltage on the right-hand side plate of the 1 μF capacitor) so that the bias on the control grid of T_4 remains constant during the application of the pulse. As a result, a tone pulse with a carrier frequency of about 3 kc/sec is produced at the output of the tone manipulator.

The length of the tone pulse is proportional to the amount of charge stored on the central collecting electrodes.

During the airplane experiment, pulses from the output of the tone manipulator were fed into a scaling circuit which counted the number of such pulses. In balloon experiments, the pulses from the tone manipulator were fed into the radio transmitter (T_5, T_6).

The operation of the relay R_1 was controlled automatically by a special programing device (Fig. 1), which also controlled the operation of a barographic probe. The complete cycle of the programer occupies about 60 seconds. During 50 seconds, the transmitter receives pulses from the barographic probe while during the remaining 10 seconds the probe is cut off and the charge on the central collecting electrodes is sampled and recorded.

The instability of the readings of the instrument is about 5% for a 10% change in the supply voltages. A change in the anode voltage of the current source can also be measured with the aid of the programing device. The latter is based on two relaxation oscillators. Thus, by measuring the length of the cycle of operation of the programer, one can obtain information about the anode voltage of the current source.

4. Experiment. The apparatus was flown five times between August 24 and August 29 on an airplane carrying out meteorological soundings of the atmosphere. The aim of this experiment was to test the apparatus and use the results to improve the circuit parameters which were originally chosen on the basis of calculated data.

The entire apparatus, including the supply sources, was placed in a plywood box. The pressure in the compensating chamber was checked with the aid of a Co^{60} γ-source which was placed in a fixed position at the top of the box. This position was chosen after preliminary laboratory experiments. It was found convenient to have an excess of ionization current in the BF_3 chamber. The magnitude of the excess current was carefully measured immediately after the adjustment of the pressure in the compensating chamber. A leakage of the gas from the compensating chamber should result in an increase in the readings of the instrument.

The selection of the correct pressure for the compensating chamber was carried out on July 31, 1959. When the chamber was examined again on August 15, it was found that a small leakage of gas had occurred. Since, however, the flight program had been agreed to, a new compensation procedure could not be carried

out. It was hoped that by having a series of control measurements at different times, it would be easy to determine the pressure in the chamber on the day of the actual experiment. Calculations showed that, owing to the leakage of nitrogen, the pressure in the compensating chamber fell from the initial value of 2.326 atm to 1.6 and 1.55 atm at the beginning and the end of the experiment respectively. This leakage of gas will be taken into account below.

Before and after each flight, a check was made of the state of the current sources and of the background in the airplane. During all five flights, the current sources retained their nominal parameters so that no corrections were necessary (they were all less than 0.5%). The calibration curve of the instrument was replotted after the completion of the five flights and no changes in the curve were found.

In order to show that the airplane engines had no effect on the readings of the instrument, special measurements were carried out with the engines on and off. These measurements showed that the engines had no effect on the readings. During all the five flights, the instrument occupied exactly the same position in the airplane and the same position relative to the surrounding objects.

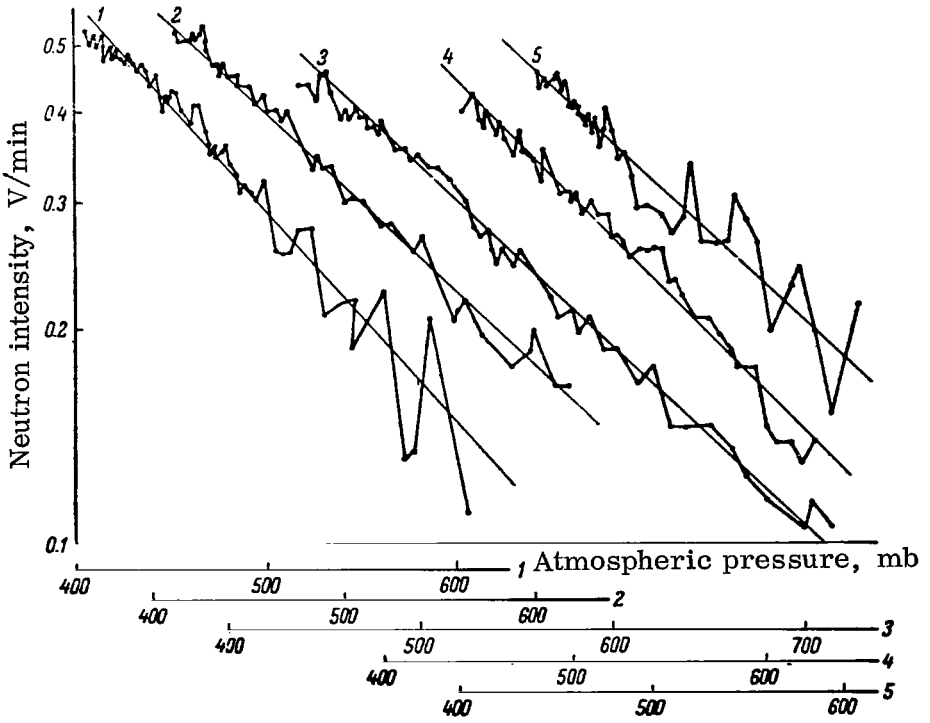

Fig. 2. Altitude variation of the neutron intensity deduced from measured ionization during five flights (1-5).

The readings of the instrument were recorded by an observer at 60-second intervals. Altitude and pressure data were obtained from the met-sounding data recorded during the flight.

In all cases, the airplane slowly gained height for 70-80 minutes and descended rapidly as soon as the observational program was completed. Fig. 2 shows the neutron intensities deduced from the ionizations recorded during the five flights.

For convenience, each flight has its own origin on the horizontal axis. The data shown in Fig. 2 refer to the layer between 600-700 and 400 mb.

Below 600-700 mb, the accuracy of the data is not sufficient and they will not be discussed. The accuracy of the 60-second data shown in Fig. 2 is 2.5% at 400 mb and 5% at 600 mb.

All the data were corrected for gas leakage from the compensating chamber. The altitude variation in the specific ionization due to cosmic rays was measured in [2-4] at a latitude equal to or near the latitude of Yakutsk. In spite of the fact that the ionization measurements were carried out at different times, the results agreed to within $\pm$ 10% at 400-700 mb. The corrections were based on the results reported in [3], since the latter were the most complete. Fig. 3 shows the altitude variation in the neutron intensity, averaged over all the five flights, before and after the corrections.

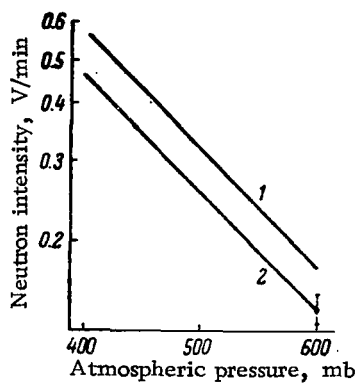

Fig. 3. Average altitude variation of neutron intensity (5 flights).

1 — Uncorrected, 2 — corrected.

The mean absorption thickness for the neutrons which were measured in these experiments was 169 $\pm$ 8 g/cm^2. This result is in good agreement with the data of other workers who used counting apparatus [5, 6].

The above results lead to the conclusion that the integrating ionization chamber working in conjunction with a compensating chamber as described above, can be successfully used to determine the neutron component of cosmic rays.

REFERENCES

1. Tobey, A.R. and Montgomery, C.G. Phys. Rev., 81, 517, 1951.

2. Grigorov, N.L. UFN, 8, No. 4, 1956.

3. Neher, H., Bowen, J.S. and Millikan, A. Phys. Rev., 53, 856, 1938.

4. Andersen, H.P. Phys. Rev., 116, 461, 1959.

5. Yuan, L.C.L. Phys. Rev., 81, 175, 1951.

6. Neuburg, H.A.C., Soberman, R.K., Swetnick, M.J. and Korff, S.A. Phys. Rev., 97, 1276, 1955.

V.D. Sokolov and I.N. Kapustin

COUNTING APPARATUS FOR THE INVESTIGATION OF THE NEUTRON COMPONENT OF COSMIC RAYS IN THE ATMOSPHERE

Measurements from artificial earth satellites have established the existence of a belt of radiation around the earth. Vernov et al [1] have suggested that one of the possible sources of particles for the inner radiation belt may consist of neutrons escaping from the earth's atmosphere and decaying in the region of the radiation belt. It is therefore of interest to investigate the neutron cosmic-ray component at large altitudes in the atmosphere.

The present note reports preliminary results obtained with a counting apparatus for balloon measurements of the density of slow cosmic-ray neutrons.

The neutron detector is in the form of a proportional SNM-5 counter filled with boron trifluoride gas (BF_3). In this counter, the amplitude of the ionization pulse due to the products of the B^{10} (n, α) Li^7 reaction is much greater than the amplitude due to relativistic particles. It follows that the latter can easily be separated out. However, events such as cosmic-ray stars, slow heavy particles, nuclear fragments, and so on, which originate in the gas and in the walls of the counter, or arrive from the outside, can give rise to pulses which are comparable with pulses due to the above reaction.

These spurious pulses cannot be distinguished but can be excluded with the aid of a device based on the principle described by Staker and Davis [2, 3]. In this method, the instrument incorporates two channels, each having identical detectors except that one of the BF_3 counters contains B^{10}-enriched gas (80-90%) while the other counter contains BF_3 gas with natural concentration of B^{10}. Such counters have different neutron sensitivities but are identical in all other respects. It is not difficult to find the rate due to the capture of neutrons, having the two sets of data obtained from these two channels.

Figure 1 shows the basic circuit of the instrument. All the tubes are directly heated and the recording channels differ only in the neutron detectors and in some of the parameters of the electronics. In each channel, the first two tubes (T_1 and T_2) are used to achieve preliminary amplification of the pulses (amplification

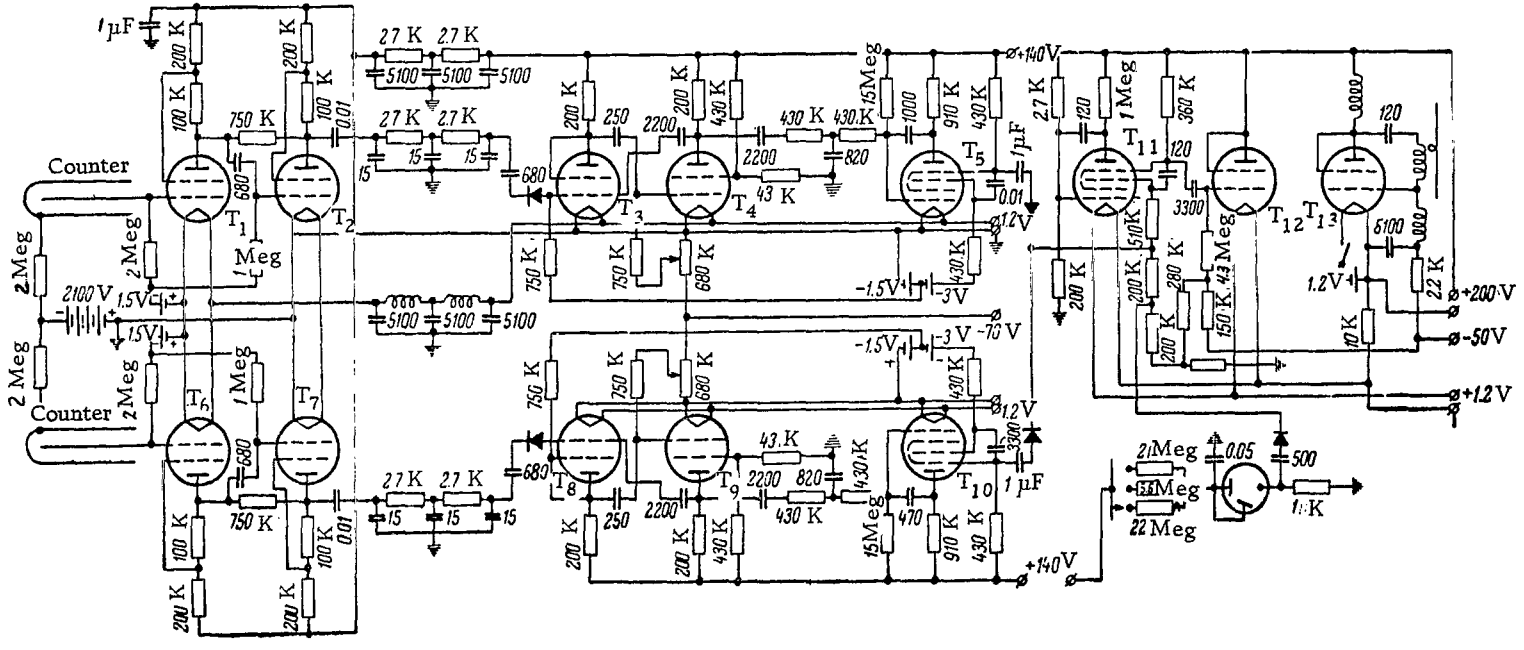

Fig. 1. Basic circuit of the instrument for cosmic-ray neutron measurements.

~75). The stages have separate anode loads in order to increase the stability. In addition, the second stage incorporates negative feedback. These two tubes are placed in a hermetically sealed compartment together with the counters and the HT batteries. Pulses from the output of the prèamplifier are fed into the grid of the flip-flop (T_3, T_8) which also serves as the final amplifier with an amplification of about 10. The discrimination is achieved by applying a negative bias to the cut off halves of the flip-flop (T_4, T_9). The amplifier as a whole has an adequate stability, i.e., the overall amplification factor changes by 2% when the supply voltage changes by 20%. The discrimination threshold is regulated by two potentiometers. In order to increase the stability of the threshold of the flip-flop against changes in the anode voltage, the screen voltage of the right-hand side tube (T_4) was chosen to be of the order of 20 V.

Pulses exceeding the discrimination threshold have a rectangular form at the output of the flip-flop with an amplitude of about 70-80 V and a length of the order of 100 μsec. They control the operation of the coding (shaping) flip-flop (T_5, T_{10}). The pulses at the output of the coding stage are positive-going. They are rectangular in shape and have a length of 0.76 and 2.0 msec in the first and second channels respectively. A low frequency filter is used to exclude triggering of the coding stage by unshaped pulses.

The coded pulses from the two channels are fed into the input of a common telemetry channel. The latter consists of a tone manipulator (T_{11}), modulator (T_{12}) and transmitter (T_{13}). A standard meteorological radiosonde element is used as a barometric probe. A change in the pressure results in a change in the repetition frequency of signals from this probe. As a result, the tone manipulator produces tone pulses from the channels with a carrier frequency of about 2 kc/sec, and single pulses from the barographic probe. These signals are used in conjunction with a modulator to operate a pulse radio transmitter working on a frequency of 80-90 Mc/sec.

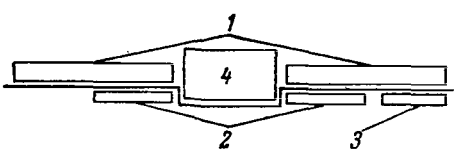

Fig. 2. Disposition of the various components in the hermetically-sealed container:

1 — counters, 2 — preamplifiers, 3 — high frequency filters, 4 — HT batteries.

The instrument as a whole was built in the form of separate units. Counters, preamplifiers (T_1, T_2, T_6 and T_7) and the HT batteries are mounted on a common

chassis and are placed in a cylindrical hermetically-sealed tinplate container which prevents corona discharge from the HT batteries and screens the sensitive part of the electronics (preamplifier) from high frequency pick-up due to the transmitter. All the leads entering the cylindrical screen are provided with decoupling high-frequency filters (Fig. 2).

The circuit is supplied by dry batteries and the total weight of the instrument is 6 kg.

The authors are indebted to Engineer V. F. Lyutenko for assistance and advice during the development of the instrument.

REFERENCES

1. Vernov, S.N., et al. Iskusstvennyye sputniki zemli (Artificial Earth Satellites). Collection of Papers, No. 2, p. 61, Akademizdat, 1958.

2. Staker, W.P. Phys. Rev., 80, 52, 1950.

3. Davis, W.O. Phys. Rev., 80, 150, 1950.

D. D. Krasil'nikov, N. N. Yefimov, M. A. Nifontov and V. A. Orlov

THE EFFECT OF A LIGHT COVER ON THE FREQUENCY OF RECORDED EXTENSIVE AIR SHOWERS

The "small" apparatus for recording of extensive air showers [EAS] at Yakutsk which operated up to January 1958 [1] and the present "large" apparatus [2] were both used under special light cover with $t < 3$ g/cm^2. The material above the recording counters should not appreciably affect the number of recorded showers. The material was therefore taken to be as thin and as similar to air as possible (moss, plywood).

It is known from previous work on the effect of the material covering the counters [3, 4] that it is very difficult to allow for this effect exactly.

The effect of the cover on the number of recorded showers for our apparatus is closely connected with the energy spectrum of the shower particles, the angular distribution function, and the effective area of the counters, and therefore with the determination of the various time variations and the influence of meteorological effect of EAS.

The following two experiments were carried out in order to determine the effect of the cover on the number of recorded showers for installations with different effective areas.

1. The apparatus in the second pavilion, which consists of three trays of counters connected in coincidence (there are 30 GS-60 counters per tray; the effective area is $\sigma_1 \simeq 1.0$ m^2), was brought out into the open air without changing the existing geometry ($D_1 = 3.8$ m). Only 0.1 mm of dural remained above the counters. The apparatus was switched on in daytime for 3-4 hours and operated for a total time of 24 hours between September 5 and September 12, 1958. The nearest wooden building occupied less than 4% of the surrounding hemisphere.

In order to exclude the influence of meteorological effects and time variations, a comparison was made of the recorded results for the same times of day.

The data obtained with the apparatus operating in open air without any cover were compared with three other identical arrays operating under a constant cover (roof). The latter data were first combined using a prolonged series of observations.

2. The second analogous experiment was carried out with an apparatus in which the effective area of each of the three groups of counters was $\sigma_2 \simeq 0.1$ m^2. The apparatus was switched on in open air for a total of 149 hours between August 10 and August 19.

The results were compared using the same method as in the preceding case.

The results of the experiment are given in the table below where N (0) is the number of recorded showers without the cover and N 3 g/cm^2 is the number of showers under a cover of 3 g/cm^2.

Counter area, m^2	Operating conditions	Number of hours	N (0)	N(3 g/cm^2)	$\frac{N(0)}{N(3\ g/cm^2)}$
$\sigma_1 \simeq 1.0$	Without cover	24	10108±28	—	98.0±0.8%
	Under cover of 3 g/cm^2	24	—	10314±48	
$\sigma_2 \simeq 0.1$	Without cover	149	2624±18	—	97.8±1.5%
	Under cover of 3 g/cm^2	149	—	2684±21	

It may be concluded from the above data that, under the above conditions, the number of recorded showers does not decrease when the apparatus is placed under the light roof (within the experimental error), as was to be expected on the basis of the approximate calculation of G.T. Zatsepin [4]. On the contrary, there is a tendency for the number of the recorded showers to increase by 1-1.5%. This may be explained by a small increase in the effective area of the counters owing to the transition effect of the cover.

REFERENCES

1. Krasil'nikov, D.D. ZhETF, 35, 295, 1958.

2. Krasil'nikov, D.D. Tr. YaFAN SSSR, ser. Fizich., No. 3, 62, 1960.

3. Cocconi, G., Loverdo, A. and Tongiorgi, V. Phys. Rev., 70, 841, 1946.

4. Zatsepin, G.T. Dissertation, FIAN SSSR, Moscow, 1950.

D. D. Krasil'nikov

ON THE RELATION BETWEEN THE MAGNITUDE OF AN IONIZATION BURST AND THE SIZE OF A SHOWER IN HIGH-PRESSURE CHAMBERS

1. Comparison of the theoretically expected shower frequencies and the observed frequency of ionization bursts in large C-type high-pressure chambers [1-2] is usually complicated by the following difficulty. The medium (usually lead) for which the cascade process is computed and the working volume of the gas (argon) are separated by the steel walls of the chamber and the collecting electrode is made of copper or steel with a total thickness of the order of 1-2 shower units.

Next, the mean path in the gas filling the chamber is of the order of 1-2 g/cm^2 so that the working volume cannot be regarded as a thin cavity. For a soft energy spectrum of the cascade shower particles, this design should give rise to considerable transition effects [3, 4]. In fact, there are at least two transition effects, i.e., lead-iron and iron-argon.

On the other hand, the integral spectrum of the magnitudes of the ionization bursts obeys a power law with an exponent of about 1.5-2. It follows that considerable errors may be introduced unless the transition effects are accurately allowed for. Christy and Kusaka [5], who carried out the early careful study of the spectrum of large ionization bursts in high-pressure chambers, came to the conclusion that the pulse spectrum observed at sea level is consistent with μ-mesons having spin 0 and magnetic moment 0, while according to our results [6], μ-mesons with spin 1/2 can explain only a proportion of the observed bursts.

The correlation between the magnitude of a burst and the size of a cascade shower reported by Christy and Kusaka has also been questioned by other workers [3, 7]. In fact, in their rough calculation of the transition effect, Christy and Kusaka erroneously assumed that the thickness of the Compton chamber was 0.8 t-units (in reality it is greater than 1 t-unit), and the ionization in the gas of the chamber was taken by them to correspond to a thin cavity, i.e., the wall-gas transition effect was neglected altogether.

Our previous work [6] also suffered from the disadvantage that the lead-iron and iron-gas transition effects were not adequately allowed for. The thickness of the walls was assumed to be 0.8 t-units and the wall-gas transition effect was neglected altogether.

We have now used recent calculations of cascade showers with low initial energies in different materials [8, 9, and others] to recalculate the lead-iron and iron-argon transition effects in order to establish the relation between the magnitude of a burst and the size of the cascade shower. The results of these calculations for the C-2 chamber are given below. /16

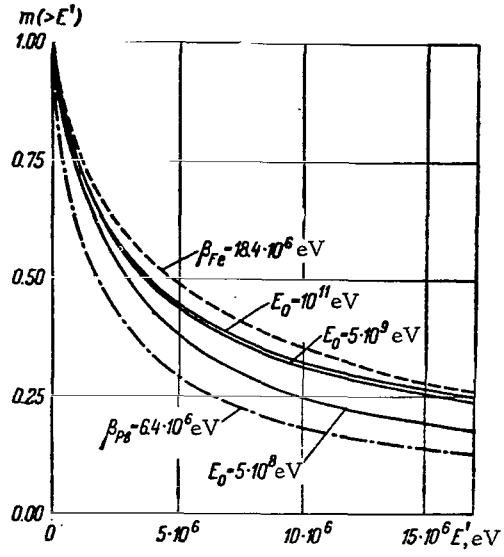

2. The C-2 chamber is spherical in form and is surrounded by a lead screen having a thickness $t_{Pb} \simeq 24$. The thickness of the walls of the chamber is $t_{Fe} = 1.59$ (including the sphere and the insulating packing); the mean path in the gas (argon) is $t_A = 0.102$.

We assume that at the lead-iron boundary all the showers are near the maximum, and hence the integral spectrum of the charged particles in a shower of any size can be described by the "equilibrium spectrum" [3] referred to a single shower particle:

$$n_e(>E) = \chi(\varepsilon) = 1 - \varepsilon e^{\varepsilon} \int_{\varepsilon}^{\infty} \frac{e^{-t}}{t}\, dt, \qquad (1)$$

where

$$\varepsilon = \frac{2.29}{\beta} E, \quad E_0 \gg E,$$

$$\beta = 6.4 \cdot 10^6 \text{ eV}.$$

The corresponding differential electron spectrum is

$$k_e(E)\,dE = \frac{\partial \chi(\varepsilon)}{\partial E} dE, \tag{2}$$

and the photon spectrum is

$$k_{ph}(E)\,dE = 3.49 \cdot 10^6 E^{-2} dE.$$

The total number of charged particles and photons with energies greater than E' after passing through $t_{Fe} = 1.59$ of iron is respectively given by

$$\left.\begin{aligned} m_e(E_0, >E') &= \int_{E'}^{E_0} k_e(E)\, N_e^e(E, t_{Fe}, E')\,dE + \\ &+ \int_{E'}^{E_0} k_{ph}(E)\, N_e^{ph}(E, t_{Fe}, E')\,dE, \\ m_{ph}(E_0, >E') &= \int_{E'}^{E_0} k_e(E)\, N_{ph}^e(E, t_{Fe}, E')\,dE + \\ &+ \int_{E'}^{E_0} k_{ph}(E)\, N_{ph}^{ph}(E, t_{Fe}, E')\,dE, \end{aligned}\right\} \tag{3}$$

where N_e^e and N_e^{ph} represent the electrons due to electrons and photons and N_{ph}^e and N_{ph}^{ph} represent the photons due to electrons and photons respectively.

These functions were taken from the corresponding curves given in [8, 9], while m_e and m_{ph} were calculated by numerical integration. The figure shows the final results for different primary energies E_0 (continuous curves). The dot-dash and dashed curves show the equilibrium spectra for lead and iron respectively. It turns out that even when the scattering of the shower particles is neglected (in lead practically all the particles are scattered [3]), the walls of the chamber absorb about 50% of the particles. Gupta has recently come to the same conclusion [10].

The distribution curves $m_e(>E')$ in the energy range $0 < E \leqslant 2 \cdot 10^6$ eV can be approximately replaced by the equilibrium spectrum for $\mathcal{E}_{eff} \simeq 15 \cdot 10^6$ eV.

Next, in order to estimate the ionization in the gas filling the chamber, we should separately allow for the ionization due to m_e and m_{ph}.

1) Ionization due to m_e in number of pairs of ions (p. i.);

$$i_e\ (\mathrm{Fe}) = \frac{1}{26.9}\int_0^{E_1} E\frac{\partial\chi(\varepsilon)}{\partial E}\,dE + 9.3\cdot 10^4\cdot\chi(\varepsilon_1) = \\ = \frac{1}{26.9}E[1-\chi(\varepsilon_1)] + 9.3\cdot 10^4\cdot\chi(\varepsilon_1), \tag{4}$$

where

$$E_1 = \beta_A t_A = 26.5\cdot 10^6\cdot 0.102 = 2.7\cdot 10^6\ \text{eV}; \quad \varepsilon = \frac{2.29}{\beta_{\text{eff}}}E = \frac{2.29}{15\cdot 10^6}E;$$

$$\varepsilon_1 = \frac{2.29}{15\cdot 10^6}E_1 = 0.412;$$

and 9.3×10^4 is the ionization due to relativistic particles in the C-2 chamber. The average energy is

$$\bar{E} = \overline{E(\leqslant E_1)} = \\ = -\frac{\beta_{\text{eff}}}{2.29}\cdot\frac{[C + \ln\varepsilon_1 + \varepsilon_1 e^{\varepsilon_1}E_i(-\varepsilon_1) - e^{\varepsilon_1}E_1(-\varepsilon_1) - \varepsilon_1 - \varepsilon^2, e^{\varepsilon_1}E(-\varepsilon_1)}{\varepsilon_1 e^{\varepsilon_1}E_i(-\varepsilon_1)}, \tag{5}$$

where $E_i(-\varepsilon_1) = -\int_{\varepsilon_1}^{\infty}\frac{e^{-t}}{t}\,dt$, and C = 0.577 is Euler's constant.

Estimates show that $\bar{E} = 9.25\cdot 10^5$ eV, $\chi(\varepsilon_1) = 0.575$.

Hence, the ionization due to the charged shower particles (per iron particle) is:

$$i_e\ (\mathrm{Fe}) = \frac{1}{26.9}\cdot 9.25\cdot 10^5 + 9.3\cdot 10^4\cdot 0.575 = \\ = (1.46 + 5.35)\cdot 10^4 = 6.81\cdot 10^4\ \text{p. i.} \tag{6}$$

The ionization per lead particle is

$$i_e(\mathrm{Pb}) = 0.47\cdot 6.81\cdot 10^4 = 3.2\cdot 10^4\ \text{p. i.} \tag{7}$$

2) Ionization due to photons per lead particle

$$i_{\text{ph}}(\mathrm{Pb}) = \frac{1}{26.9}\int_{\frac{mc^2}{2}}^{E_2} E k_{\text{ph}}(E)[1 - e^{-\sigma(E)_c t_A}]\,dE + \frac{1}{2}\cdot 9.3\cdot 10^4\cdot t_A\int_{E_2}^{E_0} k_{\text{ph}}(E)\times \\ \times[(1 - e^{-\sigma(E)_c t_A}) + 2(1 - e^{-\sigma(E)_p t_A})]\,dE, \tag{8}$$

where

$$\frac{mc^2}{2} = 2.5\cdot 10^5\ \text{eV}, \quad E_2 = \frac{1}{2}\beta_A t_A; \quad \sigma(E)_c \text{ and } \sigma(E)_p$$

are the Compton and pair-production cross-sections respectively [3]. The final result is

$$i_{ph}(Pb) = 0.663 \cdot 10^4 \text{ p.i.} \tag{9}$$

Combining (7) and (9), we have the following results for the mean ionization per shower particle in lead:

$$i(Pb) = (3.2 + 0.66) \cdot 10^4 \text{ p.i.} \simeq 3.9 \cdot 10^4 \text{ p.i.} \tag{10}$$

The mean ionization due to particles leaving the walls is

$$i(Fe) = \left(6.81 + \frac{0.663}{0.47}\right) \cdot 10^4 = 8.22 \cdot 10^4 \text{ p.i.} \tag{11}$$

The mean ionization due to shower particles from the iron at the beginning of their path (in a thin layer) in argon is

$$i(\delta A) = \frac{\beta_{Fe}}{26.9} \cdot \frac{t_A}{t_{Fe}} = \frac{18.4 \cdot 10^6}{26.9} \cdot \frac{18}{12.5} = 9.85 \cdot 10^4 \text{ p.i.} \tag{12}$$

Comparing (11) and (12), we see that the iron-argon transition effect leads to a reduction in the mean ionization due to shower particles by 16%.

A qualitatively similar result is obtained by using the approximate formulas for the transition effect given by Belen'kiy [3, Chapt. 6]. This gives the following figure for the mean ionization

$$i_{[3]} = 8.9 \cdot 10^4, \text{ p.i.} \tag{13}$$

which corresponds to an iron-argon transition effect (in the ionization) of about 10%.

No allowance was made in the above calculations for the scattering of the shower particles and ion recombination effects. The latter are particularly appreciable [12]. The following conclusions may be drawn from the above analysis of the lead-iron and iron-argon transition effects in the C-2 chamber:

1. The walls of the chamber absorb about 50% of the shower particles.

2. The iron-argon transition effect is appreciable and cannot be neglected: it corresponds to about 10-20% of the ionization.

3. In previous papers [5, 11, etc.], the expected frequency of bursts was apparently overestimated owing to errors in the relation between the magnitude of a burst and the size of the shower.

REFERENCES

1. Compton, A.H. and Bennett, W.H. Rev. Sc. Instr., 5, 415, 1934.
2. Shafer, Yu.G. Tr. YaFAN SSSR, ser. fizich., No. 2, 7, 1958.
3. Belen'kiy, S. Z. Lavinnyye protsessy v kosmicheskikh luchakh (Avalanche processes in cosmic rays). Moscow, 1948.
4. Vavilov, O.N. Dissertation, FIAN SSSR, Moscow, 1948.
5. Christy, R.F. and Kusaka, S. Phys. Rev., 59, 414, 1941.
6. Krasil'nikov, D.D. and Nikol'skiy, S.I. Tr. YaFAN SSSR, ser. fizich., No. 1, 48, 1955.
7. Rossi, B. Chastitsy bol'shikh energiy (High energy particles). Moscow, 1955.
8. Ivanenko, I.P. ZhETF, 33, 135, 1957.
9. Belen'kiy, S.Z. and Ivanenko, I.P. UFN, 69, 591, 1959.
10. Gupta, M.R. Nuovo Cimento, 7, 39, 1958.
11. Shein, M.M. and Gill, P. Rev. Mod. Phys., 11, 267, 1939.
12. Krasil'nikov, D.D. Nauchnyye Soobscheniya YaFAN SSSR, No. 1, 75, 1958.

D. D. Krasil'nikov, N. N. Yefimov, M. A. Nifontov and
F. K. Shamsutdinova

DEPENDENCE OF THE SEPARATION CURVE ON THE MEAN SIZE OF AN EXTENSIVE AIR SHOWER

I. The separation curve C(D), i.e. the dependence of the frequency of recorded extensive atmospheric showers (EAS) on the distance D between the counters, has recently attracted considerable attention, mainly because it may provide an additional source of information for the experimental verification of the following:

1) The assumption which we have made in designing our EAS recording apparatus [1] that the spatial distribution of particles in the shower is of the form

$$\varphi(r)=\begin{cases} a_1 r^{-1}, & r<10 \text{ м}, \\ a_2 r^{-1}\exp\left(-\frac{r}{55}\right), & 10<r<100 \text{ м}, \\ a_3 r^{-2.6}, & r>100 \text{ м} \end{cases}$$

and that $\varphi(r)$ is independent of the size N of the shower;

2) The correctness of the differential EAS spectrum

$$k(N)\,dN=\begin{cases} A_1 N^{-2.40}dN, & N<10^5, \\ A_2 N^{-2.70}dN, & N>10^5. \end{cases}$$

which we are using at the present time [2].

Moreover, the dependence of C on D is of interest as a possible method of approximate estimation of the geometrical effects of EAS frequency variations by the method described in [3, 4] and in other papers. This has been critically reviewed in [5].

Generally speaking, C(D) depends both on k(N)dN and on $\varphi(r)$, and calculations show that this should lead to an appreciable dependence of C(D) on the mean size $\overline{N}$ of the recorded showers. We are particularly interested in separations of the order of D = 40—100 m where the slope of the C(D) curve

is found to vary rapidly [6]. It follows that great care must be taken during the experiment in determining the experimental point.

From this point of view the experiments of Eydus [6] appear to be somewhat unsatisfactory. Eydus' measurements may suffer from differences in the counter areas and from barometric effects. Therefore, although Eydus' results do reflect the general form of C(D) since they are based on a large number of experimental points covering a wide range of values of D, they cannot be used to establish the fine structure of the function C(D) within a restricted region. In particular, there is some doubt about the form of the C(D) curve given by Eydus for $30 < D < 100$ m.

II. In our measurements, the GM counters were placed at the corners of a square. Measurements were made of six-fold coincidences over the area of counter groups with 1.0, 0.5 and 0.17 m^2, separately between two points lying (1) along one side of a square ($D_1 = 57$ m), and (2) along the diagonal of the square ($D_2 = 81$ m). Later, only simultaneous measurements were analyzed, i.e. six-fold coincidences along a side and a diagonal of the square. With this geometry, differences in the counter areas between D_1 and D_2 were excluded because the same counters were employed throughout. Barometric effects were also excluded because the measurements for both D_1 and D_2 were carried out over a long period of time.

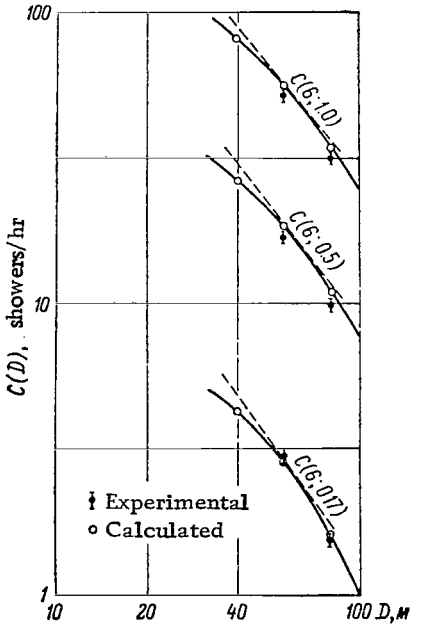

In order to compare theory and experiment we have calculated the expected frequencies for $D_1 = 57$, $D_2 = 81$ and $D_3 = 40$ m. The results are shown in the figure. The errors on the experimental points are less than 1%, while the errors on the expected points are less than 5%.

σ, м^2

$C(n, \sigma)$	$C(6; 1.0)$	$C(6; 0.5)$	$C(6; 0.17)$
d	1.25	1.33	1.44
$\bar{N}$	$1.36 \cdot 10^5$	$2.35 \cdot 10^5$	$7 \cdot 10^5$

It is evident that there is good agreement between the expected and experimental frequencies in all the cases which were considered. This confirms the correctness of the form which we assumed for the functions $\varphi(r)$ and $k(N)\,dN$. The fact that the expected frequencies are slightly higher than the experimental frequencies may be due to an inaccuracy in the effective areas of the GM counters and also to errors in the constants in the EAS size spectrum. If it is assumed that over a small range of values of D the curve may be fitted by an expression of the form $C(D) = bD^{-d}$, then it is found that near the point $D_1 = 57$ m we have

$$\frac{\partial \ln C(D_1)}{\partial \ln D_1} = -d$$

(in the figure this is shown by the dashed curve). It turns out that $d = d(\sigma)$ where σ is the area of the counter group, or $d = d(N)$ (cf. Table).

CONCLUSIONS

1. The spatial distribution function $\varphi(r)$ which we have used, and the size spectrum $k(N)dN$ which we found earlier [2], are apparently in close agreement with the experimental results and may be used to represent the true values of $\varphi(r)$ and $k(N)dN$ at our point of observation.

2. The exponent d in the separation curve C(D) is, as was expected, appreciably sensitive to the mean size of the EAS, i.e. it is a function of N.

$$d = d(\bar{N})$$

and increases with the growth N.

REFERENCES

1. Krasil'nikov, D.D. Tr. YaFAN SSSR, ser. fizich., No. 3, 22, 1960.

2. Krasil'nikov, D.D. Proc. International Conference on Cosmic Rays, II, 188, 1960.

3. Daudin, A. and Daudin, J. J. Phys. Rad., 10, 394, 1949.

4. Hodson, A.L. Proc. Phys. Soc. (London), A64, 1061, 1951.

5. Krasil'nikov, D.D. Tr. YaFAN SSSR, ser. fizich., No. 4, 51, 1961.

6. Eydus, L.Kh. Dissertation, FIAN SSSR, Moscow, 1953.

A.I. Kuz'min, G. F. Krymskiy and G.V. Skripin

UNDERGROUND ANGULAR DISTRIBUTION OF COSMIC-RAY INTENSITY AT DEPTHS OF 0-60 METERS OF WATER EQUIVALENT

1. A knowledge of the angular distribution is important in the study of the energy characteristics of time variations in the cosmic-ray intensity at different depths below ground level, and in the determination of the absolute flux.

A number of papers have been devoted to this problem [1-4]. According to [1], it is expected that as the depth increases the cosmic-ray intensity should become more and more concentrated near the vertical direction.

We have used continuously operating triple-coincidence counter telescopes at depths of 0, 7, 20 and 60 m of water equivalent below ground level, at angles of 0, 30 and 60° to the zenith, to determine the effective value of the exponent in the angular distribution at the above recording levels.

2. Figure 1 gives a schematic illustration of the counter telescopes [5].

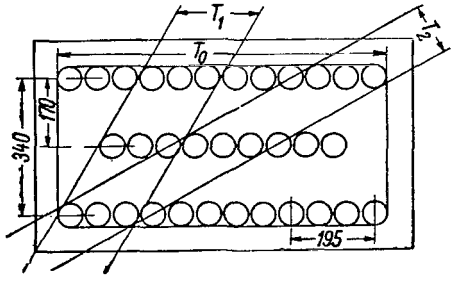

Fig. 1. Arrangement of triple-coincidence counter telescopes.

The vertical counter telescope T_0 records triple coincidences between the three counter arrays. Three telescopes of the form of T_1 are at an angle of 30° to the zenith in the north and south directions. Each of the T_1 telescopes consists of

nine counters and records triple coincidences between three trays of three counters.

The telescope T_2 also consists of nine counters, but its axis is at 60° to the zenith. As can be seen from Figure 1, the three telescopes T_0, T_1 and T_2, have different geometric configurations, and therefore their relative counting rates will depend on the angular distribution of the intensity. It is possible to calculate the expected counting rates for different angular distributions, and by comparing the results with experiment to obtain information about the angular distribution of the intensity at the point of recording.

3. Following [1], it is possible to express the angular intensity distribu- in the form $I = I_0 \cos^{\gamma}\varphi$ where φ is the zenith angle, I, I_0 are respectively the intensity in the vertical direction and at a zenith angle φ, and γ is the exponent of the angular distribution ($\gamma > 0$).

Figure 2 shows a telescope arrangement which is convenient for calculations. The telescope is represented in the two systems of coordinates by two planes. In terms of the notation indicated in Figure 2, the total number of particles recorded by the telescope per unit time is

$$N = SI_0 = I_0 H^{2+\gamma} \int_0^L \int_0^L \int_{-a}^{l-a} \int_0^l \frac{dx_1 dx_2 dy_1 dy_2}{[(x_1 - x_2)^2 + (y_1 - y_2)^2 + H^2]^{2+\frac{\gamma}{2}}},$$

where l, L and H are respectively the width, length and height of the telescope, and a is the displacement of the upper plane relative to the lower plane.

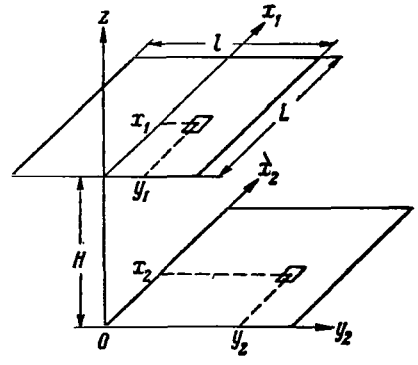

Fig. 2. Telescope arrangement for calculating the relative aperture.

This integral was evaluated in [6] by changing the variables, and was found to be of the form

$$N = I_0 2L^2 (\beta_1 I_1 + \beta_2 I_2 - 2\beta_3 I_3); \tag{1}$$

where

$$I_i = \int_0^1 \int_0^1 \frac{(1-u)(1-v)\,du\,dv}{(au^2 + \beta_i v^2 + 1)^{2+\frac{\gamma}{2}}};$$

$$a = \frac{L^2}{H^2};\ \beta_1 = \frac{(l-a)^2}{H^2};\ \beta_2 = \frac{(l+a)^2}{H^2};$$

$$\beta_3 = \frac{a^2}{H^2};\ u = \frac{x_1 - x_2}{L};\ v = \frac{y_1 - y_2}{l}.$$

The integral I_i was solved for three values of γ, namely, 0, 2 and 4. The results were as follows:

1) $\gamma = 0$:

$$I = \frac{\sqrt{1+\beta}}{2\beta\sqrt{a}} \tan^{-1}\sqrt{\frac{a}{1+\beta}} + \frac{\sqrt{1+a}}{2a\sqrt{\beta}} \tan^{-1}\sqrt{\frac{\beta}{1-a}} - \frac{1}{2\beta\sqrt{a}} \times$$

$$\times \tan^{-1}\sqrt{a} - \frac{1}{2\sqrt{\beta}\,a} \tan^{-1}\sqrt{\beta} + \frac{1}{4a\beta} \ln\frac{(1-a)(1+\beta)}{1+a+\beta};$$

2) $\gamma = 2$:

$$I = \frac{2\beta+1}{8\sqrt{a}\,\beta\sqrt{1+\beta}} \tan^{-1}\sqrt{\frac{a}{1-\beta}} + \frac{2a+1}{8\sqrt{\beta}\,a\sqrt{1+a}} \tan^{-1}\sqrt{\frac{\beta}{1-a}} -$$

$$- \frac{1}{2\beta\sqrt{a}} \tan^{-1}\sqrt{\beta} - \frac{1}{8\beta\sqrt{a}} \tan^{-1}\sqrt{a};$$

3) $\gamma = 4$:

$$I = \frac{3+12\beta+8\beta^2}{48\sqrt{a}\sqrt{1+\beta}\,\beta(1+\beta)} \tan^{-1}\sqrt{\frac{a}{1-\beta}} + \frac{3+12a+8a^2}{48\sqrt{\beta}\sqrt{1+a}\,a\sqrt{1-a}} \tan^{-1}\sqrt{\frac{\beta}{1-a}} -$$

$$- \frac{1}{16a\sqrt{\beta}} \tan^{-1}\sqrt{\beta} - \frac{1}{16\beta\sqrt{a}} \tan^{-1}\sqrt{a}.$$

It is evident from [1] that the counting rate N of the telescope is proportional to the vertical intensity I_0. The coefficient of proportionality is

$$S = 2L^2 (\beta_1 I_1 + \beta_2 I_2 - 2\beta_3 I_3) \tag{2}$$

It can be interpreted as the relative aperture of the telescope and depends on its geometry and the angular intensity distribution.

4. Equation (2) was used to calculate the relative aperture of each of the three telescopes T_0, T_1 and T_2 for the three angular distributions indicated in Table 1, namely, an isotropic distribution, and the distributions $I = I_0 \cos^2 \varphi$ and $I = I_0 \cos^4 \varphi$. The thickness of the counters and the gaps between them were taken into account in the calculations.

The ratios of the relative apertures were found for $\gamma = 0$, 2 and 4 and were used to determine γ.

It was found that the logarithm of the ratio of the relative apertures is very nearly a linear function of γ, and therefore the calculated values are sufficient for the determination of γ from the experimental counting rate ratios because the latter are equal to the ratios of the relative apertures. Table 2 shows the logarithms of the relative aperture ratios for $\gamma = 0$, 2 and 4, and the experimental counting rate ratios for a telescope at a depth of 0, 7, 20 and 60 m of water equivalent.

Table 1

Relative aperture of telescope for $\gamma = 0$, 2 and 4 ($cm^2 \cdot$ sterad).

Telescope	$\gamma = 0$	$\gamma = 2$	$\gamma = 4$
T_0	$4.36 \cdot 10^3$	$3.00 \cdot 10^3$	$2.18 \cdot 10^3$
T_1	$3.81 \cdot 10^2$	$2.65 \cdot 10^2$	$1.94 \cdot 10^2$
T_2	$8.29 \cdot 10$	$2.26 \cdot 10$	6.25

Knowing the dependence of the relative aperture S_{T_0} of the vertical telescope on γ, and having determined γ itself, it is possible to determine the relative aperture for a given angular distribution. The absolute vertical intensity can then be found from the counting rate of the telescope and its relative aperture:

$$I_0 = \frac{N_{T_0}}{S_{T_0}}.$$

Table 2

Ratios of relative apertures of telescopes for $\gamma = 0$, 2 and 4, and the experimental counting rates

	Calculated ratios			Experimental ratios			
	γ			Depth, m water equivalent			
	0	2	4	0	7	20	60
$\lg \frac{S_{T_0}}{S_{T_1}}$	1.058	1.054	1.050	1.056	1.056	1.056	1.053
$\lg \frac{S_{T_0}}{S_{T_2}}$	1.721	2.121	2.542	1.992	2.046	2.090	2.120
$\lg \frac{S_{T_1}}{S_{T_2}}$	0.662	1.068	1.491	1.936	0.990	1.034	1.067

5. Table 3 shows the values of the exponent γ and of the absolute vertical intensity at four levels.

The accuracy to which γ can be determined depends largely on the errors in the determination of the relative apertures of the telescopes, which are 2, 4 and 6% for T_0, T_1 and T_2 respectively. This corresponds to an error in γ of less than 0.2.

We see from Table 3 that as the depth of recording increases, the exponent of angular velocity γ increases as well, and exceeds the limit of error. This corresponds to the intensity versus depth curve for μ-mesons [1] and may be explained by the increase in the exponent of the energy spectrum of μ-mesons with energy.

Table 3

Values of the exponent in the angular distribution of cosmic-ray intensity and the vertical intensity for 0, 7, 20 and 60 m water equivalent.

Level, m water equivalent	γ	I_0, particles/ $cm^2 \cdot min \cdot sterad.$
0	1.3±0.2	0.38±0.03
7	1.6±0.2	0.27±0.02
20	1.8±0.2	0.12±0.01
60	2.0±0.2	0.027±0.002

An important characteristic of cosmic rays is their absolute intensity. Our result for the vertical intensity at sea level is lower than that reported by Greisen [7]. This may be explained by the difference in the exponent γ (angular distribution) which in [1] was assumed to be equal to 2.

The above values for the exponent of the angular distribution and the absolute intensity are consistent with the primary spectrum calculations in [8], and the character of the transmission of cosmic rays through the atmosphere [9]. They are also in agreement with the exponent in the μ-meson production spectrum obtained in [10] from the barometer effect.

CONCLUSIONS

1. Simultaneous measurements at ground level and at depths of 7, 20 and 60 m of water equivalent show that if the angular distribution of the cosmic-ray intensity is written in the form $I(\varphi) = I_0 \cos^{\gamma} \varphi$, where I_0 is the vertical intensity and φ is the zenith angle, then the values of γ at 0, 7, 20 and 60 m of water equivalent are respectively 1.3, 1.6, 1.8 and 2.0.

2. The absolute vertical intensities at 0, 7, 20 and 60 m of water equivalent were found to be 0.38, 0.27, 0.12 and 0.027 $cm^{-2}\ min^{-1}\ sterad^{-1}$.

3. The above values for the exponent of the angular distribution and the vertical intensity are consistent with the existing ideas about the primary spectrum and the character of the processes which accompany the passage of cosmic rays through the atmosphere.

REFERENCES

1. George, E. Fizika kosmicheskikh luchey (Progress in cosmic ray physics), Vol. 1, ed. J.G. Wilson, Chapter 7, Moscow, 1954.

2. Follet, D.H. and Grawshow, I.D. Proc. Roy. Soc., A, 155, 546, 1946.

3. Randoll, C.A. and Hazen, W.T. Phys. Rev., 81, 144, 1951.

4. Bollinger, L.M. Bull. Amer. Phys. Soc., 25, No. 3, 16, 1950.

5. Kuz'min, A.I. and Yarygin, A.V. Tr. YaFAN SSSR, ser. fizich., No. 2, 36, 1958.

6. Makarov, S.V. Tr. YaFAN SSSR, ser. fizich., No. 3, 46, 1960.

7. Greisen, K. Phys. Rev., 61, 212, 1942.

8. Charakhch'yan, A.N. and Charakhch'yan, T.A. ZhETF, 35, 1090, 1958.

9. Dobrotin, N.A. Kosmicheskiye luchi (Cosmic rays). pp. 280-285, Moscow, 1954.

10. Kuz'min, A.I. and Danilov, A.A. Tr. YaFAN SSSR, ser. fizich., No. 3, 58, 1950.

Yu. A. Nadubovich

AUTOMATIC FRAME-BY-FRAME PHOTOMETRY OF ALL-SKY PHOTOGRAPHS

1. INTRODUCTION

According to the plan for the processing of IGY observations [1], it was intended to study the instantaneous characteristics of auroras using photographs obtained with the C-180 camera. The high quality of such photographs ensures that it is possible to study the development and the space-time distribution of auroras, and also to determine (by photometric methods) temporal variations in the energy flux radiated by them. Such data may be of interest in their own right, but may also serve as a valuable source of information for comparisons between auroras and other geophysical phenomena [2].

In order to achieve this aim, it is necessary to carry out photometric measurements at a large number of points on each frame, and then use these measurements to determine the luminous flux (within the limits of the spectral sensitivity of the negative) which reaches the frame during the exposure time. Since, however, the volume of the material which has to be processed is very large, and the most widely used microphotometers (for example, the MF-2), are inconvenient for this kind of analysis, this method turns out to be unsuitable because it is laborious and inefficient.

Below, a description is given of a special automatic frame-by-frame photometer which is suitable for all-sky photographs. The basic difference between this photometer and other instruments is that each frame is examined as a whole rather than point by point. This yields a mean value for the blackening over the frame, which can then be converted to the mean luminous flux by the method described in Section 3. The apparatus functions automatically and converts the measurements directly into graphs showing the luminous flux as a function of time. The photometer can examine 720 frames per hour, which corresponds to about 14 m of the film.

The instrument was developed on the basis of the automatic mechanism of the C-180 camera which was designed by Prof. A.I. Lebedinskiy and can easily be assembled by laboratories intending to analyze all-sky photographs.

It must, however, be noted at once that the automatic photometer can be employed without any modification for the photometry of sections of the sky rather than the entire sky. It may be used to obtain photometric information for those points on auroras for which special photoelectric observations are not available.

Moreover, the design and theoretical consideration on which the automatic photometer is based may be used for the development of other automatic instruments for the examination of all-sky photographs.

The present method suffers from the disadvantage that it has a low accuracy (of the order of 15—20%), and also from its inability to deal with rapid changes in the luminous flux (for example, in pulsating auroras), owing to the low time resolution of all-sky photographs. This resolution is limited at one end of the scale by the exposure time (20 or 5 sec), and at the other end by the large time intervals (30 sec) between successive series of frames.

Much more accurate data on the variations in the luminous flux emitted by auroras may be obtained by designing an electrophotometer with a 180° field of view and continuous automatic recording of the measurements.

Various workers, including the present author [2, 3], have proposed designs for this kind of instrument, but a comparison of data obtained with the 180° electrophotometer and the automatic photometer described below shows that the method of frame-by-frame photometry is quite reliable and is capable of satisfactory determination of the development of the various auroral forms, and therefore, owing to its simplicity and potential availability, may find extensive applications.

2. CONSTRUCTION OF THE PHOTOMETER

A photograph of the automatic frame-by-frame photometer (AFP) is shown in Fig. 1 and its optical and electrical systems in Figs. 2 and 3.

Light from the point source 1 (Fig. 2), which is located at the focus of the condenser 2, is collimated by the latter and reaches the frame 3 which is to be examined. The frame to be examined is positioned within the window 4 and the light transmitted by it is intercepted by the vacuum-tube photocell 5.

The photocurrent produced by the cell flows through the resistance R_2 which is of the order of 100 Ω (Fig. 3). The potential difference across R_2 is recorded by the automatic self-recording potentiometer EPP-09 and is a measure of the blackening of the negative.

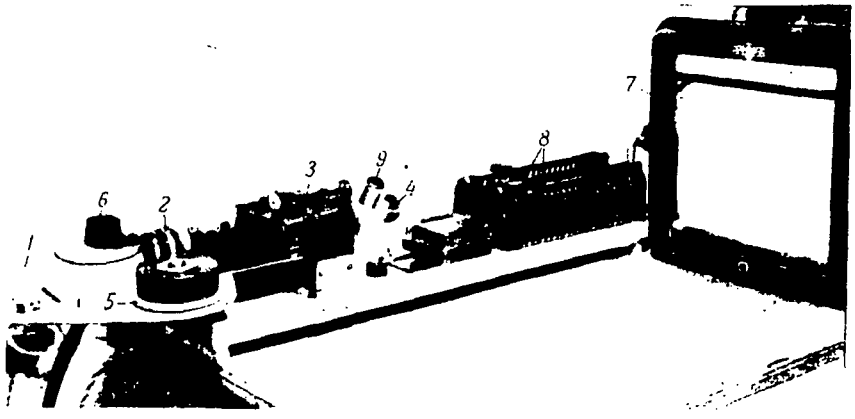

Fig. 1. Photograph of the automatic frame-by-frame photometer.

1 - lamp (with cover removed; 2 - condenser; 3 - motion picture camera; 4 - photocell; 5, 6 - spools carrying the film; 7 - EPP-09 penrecorder; 8 - rheostats controlling the current through the lamp; 9 - demountable prism for inspecting the position of the frame.

Since the markers produced by the C-180 camera and the images due to local sources and objects at the edge of the frame may affect the final result, a special mask 7 (Fig. 2) is mounted in front of the film and defines a region near the horizon up to $z \approx 80°$. It must be remembered that the image of the upper mirror of the camera also restricts the region which is photometered by the instrument (up to $z = 11°$).

The mask 7 is demountable and designed so that it defines only a small part of the image. The AFP then functions as an ordinary automatic microphotometer and measures the blackening at preselected points on the sky. If instead of measuring the magnitude of the photocurrent, one simply records the fact whether a blackening is present at a particular part of the negative or not, then the AFP may be used to determine the frequency of appearance of auroras at a particular point, and so on.

The accurate automatic transport of the film through one frame at a time is achieved by the motion picture mechanism of the C-180 camera without any modification.

The light source and the condenser are mounted on the modified cassette of the C-180. The cassette carrying the film under investigation is placed in the motion picture camera so that the frame fits exactly into the frame aperture. The motion picture camera is then connected to the command device of the

C-180, the shutter is set in the open position and the speed selector is set in position II (one complete revolution of the shutter per cycle of operation of the motor of the camera). The command device replaces the frame every five seconds.

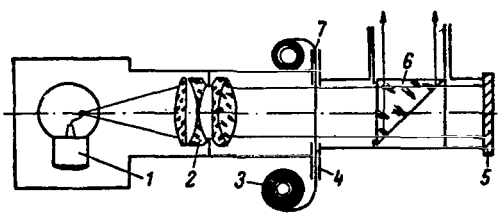

Fig. 2. Optical system of the AFP
(see text for explanation)

So long as the shutter remains in the open position, the pen of the potentiometer draws a small "step" which represents the mean blackening on the particular frame.

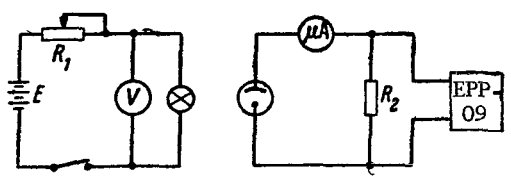

Fig. 3. Electrical circuit of the AFP.

When the current pulse produced by the command device is applied to the motor of the motion picture camera, the grab moves the negative through one frame, and the shutter simultaneously cuts off the luminous flux for a very short period of time so that the pen draws a peak on the pen recorder chart which indicates the frame change. The next frame is then photometered for about four seconds and the process is repeated again. A specimen recording is shown in Fig. 4.

If the time at which one of the frames has been exposed is known, then there is no difficulty in the calibration of the time axis on the AFP trace.

As was pointed out above, the time spent on photometering one frame is about four seconds, and this is quite sufficient for the pen to reach its equilibrium position.

Under the conditions described above, the film can be examined at the rate of 12 frames per minute, or about 14 m of the negative per hour. This can be increased still further by using a lower-inertia recording device and applying pulses with a higher repetition frequency to the motor.

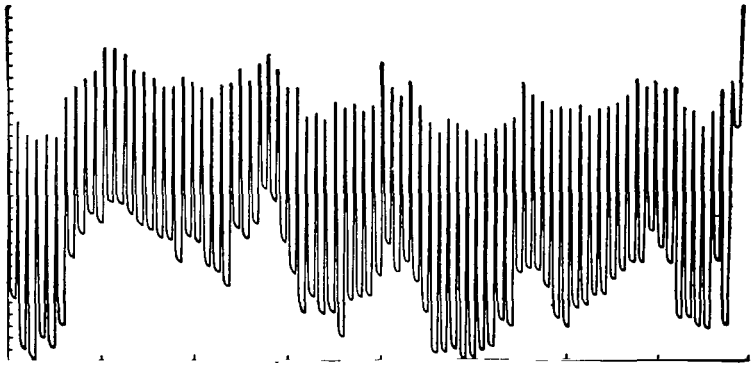

Fig. 4. Specimen recording obtained with the AFP.

The true readings are represented by the lower envelope of the trace, the sharp peaks represent displacement of the frame.

The demountable prism 6 (Fig. 2) is used for periodic visual inspection of the operation of the grab which governs the correct positioning of the film within the frame aperture.

The illuminating lamp is supplied by a battery of storage cells (Fig. 3). The intensity of the lamp is kept constant by means of the rheostat R_1 and is controlled by the voltmeter.

The AFP which we have used incorporates the following components: K-10 lamp (12 V, 50 W), Industar-51 objective (used as the condenser), the FESS-U10 silver sulfide photocell, self-recording potentiometer EPP-09 with a 0—10 mV scale and a full-scale traverse time of 2.5 sec.

3. DETERMINATION OF THE LUMINOUS FLUX FROM AURORAS

During the potometry of the film, the area S defined by the mask receives a uniform luminous flux Φ_0 which produces an illuminance A_0 at

each point on the frame, where

$$\Phi_0 = A_0 S.$$

Consider an element of area ds on the frame, which intercepts a luminous flux $A_0 ds$. If the particular element of the negative is blackened, then the illuminance due to this element at the photocell will be less than A_0, and the luminous flux transmitted by ds will be A(s)ds. By definition of the transmittance τ,

$$A(s) = A_0 \tau(s),$$

where $\tau(s)$ is the transmittance of the element of area ds. Therefore, the total luminous flux reaching the photocell may be written

$$\Phi = \int A(s)\, ds = A_0 \int \tau(s)\, ds,$$

and the mean transmittance of the frame as a whole is

$$T = \frac{\Phi}{\Phi_0} = \frac{\int \tau(s)\, ds}{S}, \quad 1 \geqslant T \geqslant 0. \tag{1}$$

Using the sensitogram which is available on each film, it is possible to construct the characteristic curve for the film by plotting the absolute exposure Et in lux-seconds as a function of the transmittance τ (Fig. 5). The straight line portion of the curve may be described by

$$\tau(s) = b - ktE(s),$$

where b is the length of the intercept on the τ axis and $k = \tan \alpha$ is the slope of the line. The parameter t represents the exposure time and E(s) the illuminance in lux-seconds which gives rise to a blackening on the negative which has a transmittance $\tau(s)$. Equation (1) then yields

$$T = \frac{bS - kt \int E(s)\, ds}{S},$$

but since

$$\int E(s)\, ds = F$$

is the luminous flux reaching the frame during the exposure we have

$$F = \frac{S}{kt}(b - T) = K(b - T). \tag{2}$$

We have thus obtained an expression which relates the mean blackening of the frame, T, to the luminous flux, F, from the aurora. In addition, equation (2) includes constants which depend on the conditions of exposure (exposure time t) and experiment, the properties of the photographic material (b and k), and the AFP parameter S (the area of the photometered part of the frame).

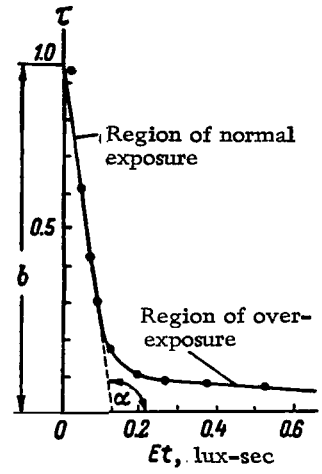

Fig. 5. Characteristic curve of the all-sky film determined by measurements on the sensitogram of the negative copy No. 16, in the Bay of Tiksi.

It is easy to show that, if S is in square meters, t is in seconds and k is in $(\text{lux-sec})^{-1}$ (Fig. 5), then the luminous flux F is in lumens. The quantities b and T are dimensionless.

Let us now consider equation (2) in greater detail by discussing two special cases. Suppose that the photometered frame has the maximum possible blackening over the entire field. This means that $T \to 0$ and $F = Kb = F_\infty$ is the magnitude of the uniformly distributed luminous flux which produces the maximum blackening on the negative. It follows that, in general, $F = F_\infty - KT$, where F_∞ is a new constant which is determined by the exposure time, by the properties of the photographic film, and by the area S.

In practice, the maximum blackening cannot be infinite and is limited to values of τ of the order of 0.001. However, this does not affect our discussion to any great extent, since in practice the range of values of T which is employed in the case of the AFP is 1—0.05.

Consider now the second limiting case in which there is no blackening at all. Here $\tau(s) = 1$ for all the elements of the film and $\Phi = \Phi_0$. It follows that $T = \frac{\Phi}{\Phi_0} = 1$. Physically, it is clear that under these conditions $F = 0$, although according to (2), $F = K(b-1) = F' \neq 0$. This is due to the fact that equation (2) is in general valid only for an idealised characteristic for which $b = 1$. However, for the majority of films used with all-sky cameras, b does not differ greatly from unity and the above analysis may be regarded as valid to an acceptable degree of accuracy.

The departure of F' from zero characterizes the accuracy of this method in each specific case in so far as the properties of the film are concerned.

The above discussion suggests the method of application of the AFP. If the scale of the recording device is calibrated in values of T (cf. below), then by using the basic equation (2) we can determine the magnitude of F for a series of successive frames exposed at known intervals of time, and thereby determine the luminous flux received from auroras as a function of time.

The scale of the recording device may be calibrated directly for values of F, but then each all-sky photograph would need its own calibration.

We have already shown that with a suitable choice of units, the luminous flux is obtained in lumens. In order to convert this into the CGS system, the result must be multiplied by the mechanical equivalent of light $M(\lambda)$ which corresponds to the effective wavelength λ of a particular negative. For panchromatic films it may be assumed that $M = 0.0016$ W/lumen at $\lambda = 5550$ Å.

In order to find the illuminance of the earth's surface in energy units, the luminous flux F reaching the frame must be divided by the area of the entrance pupil of the C-180 camera, which corresponds to the zenith distances within which the measurements are carried out.

4. CALIBRATION OF THE PHOTOMETER AND CORRECTIONS FOR THE BACKGROUND ON THE NEGATIVE

The simplest method of calibrating the scale of the recording device in terms of the absolute values of T by the method of error on AFP films is to use a film with known densities.

For this purpose the C-180 camera is used to obtain the calibration film which consists of a series of photographs of the night sky covered by uniform cloudiness, using different exposure times between 2 and 150—200 sec. An instrument capable of measuring the absolute values of the transmittance, for example, the MF-2 microphotometer, is then employed in a very careful determination, using a large number of points, of the mean transmittance T of each frame on the calibration film. Prior to the measurements on the actual

auroral photographs, measurements are made on the calibration film, using the same lamp with the same filament current, and the known values of T are used to plot a calibration curve for the AFP.

The calibration can also be carried out using some other known optical densities, although in this case it is necessary to introduce a correction for the part of the frame which includes the image of the upper mirror of the camera. If the calibration film is obtained with the C-180 camera, then this correction is introduced automatically.

The determination of the background density on the negative is an important problem in frame-by-frame photometry. Since the aurora usually occupies a small part of the frame, and the background is distributed over the entire field, it follows that this source of error may have a considerable influence on the final result.

We shall define the background as the blackening on the negative due to the glow of the night sky, the stellar light scattered in the atmosphere, the radiation due to local sources, and also the intrinsic fog on the negative, i.e. all the blackening apart from that due to the aurora. We shall assume also that the background density is uniformly distributed over the frame (this condition is reasonably satisfied in the absence of twilight, during moonless nights, and under the condition of good atmospheric transmittance).

The background transmittance, i.e. the level $T = 1$, from which all the subsequent measurements are made, may be determined by measurements on AFP frames on which there are no auroras.

In order to obtain a more accurate calibration of the AFP and to simplify the associated calculations, it is desirable to try to ensure that the background on the all-sky photographs and the background on the calibration film should be as equal to each other as possible.

It is obvious that only those all-sky photographs on which there has been no extraneous illumination, and which have been obtained during moonless nights under the condition of good atmospheric transmittance may be used in frame by frame photometry.

5. PHOTOMETRIC PROPERTIES OF ORIGINAL ALL-SKY PHOTOGRAPHS AND OF THEIR NEGATIVE COPIES

In the USSR, the "Dn" motion picture film is used by the network of stations concerned with the photographic observation of auroras.

According to our measurements, which are in good agreement with those reported in [4], the characteristic curve of this film has a very long straight line portion. A twenty-minute development in No. 2 developer at +20°C produces a maximum optical density of approximately 3 ($\tau = 0.001$), while the useful interval of exposures amounts to 2.5 (on the logarithmic scale).

These properties show that the "Dn" film is very close to the ideal film which we considered in the derivation of equation (2).

In many cases it is the negative copies rather than the original all-sky photographs which are subjected to the analysis. Measurements on the sensitograms of these negative copies show that they have a much lower maximum optical density and much shorter range of exposures (on the average 1.5 and 1 respectively).

The short straight line portion of the characteristic curve of the negative copies complicates the photometric process. In the case of the original all-sky photographs, it is sufficient to photometer frames with 20 sec exposures, since practically all the auroral images then lie on the straight line portion. In the case of very bright auroras, frames obtained with a 5 sec exposure must be additionally examined in order to ensure that the maximum blackening does not fall on the curved part of the characteristic curve (Fig. 5). Under-exposures are, in this sense, less serious since the corresponding part of the characteristic curve in the case of the "Dn" film is short and not very curved.

The gamma factors of the original all-sky photographs and of the negative copies are not very different from each other. Low blackening due to very weak auroras is satisfactorily reproduced on the copies.

6. SOURCES OF ERROR

The quantity S in the basic formula (2) can be determined with practically any degree of accuracy. The exposure time t is also a constant quantity which is determined by the accuracy of the chronometer in the C-180 camera. With careful calibration of the AFP, the values of T may be obtained to an accuracy of the order of 10%. Thus, the error in luminous flux measurements is largely determined by the degree to which the characteristic curve may be represented by a straight line within the region under consideration, and by the adequate correction for the effect of the background.

Distortion in the optics of the C-180 camera does not introduce considerable errors into the measurements, since a reduction in the area of the image at the horizon is compensated by a corresponding increase in the luminous flux falling on the selected elementary area, and the directly proportional increase in the blackening (the gamma factor of all-sky films is approximately unity).

Much greater errors may be due to difficulties in introducing adequate corrections for atmospheric absorption, since auroras often occupy a considerable range of zenith distances. If the aurora under consideration is small in area and lies near the zenith, then absorption may be allowed for in the usual way [5]. In the case of extended auroras, it is possible to carry out the photometry over successive annular regions centered on the zenith, with subsequent correction for the absorption within each ring, and integration of the resulting luminous fluxes.

7. AN EXAMPLE OF FRAME-BY-FRAME PHOTOMETRY

Figure 6 shows the illuminance of the earth's surface in energy units, due to an aurora photographed on January 21, 1958, in the Bay of Tiksi. The curve was obtained as a result of measurements on a negative copy.

The aurora was in the form of a bright, very mobile band near the zenith, exhibiting a ray structure. Fig. 6 shows the increase in the luminous flux and the subsequent slower decrease accompanied by appreciable "bursts", which is characteristic for ray auroras. Photoelectric observations show that at the maximum development of ray auroras, there are rapid oscillations in the luminous flux, although in Fig. 6 the time resolution was inadequate to

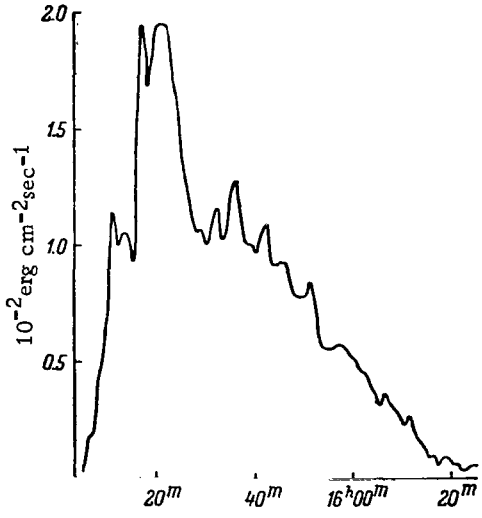

Fig. 6. Energy illuminance of the earth's surface due to the aurora observed on January 21, 1958, in the Bay of Tiksi (UT).

show it, and the smoothed-out fine structure is represented by a slight plateau at the peak.

The values for the energy illuminance obtained by the frame-by-frame photometry are in agreement with the determinations of other authors [6].

The author would like to thank Candidate of Physicomathematical Sciences Ye.A. Ponomarev for valuable advice and direct help in the construction of the device, and Senior Technician-Geophysicist Ye.M. Vasyuto for his help in building the apparatus.

REFERENCES

1. IGY Information Bulletin, No. 5, Moscow, 1958.

2. Korotin, A. Sopostavleniye fotoelektricheskoy registratsii yarkosti nebosvoda s magnitnym polem. Doklad na rasshirennom seminare Otdela fiziki verkhney atmosfery (Comparison of photoelectric recording of the brightness of the sky with the state of the magnetic field. Paper read at an extended seminar in the Department of the Physics of the Upper Atmosphere), IFA AN SSSR, Moscow, April 25-27, 1960.

3. Nadubovich, Yu. Izucheniye mgnovennykh svetovykh kharakteristik polyarnykh siyaniy pri pomoshchi elektrofotometra s uglom zreniya 180°. Doklad na rasshirennom seminare Otdela fiziki verkhney atmosfery (Studies of the instantaneous light characteristics of auroras using a 180° electrophotometer. Paper read at an extended seminar in the Department of the Physics of the Upper Atmosphere), IFA AN SSSR, Moscow, April 25-27, 1960.

4. Svoystva fotograficheskikh materialov na prozrachnoy podlozhke. Sensitometricheskiy spravochnik (The properties of photographic materials on a transparent base), Sensitometric Handbook, GITTL, Moscow, 1955.

5. Sytinskaya, N. Absolyutnaya fotometriya protyazhnykh nebesnykh ob"ektov (Absolute photometry of extended celestial objects), Leningrad University Press, 1948.

6. Dzhordzhio, N. Izv. AN SSSR, ser. geofiz., 5, 692-695, 1957.

E. P. Zubareva and Yu. Z. Nadubovich

A NEW METHOD FOR RECORDING EARTH CURRENTS

The existing method of recording the components of the electrotelluric field, which is based on the use of mirror galvanometers, is complicated and inconvenient. The recording apparatus must be mounted on massive foundations, the recording itself is carried out in a dark enclosure which prevents efficient servicing, and finally, the photographic method of recording prevents the monitoring of the state of the field during the measurements.

All this increases the cost of earth current stations and frequently leads to a reduction in the quality of the resulting tellurograms. Since the recording cannot be controlled, the galvanometer light-spot is thrown beyond the limits of the recording drum during strong disturbances, and the recording process terminates. Moreover, this can only be discovered after the film has been developed. The result may be that many hours of possible recording are lost, particularly the most interesting periods which correspond to the disturbed state.

At the same time, the amplitude of the recorded signals is sufficient for a less sensitive recording instrument, which may be more convenient and may not suffer from the above shortcomings.

Trial records of the electrotelluric field with the aid of the automatic electronic self-recording potentiometer EPP-09 have been carried out at the earth current station in the Bay of Tiksi. The quality of the tellurograms is comparable with the records obtained by the galvanometer method. However, it is now possible to have visual control of the state of the field, there is no need for a dark enclosure and massive foundations, and the difficulties of photographic processing are avoided. This method may therefore become widely adopted both for the trial recordings in preliminary searches for suitable places for the electrodes, and also at continuously operating stations. Moreover, the use of the EPP-09 recorders will facilitate automatic adjustment of the sensitivity during strong disturbances.

The EPP-09 recorders are manufactured in a number of versions which differ in the range, the number of channels (the number of recorded parameters may be between 1 and 24) and the time constant (1, 2.5 and 8 seconds). The waveform is recorded by a pen on a paper strip which is 27.5 cm wide. The

speed of the paper strip may be varied between 6 and 960 cm/hr. The instrument is supplied from the mains at 127 V, 50 cps. The estimated accuracy of the instrument is ± 0.5%.

The basic circuit of the apparatus is illustrated in Figure 1. The current flowing along the line connecting the electrodes to the earth current station gives rise to a potential difference u_H across the resistance R_H which is recorded by the EPP-09. The potential difference between the electrodes is then given by the obvious relation $U = u_H (R_M/R_H)$ where U is the required potential and R_M is the resistance between the electrodes. The potential difference u_H is read off the EPP-09 chart directly in millivolts.

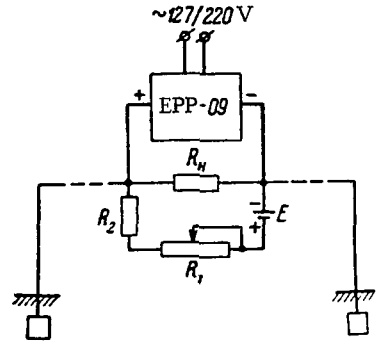

Fig. 1. Basic circuit for recording earth currents with the EPP-09 potentiometer.

The sensitivity is directly proportional to R_H although under normal conditions it is necessary that $R_H \leq 100\ \Omega$. The resistor R_H should be a high stability component with a low temperature coefficient.

Since the zero of the EPP-09 is on the left rather than at the center of the scale, which is inconvenient for our measurements, the instrument is provided with a zero shifting device which consists of a cell E (of the order of 1 volt) and the resistors R_1 and R_2. In this way the position of the zero can be adjusted until it lies at the center of the scale by altering the position of the slider of R_1. The fixed resistance R_2, which is of the order of 10-30 KΩ, protects the EPP-09 from overloading when R_1 is removed.

The precise values of all the resistances are chosen empirically.

If a large constant potential difference exists between the electrodes (for example, a potential difference due to the electrochemical interaction between the electrodes and the soil), it can be backed off by the circuit $E-R_1-R_2$. The polarity of the cell must be arranged so that the voltage drop due to the cell E is subtracted from the potential difference between the electrodes.

Since the output of the cell E is applied to the electrodes, the circuit shown in Figure 1 cannot be used for simultaneous recording with the usual galvanometric apparatus.

Figure 2 shows typical tellurograms obtained with the EPP-09 and the usual galvanometric method. The tracings were obtained with 75 × 50 × 0.3 cm electrodes at a distance of 500 m from each other. The resistance between the electrodes was 2420 Ω.

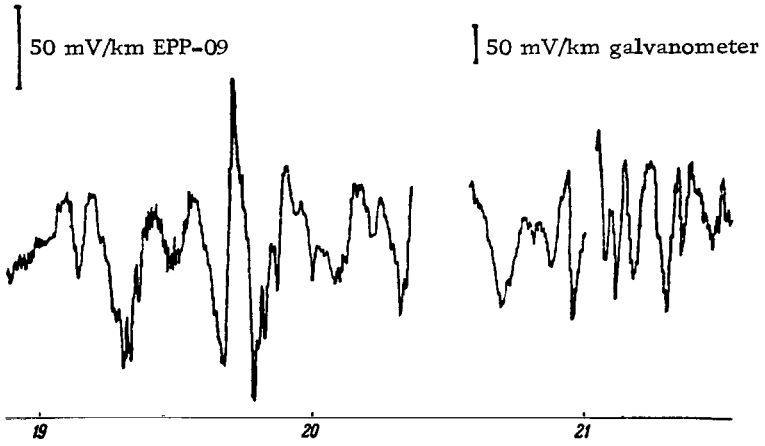

Fig. 2. Earth current records obtained with the EPP-09 and the standard galvanometer apparatus.

Bay of Tiksi, June 29, 1959, UT.

We used a single-channel EPP-09 with a 0-10 mV scale and a time constant of one second. The circuit parameters were as follows: $R_H = 100\ \Omega$, $R_1 = 15\ k\Omega$, $R_2 = 12\ k\Omega$, and $E = 0.8$ V. The constant potential difference between the electrodes which had to be backed off was 20 mV.

The galvanometric record which was obtained with a continuously operating installation in the Bay of Tiksi, incorporated a "Fi" galvanometer with R_{int} = 240 Ω, R_{crit} = 1350 Ω and T = 9 sec. The recording obtained with this apparatus is shown on the right of Figure 2. In each case the rate of scanning was 9 cm/hr.

Since simultaneous recording with the two installations was impossible, the recording was first carried out with the EPP-09 and then the electrodes were connected to the standard apparatus.

It is evident from Figure 2 that the EPP-09 recording shows a greater number of details than the tracing obtained by the standard apparatus, which is an additional feature apart from the ease with which the record can be obtained.

A.V. Sergeyev and A.A. Luzov

OPERATION OF SNM-8 COUNTERS AT VOLTAGES UP TO 3 kV

A study of the slow-neutron proportional counters SNM-5 was reported in [1] together with the main relationships connecting the counter parameters. The latter may be written in the form

$$\ln A = \ln 2\left[\frac{V_B}{U_i \ln \frac{b}{a}} - a\frac{P}{\lambda_0}\right] + \ln \frac{e\eta_0}{c}, \quad (1)$$

$$V_i = U_i \ln \frac{b}{a}\left[1 + \frac{a}{\lambda_0} P\right], \quad (2)$$

Where a, b and P are respectively the anode radius, the cathode radius and the gas pressure in the counter; A is the pulse amplitude for a voltage V_i between the electrodes, U_i is the ionization potential of the BF_3 gas, and λ_0 is the mean free path of electrons in the gas at P = 76 cm Hg.

It follows from (1) that the relation $\ln A \sim f(V)P$, b, a = const is satisfied in the proportional region of the counters. On the other hand, according to [2, 3], neutron counters function as proportional counters for gas amplification factors up to $K = 10^5$.

We have made an attempt to determine the maximum value of V_B at which the SNM-8 counters will operate as proportional counters. Two counters were investigated. Figure 1 shows their average amplitude characteristic. It follows from this figure that the pulse amplitude is a linear function of the applied voltage up to $V_B = 2900$ V. The slope of the plateau may be estimated from an analysis of the counting characteristics shown in Figures 2 and 3. Thus, for example, for $V_D = 40 - 80$ V on the $V_B = 2900$ V curve the slope is 1% per volt, while for $V_B =$ 2800 - 3000 V on the $N = f(V_B)_{V_D = 60\ V}$ curve the slope is less than 6% per 100 V. At $V_B = 2900$ V the gas amplification factor was $K \leq 10^5$.

The high-voltage (up to 3000 V) characteristics of the SNM-8 counters do not provide a complete guarantee that the total number of the recorded neutrons does not include a fraction due to particles producing direct ionization of the BF_3 gas. This point was checked in an experiment with a γ-source.

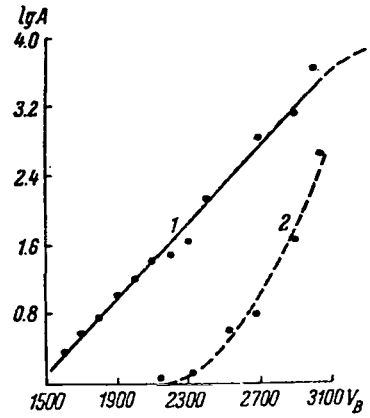

Fig. 1. Logarithm of the pulse amplitude as a function of the voltage across the counter:

1 — most probable amplitude due to neutrons; 2 — most probable amplitude due to γ-rays.

The amplitude characteristics were recorded both with a Po-Be neutron source and with a Co^{60} γ-source.

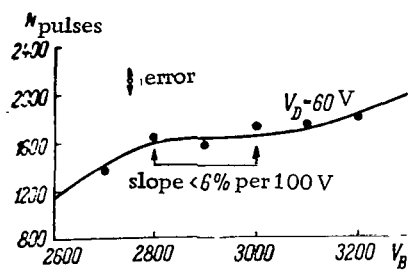

Fig. 2. Counting rate as a function of voltage across the counter.

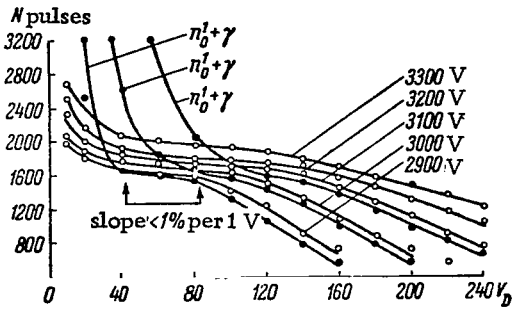

Fig. 3. Counting rate as a function of discriminator threshold.

It is evident from Figure 4 that the difference between the amplitudes due to neutrons and γ-rays is very large (factor of 10) even at V_B = 3000 V. The pulses can therefore be easily distinguished and only the true neutron counting rate recorded.

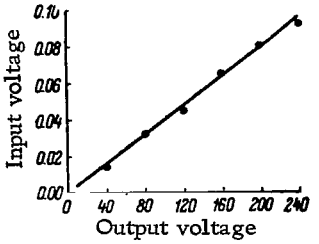

Fig. 4. Amplitude characteristic of the amplifier.

All the experiments were carried out with the commercial SCh-3 apparatus up to counter voltages of 2200 V. At higher voltages the electronics of the SCh-3 apparatus was modified without affecting the linearity of the amplifier or the resolution of the circuit. This is confirmed by the amplitude characteristic shown in Figure 4.

In conclusion, we report the recorded variation in the neutron component for a period of three months (Fig. 5). The counting rates were recorded with a three-counter array having the same geometrical dimensions as the screening block of the standard neutron monitor described in [4]. The voltage across the counters was V_B= 2950 V, the pulse amplifier had an amplification factor of 125, and the discrimination level was V_D = 12.5 V.

Although it was not intended to carry out a detailed study of the processes which occur in the SNM-8 proportional counters, the preliminary results which we have obtained lead to the following conclusions:

1. The logarithm of the pulse amplitude due to neutrons is a linear function of the voltage across the counter; the amplitude is 80 mV at V_B = 3000 V.

2. For $V_B \geq 3000$ V, the logarithm of the neutron pulse amplitude follows a non-linear law, but up to V_B = 3000 V the ratio of pulse amplitude due to neutrons and γ-rays remains greater than 5.

3. Up to V_B = 3000 V, the SNM-8 counters can be used with an amplifier giving an amplification of about 200 with the discriminator level at the output of V_D = 12 V.

4. Compared with the existing pulse amplifier of the SCh-3 (K = 50,000, V_B = 1800 V, V_D = 8 V), the recording of variations in the neutron component of cosmic rays can be carried out with higher stability if the amplifier with K ~ 200 is employed [4]. This will, of course, also ensure greater reliability.

It is possible to construct a transistorized version of this kind of amplifier.

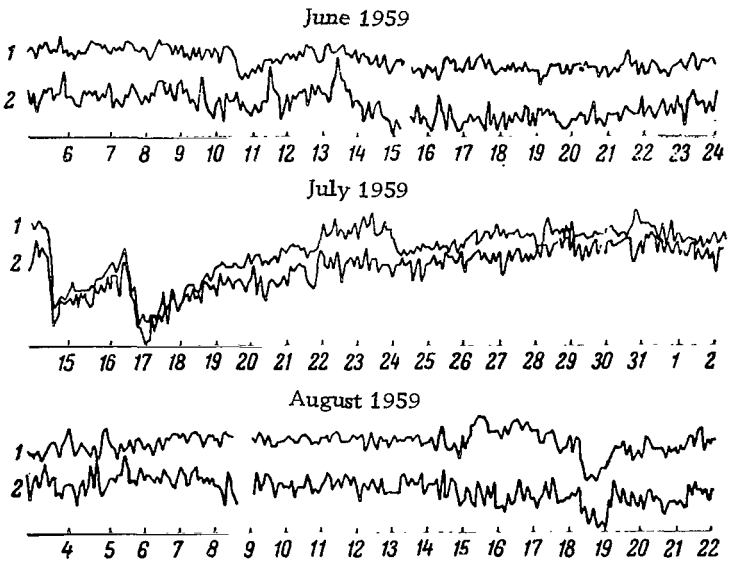

Fig. 5. Variations as measured by the three-counter apparatus (2). For comparison, (1) gives the variations recorded by a standard neutron monitor. These tracings represent two hourly values of the intensity which have been corrected for the P-effect.

REFERENCES

1. Savel'yev, V.Ya. and Kononenko, V.A. Pribory i tekhnika eksperimenta, 1, 61, 1958.

2. Veksler, V., Groshev, L. and Isayev, B. Ionizatsionnyye metody issledovaniya izucheniy (Ionization methods for studying radiation). Moscow, 1949.

3. Korff, S.A. Schetichiki elektronov i yadernykh chastits (Electron and nuclear counters). Moscow, 1947.

4. Kopylov, Yu.M. Sovetskiye stantsii kosmicheskikh luchey (Soviet cosmic ray stations). Moscow, 1960.

PART II

METEOROLOGICAL EFFECTS IN THE INTENSITY OF COSMIC RAYS

A.A. Danilov, G.F. Krymskiy and V.A. Filippov

RESULTS OF A STUDY OF THE QUANTITY γ_{eff} IN THE DIFFERENTIAL π-MESON PRODUCTION SPECTRUM

Comparison of variations in cosmic-ray intensities obtained with a meson semi-cubic telescope and an ionization chamber showed that in the former case the diurnal variations, the effects of magnetic storms, and the 27-day variations are considerably greater than the corresponding variations indicated by the ionization chamber.

It has been suggested that this difference is due to two factors:

1) The ionization chamber determines the intensity from the total ionization, while the telescope measures the number of particles whatever their energy. It follows that the energy spectrum of μ-mesons measured by the ionization chamber should differ from the energy spectrum measured by the telescope.

2) The ionization chamber and the semi-cubic telescope have different directional properties, e.g. the chamber collects radiation within an angle of about 2π, while the semi-cubic telescope has an acceptance angle of π. Particles arriving from different zenith angles ξ are attenuated by the atmosphere in proportion to $\cos\xi$. If follows that variations of extra-atmospheric origin should manifest themselves differently in the above two situations. In order to verify these hypotheses, consider each of them in turn.

1. Suppose that the energy spectra determined with the ionization chamber and the semi-cubic telescope are different. The quantity γ_{eff} in the π-meson production spectrum, which is given by the function [1],

$$f_{\pi}(\varepsilon,\ h,\ x)=\frac{A}{\varepsilon^{\gamma+1}}e^{-\frac{h_1}{L\varepsilon}}$$

where A is a constant, L is the free path for absorption of the meson-producing component, h is the level at which the π-mesons are produced, and $x = \cos \xi$, is different for the two instruments. This will lead to a difference in the temperature effect which should be verified by comparing theoretical and experimental seasonal variations in the μ-meson intensity. To do this, let us first calculate the expected seasonal variations for different γ_{eff}. Then, by comparing the calculated seasonal variations with experimental values it will be possible to determine γ_{eff} for the ionization chamber and the semi-cubic telescope.

In order to verify this hypothesis we have considered the results obtained with the S-2 ionization chamber [2], for which the minimum recorded energy is $\Delta\epsilon = 0.28$ BeV, and the semi-cubic telescope with $\Delta\epsilon = 0.24$ BeV [3]. The minimum recorded energy $\Delta\epsilon$ was calculated from the following formula [4]

$$\frac{d\varepsilon}{dx}=a+b\varepsilon+c\ln\left(\frac{\varepsilon}{10^3}\right),$$

where a is the loss of energy by ionization, $b\epsilon$ is the total loss of energy by radiation, pair production, production of stars and showers as a result of nuclear disintegration, and the production of secondary penetrating particles, and $c\ln\left(\frac{\varepsilon}{10^3}\right)$ is the energy loss by Čerenkov radiation. The third term is small and can be neglected.

The magnitude of $\Delta\epsilon$ for the ionization losses was assumed to be 2×10^6 eV g^{-1} cm^{-2} for air and 1.3×10^6 eV g^{-1} cm^{-2} for lead.

The expected variations of atmospheric origin were calculated from the formula [5]

$$\frac{dI}{I}=\beta_0\delta p+\int_0^{h_0}W(h)\,\delta T(h)\,dh,$$

where β_0 is the barometer coefficient and W(h) is the temperature-coefficient density function.

The density function W(h) was calculated from the Feynberg-Dorman expression [1]

$$W_T(h,\ h_0,\ \Delta\varepsilon,\ x)=W_T^{\pi}(h,\ h_0,\ \Delta\varepsilon,\ x)+W_T^{\mu}(h,\ h_0,\ \Delta\varepsilon,\ x),$$

where $W_T^{\pi}(h, h_0, \Delta\varepsilon, x)$ is the π-meson effect due to the competition between the decay and capture of π-mesons and $W_T^{\mu}(h, h_0, \Delta\varepsilon, x)$ is the μ-meson effect due to the instability of μ-mesons. These functions are given by

$$W_T^{\pi}(h, h_0, \Delta\varepsilon, x) = \frac{he^{-\frac{h}{Lx}}\chi(s, \nu)}{\alpha x \lambda b_{\pi}(h) T(h) (h_0 - h + \Delta\varepsilon)^{\gamma} N_{\gamma}(h_0, x)},$$

$$W_T^{\mu}(h, h_0, \Delta\varepsilon, x) = \frac{q_{\mu}}{N_{\gamma}(h_0, x) h} \int_0^{\infty} \frac{e^{-\overline{Lx}} f_{\gamma}(s, k, \nu) dh_2}{(h_0 - h_2 + \Delta\varepsilon)^{2+\gamma}}.$$

Figure 1 shows the temperature-coefficient density function for a parallel μ-meson beam calculated from the above formula for an S-2 chamber with a screen corresponding to $\Delta\epsilon = 0.28$ BeV and a semi-cubic telescope with $\Delta\epsilon = 0.24$ BeV. Curves 1—3 represent the μ-meson effect, while curves 4—6 show the π-meson effect (the signs of the two effects are opposite).

Figure 2 shows the total temperature-coefficient density functions with corrections for the geometry of the apparatus.

The directional properties of the chamber were calculated from the formula [1]

$$I(\xi, \varphi) d\xi d\varphi = \cos^2 \xi \sin \xi d\xi d\varphi.$$

while the corresponding properties of the telescope were calculated from [6]

$$I(\xi, \varphi) d\xi d\varphi = \cos^3 \xi \sin \xi d\xi d\varphi \rho(\xi, \varphi),$$

where $I(\xi, \varphi)$ is the cosmic-ray flux density per unit solid angle at a zenith angle ξ and azimuth φ, and $\rho(\xi,\varphi)$ represents the part of the plane which intercepts the cosmic-ray flux from the direction (ξ,φ) and gives triple coincidences.

In order to obtain seasonal variations in the intensity of cosmic rays, the results for the S-2 chamber and the semi-cubic telescope were converted into monthly averages. Radiation errors were avoided by confining the analysis to night data only. In order to increase the accuracy, four-hourly averages were taken over the times at which the atmosphere was sounded.

All cases of magnetic storms were excluded from the data in order to reduce errors due to non-meteorological effects. Comparability of the data was ensured by selecting only those data which corresponded to the simultaneous operation of the chamber and the telescope.

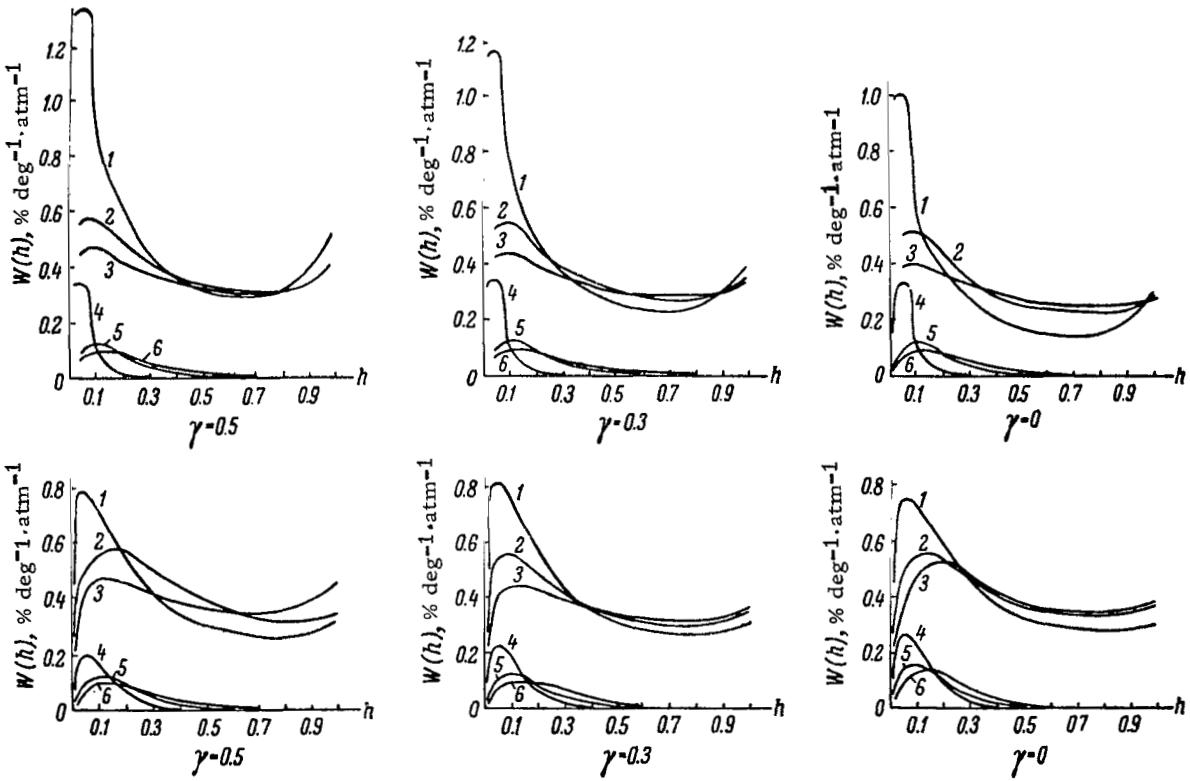

Fig. 1. $W_T(h)$ for a parallel beam of μ-mesons at the earth's surface:

The upper three curves correspond to $\Delta\epsilon = 0.28$ BeV (S-2 ionization chamber); μ-meson effect (opposite sign): 1 - $\gamma = 0.3$, 2 - $\gamma = 0.8$, 3 - $\gamma = 1.0$; π-meson effect: 4 - $\gamma = 0.3$, 5 - $\gamma = 0.8$, 6 - $\gamma = 1.0$. Lower three curves correspond to $\Delta\epsilon = 0.24$ BeV (semi-cubic telescope); μ-meson effect (opposite sign): 1 - $\gamma = 0.5$, 2 - $\gamma = 0.8$, 3 - $\gamma = 1.0$; π-meson effect: 4 - $\gamma = 0.5$, 5 - $\gamma = 0.8$, 6 - $\gamma = 1.0$.

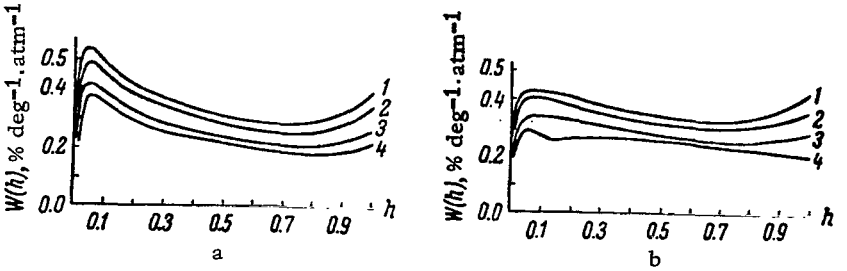

Fig. 2. The total temperature-coefficient density function for different γ:

a - for the S-2 ionization chamber with $\Delta\epsilon = 0.28$ BeV; b - for the semi-cubic telescope with 1 - $\gamma = 0.5$, 2 - $\gamma = 0.3$, 3 - $\gamma = 0.1$, 4 - $\gamma = -0.2$.

The atmospheric pressure and temperature data above the observational point were supplied by the Yakutsk Meteorological Station of the Yakutsk Hydrological and Meteorological Service.

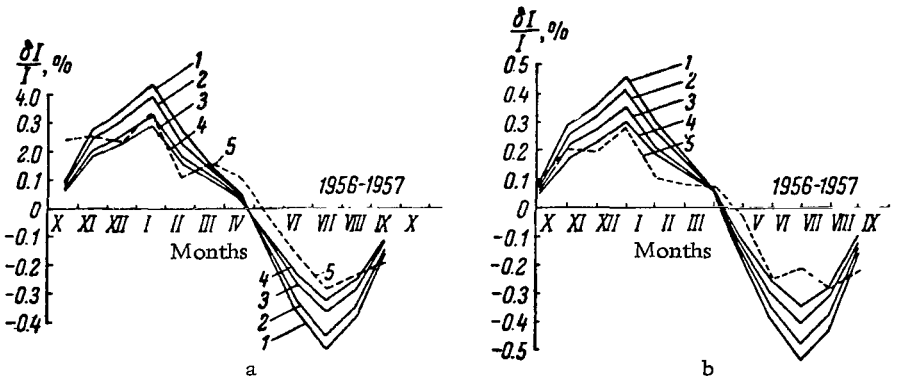

Fig. 3. Seasonal variations in the intensity of the μ-meson component:

a - S-2 ionization chamber with $\Delta\epsilon = 0.28$ BeV; b - semi-cubic telescope with $\Delta\epsilon = 0.24$ BeV. 1—4 - calculated seasonal variations with $\gamma = 0.5$, 0.3, 0 and 0.2 respectively; 5 - seasonal variations from experiment.

The mean hourly statistical accuracy for the telescope and the chamber was 0.37 and 0.30% respectively. The mean monthly error was 0.04 and 0.03%.

The barometer coefficient was found to be 0.13%/mb and 0.14%/mb for the telescope and chamber respectively.

Figure 3 shows the seasonal variations in the intensity of the μ-meson component for the telescope and the chamber, and also the expected variations calculated with the aid of the temperature-coefficient density functions in Fig. 2.

The following table shows the amplitudes of the first harmonics calculated from the seasonal variation curves and the expected variations for different γ.

Amplitudes of the first harmonic of the seasonal variations.

	Calculated variations				Observed variations	
	$\gamma = 0.5$	$\gamma = 0.3$	$\gamma = 0$	$\gamma = -02.$	Without secular correction	With secular correction
Semi-cubic μ-meson telescope	4.45±0.12	3.96±0.12	3.36±0.12	2.50±0.12	2.50±0.03	2.20±0.03
Ionization chamber (S-2)	4.15±0.12	3.70±0.12	3.05±0.12	2.36±0.12	2.63±0.03	2.19±0.03

It is evident from Fig. 3 and the table that the observed seasonal variations are much smaller than those expected for γ = 0.5, 0.3 and 0. The best agreement between theory and experiment is obtained for the semi-cubic telescope at γ = 0.3 and for the ionization chamber at γ = -0.2. The following are the possible disturbing factors which affect the seasonal variations.

1) secular variation due to the 11-year cycle of solar activity;

2) reduction in the intensity immediately after storms; these may not have been completely excluded owing to the considerable duration of some of the storms.

Comparison of the amplitudes of the seasonal variations before and after the introduction of the correction for the secular variation, showed that this correction had no effect on γ_{eff}.

During the period under consideration, the most intense storms were those of August and September 1957. Inadequate allowance for these storms may lead to a reduction in the mean monthly value during the minimum in the

seasonal variation, which in turn may give rise to an increase in the amplitude.

Since the effect of storms on the telescope was greater by a factor of ~ 1.3 than in the case of the chamber, the effect may give rise to a large reduction in the amplitude of the seasonal wave given by the telescope. This would correspond to a large reduction in the value of γ_{eff} for the telescope.

It is evident from the above discussion that γ_{eff} for the telescope and the ionization chamber has the same value to within experimental error. This result may be explained as follows. Variations in the μ-meson intensity are largely due to low-energy particles. Since the contribution of low-energy particles to the total ionization measured by the chamber is smaller than the contribution due to an equal number of high-energy particles, it follows that the ionization chamber is less sensitive to low-energy particles than the semi-cubic telescope, which is equally sensitive to particles of all the energies.

It follows that the energy spectrum deduced from the ionization may be "harder" than the energy spectrum deduced from the number of particles; i.e. the mean energy measured from the ionization is higher than the mean energy of the particles determined from the number of pulses. This will correspond to $\gamma_{eff}(\text{chamber}) < \gamma_{eff}(\text{telescope})$.

2. Since the chamber collects radiation from a larger solid angle than the telescope, the number of particles arriving obliquely in the chamber will be greater than in the telescope; according to [1] γ increases with increasing energy. This means that the chamber will record more energetic particles, for which γ increases with increasing energy, so that $\gamma_{eff}(\text{chamber}) > \gamma_{eff}(\text{telescope})$.

It is, therefore, evident that the resultant γ_{eff} represents a superposition of two effects, which act in opposite directions and may cancel out each other, thus leading to the same value for both the chamber and the telescope. Dorman [1] compared the altitude variation in the intensity of the μ-meson component with the calculated result for $\gamma = 1$ and $\gamma = 0$ and concluded that γ_{eff} lies between 0 and 1. In our calculations the best agreement between theory and experiment obtains when $\gamma_{eff} = -0.2 - 0.3$.

This can be explained by the fact that the low-energy particles are particularly sensitive to the temperature effect and the value of γ for them is small. Thus, the contribution to γ_{eff} due to the temperature effects is mainly due to low-energy particles, while the γ_{eff} for the altitude variation is an effective value for all energies.

3. It is pointed out in [6] that the difference in the directional properties of the chamber and the telescope may be responsible for the above difference

in the observed effects. In order to estimate this phenomenon, we have determined the coefficient of coupling with the π-meson spectrum for the hard component recorded by the ionization chamber and the telescope.

It is assumed in the calculations that the π-mesons are generated largely in the first two primary particle interactions. This corresponds to an average depth of about 100 mb. The mean path for the decay of a π-meson is

$$l=\frac{\tau_\pi^0 c\varepsilon_\pi}{m_\pi c^2},$$

where m_π, τ_π^0 is the mass and the lifetime of a π-meson at rest, and ε_π is the energy of the π-meson.

In grams, the free path for decay is given by

$$L_p=\frac{l\rho_0 h}{h_0}=\frac{\varepsilon_\pi \tau_\pi^0 c h \rho_0}{h_0},$$

where h is the pressure at the point where the decay occurs, and h_0 and ρ_0 are the pressure and density at sea level. For ε_π = 20 BeV and h = 100 mb the mean range is L_p = 10 g cm^{-2}, and hence the spread in the level at which the μ-mesons are produced may be neglected. The equation for the altitude variation can then be written in the form

$$\frac{\partial N_\mu(h,\ \varepsilon_\mu,\ \xi)}{\partial h}=\frac{\partial N_\mu(\varepsilon_\mu,\ h,\ \xi)}{\partial \varepsilon_\mu}\cdot\frac{a}{\cos\xi}-N_\mu(\varepsilon_\mu,\ h,\ \xi)R(\varepsilon_\mu,\ h,\ \xi), \qquad (1)$$

where ξ is the zenith angle, a is the specific ionization in air, and $R(\varepsilon_\mu, h, \xi)$ is the probability of decay of a μ-meson with energy ε_μ at the depth h.

In the case of an isothermal atmosphere

$$R(\varepsilon_\mu,\ h,\ \xi)\,dh=\frac{d\tau}{\tau}=\frac{dlm_\mu c^2}{c\tau_\mu^0\varepsilon_\mu}=\frac{m_\mu c^2 dh}{c\tau_\mu^0\rho(h)\varepsilon_\mu}=\frac{m_\mu c^2 h_0}{c\tau_\mu^0\rho_0}\cdot\frac{dh}{h\varepsilon_\mu}=\frac{A}{\varepsilon_\mu h}\,dh.$$

The solution of (1) is

$$N_\mu(\varepsilon_\mu,\ h,\ \xi)=\left\{\frac{h\varepsilon_\mu}{h_0\left[\frac{a}{\cos\xi}(h_0-h_1)+\varepsilon_\mu\right]}\right\}^{\frac{A}{ah_0+\varepsilon_\mu\cos\xi}} D\left[\frac{a}{\cos\xi}(h_0-h_1)+\varepsilon_\mu\right], \qquad (2)$$

where $h_1 = 100$ mb is the level at which the μ-mesons are generated, and $D(\varepsilon)$ is the differential μ-meson production spectrum and corresponds to the π-meson spectrum $D(\varepsilon_\pi)$ if the nuclear interaction of π-mesons is neglected.

Assuming that the fraction of the energy which is carried by μ-mesons in the decay of π-mesons is on the average $\alpha = 0.65$, we have

$$\varepsilon_\mu = \alpha\varepsilon_\pi - \frac{a}{\cos\xi}(h_0 - h_1).$$

Substituting this into (2) we have

$$N_\mu(\varepsilon_\pi, h, \xi) = \left\{ \frac{h_1\left[\alpha\varepsilon_\pi - \frac{a}{\cos\xi}(h_0 - h_1)\right]}{h_0\alpha\varepsilon_\pi} \right\}^{\frac{A}{\alpha\varepsilon_\pi\cos\xi + ah_1}} D(\varepsilon_\pi).$$

Integrating with respect to the angles with allowance for the directional properties of the instrument, we have

$$W_\mu(\varepsilon_\pi, h_0) = \int_0^{\xi(\varepsilon_\pi} I(\xi) N_\mu(\varepsilon_\pi, h_0, \xi)\, d\xi, \qquad (3)$$

where $I(\xi)$ is the directional characteristic for isotropic radiation and $\xi(\varepsilon_\pi)$ is the maximum zenith angle at which the μ-mesons emitted by disintegrating π-mesons with energies ε_π can pass through the screen of the instrument.

Normalizing $W_\mu(\varepsilon, h_0)$ so that

$$\int_0^\infty W_\mu(\varepsilon_\pi, h_0)\, d\varepsilon_\pi = 100\%,$$

we obtain the coefficient of coupling between the intensity recorded by the instrument and the π-meson spectrum.

The coupling coefficients for the ionization chamber and the semi-cubic telescope calculated from (3) are shown in Fig. 4.

If it is assumed that π-mesons with energies less than 10 BeV are responsible for the variations in the μ-meson component, then the amplitude of the variations recorded by the telescope will be larger by a factor of 1.30 ± 0.15 than for the chamber.

The above calculations are valid for an isothermal atmosphere. When the latter is replaced by the real atmosphere, there will be an increase in the

coupling coefficients in the low-energy region, owing to the smaller number of μ-meson decays in the layer between 100 and 500 mb.

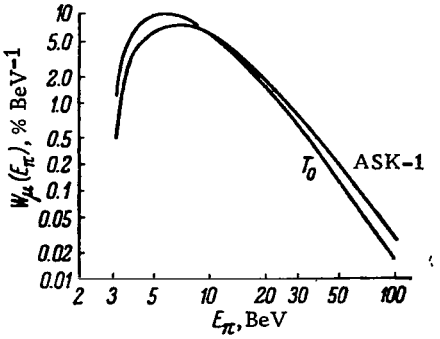

Fig. 4. Coupling coefficients $W_\mu(E_\pi)$ as functions of π-meson energy.

The maximum increase in the coefficients (roughly by a factor of 1.2) will occur at ε_π = 3—4 BeV. The change in the coupling coefficients will give rise to a change of less than ~0.03 in the ratio of the variation amplitudes for the telescope and the chamber.

The nuclear absorption of π-mesons, which has not been allowed for, would tend to increase the observed difference between the effects, but the correction for this phenomenon lies within the limits of error indicated above.

CONCLUSIONS

1. The magnitude of γ_{eff} in the π-meson production spectrum, as calculated from the altitude variation of the μ-meson intensity, does not reflect the true situation in the calculation of meterological coefficients.

2. The magnitude of γ_{eff} calculated from the seasonal variation in the cosmic-ray intensity is the same, to within experimental error, for the ionization chamber and the semi-cubic telescope.

3. The differences in the effects of storms and 27-day recurrences and diurnal variations on the cosmic-ray intensity recorded by the ionization chamber and the semi-cubic telescope may be explained by differences in the directional properties of these instruments.

The authors wish to express their gratitude to A.I. Kuz'min for his advice and a number of valuable suggestions.

REFERENCES

1. Dorman, L.I. Variatsii kosmicheskikh luchey (Cosmic ray variations), Gostekhizdat, Moscow, 1957.

2. Shafer, Yu.G. Dissertation, FIAN USSR, Moscow, 1950.

3. Kuz'min, A.I. and Yarygin, A.V. Tr. YaFAN SSSR, ser. fizich., No. 2, 34, 1958.

4. George, E. In the book: Progress in cosmic ray physics. Vol. 1, ed. J.G. Wilson, IL Moscow, 1954.

5. Dorman, L.I. DAN SSSR, 95, 49, 1954.

6. Kuz'min, A.I. Dissertation, NIYaF, MGU, Moscow, 1959.

Yu. G. Shafer and V. D. Sokolov

SEASONAL EFFECT IN THE INTENSITY OF COSMIC RAYS DEDUCED FROM MEASUREMENTS IN THE STRATOSPHERE

We have used the mean monthly values of the intensity at different pressure levels, deduced from stratospheric measurements for 1958, to estimate the seasonal effect in the intensity of cosmic rays. The intensity was measured by a counter telescope [1]. The figure shows the results of the analysis. As can be seen, the amplitude of the seasonal variation reaches 8% at the 300 mb level, and decreases with height reaching approximately 6% at the 60 mb level.

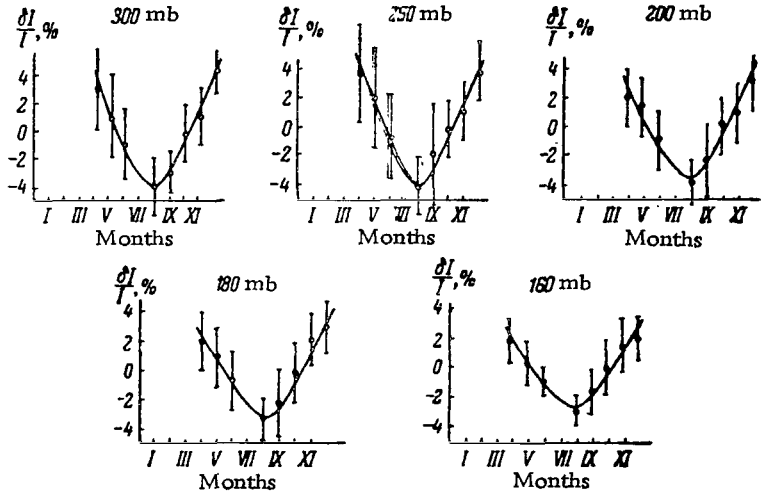

Fig. 1. Seasonal effect in the intensity of cosmic rays from measurements in the stratosphere.

This large amplitude of the seasonal variation apparently indicates the existence of a considerable contribution of low-energy μ-mesons and shower processes due to the change in the atmospheric density to the intensity of cosmic rays in the stratosphere. Both effects act in the same direction. Thus, in the summer,

the increase in the geometrical height of the atmosphere gives rise to an increase in the probability of the decay of the low-energy μ-mesons. This removes both the mesons themselves and their decay products (low-energy electrons) which are not recorded by the instrument. At the same time, the reduction in the density of the atmosphere is responsible for a reduction in the flux density of shower particles and therefore a reduction in the probability of random coincidences in the telescope. The opposite situation occurs in the winter.

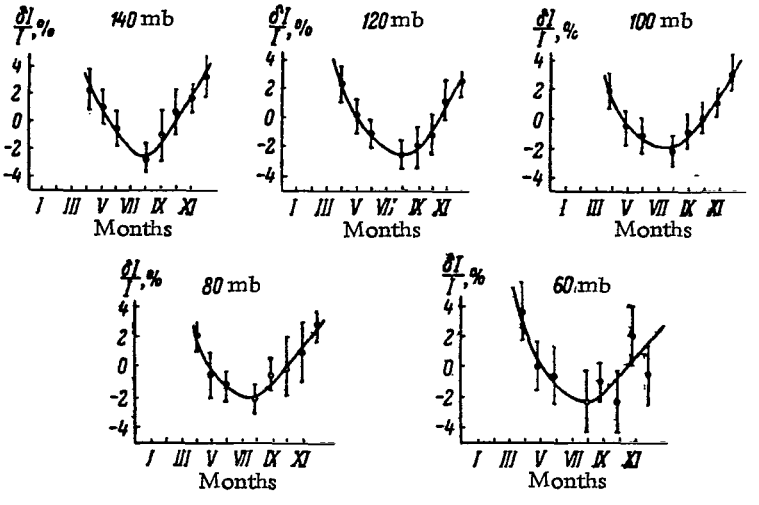

Fig. 2. Continuation of Fig. 1.

If the above mechanism for the seasonal effect in the stratosphere is in fact correct, or is largely correct, then it is to be expected that single counter measurements will not exhibit this phenomenon, or will show a very small effect, owing to the presence of a large background of radiation in the atmosphere.

The present note is only preliminary because the observational data for 1959-1960 are still to be processed.

REFERENCES

1. Belomestnykh, V.A. and Shafer, Yu.G. Tr. YaFAN SSSR, ser. fizich., No. 2, 47, 1958.

D.D. Krasil'nikov

A METHOD OF ALLOWING FOR GEOMETRIC EFFECTS IN THE EAS FREQUENCY VARIATIONS NEAR SEA LEVEL

1. The observed temporal variations in the frequency of extensive air showers may be due to both changes in the EAS size spectrum k(N), i.e. the total particle number spectrum in the shower, and a deformation of $\varphi(r)$, i.e. the spatial distribution function for EAS particles at the point of observation.

EAS frequency variations due to a deformation of $\varphi(r)$ at constant size spectrum k(N) are referred to as geometric effects. It is well known that deformations of the function $\varphi(r)$, and therefore the geometric effects in EAS, may be due to changes in the density of the atmosphere above the point of observation.

It is particularly important to allow correctly for the geometric effect when it is desired to estimate the magnitude of the changes in the size spectrum at the point of observation. Changes in the size spectrum have recently attracted considerable attention.

However, existing methods of correcting for the EAS geometric effects are not satisfactory [3—5].

2. The authors of [3, 4] have used general considerations on changes in the area of GM counters, the shower collection area, and the separation between the GM counters during changes in the atmospheric density above the point of observation, and showed that the geometric effects may be allowed for by means of the following formulas

$$\beta_T = -\left.\frac{2(\varkappa-1)-d}{T}\right|_{h=\text{const}}, \tag{1a}$$

$$\beta_h = -\left.\frac{2(\varkappa-1)-d}{h}\right|_{T=\text{const}}, \tag{1b}$$

where $\varkappa$ is the exponent in the density spectrum of the recorded showers, d is the exponent in the separation curve when it is fitted with an expression of the form $C(D) \sim D^{-d}$ and T and h are the temperature and pressure in the atmosphere respectively.

Without going into details of the accuracy of this method of allowing for geometric effects, it is possible to show that these formulas are inconvenient in practice. It is well known that geometric effects are small, while it is very difficult to determine the magnitudes of $\varkappa$ and d accurately for a given apparatus used for the determination of EAS frequency variations. This requires very laborious additional experiments. Moreover, it should be noted that the above workers do not indicate precisely the T, $\varkappa$ and d which should be employed.

It is therefore not surprising that when these formulas are employed to estimate the expected geometric effects [6], a considerable discrepancy is found between the calculated and the experimental results. Thus the expected magnitude of $2(\varkappa-1)$ - d turned out to be 0.5 for a separation of D_1 = 5 m and 0.1 for D_2 = 80 m, while the experimental values were 0.35 and -0.13.

Cranshaw and Galbraith [5] used an approach similar to that employed in [3-4] and tried to simplify further the determination of the geometric effect in the analysis of the barometer coefficient of EAS. They consider that it is possible to introduce a temperature equivalent for the pressure changes with the aid of the gas laws using the expressions

$$\frac{\delta\rho}{\rho}=\frac{\delta h}{h}\Big|_{T=\text{const}} \text{ and } \frac{\delta\rho}{\rho}=-\frac{\delta T}{T}\Big|_{h=\text{const}},$$

and hence $\delta h=-\frac{h}{T}\delta T$. Since the contribution to the barometer coefficient which is due to the geometric effect (at constant temperature) is

$$\beta_h=\frac{1}{C}\cdot\frac{\delta C}{\delta h},$$

where C is the number of showers per unit time, it follows that

$$\beta_h=-\frac{1}{C}\cdot\frac{T}{h}\cdot\frac{\delta C}{\delta T}=-\frac{T}{h}\beta_T\simeq-4\beta_T, \tag{2}$$

where T is in °K and h is in centimeters of mercury.

Next, they define the true EAS barometer coefficient at sea level by

$$\alpha_h=B-\beta_h=B+4\beta_T, \tag{3}$$

where B is the observed barometer coefficient. In this expression, the geometric correction $4\beta_T$ is deduced not from real changes in the temperature during the observation, but after the barometer coefficient B has been determined as a single correction to the final result. The temperature itself is

assumed to be constant, and $4\beta_T$ is used only as an equivalent quantity in the determination of the change in the density (and therefore the geometric effect) during changes in the pressure.

The above method of estimating geometric effects (in the determination of barometer effects) is of doubtful validity:

1) In the real atmosphere, pressure changes at the point of observation are always accompanied by changes in the air temperature [7], and therefore the geometric effect cannot be simply reduced to β_h;

2) In the most important cases of meteorological processes, the changes in the temperature and pressure in the troposphere have different signs, and this should lead to a much smaller geometric correction than is indicated by equation (2), i.e.

$$|\beta_h \delta h + \beta_T \delta T| < |\beta_h \delta h|.$$

The conclusion reached in [5] that the particle absorption coefficient in the shower is independent of the size of the EAS must therefore also be regarded as of doubtful validity. Our own results for the barometer coefficient of EAS of different sizes have led us to a different conclusion [7, 8].

Assuming that the ground layer of the atmosphere governs the form of the spatial distribution of EAS particles [2], it was shown in a recent paper [9] that the geometric effect of the temperature may be calculated from

$$\beta_T = -\frac{2(\varkappa - 1) - d}{T_{h-100}},$$

where T_{h-100} is the temperature at h -100 mb where h is the pressure at the point of observation.

Here we must note the following points:

1) In the real situation, the atmospheric layer which governs the form of the spatial distribution of EAS particles will be thicker than h - 100 mb [10].

2) The temperature at a particular level of pressure cannot be representative of the entire layer under consideration.

However, it is evident that all the above methods of allowing for the geometric effect in EAS frequency near sea level are either insufficiently accurate or are inconvenient in practice.

Below, we propose a different method for estimating the geometric effects in the EAS frequency, which is based on the variation of the shower function with the height of the atmospheric layer at constant EAS size spectrum.

3. It follows from the altitude variation of the form of the spatial distribution $\varphi(r)$ that the parameter R which characterizes this function is related to the atmospheric density by

$$R(\rho) \sim \frac{1}{\rho},$$

but $\rho \sim h/T$ or $\rho \sim H^{-1}$, where H is the height in meters of the atmospheric layer, for example, h - 100 mb, h - 200 mb, or in general, the mean height in the lower half of the atmosphere (T is the temperature of the layer in °K and h is the atmospheric pressure at the point of observation). It may, therefore, be assumed that $R(H) = R(H_0)\ (H/H_0)$, where $R(H_0) = 55$ m for our point of recording of the EAS, and H_0 is the mean height of the layer under consideration.

The choice of H as an indicator of the density of air, and therefore the parameter R, is due to the fact that: (1) H is related to the integrated (over the entire layer) change in the atmospheric density and is therefore a more representative characteristic than the separate value of T or h, and (2) the use of H avoids the consideration of the complicated relation between changes in h and T in the case of real meteorological processes. The values of H may be deduced from aerological sounding data.

The shower recording function, i.e. the frequency of shower coincidences of multiplicity n for a counter group area σ per unit of time is given by

$$C(n, \sigma, H) = \int_0^\infty k(N)\,dN \iint_{(S)} W[N, n, \sigma, \varphi(r_1, H), \ldots, \varphi(r_n, H)]\,dS, \qquad (4)$$

where k(N)dN is the differential size spectrum (number of particles) of the global EAS intensity, $W[N, n, \sigma, \varphi(r_1, H), \ldots, \varphi(r_n, H)]$ is the probability of recording by the given apparatus of a shower with N particles, whose axis passes through the element of area dS and

$$\varphi(r, H) = \begin{cases} 2.18 \cdot 10^{-3} \frac{H_0}{H} r^{-1} e^{-\frac{r}{55} \cdot \frac{H_0}{H}} & \text{with } r \leqslant 100, \\ 0.56 \left(\frac{H}{H_0}\right)^{0.6} r^{-2.6} & \text{with } r > 100, \end{cases}$$

where $r_1, \ldots, r_n$ are the distances of the corresponding groups of counters from the axis.

The shower-frequency variation coefficient, due to the change in the radius of the shower alone which occurs as a result of a change in the height of the layer next to the point of observation, H, i.e. the geometric coefficient for the EAS frequency, can be found by varying the function C(n, σ, H) with respect to H:

$$\frac{\partial C(n,\sigma,H)}{\partial H}=\int_0^\infty k(N)\,dN\,\frac{\partial}{\partial H}\iint_{(S)} W[N,\ n,\ \sigma,\ \varphi(r_1,\ H),\ \ldots,\ \varphi(r_n,\ H)]\,dS=$$

$$=\int_0^\infty k(N)\,dN\iint_{(S)}\left\{\frac{\partial W}{\partial\varphi(r_1,\ H)}\cdot\frac{\partial\varphi(r_1,\ H)}{\partial H}+,\ \ldots,\right.$$

$$\left.\ldots+\frac{\partial W}{\partial\varphi(r_n,\ H)}\cdot\frac{\partial\varphi(r_n,\ H)}{\partial H}\right\}dS, \tag{5}$$

$$\frac{\partial\varphi(r_i,\ H)}{\partial H}=\frac{\partial\varphi(r_i,\ H)}{\partial R}\cdot\frac{\partial R}{\partial H}\simeq$$

$$\simeq\begin{cases}-1.82\cdot10^{-2}\,\dfrac{\varphi(r_i,\ H_0)}{H_0}\,(55-r_i) & \text{when } r_i\leqslant 100\text{ м},\\[2ex] 0.6\,\dfrac{\varphi(r_i,\ H_0)}{H_0} & \text{when } r_i>100\text{ м}.\end{cases}$$

The height H_0 may be identified, for example, with the mean height of the h - 100 mb layer. In our case it is equal to 930 m. In the case of three-fold coincidences, we can neglect in our data the separation of the counters (D_1 = 3.8 m), so that with H_0 = 930 m we have

$$\frac{\partial C(3;\ \sigma,\ H)}{\partial H}\simeq 6\pi\sigma\int_0^\infty k(N)\,dN\left\{-4.25\cdot10^{-8}N\int_0^{100}[1-e^{-N\varphi(r,\ H_0)\sigma}]^2\times\right.$$

$$\left.\times\,e^{-N\varphi(r,\ H_0)\sigma-\frac{r}{55}}(55-r)\,dr+3.61\cdot10^{-4}N\int_{100}^\infty[1-e^{-N\varphi(r,\ H_0)\sigma}]^2 r^{-1.6}\,e^{-N\psi(r,H_0)\sigma}dr\right\}. \tag{6}$$

Similarly, for six-fold coincidences (D_2 = 57 m) we have

$$\frac{\partial C(6;\ \sigma,\ H)}{\partial H}\simeq 3\sigma\int_0^\infty k(N)\,dN\iint_{(S)}\left\{[1-e^{-N\varphi(r_1,\ H_0)\sigma}]^2[1-e^{-N\varphi(r_2,\ H_0)\sigma}]^3\times\right.$$

$$\times\,e^{-N\varphi(r_1,\ H_0)\sigma}N\frac{\partial\varphi(r_1,\ H)}{\partial H}+[1-e^{-N\varphi(r_1,\ H_0)\sigma}]^3[1-e^{-N\varphi(r_2,\ H_0)\sigma}]^2\times \tag{7}$$

$$\left.\times\,e^{-N\varphi(r_2,\ H_0)\sigma}N\frac{\partial\varphi(r_2,\ H)}{\partial H}\right\}dS.$$

It is evident that the sign of the geometric effect changes at distances from the axis of the shower r > 55 m.

According to our measurements, one can use the following EAS size spectrum

$$k(N)\,dN = \begin{cases} AN^{-2.40}dN & \text{with } N < 10^5. \\ BN^{-2.70}dN & \text{with } N > 10^5. \end{cases}$$

The geometric coefficient, in percent, is then given by

$$\alpha_r(n,\ \sigma)\,\%\cdot \text{м}^{-1} = \frac{100}{C(n,\ \sigma,\ H_0)} \cdot \frac{\partial C(n,\ \sigma,\ H)}{\partial H}\ .$$

The calculated values of this coefficient for our measurements are given in the Table below.

$C(n\ \sigma)$	$D_1 = 3.8$ м			$D_2 = 57$ м		
	$C(3;\ 1.0)$	$C(3;\ 0.5)$	$C(3;\ 0.17)$	$C(6;\ 1.0)$	$C(6;\ 0.5)$	$C(6;\ 0.17)$
$\alpha_r(n,\ \sigma)\,\%\cdot \text{м}^{-1}$	—0.059	—0.073	—0.093	0.013	0.010	0.008

Comparison with experimental data shows that the values of $\alpha_r(n,\ \sigma)$ are in good agreement with the true geometric effects both in sign and in the order of magnitude.

Thus, if it is assumed that all the change δH is due only to the change δT in the atmospheric layer under consideration (lower half), then $\alpha_r(3;\ 1.0)$ and $\alpha_r(6;\ 1.0)$ correspond to temperature coefficients of -0.21% and +0.05% per °K, since

$$\beta_T = \frac{100}{C} \cdot \frac{\partial C}{\partial T} = \frac{H}{T}\alpha_r.$$

If on the other hand one starts with our measurements of $\bar{x}$ and $\bar{d}$ [11] and calculates the temperature coefficient from (1a), then it is found that

$$\beta_T(3;\ 1.0) = -\frac{2 \cdot 1.45 - 2 - 0.15}{260} \cdot 100 = -\frac{75}{260} = -0.29\,\%\ \text{per } 1°\text{K}$$

and

$$\beta_T(6;\ 1.0) = -\frac{2 \cdot 1.58 - 2 - 1.25}{260} \cdot 100 = \frac{9}{260} = 0.035\,\%\ \text{per } 1°\text{K}.$$

The method for allowing for geometric effects which is recommended above does require preliminary calculations but is convenient in practical applications. It does not require laborious additional experiments.

I should like to thank M. A. Nifontov and F. K. Shamsutdinova who assisted in the numerical integration.

REFERENCES

1. Euler, H. Zs. f. Phys., 116, 73, 1940.

2. Daudin, A. and Daudin, J. J. Phys. Rad., 10, 394, 1949.

3. Janossy, L. Cosmic rays, Foreign Literature Press, Moscow, 1949.

4. Hodson, A. L. Proc. Phys. Soc. (London), A64, 1061, 1951.

5. Cranshaw, T. E. and Galbraith, W. Nuovo Cimento, Supplement, 8, No. 2, 571, 1958.

6. Daudin, A. and Daudin, J. J. Atm. Terr. Phys., 3, 245, 1953.

7. Janossy, L., Sandor, T. and Somogyi, A. Nuovo Cimento, Supplement, 8, No. 2, 701, 1958.

8. Krasil'nikov, D. D. Tr. YaFAN SSSR, ser. fizich., No. 3, 65, 1960.

9. Krasil'nikov, D. D. Proc. International Conference on Cosmic Rays, II, 188, 1960.

10. Herlofson, N. The Oxford Conference on Extensive Air Showers, p. 46, April, 1956.

11. Krasil'nikov, D. D., Yefimov, N. N., Nifontov, N. A. and F. K. Shamsutdinova. Tr. YaFAN SSSR, ser. fizich., No. 4, 20, 1961.

G. F. Krymskiy

ON THE PROBLEM OF MULTIPLICITY

1. The relation between the secondary components and the primary flux must be known before the energy spectrum of primary cosmic-ray variations can be determined. This relation is determined by the contribution of different energies in the primary spectrum to the given component.

The contribution due to different energies of the primary spectrum is proportional to $D(E)m^i(E, h_0)$ where $D(E)$ is the differential spectrum of the primary flux and $m^i(E, h_0)$ is the multiplicity for the component of type i at the recording level h_0 and shows how many particles belonging to a given component, which are produced by a single primary particle of energy E, will reach the level at which the recording is carried out. The function which represents this contribution is called the coefficient of coupling [1] (usually normalized to 100%). It is given by

$$W^i(E, h_0) = \frac{D(E)\, m^i(E, h_0)}{N^i(h_0)}$$

The coefficients of coupling may be used to determine variations in the primary spectrum from variations in the various components. In the energy region $E \lesssim 15$ BeV, the coupling coefficients may be determined from the latitude effect. The values of the coefficients are extrapolated to energies greater than 15 BeV by means of matching and normalization conditions.

The extrapolated coefficients are not very reliable in the high energy range, and are not in agreement with the coefficients calculated from the intensity versus depth relation [2].

2. The variation of the coefficients is known when the variation of the multiplicity $m^i(E, h_0)$ has been determined. Some information about the multiplicity of the μ-meson component can be obtained from the form of the primary

spectrum, D(E), and the spectrum of the recorded μ-mesons, $N_\mu(E_\mu)$, by using certain assumptions about the production of the μ-meson component.

Let $w(E, E_\mu)dE_\mu$ be the probability that a particle produced by a primary particle of energy E has an energy between E_μ and $E_\mu + dE_\mu$ at the detector. The number of μ-mesons due to primary particles with energies between E and E + dE which reach the detector is D(E)m(E)dE. Of these,

$$dN_\mu(E_\mu)\,dE_\mu = D(E)\,m(E)\,w(E, E_\mu)\,dE\,dE_\mu \tag{1}$$

have energies between E_μ and $E_\mu + dE_\mu$.

In order to obtain the number of all the μ-mesons which reach the detector with energies between E_μ and $E_\mu + dE_\mu$ the expression given by (1) must be integrated over the entire primary spectrum between $f(E_\mu)$ and ∞, where $f(E_\mu)$ is the lower limit of the primary spectrum at which μ-mesons with energies E_μ still reach the detector. Thus, /58

$$N(E_\mu)\,dE_\mu = \int_{f(E_\mu)}^{\infty} D(E)\,m(E)\,w(E, E_\mu)\,dE\,dE_\mu.$$

On cancelling dE_μ, we have the following expression for the differential spectrum of the μ-mesons

$$N(E_\mu) = \int_{f(E_\mu)}^{\infty} D(E)\,m(E)\,w(E, E_\mu)\,dE. \tag{2}$$

Suppose now that the average fraction of energy of the primary particle carried by the meson is independent of the primary energy. If it is further assumed that the elementary interaction remains essentially unaltered in the energy range 10^{10}-10^{12} eV, then the probability function will depend only on the ratio E_μ/E:

$$w(E, E_\mu) = r w_1\left(\frac{E_\mu}{E}\right). \tag{3}$$

The lower limit of the primary spectrum will then be

$$f(E_\mu)=\frac{E_\mu}{K}, \tag{4}$$

where K is a constant which is less than unity. The probability w will be identically zero when $E'_\mu/E \geq K$. The normalization factor r is defined by

$$\int_0^{KE} w(E,\ E_\mu)\,dE_\mu = r\int_0^{KE} w_1\left(\frac{E_\mu}{E}\right)dE = rEa = 1,$$

and hence r = 1/aE where a is a constant.

The primary differential spectrum for energies in the range 10^{10}-10^{12}eV may be written in the form [3]

$$D(E)\sim E^{-\delta_{\text{eff}}}, \tag{5}$$

where $\delta_{\text{eff}} = 2.5$-$2.8$.

We shall write the multiplicity in the form

$$m(E)\sim E^{\beta}. \tag{6}$$

Substituting (3)-(6) into (2) we have the following differential spectrum for the μ-mesons

$$N_\mu(E_\mu)=c\int_{\frac{E_\mu}{K}}^{\infty} E^{-\delta_{\text{eff}}+\beta-1} w_1\left(\frac{E_\mu}{E}\right)dE;$$

Finally, substituting $t = E_\mu/E$ we have

$$N_\mu(E_\mu)=c_1 E_\mu^{-\delta_{\text{eff}}+\beta}.$$

Experiment shows that the differential μ-meson spectrum is of the form [3]

$$N_\mu(E_\mu)\sim E_\mu^{-\gamma}, \text{where}\ \gamma = 2.8\text{—}3.2.$$

Hence, $\beta = \delta_{\text{eff}} - \gamma$.

3. It might be thought that the latter expression can be used to determine the exponent β. However, the above assumption that the fraction of primary energy per meson is constant is not sufficiently precise, since it is in conflict with the increase in the number of mesons with increasing energy of the generating particles. The meson production multiplicity increases with primary energy in proportion to E^{λ} where $\lambda = 0.25$ [4].

Since the average fraction of energy transmitted to the mesons in a single interaction remains constant [5], it follows that the average fraction of primary energy per meson falls off as $\sim E^{-\lambda}$.

If the meson production mechanism remains essentially the same in the energy range under consideration, then it may be assumed that the probability function will depend on $E_\mu/E^{1-\lambda}$. The normalized probability function will then be of the form

$$w(E, E_\mu) = \frac{w_1\left(\frac{E_\mu}{E^{1-\lambda}}\right)}{E^{1-\lambda}},$$

and vanishes when

$$\frac{E_\mu}{E} \geqslant kE^{-\lambda}.$$

The lower limit of the primary spectrum for energy E_μ will be $E_\mu/kE^{-\lambda}$. The differential spectrum of the μ-mesons will then be

$$N_\mu(E_\mu) = c \int_{\frac{E_\mu}{kE^{-\lambda}}}^{\infty} E^{-\delta_{\text{eff}}+\beta-1+\lambda} w_1\left(\frac{E_\mu}{E^{1-\lambda}}\right) dE;$$

Finally, substituting $t = E_\mu/E^{1-\lambda}$ we have

$$N_\mu(E_\mu) = c_1 E_\mu^{\frac{-\delta_{\text{eff}}+\beta+\lambda}{1-\lambda}} = c_1 E_\mu^{-\gamma}.$$

On equating the exponents and rearranging, we obtain the following expression for the exponent in dependence of the multiplicity on energy:

$$\beta = \delta_{\text{eff}} - \gamma + \lambda(\gamma - 1). \tag{7}$$

Assuming that δ_{eff} and γ are respectively equal to 2.8 and 3.2, we find that $\beta \approx 0$, i.e., the multiplicity is independent of energy.

If the number of interactions per primary particle increases with energy, then there should be a slower increase in the average meson energy and an increase in λ. In order to estimate the effect of the number of interactions we may

assume that the coefficient of inelasticity is 0.5, the recoil nucleon carries off a negligible fraction of energy, and only nucleons give rise to interactions which are effective for the recording of μ-mesons.

Estimates carried out for this model showed that as the number of inelastic interactions produced by the primary particle increases by an order of magnitude, the average energy of the secondary particles decreases by a factor of 2-3. The reduction in the average energy of the secondary particles will be smaller still when it is recalled that the interactions of high energy particles become ineffective, beginning with a certain depth, because of the production of μ-mesons as a result of the nuclear absorption of π-mesons in the dense lower layers of the atmosphere. Since at energies of 10^{10}-10^{12} eV the number of cascades will apparently be of the same order of magnitude, it follows that the variation in the average energy of the mesons with the number of cascades need not be taken into account.

If it is assumed that the multiplicity is proportional to the energy, then provided the fraction of energy transmitted to the mesons remains constant, it follows from (7) that the number of mesons produced per elementary interaction should be approximately proportional to $E^{0.7}$, which is in contradiction with both theoretical and experimental data.

The multiplicity may also be approximately proportional to E if the number of mesons produced per elementary interaction does not increase faster than $E^{0.25}$, but the average fraction of energy transmitted to the mesons per interaction will then be $\sim E^{-(0.4-0.5)}$. This is also in apparent contradiction with existing data about the elementary interaction [5].

4. The suggested increase in the multiplicity can be made to agree both with theory and experiment if it is assumed that the π-mesons multiply during collisions with air nuclei.

Thus, suppose that there exists a minimum energy $E_{\pi}^{\min}$ below which the π-mesons cannot multiply. Then, even if one neglects π-meson losses through the formation of nuclear fragments and the conversion of a part of the energy into the soft component through π^0-mesons, it is found that the number of π-mesons produced by a single primary particle of energy E is

$$N_{\pi}(E) = \frac{a}{E_{\pi}^{\min}} E,$$

where α is the fraction of primary energy transmitted to the mesons. It follows that the multiplicity is approximately proportional to E. When the conversion of energy into the soft component and losses due to star formation are allowed for, the increase with energy is slower still.

Thus, it turns out that in the energy range 10^{10}-10^{12} eV the multiplicity is approximately proportional to E^{β} where $0 < \beta < 1$.

With increased screening of the detector, the effective exponent β should increase owing to the removal of low energy mesons.

In conclusion, I should like to express my gratitude to Candidate of Physicomathematical Sciences, A. I. Kuz'min for his help and interest in this work.

REFERENCES

1. Dorman, L.I. Variatsii kosmicheskikh luchey (Cosmic-ray variations). Gostekhizdat, Moscow, 1957.

2. Kuz'min, A.I. Dissertation, NIYaF MGU, Moscow, 1959.

3. Progress in cosmic ray physics. Vol. 1, ed. by J.G. Wilson, IL, 1954.

4. Landau, L.D. Izv., AN SSSR, ser. fizich., 17, 51, 1953.

5. Grigorov, N.L. and Murzin, V.S. Izv., AN SSSR, ser. fizich., 17, 21, 1953.

A.I. Kuz'min

THE CONTRIBUTION OF THE UPPER ATMOSPHERE TO SMALL EFFECTS IN THE HARD COMPONENT OF COSMIC RAYS DURING CHROMOSPHERIC FLARES

1. Five large sudden increases in the cosmic-ray intensity, N, which were associated with particularly large chromospheric flares, were observed during the last twenty years. These increases were detected by many stations, and the last two of them were also recorded at the Yakutsk station. However, chromospheric flares are not rare occurrences, and hence many authors [1, 2] have investigated the effect of small chromospheric flares on the intensity of cosmic rays. It was established that during daytime radio fadeouts, the intensity of the hard component increases by $0.3 \pm 0.06\%$ [1], but no changes in N are observed during radio fadeouts at night. According to [2], the effect of small solar flares on the intensity of the neutron component gives rise to an effect with an amplitude of $0.6 \pm 0.15\%$. Analysis of these results given in [3] shows that cosmic-ray particles with energies less than or approximately equal to 10 BeV are generated in practically all chromospheric flares, and that the increases in the intensity of the hard component must be of a different origin.

One of the possible reasons for the increased intensity of the hard component at sea level [4] may be due to the reduction in the temperature of the ozone layer, which is associated with the increase in the ultraviolet flux during a solar flare. This possibility has recently been verified as a result of the continuous recording of the hard component at sea level [5].

More direct data on the change in the temperature of the ozone layer during solar flares may be obtained as a result of composite ground and underground measurements of the hard component of cosmic rays [6].

The aim of the present paper is to estimate the importance of the upper atmosphere in the effect of small solar flares, using the data obtained as a result of continuous recording of the hard component of cosmic rays by ground-level and underground apparatus during 1957-1959.

2. The energy characteristics of cosmic-ray variations were investigated at the Yakutsk laboratory with the aid of triple-coincidence counter telescopes at

ground level and at depths of 7, 20 and 60 meters of water equivalent [4]. This apparatus has been used since February 1957 in continuous measurements of the intensity of the hard component of cosmic rays.

A theoretical analysis [3] of the meteorological effects in the case of the two-meson theory of the generation of the hard component shows that the density function for the negative temperature effect falls off rapidly with depth, while the density function for the positive temperature coefficient increases with depth. These results were confirmed experimentally in [7] but in that paper the temperature coefficients were estimated only approximately. Figure 1 shows the results of the calculations [6] using the exact formulas given in [3] for the density function of the temperature coefficient for our system of telescopes. In distinction from [3, 7], in the present calculations the density functions of the temperature coefficient for fractional values of the effective exponent in the μ-meson spectrum were obtained directly by calculation, while in [3, 7] the densities for fractional γ were obtained by interpolation.

It is clear from Figure 1 that the total density function of the temperature coefficient for the semi-cubic telescope varies appreciably with depth. Thus, if the total density function of the temperature coefficient in the atmosphere remains negative, then the positive effect in the upper atmosphere due to the competition between the decay and capture of π-mesons is predominant even at depths of 60 m of water equivalent.

Thus, if the reduction in the temperature of the ozone layer does, in fact, take place during small chromospheric flares, then the intensity of the hard component at the ground level and underground at a depth of 60 m water equivalent should exhibit opposite effects.

Following Elliot [1], we have used shortwave radio fadeouts as indicators of chromospheric flares. The onset of a radio fadeout as given by the Yakutsk ionospheric station, corresponds to zero values in Chree's scheme. Moreover, the table includes six preceding and six subsequent hours. During the entire period there were 87 radio fadeouts between 0900 and 1600 hrs local time. The intensities corrected for the barometer effect were averaged, and the average diurnal variation was subtracted from the result [6, 8].

Figure 2 shows the final results. It is evident that no appreciable changes in the intensity of the μ-mesons at ground level and at 7, 20 and 60 m of water equivalent below ground were observed (to within experimental error) during and after the shortwave fadeouts. If it is assumed that the effect in the intensity of the μ-mesons at the earth's surface was 0.05% then, according to Figure 1, the expected oscillation in the mean temperature of the 0-25 mb layer is $t(0\text{-}25) = 0.05 : 0.01 \approx 5°$.

Such temperature changes could, according to the density function of the temperature coefficient (the 10-15 layer), give rise to opposite changes in the underground intensity at a depth of 60 m of water equivalent, with an amplitude

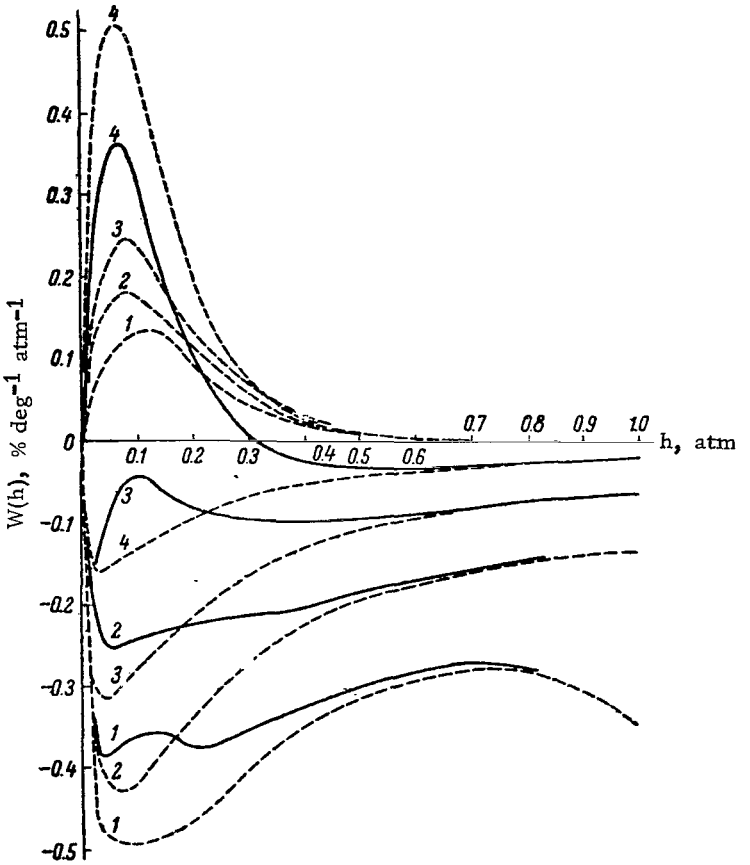

Fig. 1. Density function of the temperature coefficient for the semi-cubic telescope:

1 — at the earth's surface, 2 — at a depth of 7 m water equivalent, 3 — at a depth of 20 m water equivalent, 4 — at a depth of 60 m water equivalent. Dashed curves — $W_{\mu}(h)$ or $W_{\pi}(h)$ - negative (μ-meson) or positive (π-meson) effects; continuous lines — $W_T(h) = W_{\mu}(h) + W_{\Omega}(h)$.

of about 0.07%. It is clear from Figure 2 that the effect in the intensity of the hard component at the depth of 60 m of water equivalent is absent to within 0.1%. Hence, the above estimate of the temperature oscillation in the 0-25 mb layer may be regarded as the maximum possible temperature change in the ozonosphere during 1957-1959.

It should be noted that this estimate is consistent with the results of an analysis of continuous measurements of the hard component between 1955 and 1956 which were reported by Kaminer [5].

4. In order to verify the existence of the effect of small solar flares during maximum solar activity, we have analyzed a number of radio fadeouts with allowance for the zones of incidence. The data were analyzed by the method of superposition of epochs when Yakutsk was inside and outside the zone of incidence respectively. This analysis was based on the zone of incidence calculations given by Kaminer [9].

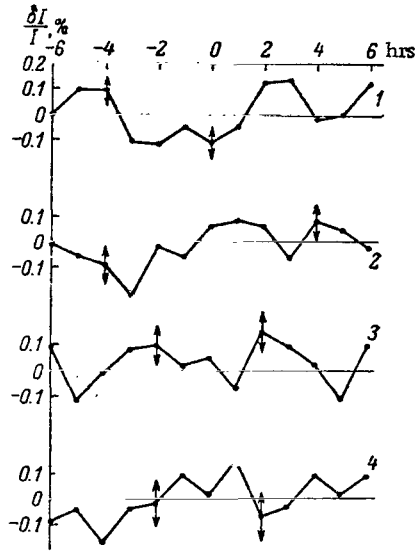

Fig. 2. Dependence of cosmic-ray intensity on small chromospheric flares in daytime (0900-1600 hrs local time) in 1957-1959.

1-4 — semi-cubic telescope at ground level and at 7, 20 and 60 m water equivalent respectively.

Altogether there were 37 cases of radio fadeout when Yakutsk was within the zone of incidence, and 38 cases when it was outside this zone. The correction for the diurnal effect in the intensity was introduced for each day separately.

The results of the analysis are shown in Figure 3 from which it is evident that in both cases, i.e., whether Yakutsk was inside or outside the zone of incidence, there were no noticeable changes in the intensities of the neutron and hard components at any time. The absence of an appreciable effect of small flares in the intensity of the neutron component during maximum solar activity is in agreement with the results obtained by Lockwood [10] and Dzhemel'di et al. [11].

Thus, it may be concluded that during the period of maximum solar activity the effect of small flares, due to the direct generation of low-energy particles, is absent.

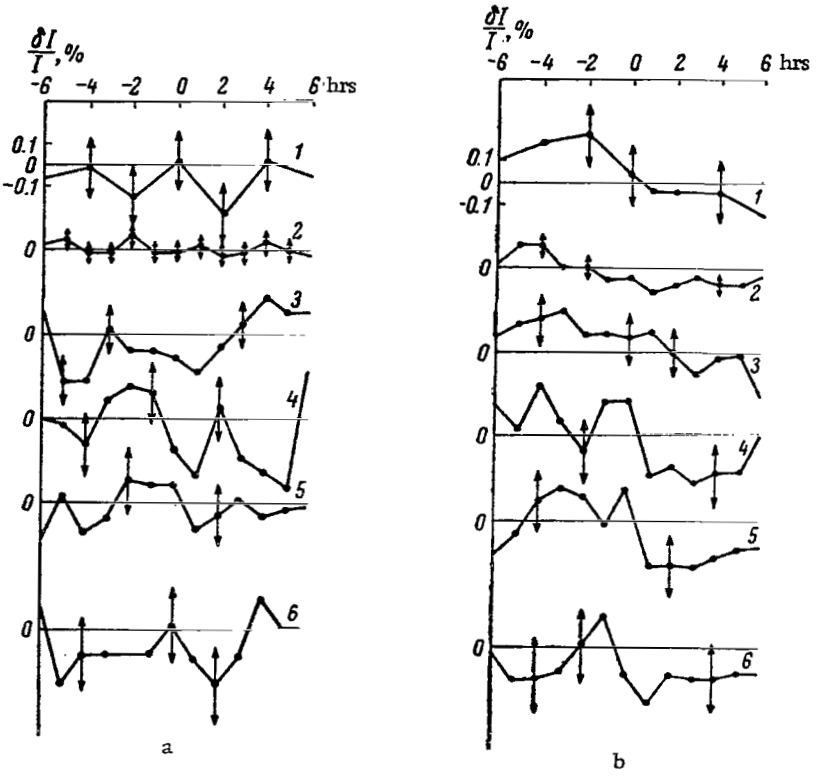

Fig. 3. Dependence of the intensity of cosmic-rays on small chromospheric flares, with allowance for the zones of incidence in 1957-1959:

a — inside the zone, b — outside the zone. 1 — neutron monitor, 2 — ionization chamber, 3-6 — semi-cubic telescope at ground level and at depths of 7, 20 and 60 m water equivalent respectively.

In conclusion, we list the main results of this work.

1. No appreciable changes in the average temperature of the ozonosphere are observed during shortwave radio fadeouts. The maximum average changes in the temperature of the ozonosphere in 1957-1959 during small chromospheric flares did not exceed 5°.

2. In 1957-1959 no appreciable changes were observed in the intensity of cosmic rays at the earth's surface during small chromospheric flares.

REFERENCES

1. Dolbear, D., Elliot, H. and Danton, D. J. Ter. Phys., 1, 187, 1951.

2. Firor, J. Phys. Rev., 94, 1017, 1954.

3. Dorman, L.I., Kuz'min, A.I., Tyanutova, G.V., Shafer, Yu.G. and Feynberg, Ye.L. ZhETF, 26, 537, 1954.

4. Dorman, L.I. Variatsii kosmicheskikh luchey (Cosmic ray variations). Gostekhizdat, Moscow, 1957.

5. Kaminer, N.S. Tr. YaFAN SSSR, ser. fizich., No. 3, 92, 1960.

6. Kuz'min, A.I. Dissertation, NIYaF MGU, 1959.

7. Kuz'min, A.I. and Danilov, A.A. Tr. YaFAN SSSR, ser. fizich., No. 3, 58, 1960.

8. Kuz'min, A.I. Tr. YaFAN SSSR, ser. fizich., No. 3, 99, 1960.

9. Kaminer, N.S. Tr. YaFAN SSSR, ser. fizich., No. 3, 148, 1960.

10. Towell, L.C. and Lockwood, J.A. Phys. Rev., 113, 64, 1959.

11. Dzhemel'di, et al. International Conference on Cosmic Rays, Mowcow, p. 223, 1959.

PART III

MAIN PROPERTIES AND NATURE OF VARIATIONS IN THE INTENSITY OF COSMIC RAYS

A.I. Kuz'min and G.V. Skripin

UNDERGROUND VARIATIONS IN THE INTENSITY OF COSMIC RAYS IN 1957-1959

1. INTRODUCTION

Studies of variations in the intensity of cosmic rays at different depths below ground level yield important information on the changes in the energy spectrum of the primary particles in the high-energy range, on the absorption and decay of particles generating μ-mesons, on the dynamics of the meteorological state of the lower stratosphere, and so on.

Underground cosmic-ray variations have been studied by a number of workers at various times and depths below ground level [1—8]. However, these investigations have not as yet produced reliable information about the energy characteristics of the various variations in the intensity of cosmic rays. This information can be deduced with the aid of the coupling coefficients $W(h, \epsilon)$ [9, 10], using simultaneous measurements of the intensity of the secondary components of cosmic rays at different longitudes and latitudes at sea level and at various depths underground [11].

Calculations of the coupling coefficients cannot be successfully completed, owing to the lack of information about the fundamental interactions of high and very high energy particles with atmospheric nuclei. Therefore, in order to determine the coupling coefficients and to carry out an independent study of the energy characteristics of these variations, using simultaneous measurements of the μ-meson component in a wide range of energies, we built in 1957 an underground installation for the systematic recording of the hard component at the earth's surface and at depths of 7, 20 and 60m water equivalent [12, 13].

The present paper reports the results of an analysis of the 1957-1959 underground measurements of the intensity of cosmic rays.

2. MAIN CHARACTERISTICS OF THE UNDERGROUND INSTALLATION AND THE EXPERIMENTAL METHOD

The underground installation for the recording of the μ-meson component is located at Yakutsk and consists of a system of counter telescopes at different levels within a special shaft. The disposition of the telescopes at the earth's surface and at depths of 7, 20 and 60 m water equivalents is illustrated schematically in Fig. 1, which also indicates the variation in the

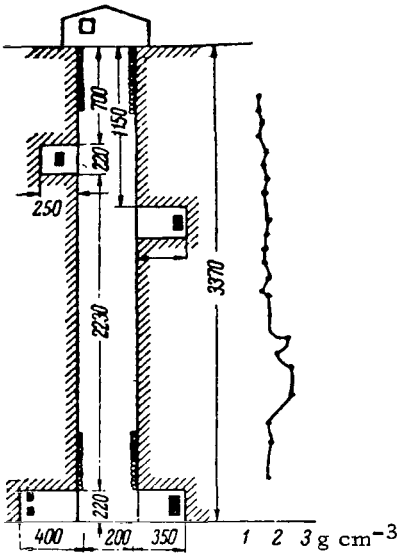

Fig. 1. Disposition of the counter telescopes in the underground laboratory of the Yakutsk Branch, Siberian Division, Academy of Sciences, USSR.

density of the rocks with depth. The installation may be used to investigate variations in the μ-meson component at sea level in the energy range 2×10^8 — 2×10^{10} eV, which approximately corresponds to the average energies of the primary particles between 40 and 200—400 BeV. /67

At each of the levels indicated in Fig. 1, measurements are made of the vertical intensity within a solid angle $\omega \sim \pi$, and the intensity in the southern and northern directions at 30° to the zenith, using triple-coincidence telescopes.

Table 1 shows the average statistical accuracy of the μ-meson measurements at different depths underground.

Table 1

Accuracy of the measured intensity of the hard component of cosmic rays at the earth's surface and at different depths underground (%).

Depth, m w.e.	Vertical telescope		Telescope at 30° to the zenith	
	1 Hour	24 Hours	1 Hour	24 Hours
Surface	0.35	0.07	0.7	0.14
7	0.5	0.10	0.8	0.17
20	0.5	0.10	0.9	0.18
60	0.7	0.14	1.10	0.20

The statistical accuracy of each component at every depth was calculated using the calculations of all the identical double telescopes. It is evident from Table 1 that the accuracy of fine effects when the recording is continued over a period of some months or more.

3. RESULTS OF MEASUREMENTS OF REGULAR AND IRREGULAR VARIATIONS IN THE μ-MESON COMPONENT OF COSMIC RAYS

a) Meteorological effect and seasonal variations. In studying the various variations in the intensity of the hard component, it is important to allow correctly for the temperature effect in the free atmosphere which, in the case of a non-equilibrium atmosphere, cannot be reduced to the concept of a single temperature coefficient, as was first shown by Feynberg [14]. Later, this problem was discussed by Dorman in the case of a two-meson scheme for the generation of μ-mesons. The main results obtained by Dorman are summarized in his monograph "Cosmic-Ray Variations " [9].

The starting point of Dorman's theory was the generally accepted fact that the μ-mesons are the decay products of π-mesons which are generated in the entire atmosphere in accordance with a law which is a consequence of the law of absorption of the meson-producing component. The conclusions of this theory [9] and also of the single-meson theory [14] can be represented by the expression

$$\frac{\delta N_\mu}{N_\mu} = \beta \delta h_0 + \int_0^{h_0} W(h)\, \delta T(h)\, dh,$$

where β is the barometer coefficient, $W(h) = W^\pi(h) + W^\mu(h)$, where $W^\pi(h)$ is the density function of the positive temperature coefficient which is due to the competition between the decay and the absorption of π-mesons, and $W^\mu(h)$ is the density function of the negative temperature coefficient which is due to the decay of the μ-mesons.

We have used the temperature-coefficient density function W(h) given in [15] to calculate for our experimental installation the expected variations due to changes in the temperature of the free atmosphere between ground level and 50 mb.

In the determination of the barometer effect (Table 2), the mean daily values of the intensity $\overline{N}_\mu$ were compared with the mean daily values of the barometic pressure and of W(h) determined from three daily radio-soundings of the atmosphere. Observational data for the period December 1, 1957—January 30, 1958 were employed. It was assumed that the change in the intensity $\delta N\mu$ is given by

$$N_\mu - \bar{N}_\mu = \beta (h - \bar{h}) + (W - \bar{W}),$$

where N_μ and $\overline{N}_\mu$ are the mean daily values of the μ-meson intensity and their average over the given period, and h, $\overline{h}$ and W, $\overline{W}$ are the mean daily values of the barometric pressure and the expected value of the intensity W for a given temperature profile.

The notation in Table 2 is as follows: $r_{Nh(W)}$ - partial correlation coefficient between the intensity N and the barometric pressure h at constant W; $r_{NW(h)}$ - partial correlation coefficient for NW for h = const.; β - barometer coefficient; β_h the theoretically expected part of the barometer coefficient due to the decay of the μ-meson [9], $_{ab}$ - theoretically expected

Table 2

Barometer coefficient for μ-mesons recorded at different depths underground [15].

Depth, m w.e.	$r_{Nh(W)}$	β	$r_{NW(h)}$	ρ	Expected barometer coefficient (theoretical)			
					γ	β_h	β_{ab}	$\beta_{ab}+\beta_h$
Surface	—0.8	—0.13±0.01	0.7	0.85	0.45	—0.07	—0.07	—0.14
					0.3	—0.06	—0.06	—0.12
7	—0.9	—0.10±0.01	0.7	0.8	0.45	—0.034	—0.065	—0.10
20	—0.85	—0.08±0.01	0.5	0.9	0.45	—0.017	—0.060	—0.08
					0.8	—0.018	—0.072	—0.09
60	—0.75	—0.05±0.01	0.45	0.8	0.45	—	—0.03	—0.03
					1.0	—	—0.04	—0.04

part of the barometer coefficient due to absorption, and ρ - the generalized correlation coefficient between the intensity N and the meteorological factors.

In addition to the experimental data on the barometer coefficient, Table 2 gives the coefficients calculated from Dorman's theory [9].

It is evident from Table 2 that the experimental and theoretical values for the barometer coefficient agree at the following values of the exponent in the integral μ-meson spectrum:

earth's surface — $\gamma + 1 = 1.3$
7 m w.e. — $\gamma + 1 = 1.5$
20 m w.e. — $\gamma + 1 = 1.8$
60 m w.e. — $\gamma + 1 = 2.0$

For $h \geqslant 20$ m w.e., these values of γ are in agreement with the intensity-depth relation [8].

The partial correlation coefficient $r_{NW(h)}$ is significant, though small at all levels at which the μ-mesons were recorded ($r_{NW(h)} \geqslant 0.5$). At the same time, the generalized correlation coefficient is found to be $\rho \geqslant 0.8$. The small magnitudes of the correlation coefficient $r_{NW(h)}$ may possibly be due to the fact that these values were found over short periods of time within which the changes in the expected variations due to the temperature effect were small. Moreover during 1957-1958, the role of extra-atmospheric effects in N was particularly significant, but these effects were not adequately allowed for.

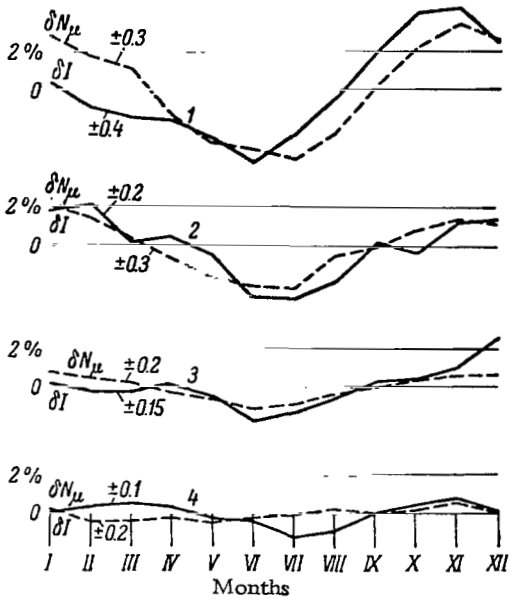

Fig. 2. Seasonal variation in the μ-meson intensity at different depths and at the earth's surface for 1958:

δI - experimental curve; δN - intensity expected on the basis of temperature oscillations. 1—4 - at depths of 0, 7, 20 and 60 m water equivalent, respectively.

When all these points are taken into account, the resulting data on the meteorological effect at different levels underground are found to be in good agreement with the theoretical predictions [9].

This conclusion is confirmed by the fact that the observed seasonal variations in the μ-meson intensity at different depths and the predicted changes due to the temperature effect agree to within experimental and computational errors (Fig. 2). The discrepancies between the theoretical and experimental results will be considered in greater detail below.

b) Solar diurnal variation. Studies of the main properties of solar diurnal variations should be based on continuous measurements in different parts of the energy spectrum of the primary beam at a given point in order to exclude the effect of the geomagnetic field on the isotropic flux [9] and correctly allow for the meterological factors [16—18]. It is also important to make use of composite data for a given period of observation. In 1958, we were able to determine [16] the properties of quiet solar diurnal variations from simultaneous measurements of the intensity of cosmic rays in a wide range. Table 3 shows the results of a Fourier analysis of the diurnal variations.

Table 3

Amplitude and time of maximum of the first two harmonics of diurnal variations measured by different installations during 1957-1958 and 1958-1959.

Period	Meteorological corrections	Harmonic	Neutron component at sea level	Hard component at earth's surface		Hard component underground		
				Ionization chamber	Semi-cubic telescope	7 m.w.e.	20 m w.e.	60 m w.e.
VII 1957—VII 1958	Barometer effect allowed for	A_h, %	0.28±0.03	0.080±0.002	0.160±0.015	0.17±0.02	0.18±0.02	0.05±0.02
		t_h, hr	14.4±0.5	13.6±0.1	16.5±0.5	15.2±0.6	15.7±0.6	16.2±1.2
	Barometer and temperature effects allowed for	A_{hW}, %	—	0.28±0.03	0.36±0.04	0.27±0.03	0.180±0.025	0.05±0.02
		t_{hW}, hr	—	14.0±0.5	14.0±0.5	14.4±0.6	15.4±0.7	16.2±1.2
VIII 1958—III 1959	Barometer effect allowed for	A_h, %	0.28±0.04	0.10±0.02	0.22±0.02	0.150±0.030	0.15±0.03	0.06±0.03
		t_h, hr	14±0.5	13±0.0	14	14	14.9	15
	Barometer and temperature effects allowed for	A_{hW}, %	0.28±0.04	0.27±0.05	0.38±0.06	0.24±0.04	0.16±0.03	0.06±0.03
		t_{hW}, hr	14±0.5	13±0.7	13.5±0.66	14±0.6	14.9±0.7	7.15±1.8

The following facts are evident from Table 3. Firstly, the character of the diurnal variations in N_h does not change appreciably with increasing energy of the recorded particles. However, the amplitude of the diurnal variations in the hard component of cosmic rays at the earth's surface, before it is corrected for the temperature effect, is smaller than the corresponding amplitude underground at depths of 7 and 20 m water equivalent. At 60 m water equivalent, the amplitude falls sharply and, as the energy of the recorded particles increases, the maximum shifts to a later time. This dependence of the amplitude of the diurnal variation N_h indicates that the negative temperature effect [9] masks the true diurnal variations in the hard component more effectively at the earth's surface than at depths of 7 and 20 m water equivalent. This is in full agreement with the change in the temperature-coefficient density function with depth. It also follows that the diurnal variations in the μ-meson component are of non-atmospheric origin and this extra-atmospheric part of the diurnal variation in N_h decreases with increasing energy of the μ-mesons much more slowly than the atmospheric part. When the effect of the expected dirunal variations in W due to diurnal oscillations in temperature of the free atmosphere is allowed for in accordance with the Feynberg-Dorman scheme [9], it turns out that the true variations decrease appreciably with increasing energy of the recorded μ-mesons.

Secondly, the amplitude of the first harmonic of the diurnal variation in the hard component, N, determined from the ionization is much smaller than the corresponding variation determined from the number of particles. This difference may be due to the fact that the screened ionization chamber records both mesons and other particles, and the fact that the ionization losses of μ-mesons increase slowly with energy. Hence the average energy of particles recorded by the ionization chamber is greater than the average energy of the particles recorded by the semi-cubic telescope.

Thirdly, the amplitude of the diurnal variation in the neutron component at the geomagnetic latitude of 50° is not greater than that of the corresponding true diurnal variation in the hard component at this latitude. This suggests that the particles which are responsible for the primary diurnal variations are of high energy and that low-energy particles exhibit practically no diurnal variations.

Fourthly, comparison of diurnal variation measurements by identical installations at different levels can, after correction for meteorological effects, be used to determine the changes in the energy spectrum of the μ-mesons which are related to the primary variations. To do this, it is sufficient to subtract the exponent in the energy spectrum of the undisturbed flux from the exponent of the disturbed μ-meson flux. Calculations showed that the exponent in the integral energy spectrum of the disturbed flux of μ-mesons which are responsible for the extra-atmospheric diurnal variation is $\gamma = 2.5—2.7$, while the result for the undisturbed flux is $\gamma = 1.6—1.8$. It follows that, if the

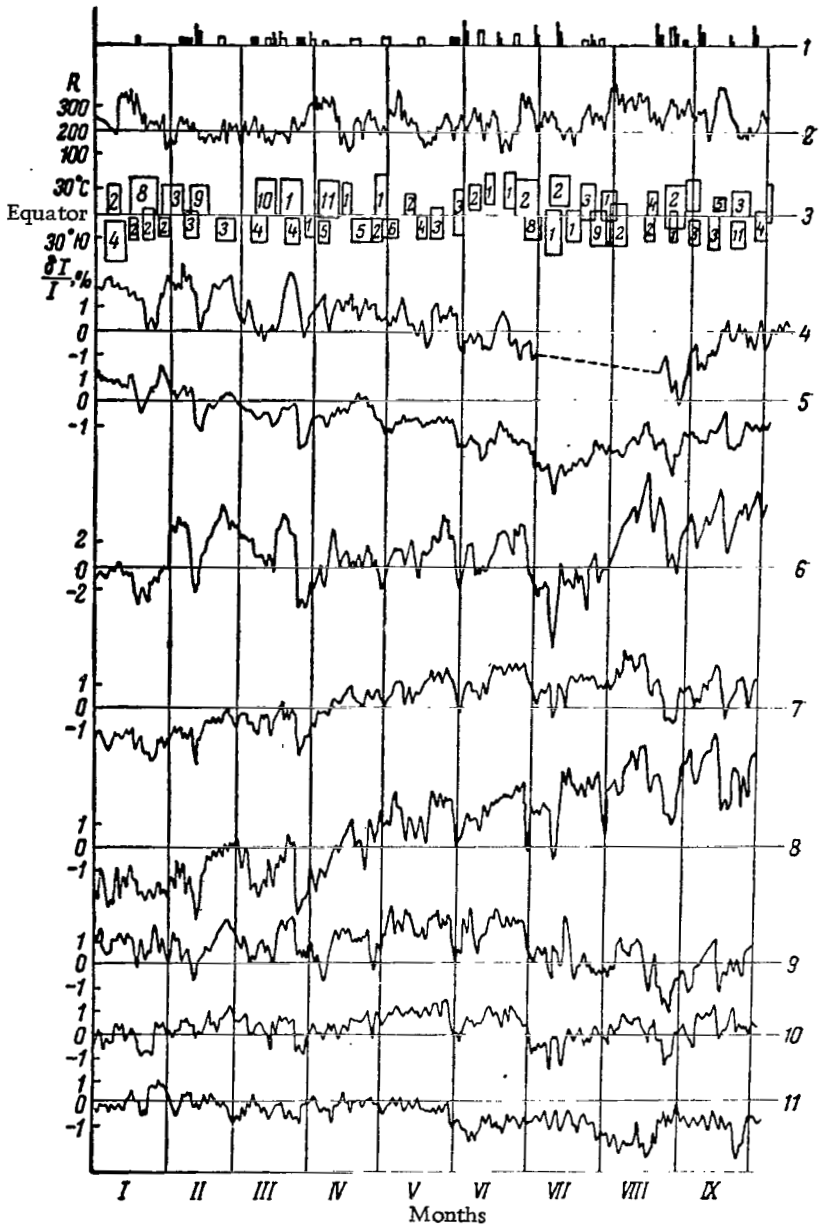

Fig. 3. Mean daily variation in the intensity of the various cosmic-ray components between January 1 and October 1, 1958:

1 - commencement and end of magnetic storms; 2 - relative sunspot number; 3 - position of active regions on the sun relative to the solar equator and the central meridian; 4 - Ih - ionization chamber, Moscow; 5 - Ih - ionization chamber, Tiksi; 6 - neutron monitor data, Yakutsk; 7 - ionization chamber data Yakutsk; 8—11 - semi-cubic telescopes at 0, 7, 20 and 60 m water equivalent respectively.

μ-meson production spectrum is similar to the primary spectrum, it may be assumed that the spectrum of the primary variations is of the form

$$\frac{\delta D(\varepsilon)}{D(\varepsilon)} \sim \varepsilon^{-0.7-1.0}.$$

c) Effects in the intensity of cosmic rays during magnetic storms. Fig. 3 shows the variation in the mean daily values of the intensity of the hard component corrected for the meteorological effects. For comparison, this figure also shows the neutron data obtained at Yakutsk and other stations. It is evident from this figure that, if a reduction in the intensity is observed at the earth's surface, then it can also be detected underground at depths of 7, 20 and 60 m water equivalent, and that the amplitude of the variations decreases with depth. Since it is very important to have reliable information about the presence of the reduction in the intensity at the depth of 60 m water equivalent, we have used the method of superposition of epochs to analyze the data given in [17, 19]. The results for eight effective storms are shown in Fig. 4. It is clear from this figure that the decrease in the cosmic-ray intensity does in fact also occur at 60 m water equivalent where it amounts to about 0.3%. The fact that this is a real effect is confirmed by the appreciable correlation between the underground variation in the intensity and the surface variation for a number of storms (Table 4).

These data indicate that the characteristic changes in the cosmic-ray intensity during some of the magnetic storms occur not only for the components measured at the earth's surface, but also underground down to the depths of 60 m water equivalent. Hence, cosmic-ray particles with energies of a few hundred BeV undergo the intensity decrease.

In addition, Fig. 5 shows that some storms are preceded by an increase in the intensity, for example, January 17, February 8, March 24, May 26, August 17 and September 16. This increase is not due to meteorological effects since it is still present after the introduction of corrections for the barometer and temperature effects.

Assuming that the intensity-depth relation for the undisturbed flux of μ-mesons, N, and for the disturbed flux, N', during magnetic storms can be described by functions of the form $N = N_0\varepsilon^{-\gamma_0}$ and $N = N'_0\varepsilon^{-\gamma}$, it is possible to determine the difference $\gamma_0 - \gamma$, i.e. the change $\Delta\gamma$ in the exponent γ during magnetic storms.

The undisturbed μ-meson flux at different depths (corrected for atmospheric effects) is in the ratio $N_{10} : N_{17} : N_{30} : N_{70} = 1 : 0.67 : 0.34 : 0.064$.

The result for the disturbed flux (Table 4) is $N'_{10} : N'_{17} : N'_{30} : N'_{70} = 1 : 0.45 : 0.17 : 0.013$.

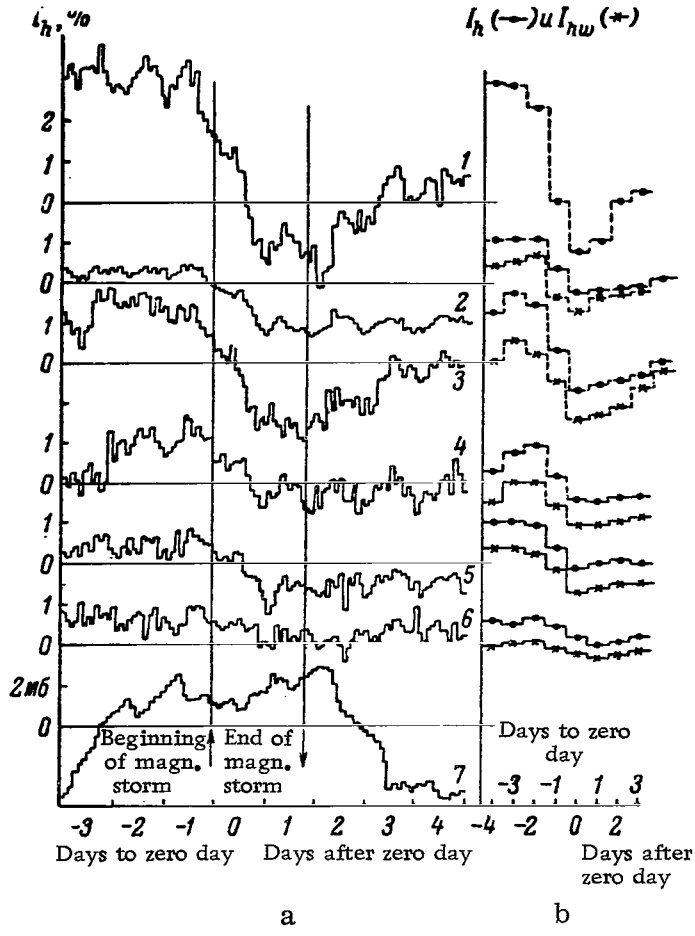

Fig. 4. Mean variation in the intensity of different cosmic-ray components during eight effective magnetic storms.

a - two-hourly intensities; b - mean daily intensities. 1 - neutrons, sea level; 2 - ASK-2; 3 - counter telescope, sea level; 4 - ditto at 7 m w.e.; 5 - ditto at 20 m w.e.; 6 - ditto at 60 m w.e.; 7 - surface pressure.

We have used this ratio to calculate the change

$$\Delta\gamma = \gamma = \gamma_0.$$

The results of calculations of the μ-meson energy spectrum during magnetic storms are shown in Table 4. If it is assumed, on the first approximation, that changes in the μ-meson energy spectrum during magnetic storms

reflect variations in the primary spectrum, then it is evident from Table 4 that these variations are of the form

$$\frac{\delta D(\varepsilon)}{D(\varepsilon)} \sim \varepsilon^{-0.75 \pm 0.25}.$$

Table 4

Change in the exponent γ in the effective integral μ-meson spectrum during magnetic storms.

Level with allowance for the atmosphere, m w.e.	γ_0 for the undisturbed μ-meson flux	γ for the disturbed μ-meson flux	$\gamma-\gamma_0$
10—17	—0.76	—1.50	—0.74
10—30	—1.04	—1.62	—0.58
10—70	—1.38	—2.21	—0.52
17—30	—1.49	—1.72	—0.23
17—70	—1.62	—2.48	—0.86
30—70	—1.77	—2.97	—1.20
Mean . .	—	—	—0.75±0.25

Primary particles with energies up to 300—400 BeV, which is the mean energy of primary particles at 60 m w.e., undergo the reduction in intensity.

27-day variations. In estimating 27-day variations in the underground cosmic-ray intensity at depths $h \geqslant 60$ m w.e., it is important to consider temperature changes not only in the troposphere but also in the upper atmosphere. According to the hypothesis advanced by Rora [20], oscillations in the temperature and the ozonosphere can fully explain the 27-day variations in the hard component at ground level. This hypothesis may be verified by comparing 27-day variation data obtained as a result simultaneous measurements at various depths down to 60 m w.e.

The analysis of continuous measurements of cosmic-ray intensity at 0, 20 and 60 m w.e. was completed in the middle of 1958 [21]. The basic data were the mean daily intensities corrected for the barometer effect. The processing was carried out by the method of superposition of epochs. The processing of hard-component data included corrections for the barometer and temperature effects. Starting with the estimated magnitude of the temperature effect in the hard component at ground level, a rough calculation was made of the temperature effect due to the troposphere and the lower stratosphere in the underground cosmic-ray intensity. The data processed in [21] may also be subject to instrumental errors and long-period variations.

We have therefore carried out a second and more careful analysis of the data. All the measurements were smoothed with a 27-day period and the deviations of the mean daily values from the smoothed values were determined. This procedure was applied to data corrected for both the barometer effect and

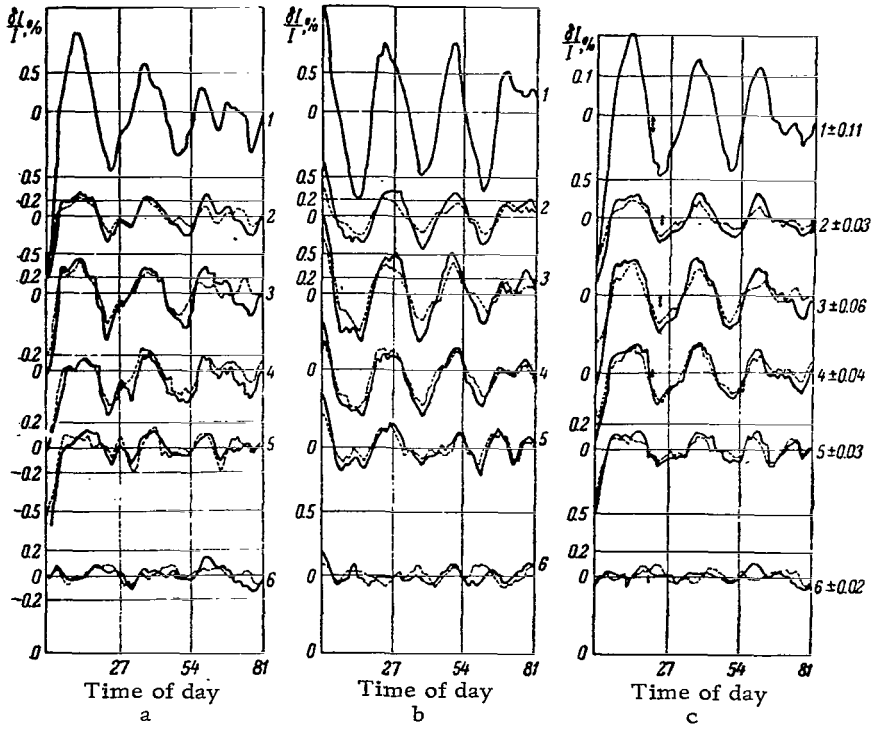

Fig. 5. 27-day recurrence of I_h and I_{hW} for different components measured at Yakutsk.

a - negative pulses; b - positive pulses; c - mean difference between curves a and b. 1 - neutron monitor; 2 - ionization chamber; 3—6 - telescopes at 0, 7, 20 and 60 m w.e. respectively.

the barometer and temperature effects. The deviations were then used to select five maximum and five minimum "zero days" for each month. All the independently chosen days for each level of observation and for each component coincided to within 24 hours both before and after the introduction of the temperature correction. These data were then analyzed by the method of superposition of epochs.

Figure 5 shows the result of this analysis in the form of difference curves. It is evident from this figure that there are 27-day variations in the cosmic-ray intensity at all the levels, both before and after the introduction of corrections for the temperature effect in the troposphere and the lower stratosphere (the correction is introduced at all heights up to h = 50 mb). The introduction of the corrections tends to reduce the amplitude of the 27-day variations in the hard component at the earth's surface and at the depth of 7 m water equivalent. At 20 and 60 m water equivalent, the corrections for the temperature effect are negligible. The curves for all the recording levels exhibit a positive correlation. The correlation coefficient between the surface and the 7 and 20 m w.e. measurements is $r \geqslant 0.75$.

The correlation coefficient for the curve obtained at 60 m. w.e. is 0.3.

It follows that all the curves reflect real extra-atmospheric changes in the cosmic-ray intensity with a period of approximately 27 days, except for the variations at the depth of 60 m w.e. In view of the low correlation coefficient, the variations at 60 m w.e. may be considerably affected by the temperature effect in the atmospheric layer between 0 and 25 mb. If it is assumed that the regular deviations which recur with a period of about 27 days on the curve taken at 60 m w.e. are a consequence of the 27-day variations in the temperature of the 0—25 mb layer, then these oscillations should amount to 0.05% : 0.014% / 1°C = 4°C since the temperature coefficient is ±0.014%.

Such oscillations may give rise to an increase in the amplitude of the variations in the hard component at the earth's surface of about 0.04%. At 7 and 20 m w.e., the increase may amount to 0.03 and 0.02% respectively. Thus, it may be concluded that, firstly, the 27-day variations in the mean temperature of the ozonosphere are small and have no significant effect on the 27-day variations in the hard component of cosmic rays, and secondly, the 27-day variations in the hard component are of extra-atmospheric origin.

The amplitudes of the variations measured by the semi-cubic telescope at different depths are in the ratio of $N'_{10} : N'_{17} : N'_{30} : N'_{70} = 1 : 0.7 : 0.5 : 0.15$. Since this is the same ratio as in the case of the reduction in the cosmic-ray intensity during magnetic storms, it may be considered that the 27-day variations are in fact associated with magnetic storms [22].

d) Non-cyclic variations in the intensity of cosmic rays. Fig. 3 shows the seasonal variations in the intensity of cosmic rays at different depths in 1958. It is evident from this figure that seasonal cosmic-ray variations can almost entirely be described by a temperature effect. Moreover, the cosmic-ray intensity undergoes non-cyclic secular changes. Thus, the cosmic-ray intensity increases by 2.5% at the surface and by about 0.5% at 20 m w.e. between the beginning and the end of the year. This increase was absent at 7 and 60 , w.e. to within experimental error. It should be noted that the non-cyclic part of the variations at the depth of 7 m w.e. was either

accidentally excluded owing to inadequate "matching" of data, or the variations had a very small amplitude. At the same time, the increase in the intensity at 20 m w.e. was a real effect. At this depth, the matching of the data was carried out with the aid of the readings of two independent instruments, so that these data can be regarded as more reliable. It follows that the spectrum of the non-cyclic variations extends up to energies of a few tens of BeV.

4. DETERMINATION OF THE SPECTRUM OF PRIMARY VARIATIONS BY THE METHOD OF COUPLING COEFFICIENTS

Measurements of the μ-meson component at different levels may be compared with the spectrum obtained by the method of coupling coefficients [9]. The variations in a particular component $\frac{\delta N_i}{N_i}$ are related to the primary variations $\frac{\delta D(\varepsilon)}{D(\varepsilon)}$ by

$$\frac{\delta N_i(h)}{N_i(h)} = \int_{\epsilon_{min}}^{\infty} W_i(\varepsilon, h) \frac{\delta D(\varepsilon)}{D(\varepsilon)} d\varepsilon,$$

where $W_i(\epsilon, h)$ are the coefficients of coupling of the i-th component at the level h; and ϵ_{min} is the minimum energy of the primary particles which is determined by the geomagnetic threshold or the experimental conditions.

The coupling coefficients $W_i(\epsilon, h)$ were obtained in [10] for underground telescopes. The coupling coefficients for the neutron component and the hard component (determined from ionization) were determined with the aid of the latitude effect using the mean probable energy of the particles responsible for the given component.

Since all the variations decrease with energy, the primary variation spectrum may be of the form

$$\frac{\delta D(\varepsilon)}{D(\varepsilon)} = -\begin{cases} a\varepsilon^{-\alpha}, & \text{when } \varepsilon > \varepsilon_1, \\ b, & \text{when } \varepsilon < \varepsilon_1. \end{cases}$$

Let us try and fit the experimental data with this expression by adjusting the parameters a, b, α and ϵ_1. Moreover, in the case of a decrease in the intensity during a magnetic storm, we shall try to fit the data with the theoretical spectrum [9]:

Table 5

Predicted and experimental values for the ratios of cosmic-ray intensity variations.

Test spectrum	ε_1 BeV	$\frac{\delta N_H}{N_H} : \frac{\delta N_{T_0}}{N_{T_0}}$	$\frac{\delta N_K}{N_K} : \frac{\delta N_{T_0}}{N_{T_0}}$	$\frac{\delta N_{T_7}}{N_{T_7}} : \frac{\delta N_{T_0}}{N_{T_0}}$	$\frac{\delta N_{T_{20}}}{N_{T_{20}}} : \frac{\delta N_{T_0}}{N_{T_0}}$	$\frac{\delta N_{T_{00}}}{N_{T_{00}}} : \frac{\delta N_{T_0}}{N_{T_0}}$
Experiment	—	2.50	0.74	0.67	0.55	0.21
I $\frac{\delta D(\varepsilon)}{D(\varepsilon)} = a \begin{cases} -1, \text{ when } \varepsilon < \varepsilon_1 \\ 0, \text{ when } \varepsilon > \varepsilon_1 \end{cases}$	30	2.1	0.78	0.09	0.01	0.0
	100	1.10	0.90	0.82	0.43	0.0
	220	1.05	0.96	0.96	0.85	0.27
	260	1.04	0.98	0.97	0.85	0.37
	∞	1.0	1.0	1.0	1.0	1.0
II $\frac{\delta D(\varepsilon)}{D(\varepsilon)} = -a \begin{cases} 1, \text{ when } \varepsilon < \frac{\varepsilon_1}{4} \\ \frac{2}{\pi} \sin^{-1}\left(\frac{\varepsilon_1}{2\varepsilon} - 1\right), \text{ when } \frac{\varepsilon_1}{4} < \varepsilon < \frac{\varepsilon_1}{2} \\ 0, \text{ when } \varepsilon > \frac{\varepsilon_1}{2} \end{cases}$	30	3.8	0.95	0	0	0
	100	1.50	0.80	0.59	0.16	0
	220	1.09	0.80	0.90	0.67	0.07
	260	1.06	0.81	0.94	0.73	0.13
	300	1.05	0.84	0.95	0.80	0.19
	∞	1.0	1.0	1.0	1.0	1.0
III $\frac{\delta D(\varepsilon)}{D(\varepsilon)} = \begin{cases} -a\varepsilon^{-1}, \text{ when } \varepsilon_1 > \varepsilon_1 \\ 0, \text{ when } \varepsilon_1 > \varepsilon \end{cases}$	60	2.92	0.86	0.37	0.05	0.0
	100	2.76	0.81	0.46	0.17	0.0
	220	2.75	0.81	0.48	0.29	0.05
	260	2.75	0.81	0.48	0.29	0.07
	∞	2.70	0.82	0.49	0.31	0.12
IV $\frac{\delta D(\varepsilon)}{D(\varepsilon)} = \begin{cases} -a\varepsilon^{-0.7}, \text{when } \varepsilon_1 > \varepsilon \\ 0, \text{ when } \varepsilon_1 < \varepsilon \end{cases}$	100	2.02	0.76	0.55	0.24	0.0
	180	2.00	0.80	0.60	0.39	0.05
	260	2.00	0.81	0.61	0.41	0.12
	∞	2.00	0.84	0.63	0.45	0.23
V $\frac{\delta D(\varepsilon)}{D(\varepsilon)} = \begin{cases} -0\varepsilon^{-0.5}, \text{ when } \varepsilon_1 > \varepsilon \\ 0, \text{ when } \varepsilon_1 < \varepsilon \end{cases}$	100	1.94	0.74	0.62	0.28	0.0
	180	1.62	0.78	0.69	0.48	0.06
	260	1.60	0.80	0.71	0.54	0.16
	∞	1.60	0.83	0.71	0.57	0.35

Table 5 (Continued)

Test spectrum	ε_1 BeV	$\frac{\delta N_H}{N_H} : \frac{\delta N_{T_0}}{N_{T_0}}$	$\frac{\delta N_K}{N_K} : \frac{\delta N_{T_0}}{N_{T_0}}$	$\frac{\delta N_{T_7}}{N_{T_7}} : \frac{\delta N_{T_0}}{N_{T_0}}$	$\frac{\delta N_{T_{30}}}{N_{T_{30}}} : \frac{\delta N_{T_0}}{N_{T_0}}$	$\frac{\delta N_{T_{60}}}{N_{T_{60}}} : \frac{\delta N_{T_0}}{N_{T_0}}$
VI $\frac{\delta D(\varepsilon)}{D(\varepsilon)} = -a \begin{cases} \varepsilon^{-1}, \text{ when } \varepsilon > \varepsilon_1 \\ 1, \text{ when } \varepsilon < \varepsilon_1 \end{cases}$	3	3.23	0.81	0.48	0.31	0.12
	7	6.4	0.90	0.43	0.29	0.11
	11	6.5	0.97	0.27	0.18	0.07
	15	5.6	0.93	0.15	0.10	0.04
VII $\frac{\delta D(\varepsilon)}{D(\varepsilon)} = -a \begin{cases} \varepsilon^{-0.7}, \text{ when } \varepsilon > \varepsilon_1 \\ 1, \text{ when } \varepsilon < \varepsilon_1 \end{cases}$	3	2.16	0.80	0.63	0.45	0.23
	7	3.25	0.78	0.60	0.42	0.22
	11	3.80	0.79	0.51	0.35	0.19
	15	3.40	0.80	0.36	0.25	0.13
VIII $\frac{\delta D(\varepsilon)}{D(\varepsilon)} = -a \begin{cases} \varepsilon^{-0.5}, \text{ when } \varepsilon > \varepsilon_1 \\ 1, \text{ when } \varepsilon < \varepsilon_1 \end{cases}$	3	1.67	0.72	0.71	0.55	0.35
	7	2.08	0.75	0.69	0.53	0.34
	11	2.40	0.75	0.64	0.49	0.31
	15	2.38	0.73	0.54	0.42	0.26
IX $\frac{\delta D(\varepsilon)}{D(\varepsilon)} = -a \begin{cases} \varepsilon^{-1}, \text{ when } \varepsilon > \varepsilon_1 \\ 0, \text{ when } \varepsilon < \varepsilon_1 \end{cases}$	3	2.52	0.78	0.48	0.31	0.12
	7	1.29	0.76	0.50	0.32	0.13
	11	0.91	0.78	0.55	0.35	0.14
	15	0.52	0.78	0.63	0.41	0.17
X $\frac{\delta D(\varepsilon)}{D(\varepsilon)} = -a \begin{cases} \varepsilon^{-0.7}, \text{ when } \varepsilon > \varepsilon_1 \\ 0, \text{ when } \varepsilon < \varepsilon_1 \end{cases}$	3	1.88	0.75	0.63	0.43	0.23
	7	1.25	0.74	0.64	0.44	0.24
	11	0.92	0.74	0.68	0.47	0.25
	15	0.74	0.76	0.75	0.52	0.27
XI $\frac{\delta D(\varepsilon)}{D(\varepsilon)} = -a \begin{cases} \varepsilon^{-1}, \text{ when } \varepsilon > \varepsilon_1 \\ -0.5, \text{when } \varepsilon < \varepsilon_1 \end{cases}$	3	3.14	0.82	0.48	0.32	0.13
	7	4.15	0.83	0.46	0.30	0.12
	11	4.5	0.84	0.37	0.24	0.10
	15	8.9	0.82	0.35	0.16	0.07
XII $\frac{\delta D(\varepsilon)}{D(\varepsilon)} = -a \begin{cases} \varepsilon^{-0.7}, \text{ when } \varepsilon > \varepsilon_1 \\ -0.5, \text{ when } \varepsilon < \varepsilon_1 \end{cases}$	3	1.90	0.75	0.63	0.43	0.23
	7	2.28	0.76	0.62	0.42	0.23
	11	2.58	0.76	0.57	0.40	0.22
	15	2.55	0.75	0.50	0.34	0.19

$$\frac{\delta D(\varepsilon)}{D(\varepsilon)} = -a \begin{cases} 1, & \text{when} \quad \varepsilon < \frac{\varepsilon_1}{4}, \\ \frac{2}{\pi} \sin^{-1} \left(\frac{\varepsilon_1}{2\varepsilon} - 1 \right), & \text{when} \quad \frac{\varepsilon_1}{4} < \varepsilon < \frac{\varepsilon_1}{2}, \\ 0, & \text{when} \quad \varepsilon > \frac{\varepsilon_1}{2}. \end{cases}$$

Since the ratio of the amplitudes of the 27-day variations in the various components is, to within experimental error, identical with the amplitude ratio of the variations during magnetic storms, it is clear that their spectra can only differ in the magnitude of the parameter a. The results of the calculations [15, 18] are shown in Table 5.

It is clear from Table 5 that the experimental data on the diurnal variation of cosmic rays at a given point can be satisfactorily described in a wide energy range by a primary variation spectrum of the form

$$\frac{\delta D(\varepsilon)}{D(\varepsilon)} = \begin{cases} -a\varepsilon^{-0.7}, & \text{when} \quad \varepsilon > \varepsilon_1, \\ 0, & \text{when} \quad \varepsilon < \varepsilon_1. \end{cases}$$

The best agreement (symmetric disposition of the experimental errors) occurs for $\alpha = 0.7—1.0$ and $\epsilon_1 = 12$ BeV. When $\alpha = 0.7$, the strength of the source is a = 0.05 BeV, while for $\alpha = -1.0$ the result is a = 0.150 BeV.

Thus, the spectrum of the primary diurnal variations determined by the method of coupling coefficients is identical with the spectrum of the extra-atmospheric diurnal variations of μ-mesons and is in agreement with the mechanism postulated in [9], according to which the primary beam is modulated by the electric fields of solar corpuscular streams. The fact that particles with energies $\epsilon \geqslant 12$ BeV take part in the production of diurnal cosmic-ray variations is in agreement with the suggestion put forward in [9] that the corpuscular streams carry frozen-in magnetic fields whose intensities at the earth are of the order of $10^{-5} — 4 \times 10^{-5}$ oe, the angular width of a stream being 8—30°.

Calculations [16] also show that the source of the diurnal variations lies at an angle of 66 ± 11° left of the earth-sun line and the strength of the source in the angular range $\varphi = 20—30°$ is higher by a factor of 1.8 than in the range $\varphi = 45—50°$ (φ is the angle between the plane of the geomagnetic equator and the direction of motion of the particle at infinity).

It is clear from Table 5 that the experimental data on the cosmic-ray variations during magnetic storms are in disagreement with the primary variation spectrum of type I for all values between 40 BeV and infinity. The discrepancy is due to the fact that this spectrum does not satisfy the experimental

results for the neutron intensity and the underground variations at depths of 20 and 60 m water equivalent.

The situation is similar in the case of spectrum II. Spectra III, IV and V do not fit the experimental ratios for all values of ϵ_1 between 60 BeV and infinity. In some cases, this is due to the neutron component (when $\epsilon_1 \geqslant 100$ Bev), while in other cases it is due to the meson component at depths of 7, 20 and 60 m w.e. (for $\epsilon_1 \leqslant 260$ BeV). However, experimental data are in satisfactory agreement with the spectrum of the form

$$\frac{\delta D(\varepsilon)}{D(\varepsilon)} = \begin{cases} -b, & \text{when } \varepsilon < \varepsilon_1, \\ -a\varepsilon^{-\alpha}, & \text{when } \varepsilon > \varepsilon_1; \end{cases}$$

where $\epsilon_1 = 7 \pm 2$ BeV, a = 0.22 and b = 0.11.

For energies $\geqslant 30$ BeV, this spectrum is in disagreement with that expected on the basis of scattering of the particles by the frozen-in magnetic fields in the corpuscular streams [9], but is confirmed by the IGY data [23]. This discrepancy may be explained as follows. Firstly, the determination of the variation spectrum during magnetic storms [23] was deduced only from data for the energy range 20—50 BeV. Secondly, the coupling coefficients for underground installations in the region of relatively low energies are not reliable and are apparently too low. Thirdly, if one persists in postulating the scattering of cosmic rays by the regular magnetic field of a corpuscular stream as the factor responsible for the magnetic storm effects [9], then it is necessary to admit that an appreciable part of the stream carries irregularities or magnetized clouds which scatter particles of low and moderate energies. The width of the uniform magnetic field of a stream will then appear to contract for particles of low and moderate energies, and the variation spectrum will become similar to the experimental spectrum.

It should be noted that the spectrum of variations during magnetic storms as determined by the method of coupling coefficients is identical with the spectrum of the extra-atmospheric variations in the μ-meson component. This is not accidental and suggests that the above primary variation spectrum is in fact correct.

Since the experimental ratios of the amplitudes of the 27-day variations are identical with the corresponding ratios of the amplitudes of the decreases during magnetic storms, the spectrum of the primary 27-day variations is similar in form to the magnetic storm effect; i.e. it can be described by the spectra XI and XII in Table 5. However, the strength of the source of the 27-day variations will be smaller by a factor of approximately 4 than the source

strength of variations during the magnetic storm effect, i.e. in the case of the 27-day variations a = 0.06 and b = 0.03.

CONCLUSION

1. Meteorological effects in the intensity of the hard component at the earth's surface and at 7, 20 and 60 m water equivalent are in agreement with the two-meson scheme for the generation of the hard component in the atmosphere [9]. The best agreement between theory and experiment is achieved for the following values of the exponent in the effective differential μ-meson spectrum:

earth's surface	—	$\gamma + 1 = -2.3$
7 m w.e.	—	$\gamma + 1 = -2.5$
20 m w.e.	—	$\gamma + 1 = -2.8$
60 m w.e.	—	$\gamma + 1 = -3.0$

The introduction of the temperature correction into the above values of γ smooths out the seasonal variations in the hard component at the above depths to within experimental and computational error.

2. The main properties of solar diurnal variations deduced from composite data recorded at a given point are in agreement with Dorman's theory [9] according to which the primary beam of cosmic radiation is modulated by the electric fields of solar corpuscular streams. The lower energy limit of the particles modulated by the streams is ϵ = 12 BeV. The effective source of these variations lies at an angle of 66 $\pm$ 11° to the left of the earth-sun line.

3. The ratios of the amplitudes of the 27-day variations on the one hand, and the decreases in the intensity during magnetic storms on the other, are identical within a wide primary energy range ($2 \times 10^9 - 4 \times 10^{11}$ eV) and are therefore due to a single common mechanism. The energy spectrum of the primary variations is of the form

$$\frac{\delta D(\epsilon)}{D(\epsilon)} = -\begin{cases} b, & \text{when } \epsilon < \epsilon_1, \\ a\epsilon^{\alpha}, & \text{when } \epsilon > \epsilon_1, \end{cases}$$

where $\epsilon_1 = 7 \pm 2$ Bev, $\alpha = -0.7 \pm 0.3$, a = 0.22 and b = 0.11 in the case of the magnetic storm effect, and a = 0.06, b = 0.03 in the case of the 27-day variations. This spectrum is consistent with Dorman's theory [9] according to which the particles are scattered by the frozen-in magnetic field of corpuscular streams whose intensity at the earth's orbit is of the order of

10^{-4} oe, the stream itself being appreciably turbulent as a result of its interaction with the interplanetary medium. Thus, only low-energy particles are appreciably scattered by the uniform field.

The considerable transformation of the energy spectrum in the primary energy range above 30 BeV during magnetic storms suggests the presence of appreciable irregularities in the regular magnetic field of corpuscular streams and indicates the importance of electric fields.

REFERENCES

1. Rau, W. Naturwiss., 27, 503, 1939.
2. Forro, M. Phys. Rev., 72, 868, 1947.
3. MacAnuff, J.W. Thesis, London, 1950.
4. Barrett, J.H., Bollinger, L.M., Cocconi, G., Eisenberg, G. and Greisen, K. Rev. Mod. Phys., 24, 133-178, 1952.
5. Sherman, N. Phys. Rev., 89, 25, 1953.
6. Barrett, J.H., Cocconi, G., Eisenberg, G. and Greisen, K. Phys. Rev., 95, 1951, 1954.
7. Sherman, N. Phys. Rev., 93, 208, 1954.
8. George, E.P. In the book: Progress in cosmic ray physics. Vol. 1, ed. J.G. Wilson, IL, Moscow, 1954.
9. Dorman, L.I. Variatsii kosmicheskikh luchey (Cosmic ray variations). Gostekhizdat, Moscow, 1957.
10. Kuz'min, A.I. Proceedings of the Moscow Cosmic Ray Conference, IV, 48, 1960.
11. Kuz'min, A.I. Tr. Mezhd. konfer. po kosmich. lucham (Proceedings of the Moscow Cosmic Ray Conference). IV, 258, 1960.
12. Kuz'min, A.I. and Yarygin, A.V. Tr. YaFAN SSSR, ser. fizich., No. 2, 36, 1958.
13. Danilov, A.A., Druzhinin, S.N., Kapustin, I.N. and Skripin, G.V. Tr. YaFAN SSSR, ser. fizich., No. 3, 40, 1959.

14. Feynberg, Ye. L. DAN SSSR, 53, 421, 1946.

15. Kuz'min, A.I. and Danilov, A. A. Tr. YaFAN SSSR, ser. fizich., No. 3, 58, 1959.

16. Kuz'min, A.I. Tr. YaFAN SSSR, ser. fizich., No. 3, 99, 1959.

17. Kuz'min, A.I., Yefimov, N.N., Krasil'nikov, D.D., Skripin, G.V., Shafer, Yu.G. and Shafer, G.V. Proc. IGY Cosmic Ray Series, No. 3, 1960.

18. Kuz'min, A.I. ZhETF, 28, 614, 1955; Dorman, L.I., Kuz'min, A.I., Tyanutova, T.V., Feynberg, Ye. L. and Shafer, O.G. ZhETF, 26, 537, 1954; Fuks, L.A. and Shvartsman, B.F. Tr. YaFAN SSSR, ser. fizich., No. 2, 118, 1958; Glokova, Ye.S. Izv. AN SSSR, ser. fizich., 20, 47, 1956; Glokova, Ye.S., Kaminer, N.S. and Lepshina, N.A. Tr. YaFAN SSSR, ser. fizich., No. 2, 95, 1958.

19. Kuz'min, A.I. and Skripin, G.V. Tr. YaFAN SSSR, ser. fizich., No. 3, 121, 1959.

20. Rora, E.G. Zs. Naturforsch., 5A, 517, 1950.

21. Kuz'min, A.I., Sokolov, V.D. and Shafer, G.V. Tr. YaFAN SSSR, ser. fizich., No. 3, 111, 1959.

22. Sekido, J. and Wada, M. Rep. Jonos, Res. Japan, 9, 174, 1955.

23. Blokh, Ya., Dorman, L. and Glokova, Ye. Proc. IGY, No. 2, 2, 1958.

G. V. Skripin

MAIN PROPERTIES OF SOLAR DIURNAL VARIATIONS FROM DIRECTIONAL COSMIC-RAY MEASUREMENTS

1. Solar diurnal variations in the intensity of cosmic rays at energies up to 20 BeV have been exhaustively studied both experimentally and theoretically [1]. However, the number of papers devoted to the main properties of diurnal variations at higher energies is still quite small [2—6]. Underground measurements of diurnal variations by Rau [2] at a depth of 40 m water equivalent, and by MacAnuff [3] at a depth of 60 m water equivalent, appear to be contradictory. Rau has found a diurnal variation with two maxima while MacAnuff has reported the presence of only one maximum.

More complete underground studies of the diurnal variation were carried out at Yakutsk [4—6] with the aid of a system of counter telescopes at ground level and at a depth of 7, 20 and 60 m of water equivalent. The diurnal variation of extra-terrestrial origin which was deduced from these observations had an amplitude of 0.36, 0.27, 0.18 and 0.05 at the above four levels respectively. A more accurate determination was also made of the energy spectrum of primary particles in the diurnal variation, which was found to be of the form

$$\frac{\delta D(\varepsilon)}{D(\varepsilon)} = \begin{cases} -0.15 \cdot \varepsilon^{-1-0.7}, & \text{when} \quad \varepsilon > \varepsilon_1 = 10\text{—}15 \text{ BeV}, \\ 0, & \text{when} \quad \varepsilon < \varepsilon_1 = 10\text{—}15 \text{ BeV}. \end{cases}$$

There are no data on the dependence of the underground diurnal variation on the direction of arrival of the cosmic rays at the earth's surface. The only data available are those obtained at ground level [7—9].

Alfvén and Malfors [7] found at Stockholm in 1943 that the first harmonic of the diurnal variation from the north has an amplitude of about 0.16% with a maximum at 1330 hrs, while for particles arriving from the south the amplitude is the same, but the maximum occurs at 1900 hrs. Analogous results were obtained earlier by Kolhörster [8] in Berlin.

The more careful measurements of Elliot and Dolbear [9], who used directional counter telescopes with and without a 35 cm lead filter, indicated the possible presence of an increase in the anisotropy of primary radiation with increasing average energy of the recorded particles. In our view, the most acceptable explanation of the observed dependence of diurnal variations on the direction of arrival of particles at the earth's surface has been given by Dorman [1]. Dorman used the coupling coefficients and the entire spectrum of variations to arrive at a more correct, as compared with [10], evaluation of the effect of the geomagnetic field on the particle trajectories, and thereby explained the difference in the diurnal variations in different directions.

The effects which are still to be explained are (1) the nature of the diurnal variation of cosmic rays with energies in excess of 20 BeV which arrive from different directions, and (2) the correctness of the mechanism given in [1] for the observed anisotropy at high energies.

Below, we report results of directional measurements of the diurnal variation which were carried out with the aid of the Yakutsk counter apparatus at ground level and underground at depths of 7, 20 and 60 m water equivalent in 1958-1959. These measurements showed that the observed difference in the readings of the telescope pointing south and north at the earth's surface remains, or is even more pronounced, at the three levels underground. This behavior of the diurnal variation of high-energy primary particles is interpreted as being due to the effect of the geomagnetic field on the particle trajectories.

These data were used to show that in 1958-1959 the source of the diurnal variation was located at 80° left of the earth-sun line in the plane of the ecliptic. A determination was also made of the distribution of the source in the plane perpendicular to the plane of the ecliptic.

Observational data obtained at Yakutsk at 60 m water equivalent below ground level during the minimum of 1954-1955 are also reported.

2. Directional measurements of the diurnal variation of cosmic rays at a depth of 60 m water equivalent were begun at Yakutsk (λ = 51°N geomag. lat.) in September 1954, using a vertical counter telescope and two further counter telescopes pointing north and south at 30° to the zenith. These observations were continued until January 1956. The measurements were resumed again in July 1956 after the completion of the reconstruction of the underground laboratory. Ground level measurements of the cosmic-ray intensity, using the same apparatus as underground, were begun in January 1956. Two further counter telescopes were installed in January 1958 at depths of 7 and 20 m water equivalent [11]. Moreover, in order to increase the statistics at the 60 m water equivalent level, two further counter telescopes were added to the existing apparatus [12].

Table 1

Level, m water equivalent	Direction	Number of telescopes	Counts per two hours	Scaling factor	Statistical error per two hours	Barometer coefficient, % mb^{-1}
Earth's surface	Vertical	1	145000	128	0.25	—0.13
	South	3	40000	32	0.50	—0.13
	North	3	40000	32	0.50	—0.13
7	Vertical	1	100000	64	0.30	—0.10
	South	3	29000	16	0.55	—0.10
	North	3	29000	16	0 55	—0.10
20	Vertical	2	100000	32	0.30	—0.08
	South	7	29000	16	0.60	—0.08
	North	7	29000	16	0.60	—0.08
60	Vertical	4	53000	8	0.45	—0.04
	South	9	8000	4	1.1	—0.04
	North	9	8000	4	1.1	—0.04

Each directional telescope consists of three trays of three counters each. The C-60 counters have an effective length of 55 cm and a diameter of 6 cm. Special electronic circuits select triple coincidences between these three trays. An 8 cm lead filter is placed between the lowest and middle trays. In addition to the directional telescopes there are vertical telescopes with larger angles of acceptance at each of the levels. Table 1 gives their geometry and other parameters.

3. Figure 1 shows the two-hourly diurnal variation in the intensity of cosmic rays, which represents an average over two years (1958-1959). The data shown in Fig. 1 have been corrected for the barometer effect with the aid of the coefficients given in Table 1.

Table 2 gives the results of a harmonic analysis of the data obtained by the above apparatus. In this table A_h, A_{hW}, t_h and t_{hW} are the amplitude and the time of maximum of the first harmonic corrected for the barometer (subscript h) and temperature (subscript hW) effects respectively.

It is clear from these experimental data that in 1958-1959 the maximum amplitude of the diurnal variation at all levels was indicated by the telescopes pointing south, while the smallest amplitudes were indicated by the telescopes pointing north. The vertical telescopes indicated an intermediate result. This difference between the diurnal variations between the two opposite azimuths becomes even more clearly defined with increasing depth of recording, i.e. with increasing energy of the particles.

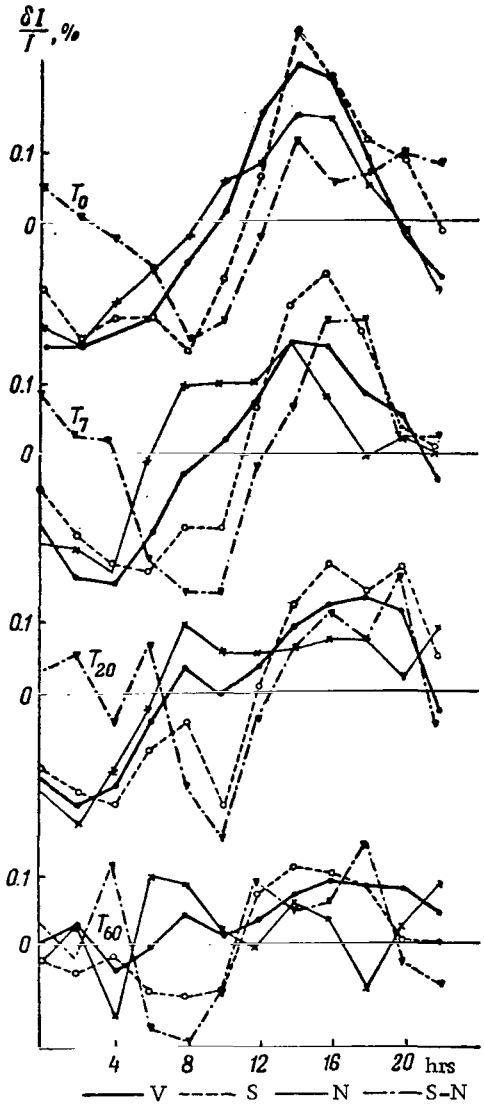

Fig. 1. Diurnal variations at Yakutsk during 1958-1959.

T_o, T_7, T_{20}, T_{60} - readings of counter telescopes at 0, 7, 20 and 60 m water equivalent; V, S and N represent the telescopes pointing in the vertical, south and north directions respectively; S-N - difference between the readings of the south and north telescopes.

Table 2

Station	Period of observation	Level, m water equivalent	Vertical				South				North				South–North	
			A_h	t_h	A_hW	t_hW	A_h	t_hW	A_hW	t_hW	A_h	t_h	A_hW	t_hW	A_h	t_h
Yakutsk	IX 1954–XI 1955	60	0.07 ± 0.02	4.0 ± 2	—	—	0.06 ± 0.02	2.0 ± 2	—	—	0.06 ± 0.02	7.0 ± 2.0	—	—	0.03	23.0
Chacaltaya	1953–1954	30	0.12	5.0	—	—	—	—	—	—	—	—	—	—	—	20.0
Yakutsk	1958–1959	Ground level	0.18	15.5	0.34	14.8	0.21	16.7	0.37	16.0	0.14	14.1	0.30	14.1	0.13	—
»	1958–1959	7	0.16	15.7	0.24	15.4	0.19	16.7	0.27	16.4	0.12	14.2	0.20	14.2	0.16	18.0
»	1958–1959	20	0.12	15.8	0.14	15.8	0.16	17.3	0.18	17.0	0.10	14.7	0.12	14.6	0.20	20.0
»	1958–1959	60	0.04	17.0	0.04	17.0	0.09	17.0	0.08	17.0	0.02	14.6	0.02	14.70	0.08	19.0
»	1958–1959	Neutrons	0.28	14.4	—	—	—	—	—	—	—	—	—	—	—	—

The time of the maximum in the diurnal variation of the north telescope occurs 2—3 hours before the maximum on the south telescope, and this holds at all levels.

Consider now the south-north difference curves for the diurnal variation. It is evident that this difference is independent of the diurnal variation of atmospheric origin. The general character of the south-north curves is the same at all levels and its maximum occurs at 1600—2000 hrs. However, the amplitude of this difference increases with increasing depth of recording. In fact, the ratio of the south-north differences and the corresponding quantities for the vertical telescope are less than unity at the surface and at a depth of 7 m water equivalent, while at 20 and 60 m water equivalent they are equal to 2.

It should be noted that the above properties of the ground-level diurnal variation at Yakutsk in 1958-1959 are in agreement with earlier (1950) studies [9]. Both series of measurements were carried out near the maximum of solar activity and the observed agreement is apparently due to this circumstance.

4. In order to explain the observed behavior of the diurnal variations, it is first necessary to determine the energy spectrum of the variation and then allow for the effect of the geomagnetic field on the trajectories of the particles reaching the earth at different angles of incidence.

The energy spectrum of the diurnal variation is best determined with the aid of the neutron monitor and the south telescopes, since the amplitude of the diurnal variation is then a maximum and, as will be shown below, the neutron monitor and the south telescopes receive particles arriving from almost the same region in the plane perpendicular to the plane of the ecliptic.

The coupling coefficients $W(\epsilon, h)$ obtained in [4], the method put forward by Dorman [1], and the neutron and μ-meson data obtained from the diurnal variation at Yakutsk were used to deduce the following energy spectrum:

$$\frac{\delta D(\epsilon)}{D(\epsilon)} = \begin{cases} -0.16 \cdot \epsilon^{-1}, & \text{when } \epsilon > 13 \text{ BeV}, \\ 0, & \text{when } \epsilon < 13 \text{ BeV}. \end{cases} \quad (1)$$

This spectrum is in good agreement with the results obtained in [1] and [4] and can now be used in conjunction with the results of Brunberg and Dattner [10] on the charged-particle trajectories in the geomagnetic field and the known directional properties of the telescopes to determine the effect of the geomagnetic field on the trajectories of the incident particles.

The effective angle of drift in the south-north plane is given by [1]

$$\Phi = \frac{\int_{\epsilon_{min}}^{\infty} \Phi(\epsilon) W(\epsilon, h) n \frac{\delta D(\epsilon)}{D(\epsilon)} d\epsilon}{\int_{\epsilon_{min}}^{\infty} W(\epsilon) \frac{\delta D(\epsilon)}{D(\epsilon)} d\epsilon}; \quad (2)$$

The corresponding result for east-west is

$$\Psi = \frac{\int_{\epsilon_{min}}^{\infty} \overline{\Psi}(\epsilon) W(\epsilon, h) n \frac{\delta D(\epsilon)}{D(\epsilon)} d\epsilon}{\int_{\epsilon_{min}}^{\infty} W(\epsilon, h) \frac{\delta D(\epsilon)}{D(\epsilon)} d\epsilon}; \quad (3)$$

In both expressions $W(\epsilon, h)$ is the coupling coefficient at the particular level of recording [4], ϵ_{min} is the minimum energy of the primary particles recorded at the level, and $\frac{\delta D(\epsilon)}{D(\epsilon)}$ is the relative change in the energy spectrum of the primary particles which are responsible for the diurnal variation.

Knowing the angle of drift in the east-west plane, the direction of the source of the diurnal variation can be determined from the formula

$$\varkappa = \Psi + 15(t_{max} - 12). \quad (4)$$

Table 3 shows the angles of drift Φ and Ψ calculated in this way, and also the direction of the source of diurnal variation $\varkappa$. It is clear from this table that all the accumulated directional data on the diurnal variations for

Table 3

Level, m water equivalent	Vertical			South			North		
	Φ	ψ	$\varkappa$	Φ	ψ	$\varkappa$	Φ	ψ	$\varkappa$
Ground level . .	20	38	80	16	22	82	24	53	84
7	32	34	85	25	11	77	50	57	90
20	42	28	85	24	6	81	59	50	89
60	50	15	90	25	3	78	72	33	74
Mean . . .	—	—	85	—	—	79	—	—	84

1958-1959 lead to the same values of $\varkappa$ in spite of the fact that the observed difference between the maxima for the south and north directions was about 4 hours.

The average value of $\varkappa$ was found to be $83 \pm 4°$. This means that the source of the diurnal variations lies left of the earth-sun line in a direction practically at right angles to this line. Thus, the geomagnetic field is responsible for the difference in the phases of the diurnal variation of cosmic rays arriving from different azimuths.

Analysis of the diurnal variation data over the seasons of 1958-1959 (this will be discussed elsewhere) shows that the general nature of the diurnal variations is almost the same in all seasons.

This means that the source of the diurnal variation takes part, together with the earth-sun line, in the annual motion about the sun, and remains left of this line throughout this period.

It is evident from Table 3 that the effective values of the angle Φ for different levels and directions of recording are not the same. This means that the source of the diurnal variation has appreciable dimensions in the plane perpendicular to the plane of the ecliptic. However, if the strength of the source is the same at all points, i.e. all parts of the source give rise to similar spectra, then the spectrum obtained in this work may be used to show that the amplitudes of the diurnal variations for neutrons at 0, 7, 20 and 60 m water equivalent, should be 0.28, 0.36, 0.26, 0.18 and 0.08% respectively.

As we can see from Table 2, these expected percentages are in agreement with the experimental results for the south telescopes only, while they are significantly smaller in the case of the vertical and north telescopes. This situation can be explained by the fact that the strength of the

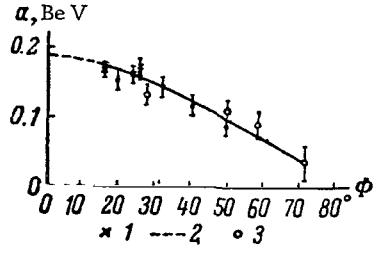

Fig. 2. Distribution of the strength, a, of the source of the diurnal variation in the plane perpendicular to the plane of the ecliptic.

1 - south telescopes; 2 - vertical telescopes;
3 - north telescopes.

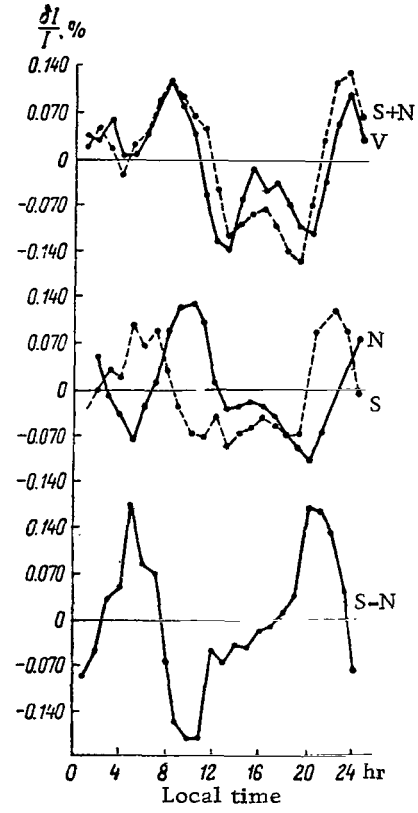

Fig. 3. Diurnal variation at 60 m water equivalent in 1954-1955.

V, S and N are the readings of the telescopes pointing vertically upward, south and north respectively; S + N and S - N are the sum and difference of the readings of the south and north telescopes respectively.

source of the diurnal variation in the plane perpendicular to the plane of the ecliptic is a function of the angle Φ, i.e. it may be written as $a(\Phi)$.

We have calculated this function using the data of Tables 2 and 3 and the spectrum quoted above. Fig. 2 shows the strength distribution for the source of the diurnal variation in the plane perpendicular to the plane of the ecliptic. It is clear from this figure that a smooth curve can be drawn through all the points. Extrapolation to $\Phi = 0°$ yields $a = 0.18$ BeV. The curve of Fig. 2 may be used to determine the amplitude of the diurnal variation in the

various cosmic-ray components with the aid of the formula

$$\frac{\delta D(\varepsilon)}{D(\varepsilon)} = a(\Phi) \int_{13}^{\infty} \frac{W(\varepsilon)}{\varepsilon} d\varepsilon.$$

Thus, the above results constitute a new experimental confirmation in the high-energy range of Dorman's theory [1] that solar corpuscular streams carrying frozen-in regular magnetic fields are the source of the average solar diurnal variation. The observed phase difference in the diurnal variation is explained by the effect of the geomagnetic field on the trajectories of the particles.

5. Figure 3 shows the diurnal variations in the cosmic ray intensity at a depth of 60 m water equivalent, which was recorded in 1954-1955 by counter telescopes pointing vertically upwards and in the south and north directions at 30° to the vertical. Comparison of Figs. 3 and 1 indicates that, at these two different times and different solar situations, the diurnal variations exhibited opposite behaviors. Thus, during the maximum solar activity of 1958-1959 the diurnal variation is clearly defined with the maximum occurring in the afternoon for all directions, while during the minimum of 1954-1955 the diurnal variation has a maximum in the morning (0600—0800 hrs) and an additional maximum at night (2200—2300 hrs). The time of the diurnal-variation maximum in opposite azimuths during the maximum solar activity, exhibits the opposite behavior as compared with 1954-1955. The measurements of Regener [13] at Chacaltaya 3°S geomag. lat. at a depth of 30 m water equivalent in 1953-1954, in which he used a vertical telescope, yielded analogous results. It is clear from Table 2 that at Chacaltaya, the diurnal variation at 30 m water equivalent had an amplitude of 0.12% and the maximum occurred at 0500 hrs local time.

The south-north difference curve shows two well defined maxima, one at 0500 hrs and the other at 2000 hrs local time, with amplitudes of less than 0.10%.

This sharp change in the properties of the diurnal variation during the period of minimum solar activity may be explained by a reduction in the frequency of ejection of corpuscular streams by the sun, and the predominance of corpuscular streams which return to the sun and are extended, highly turbulent, and are emitted earlier during the maximum of solar activity. The electric field of such streams is directed in the opposite direction to that observed during the activity maximum, and hence the source of diurnal variations should lie right of the earth-sun line, which is in agreement with observations.

This explanation must be subjected to a more detailed verification. This can be done with the aid of the Yakutsk apparatus during the next solar activity maximum.

In conclusion, the author would like to express his deep gratitude to Candidates of Physicomathematical Sciences, A.I. Kuz'min and L.I. Dorman for their valuable advice.

REFERENCES

1. Dorman, L.I. Variatsii kosmicheskikh luchey (Cosmic ray variations). Gostekhizdat, Moscow, 1957.

2. Rau, W. Naturwiss., 27, 803, 1939.

3. MacAnuff. Thesis, London, 1950.

4. Kuz'min, A.I. Dissertation, NIYaF MGU, Moscow, 1959.

5. Kuz'min, A.I. and Skripin, G.V. Tr. YaFAN SSSR, ser. fizich., No. 4, 67, 1961.

6. Kuz'min, A.I. Tr. YaFAN SSSR, ser. fizich., No. 3, 99, 1960.

7. Alfvén, H. and Malfors, K.G. Ark. Mat. Astr. Fys., 29A, 24, 1943.

8. Kolhörster, N. Phys. Zs., 42, 155, 1941.

9. Elliot, H. and Dolbear, D.W. Proc. Phys., 63, 137, 1950.

10. Brunberg, E.A. and Dattner, A. Tellus, 6, 73, 1954.

11. Kuz'min, A.I., Skripin, G.V. and Yarygin, A.V. Tr. YaFAN SSSR, ser. fizich., No. 2, 34, 1958.

12. Danilov, A.A., Druzhinin, S.N., Kapustin, I.N. and Skripin, G.V. Tr. YaFAN SSSR, ser. fizich., No. 3, 40, 1959.

13. Regener, B.X. Proceedings of the International Conference on Cosmic Rays, IV, 218, 1960.

A. I. Kuz'min and G. V. Skripin

SOME MAIN PROPERTIES OF DISTURBED DIURNAL VARIATIONS IN THE INTENSITY OF COSMIC RAYS

It has been found by a number of workers [1—3] that during and after magnetic storms there is an increase in the amplitude of the solar diurnal variation and a shift in the position of the maximum toward an earlier time.

According to Dorman's theory [4], this is explained by the fact that a corpuscular stream carrying a strong frozen-in magnetic field reaches the earth during magnetic storms. As a result, the source of the solar-diurnal variation becomes displaced toward the earth-sun line and the amplitude of the variations increases with the energy of the recorded particles.

This theory has not as yet been adequately verified experimentally. The experimental results reported by Kuz'min [5] cannot be used in a quantitive comparison between the theory and experiment, since they are based on the average characteristics of variations which do not take into account the fact that isolated storms may be ineffective in this respect.

In addition to a qualitative analysis, the present paper is concerned with the determination of the main properties of disturbed solar diurnal variations, and a quantatative comparison of theory with experiment.

1. BASIC DATA AND THEIR PROCESSING

The present work was based on cosmic-ray intensity data for 1957—1959, which were obtained with the aid of the composite installation described in [6]. The measuring instruments were located at ground level and underground at depths of 7, 20 and 60 m water equivalent (m w.e.). The cosmic-ray intensity data were corrected for the barometer effect with the aid of constant coefficients equal to -0.13, -0.10, -0.08 and -0.04% mb^{-1} for the meson component measured by semi-cubic telescopes at ground level and at depths of 7, 20 and 60 m w.e. The final results were also corrected for diurnal temperature oscillations determined from aerological sounding data and the temperature-coefficient density function [4].

The times of commencement and termination of magnetic storms and their characteristics were determined from cosmic data published by the Institute of Terrestrial Magnetism of the Academy of Sciences, USSR.

Only those periods of effective magnetic storms were considered during which there was a decrease in the intensity of not less than 1% as indicated by the ground level μ-meson detectors. The effect of the decrease in the intensity was excluded by subtracting from the two hourly values of the intensity the continuous curve corresponding to the mean variation in the intensity. The commencement of the magnetic storm was taken as the zero day in the method of superposition of epochs. Moreover, a determination was made of the mean diurnal variation during a number of preceding and subsequent days. The resulting data were compared with the mean annual diurnal variation which was adopted as the characteristic of a quiet day.

At first, magnetic storms were not sub-divided into effective and ineffective from the point of view of the degree to which they affected the diurnal variation. Subsequently, the magnetic storms which significantly disturbed the diurnal effects were subjected to further analysis.

Errors in the parameters of the diurnal effect were determined from errors in the experimental data, with allowance for diurnal oscillations in the meteorological factors.

2. MEAN DISTURBED SOLAR DIURNAL VARIATIONS OF COSMIC RAYS DURING MAGNETIC STORMS

Figure 1 shows the mean diurnal variations in the intensity of cosmic rays during magnetic storms. In order to increase the statistical weight of the data, days corresponding to subsequent days +1 and +2 are combined into a single column which is designated "after the storm." Moreover, Table 1 gives the amplitude and the time of the maximum of the first harmonic of the solar diurnal variations with allowances for the diurnal oscillations in the free atmosphere.

It is clear from these data that there is an increased diurnal variation in the "after-the-storm" days and the time of the maximum is displaced toward an earlier instant. At the same time, the amplitude of the first harmonic increases at all the levels underground, and for all components, by approximately 1.4 ± 0.4 times the relative mean annual value. It is also evident from Fig. 1 that variations at the depth of 60 m w.e. increase to a much greater extent. It may, therefore, be considered that the first harmonic of the solar diurnal variations during magnetic storms does not fully characterize the true diurnal variations of cosmic rays. In this connection the fourth and fifth lines of

Table 1 gives the values of σ, which represents the dispersion of the two-hourly values of the intensity relative to the mean diurnal value for the period of magnetic storms and the mean annual value.

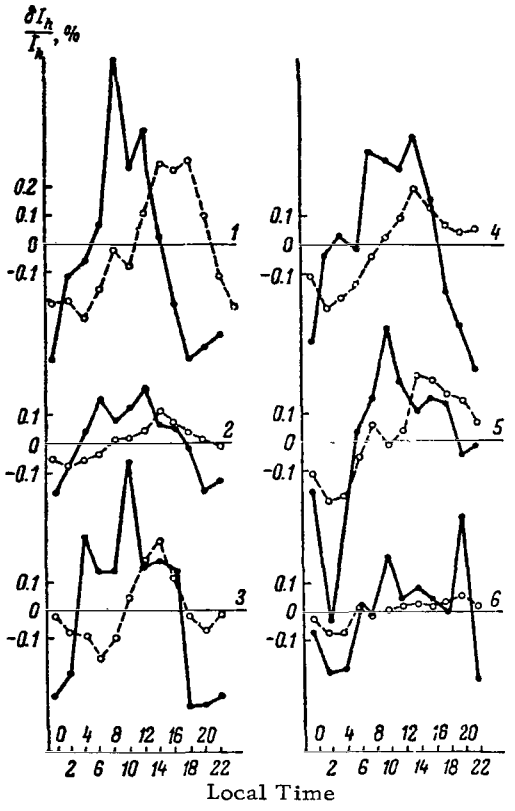

Fig. 1. Diurnal variations during eight magnetic storms in 1957-1958.

1 - neutron monitor; 2 - ionization chamber; 3 - vertical counter telescope at ground level; 4—6 - vertical telescopes at 7, 20 and 60 m w.e. respectively. Continuous lines - disturbed solar variations; broken lines - mean diurnal variation for 1958.

It is obvious that the variance is proportional to the true diurnal variation and is given by

$$\sigma = \sqrt{\sigma_N^2 + \sigma_W^2 - \sigma_{st}^2},$$

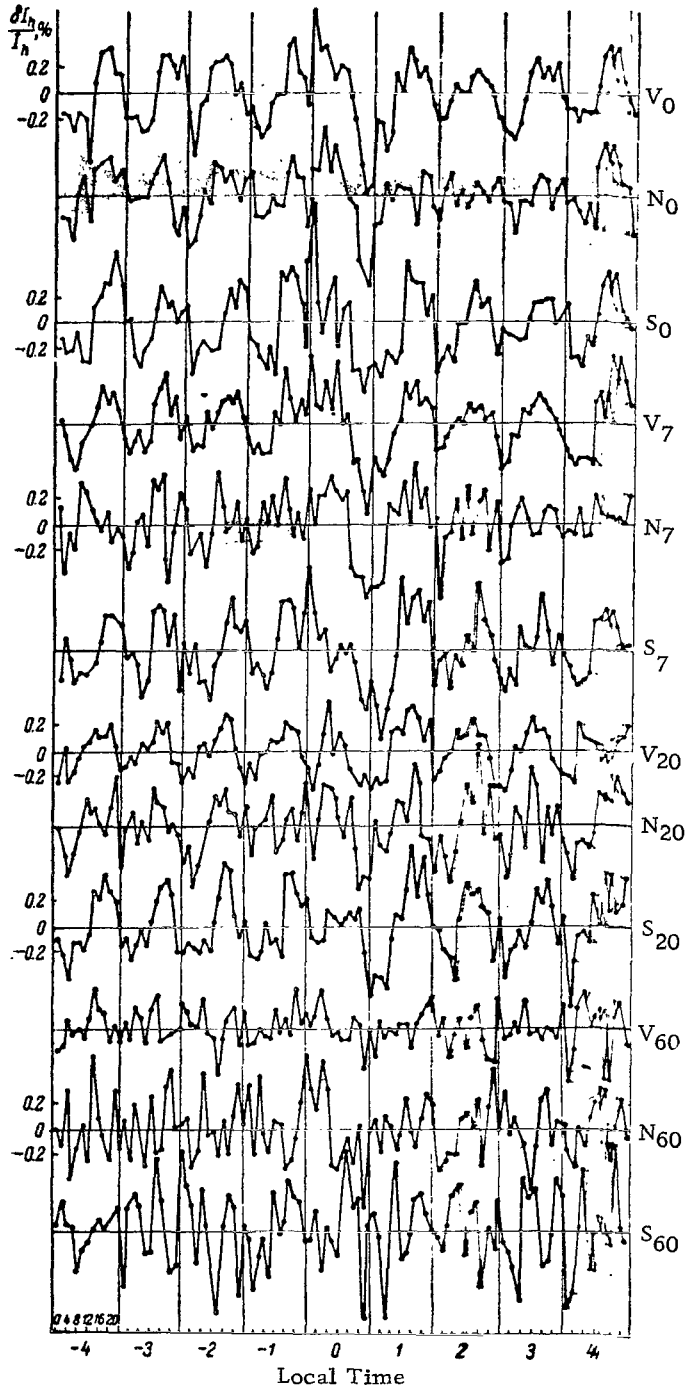

Fig. 2. Two hourly values of the cosmic-ray intensity during magnetic storms.

Subscripts 0, 7, 20 and 60 represent levels of recording below ground level; V, S, and N - directions of telescopes (vertical, and south and north at 30° to the zenith).

Table 1

Changes in the diurnal variations in cosmic-ray intensity during magnetic storms.

	Parameter	Neutrons		ASK ionization chamber		Semi-cubic telescope							
						Ground level		7 m w.e.		20 m w.e.		60 m w.e.	
		A_{hW}	t_{max}	A_{hW}	t_{max}	A_{hW}	t_{max}	A_{hW}	t_{max}	A_{hW}	t_{max}	A_{hW}	t_{max}
Storm days	1st harmonic A'_{hW}	0.43±0.06	9.1	0.32±0.06	11.0	0.47±0.08	10.0	0.35±0.07	11.0	0.30±0.51	13.20	0.9±0.04	14.0
Annual mean	A_{hW}	0.28±0.03	14	0.28±0.03	14.5	0.36±0.04	14.0	0.27±0.03	14.0	0.18±0.25	15.4	0.05±0.02	16.2
Ratio	$\frac{A'_{hW}}{A_{hW}}$	1.54±0.4	—	1.14±0.3	1.3	1.3±0.3	—	1.3±0.40	—	1.7±0.6	—	1.8±0.3	—
Storm days	standard σ'	0.58		0.34		0.50		0.50		0.50		0.28	
Annual mean	σ	0.3		0.25		0.34		0.27		0.25		0.08	
Ratio	$\frac{\sigma'}{\sigma}$	1.9		1.4		1.4		1.8		2.0		3.5	

where σ_N is determined directly from the diurnal variation in the intensity corrected for the barometer effect; $\sigma_W = \frac{A_W}{\sqrt{2}}$, where A_W is the amplitude of the expected diurnal variations due to diurnal oscillations in atmospheric temperature; and $\sigma_{st} = \frac{100}{\sqrt{N}}$.

Comparison of the third and six lines of Table 1 shows that disturbances in the diurnal variations are much greater than would be expected on the basis of the amplitude of the first harmonic. The degree of disturbance of the solar diurnal variations during magnetic storms increases with depth. Thus, it may be said that during magnetic storms there is both a change in the strength of the source and an appreciable hardening in the spectrum of the primary variations.

It must be emphasized once again that in this section we do not take into account magnetic storms which are especially effective in the sense of producing disturbances in diurnal variations. Therefore, the results obtained here may be regarded as the lower limit of the true changes during magnetic storms.

One would expect on the basis of the theoretical ideas given in [4] that the character of the diurnal variations would depend on the strength and direction of the magnetic and electric fields in the stream and the disposition of the stream relative to the earth. We have therefore selected effective magnetic storms which were accompanied by certain definite forms of the diurnal variation, both before and after the commencement of the storms. From among the magnetic storms for 1958-1959 we selected 17 storms with a well defined Forbush effect for which the diurnal variations four days before and four days after the storm had a clearly defined diurnal character with the maximum during the evening. This selection was carried out on the basis of the data obtained at 20 m w.e., where meteorological factors are relatively unimportant and statistical errors are low enough for the selection of individual diurnal variations.

Figure 2 shows the two hourly values of the cosmic-ray intensity corrected for the barometer effect during these 17 storms for the vertical, north, and south telescopes at the earth's surface and at various levels underground.

The deviation of the intensity from the average for each day is plotted along the ordinate axis and the local time (in hours) along the abscissa axis.

It is evident from Fig. 2 that the clearly defined diurnal variation with a maximum during the evening, which is normally shown by the vertical telescope data for 20 m w.e., is also present for all directions and all levels of recording both before and after the storm, except for the 60 m w.e. level where the effect is not clearly exhibited owing to large statistical errors. There is also a noticeable tendency to an increase in the amplitude of the

diurnal variation toward the zero day, i.e. the day of commencement of the magnetic storm. The south telescopes show a more clearly defined diurnal variation than the north telescopes.

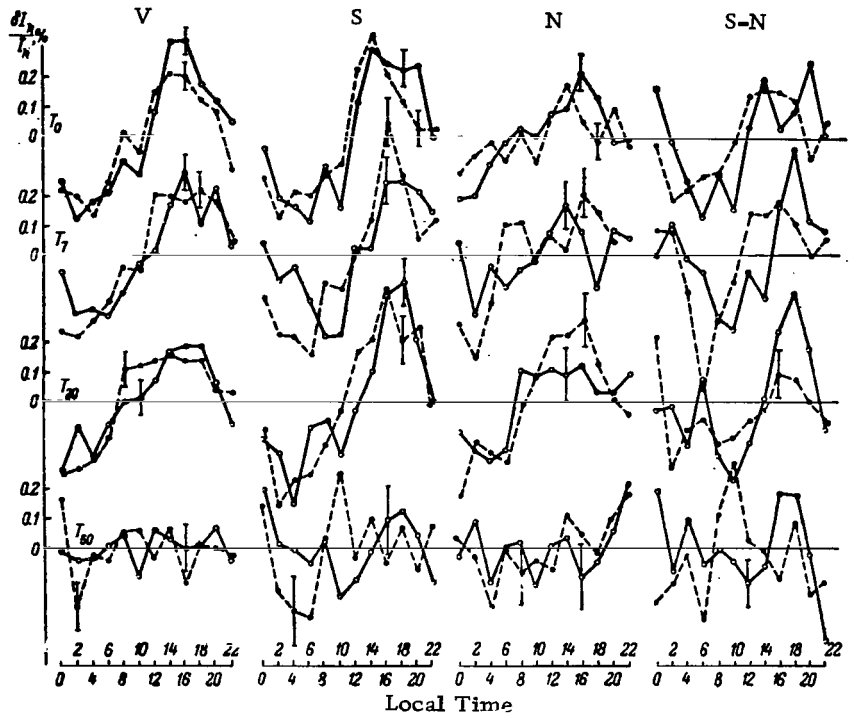

Fig. 3. Diurnal variation at different depths before (continuous line) and after (dashed line) the commencement of magnetic storms.

S—N - represents the difference between the readings of the south and north telescopes; the remaining notations are the same as in Fig. 2.

In order to increase the statistical weight of the data, the four days before the storm were combined into a single group; this was also done for the four days after the beginning of the storm. Fig. 3 shows the diurnal variations, corrected for the barometer effect, for these two groups of days in different directions at each of the above recording levels.

Table 2 gives the amplitudes and phases of the diurnal variations in the intensity, after correction for the barometer and temperature effects in these two groups, and also for the zero day after smoothing in a 24 hour interval, and the diurnal variations for two years (1958-1959).

Table 2

Parameters of diurnal variation in the cosmic-ray intensity during seventeen magnetic storms.

Level m w.e.	Period of observation	Vertical				South				North			
		A_h	t_h	A_{hW}	t_{hW}	A_h	t_h	A_{hW}	t_{hW}	A_h	t_h	A_{hW}	t_{hW}
Ground level	Before storm	0.27±0.02	16.0±0.3	0.38	15.5	0.29±0.03	16.9±0.5	0.40	16.20	0.15±0.03	14.4±0.6	0.25	14.4
	Zero day	0.27±0.02	13.2	0.45	14.0	—	—	—	—	—	—	—	—
	After the storm	0.22±0.02	15.0±0.4	0.40	14.5	0.25±0.03	15.5±0.5	0.43	15.0	0.08±0.03	15.5±0.5	0.26	14.4
	Mean for 2 years	0.18	15.5	0.36	14.8	0.22	16.7	0.40	16.2	0.14	14.1	0.32	14.1
7	Before storm	0.22±0.03	16.8±0.5	0.27	16.4	0.24±0.04	19.0±0.8	0.29	18.2	0.09±0.04	16.0±1.5	0.14	15.5
	Zero day	0.29±0.06	13.0	0.38	13.2	—	—	—	—	—	—	—	—
	After the storm	0.25±0.03	15.5±0.5	0.34	15.2	0.31±0.04	17±0.7	0.40	17.5	0.15±0.04	14.3±1.0	0.24	14.3
	Mean for 2 years	0.16	15.7	0.25	15.4	0.10	16.7	0.28	16.0	0.12	14.2	0.20	14.2
20	Before storm	0.17±0.03	17.0±0.8	0.18	17.0	0.25±0.04	17.0±0.7	0.26	17.0	0.014±0.0	44.7±1.0	0.15	14.7
	Zero day	0.24±0.06	12.0	0.26	12.2	—	—	—	—	—	—	—	—
	After the storm	0.22±0.03	15.7±0.7	0.24	15.5	0.30±0.04	16.2±0.6	0.32	16.0	0.21±0.04	14.7±0.8	0.23	14.7
	Mean for 2 years	0.12	16.0	0.14	15.9	0.16	17.3	0.18	19.0	0.10	14.7	0.12	14.7
60	Before storm	0.05	20	0.06	20	0.08±0.06	21.2±3.0	0.08	21.2	0.05±0.06	194.0	0.05	19.0
	Zero day	—	—	—	—	—	—	—	—	—	—	—	—
	After the storm	0.08	17	0.08	17.0	0.09±0.05	15.4±3.0	0.09	15.4	0.09±0.6	19±2.2	0.09	19.0
	Mean for 2 years	0.06	17.4	0.04	17.4	0.09	18.0	0.06	18.0	0.02	14.6	0.02	14.6

Remark: A_h and t_h are the amplitude and time of the diurnal variation after correction for the barometer effect respectively. A_{hW} and t_{hW} refer to the same quantities after correction for the barometer and temperature effects.

It is evident from these data that both before and after the commencement of a magnetic storm the amplitude of the diurnal variation is larger by a factor of 1.5—2 as compared with the mean diurnal variation for two years. For the zero day, the maximum is displaced by 2—4 hours toward an earlier time and the amplitude is greater than the mean value. However, there were no appreciable changes during the maximum for days before and after the storm as compared with the mean.

Table 2 also shows that the amplitude of the diurnal variation in the southern direction is much greater, and the maximum occurs later, than for the vertical and northern directions. This situation was found to occur at all the recording levels both before and after magnetic storms, and also throughout the bi-annual period of observation.

Table 3

Comparison of the amplitudes of diurnal variations.

Instrument	Vertical			South		North	
	Before	Zero	After	Before	After	Before	After
T_0	1.1	1.3	1.1	1.0	1.1	0.8	0.8
T_7	1.1	1.5	1.4	1.0	1.4	0.7	1.2
T_{20}	1.3	1.9	1.7	1.4	1.8	1.2	2.0
T_{60}	1.0	2.0	2.0	—	—	—	—

Table 3 gives the ratios of the amplitudes of the diurnal variations for days before and after the storm, and for the day corresponding to the commencement of the storm, to the amplitudes of the bi-annual mean diurnal variation. These data are corrected for the barometer and temperature effects.

It is clear from Table 3 that there is a relative increase in the diurnal variation with depth during zero days and after commencement, while prior to the storm this increase is small or is absent altogether. This suggests that there is a hardening in the energy spectrum of the diurnal variation during disturbed days as compared with the mean spectrum.

3. ENERGY SPECTRUM OF DISTURBED SOLAR-DIURNAL VARIATIONS

The energy spectrum of disturbed diurnal variations in cosmic rays will at first be determined with the aid of data on the variations in the μ-meson

component at ground level and at various depths underground, corrected for meteorological effects. Later this spectrum will be determined by the method of coupling coefficients [4, 5].

The energy spectrum of extra-atmospheric variations in the μ-meson component can be determined as follows.

The readings of identical instruments at different depths underground are reduced to a single level (sea-level intensity) and a determination is made of the integral spectrum of the μ-mesons which are responsible for the extra-atmospheric solar diurnal variations during the magnetic disturbances. This spectrum is then compared with the corresponding spectrum of the "undisturbed stream". It is clear that the ratio of these integral spectra yields the μ-meson variation spectrum $\frac{\delta D(\varepsilon_\mu)}{D(\varepsilon_\mu)}$.

When the spectrum $\delta D(\varepsilon_\mu)$ of μ-mesons which are responsible for the extra-atmospheric solar diurnal variations and the spectrum of the undisturbed stream $D(\varepsilon_\mu)$ are approximated by power functions, then the resulting spectrum of the variations in the energy range 10^{10}–10^{13} eV is independent of the particular model of the elementary interaction and the subsequent passage of secondary and primary particles through the atmosphere. Therefore, in this approximation, $\frac{\delta D(\varepsilon_\mu)}{D(\varepsilon_\mu)}$ is proportional to the spectrum of the primary variations $\frac{\delta D(\varepsilon)}{D(\varepsilon)}$.

Table 4 gives the results of calculations of the exponents in the integral spectrum of μ-mesons responsible for disturbed diurnal variations, and for the stream as a whole.

It is evident from Table 4 that the spectrum of μ-mesons undergoing disturbed diurnal variations is much softer than the spectrum of the stream as a whole. However, the spectrum is much harder than the spectrum of μ-mesons responsible for the diurnal variations during the mean quiet days [5], which is in qualitative agreement with Dorman's theory [4].

In order to obtain a quantitative estimate of the diurnal variations, it is necessary to determine the variation spectrum by the method of coupling coefficients [4, 5].

Here we determined the primary variations with the aid of two significantly different coefficients of coupling [4, 5].

Since the disturbed diurnal variations in general decrease with increasing mean energy of the recorded particles, we shall take the trial spectrum in the form

$$\frac{\delta D(\varepsilon)}{D(\varepsilon)} = \begin{cases} 0, & \text{if} \quad \varepsilon < \varepsilon_0 \\ a\varepsilon^{-\alpha}, & \text{if} \quad \varepsilon > \varepsilon_0. \end{cases} \tag{1}$$

Table 4

Comparison of the exponent in the integral spectrum of μ-mesons responsible for the disturbed diurnal variations and of the entire μ-meson beam.

	Exponents γ' for μ-mesons responsible for disturbed diurnal variations		Exponents γ_0 for the entire μ-meson beam	$\gamma' - \gamma_0 = \Delta\gamma$	
	Choice 1	Choice 2		Choice 1	Choice 2
T_0 & T_7	—1.3	—1.1	—0.8	—0.5	—0.3
T_0 & T_{20}	—1.5	—1.6	—1.1	—0.4	—0.5
T_0 & T_{60}	—2.2	—2.2	—1.4	—0.8	—0.8
T_7 & T_{20}	—1.7	—2.0	—1.5	—0.2	—0.5
T_7 & T_{60}	—2.4	—2.5	—1.7	—0.7	—0.8
T_7 & T_{60}	—2.7	—2.9	—1.8	—0.9	—1.1
Average . .				—0.6	—0.7

In addition, we shall also try the spectrum predicted by Dorman's theory [4] which is given by

$$\frac{\delta D(\epsilon)}{D(\epsilon)} = \pm \frac{f}{\epsilon} \begin{cases} 1, & \text{if } \epsilon > \frac{\epsilon_1}{2}, \\ 1 - \frac{2}{\pi} \sin^{-1}\left(\frac{\epsilon_1}{2\epsilon} - 1\right), & \text{if } \frac{\epsilon_1}{4} < \epsilon < \frac{\epsilon_1}{2}, \\ 0, & \text{if } \epsilon < \frac{\epsilon_1}{4}. \end{cases} \qquad (2)$$

Table 5 shows the results of calculations of these expected ratios of variations for different assumed primary variation spectra. In these variations the coupling coefficients for inclined telescopes were taken to be equal to the coefficients for a semi-cubic telescope at the particular depths.

Table 5 shows that the experimental data on the disturbed diurnal variations during magnetic storms is not inconsistent with (1) for $\alpha = -0.5$ and $\epsilon_1 = 10$—15 BeV. Moreover, the experimental data are in agreement with the spectrum predicted by Dorman's theory [4] to within the experimental error. The best agreement between experiment and theory is found to occur for $f = 0.3$ and $\epsilon_1 = 80$—100 BeV.

The exponent in (1) is in agreement with the exponent in the spectrum of variations determined from direct measurements by a system of identical instruments at different depths underground. Since the spectrum of the form

Table 5

Amplitude ratios for disturbed diurnal variations.

Trial spectrum	ε_1	$\frac{T_7}{T_0}$	$\frac{T_{20}}{T_0}$	$\frac{T_{60}}{T_0}$
Expected from [4, 5]				
$\frac{\delta D(\varepsilon)}{D(\varepsilon)} = \pm \frac{f}{\varepsilon}$ { 1 when $\varepsilon > \frac{\varepsilon_1}{2}$; $1 - \frac{2}{\pi} \sin^{-1}\left(\frac{\varepsilon}{2\varepsilon} - 1\right)$ when $\frac{\varepsilon_1}{4} < \varepsilon < \frac{\varepsilon}{2}$; 0 when $\varepsilon < \frac{\varepsilon_1}{4}$	20	0.51	0.31	0.12
	60	0.72	0.45	0.18
	100	1.06	0.72	0.30
	120	1.20	0.87	0.36
	160	1.90	1.74	0.76
	240	1.90	3.2	1.75
$\frac{\delta D(\varepsilon)}{D(\varepsilon)} = \begin{cases} a\varepsilon^{-0,5} \text{ when } \varepsilon > \varepsilon_1 \\ 0 \text{ when } \varepsilon < \varepsilon_1 \end{cases}$	3	0.75	0.62	0.34
	7	0.77	0.65	0.36
	10	0.82	0.70	0.38
	15	0.87	0.77	0.42
$\frac{\delta D(\varepsilon)}{D(\varepsilon)} = \begin{cases} a\varepsilon^{-0,7} \text{ when } \varepsilon > \varepsilon_1 \\ 0 \text{ when } \varepsilon < \varepsilon_1 \end{cases}$	3	0.69	0.50	0.22
	7	0.72	0.53	0.24
	11	0.77	0.58	0.26
	15	0.84	0.66	0.30
$\frac{\delta D(\varepsilon)}{D(\varepsilon)} = \begin{cases} a\varepsilon^{-1} \text{ when } \varepsilon > \varepsilon_1 \\ 0 \text{ when } \varepsilon < \varepsilon_1 \end{cases}$	3	0.60	0.37	0.17
	7	0.65	0.40	0.18
	11	0.71	0.46	0.21
	15	0.84	0.55	0.25
Experimental				
Before the storm: Vertical		0.72	0.49	0.16
Before the storm: South		0.72	0.65	0.20
Before the storm: North		0.56	0.60	0.20
After the storm: Vertical		0.88	0.68	0.23
After the storm: South		0.98	0.84	0.24
After the storm: North		1.00	1.15	0.43

$\frac{\delta D(\varepsilon)}{D(\varepsilon)} = a\,\varepsilon^{-\alpha}$ and the theoretical spectrum predict an appreciable hardening in the spectrum of diurnal variations during magnetic storms, it may be concluded that the energy spectrum deduced from the spectrum of μ-mesons is in agreement with the theoretically expected primary spectrum. The direction of the source of these variations may be determined with the aid of the diagram, given by Brunberg and Dattner [7], which represents the dependence of the angles Ψ and Φ on the particle energy in the geomagnetic field. Here we shall only estimate the effective values of these angles:

$$\Psi = \frac{\int \Psi(\varepsilon) W(\varepsilon) \frac{\delta D(\varepsilon)}{D(\varepsilon)} d\varepsilon}{\int W(\varepsilon) \frac{\delta D(\varepsilon)}{D(\varepsilon)} d\varepsilon},$$

$$\Phi = \frac{\int \Phi(\varepsilon) W(\varepsilon) \frac{\delta D(\varepsilon)}{D(\varepsilon)} d\varepsilon}{\int W(\varepsilon) \frac{\delta D(\varepsilon)}{D(\varepsilon)} d\varepsilon}.$$

The value of Ψ, will now be used to determine the direction of the effective source of the diurnal variations during the period of disturbances:

$$x = \overline{\psi} + 15\,(t_{max} - 12);$$

where t_{max} is the moment of the maximum of the diurnal variations in local time, and ψ is the effective angle of drift in the geomagnetic field.

It is clear from the results of calculations given in Table 6 that all the experimental data on diurnal variations in cosmic rays during magnetic storms lead to approximately the same value of $\varkappa$ in a large energy range (2–400 BeV). The average of all the data is 35 ± 5°. The effective value of the angle Φ increases with the energy of the recorded particles, reaching 50° at the depth of 60 m w. e. Hence it is clear that the source has large dimensions in the plane perpendicular to the planeof the ecliptic.

Table 6

Values for the angles of drift Ψ and Φ and the direction of the effective source of diurnal variations during magnetic storms.

Level, m w.e.	Vertical						South			North		
	Φ	Ψ	$\varkappa_1$	$\varkappa_0$	$\varkappa_2$	$\varkappa_3$	Φ	Ψ	$\varkappa_3$	Φ	Ψ	$\varkappa_3$
Ground level	30	35	35	35	73	87	22	20	65	38	52	88
7	36	29	29	29	75	94	23	10	93	50	55	90
20	48	26	44	41	76	101	23	5	65	59	50	90
60	50	12	42	—	87	—	23	2	53	72	30	—

Remark: $\varkappa_1$ represents the direction of the source of the diurnal variation deduced from data for days after the commencement of eight magnetic storms (choice 1); $\varkappa_0$ represents the direction of the source found from data for days of commencement of 17 storms (2nd choice); $\varkappa_2$ and $\varkappa_3$ — same as $\varkappa_0$ but for days after and before storm commencement respectively.

Table 6 also gives data on the variations before and after the storm, from which it is clear that, prior to the storm, the source lay left of the earth-sun line and became displaced toward this line as the commencement of the magnetic storm was approached. This effect was also observed after the termination of the storm, but in the reverse direction.

It follows that the source of the diurnal variations during magnetic disturbances is connected with a "mechanism" whose position in space is varying continuously.

The spectrum of the diurnal variations during magnetic disturbance is of the form

$$\frac{\delta D(\varepsilon)}{D(\varepsilon)} = \begin{cases} 0, & \text{if} \quad \varepsilon < 10\text{—}15 \text{ BeV}, \\ a\varepsilon^{-0.5}, & \text{if} \quad \varepsilon > 10\text{—}15 \text{ BeV}, \end{cases} \tag{1}$$

$$\frac{\delta D(\varepsilon)}{D(\varepsilon)} = \frac{f}{\varepsilon} \begin{cases} 1, & \text{if} \quad \varepsilon > \frac{\varepsilon_1}{2}, \\ 1 - \frac{2}{\pi} \sin^{-1}\left(\frac{\varepsilon_1}{2\varepsilon} - 1\right), & \text{if} \quad \frac{\varepsilon_1}{4} < \varepsilon < \frac{\varepsilon_1}{2}, \\ 0, & \text{if} \quad \varepsilon < \frac{\varepsilon_1}{4}. \end{cases} \tag{2}$$

Both spectra are much harder than the spectra of mean (quiet) diurnal variations [5]. This hardening of the spectrum is predicted by theory [4] and is explained by the perturbation of the cosmic rays by streams reaching the earth and carrying frozen-in magnetic fields. The effect of the electric and magnetic fields of the stream on the primary cosmic rays should lead to variations of type II.

Our experimental data can be made to agree with the theory if it is assumed that $\epsilon_1 = 100$ BeV and that the stream velocity is $u = 10^8$ cm/sec.

Since both before and after the storm there is occasionally an increase in the amplitude of the diurnal variation, the theory predicts that in such cases the frozen-in magnetic field in the stream should have a large component in the plane perpendicular to the plane of the ecliptic. If the proposed effect of corpuscular streams on cosmic ray variations is in fact correct, then it must be considered that during 1957-1959 the streams were most frequently emitted from the solar region with a latitude of about 15°.

The theoretical predictions are in good agreement with the south and north telescope data. In fact, the variations in the southern direction are greater by a factor of approximately two than the variations in the northern direction. This holds for all the recording levels. Such differences are only possible if the magnetic field is frozen-in in the plane perpendicular to the plane of the ecliptic. Experimental results on the position of the source of the variations and its change are also in agreement with the proposed effect of magnetic and electric fields on solar corpuscular streams reaching the earth.

In conclusion, let us list the main results of this work.

1. During magnetic disturbances there is a considerable change in the solar diurnal variation of cosmic rays. The disturbances in the amplitude and the position of the maximum of the diurnal cosmic-ray variation increases with increasing energy of the recorded particles (Tables 1 and 2).

2. The maximum change in the diurnal variation during magnetic storms was recorded at all the depths by the telescope pointing in a direction parallel to the plane of the ecliptic (the telescope was pointing southward at an angle of 30° to the vertical at the geographic latitude of 60°).

3. During magnetic storms the spectrum of solar diurnal variation is of the form

$$\frac{\delta D(\varepsilon)}{D(\varepsilon)} = \begin{cases} 0, & \text{if} \quad \varepsilon < 10\text{—}15 \text{ BeV}, \\ 0.03 \cdot \varepsilon^{-0.5}, & \text{if} \quad \varepsilon > 10\text{—}15 \text{ BeV}. \end{cases}$$

$$\frac{\delta D(\varepsilon)}{D(\varepsilon)} = \pm \frac{f}{\varepsilon} \begin{cases} 1, & \text{if} \quad \varepsilon > \frac{\varepsilon_1}{2} \\ 1 - \frac{2}{\pi} \sin^{-1}\left(\frac{\varepsilon_1}{2\varepsilon} - 1\right), & \text{if} \quad \frac{\varepsilon_1}{4} < \varepsilon < \frac{\varepsilon_1}{2}, \\ 0, & \text{if} \quad \varepsilon < \frac{\varepsilon_1}{4}, \end{cases}$$

where $f = 0.30$ and $\epsilon_1 = 80\text{—}100$ BeV. The source of these variations lies at an angle of $\varkappa = 35 \pm 5°$ left of the earth-sun line.

4. Many cases of considerable disturbance in solar diurnal variations were noted during 1957—1959, both during storms and before and after storms (Tables 1 and 2).

5. The main characteristics of the disturbed diurnal variations are in good agreement with the theory which explains them by the effect of electric and magnetic fields of solar corpuscular streams reaching the earth.

REFERENCES

1. Sekido, J. and Joshido, S. Rep. Ionos, Res. Japan, 4, 37, 1950.

2. Sekido, J. Rep. Ionos, Res. Japan, 4, 37, 1950.

3. Kuz'min, A.I. and Skripin, G.V. Tr. YaFAN SSSR, ser. fizich., No. 2, 107, 1958.

4. Dorman, L.I. Variatsii kosmicheskikh luchey (Cosmic-ray variations), Gostekhizdat, Moscow, 1957.

5. Kuz'min, A.I. Dissertation, NIYaF, MGU, Moscow, 1959.

6. Kuz'min, A.I., Skripin, G.V. and Yarygin, A.V. Tr. YaFAN SSSR, ser. fizich., No. 2, 34, 1958.

7. Brunberg, E.A. and Dattner, A. Tellus, 6, 73, 1954.

A.I. Kuz'min and G.V. Skripin

ON THE COEFFICIENT OF ABSORPTION OF COSMIC RAYS RESPONSIBLE FOR SOLAR DIURNAL VARIATIONS

1. In cosmic-ray variation studies it is usually necessary to compare the readings of a large number of identical instruments at different points on the earth's surface. In most cases these instruments are located in enclosures with different amounts of absorbing matter and different geometry so that the equivalent thicknesses are very different.

Since cosmic-ray variations may be due to particles with definite energy distributions, it follows that variations measured under different amounts of matter will be different. Such measurements may be used to determine the absorption coefficients and hence deduce information about the spectrum of particles undergoing the given variations.

The present note reports the results of a comparison of diurnal variations of the μ-meson component at ground level with identical ionization chamber measurements under different amounts of matter.

2. The ASK-1 and S-2 ionization chambers [1] were first used for the continuous recording of the hard cosmic-ray component at Moscow and Yatusk, and were subsequently transported to other locations with different amounts of covering matter.

The integral minimum and minimum effective filters were designed for the μ-meson spectrum at sea level [2] for each of the periods of recording, and their properties are summarized in Table 1.

The symbols in Table 1 are: D_c-thickness of the lead filter plus the steel envelope and wall of the chamber itself in g/cm^2 and D_e-thickness of the walls of the enclosure in g/cm^2.

It is evident from Table 1 that the removal of the counters from one enclosure to another gives rise to a considerable change in the integral effective filters. Moreover, there is an appreciable change in the mean compensated value of the ionization current due to μ-mesons which amounts to about 3—6% and is in good agreement with the coefficient of true absorption of μ-mesons ($\alpha_\alpha = -0.05\%$ [3]).

Table 1

Minimum and minimum effective screens for the ASK-1 and S-2 ionization chambers during 1949-1959.

Place and instrument	Period of recording	Minimum screen, g/cm^2		$D_c + D_e$	Minimum effective screen, g/cm^2		$D_c^e + D_e^e$
		D_c	D_e		D_c^e	D_e^e	
Moscow, ASK-1	1950— V 1954	120±1	70±0	190±8	147±1	90±10	237±10
Moscow, ASK-1	VII 1954—1958	120±1	20±3	140±3	147±1	26±5	173±4
Yakutsk, S-2	1949—1953	120±1	30±4	150±4	137±1	35±5	172±5
Yakutsk, ASK-1	1953—1958	120±1	90±3	210±3	147±1	120±4	267±4
Yakutsk, S-2	1955—1956	120±1	90±3	210±3	137±1	120±4	257±4
Yakutsk, S-2	IX 1956—1958	120±1	3±0.5	123±1	137±1	26±6	163±6

Table 2 gives the parameters of the diurnal component of the solar diurnal variations of the hard cosmic-ray component I_h after correction for the barometer effect and cyclic changes. These parameters were determined from the mean diurnal variation found by averaging over magnetically quiet days. The day corresponding to the onset of the storm and the two subsequent days were excluded from the analysis.

It is evident from Table 2 that a change in the location of the counters led to a considerable change in the diurnal variations. Thus, when the integral filter was altered by 90g/cm^2, the amplitude of the diurnal variation A changed by a factor of $\sim$2.

This change in the amplitude of the diurnal variations cannot be a reflection of temporal changes in these variations. In fact, the amplitudes of the diurnal variations at Moscow and Yakutsk are roughly the same, provided the instruments are located under the same amounts of matter. When the amount of matter above the instruments at Moscow was reduced from 90 ± 10 to 26 ± 4g/cm^2, the diurnal variations became greater by a factor of approximately 2 than those at Yakutsk.

This increase in the amplitude cannot be due to an increase in the meteorological contribution to the diurnal effect as a result of a reduction in the effective screen of the apparatus. In fact, a change in the role of the temperature effect during a transition from a thick to a thin filter can only lead to a reduction in the observed diurnal variations. The point is that the maximum of the diurnal variations due to diurnal temperature oscillations in

Table 2

Amplitude (A) and the time of maximum of the diurnal component of the solar-diurnal variations in the hard cosmic-ray component.

	Yakutsk				Moscow			
	1949—1953	1953—1954	1954—1955	1956—1958	1950—1953	1953—1954	1954—1955	1956—1958
	$35 \pm 5 g/cm^2$	$120 \pm 4 g/cm^2$	$120 \pm 4 g/cm^2$	$120 \pm 4 g/cm^2$	$90 \pm 4 g/cm^2$	$90 \pm 10 g/cm^2$	$26 \pm 4 g/cm^2$	$26 \pm 4 g/cm^2$
A, % . . .	0.13 ± 0.01	0.060 ± 0.005	0.06 ± 0.005	0.10 ± 0.03	0.08 ± 0.01	0.08 ± 0.01	0.14 ± 0.01	0.14 ± 0.01
t, hr . . .	13 ± 0.2	8 ± 0.1	7.8 ± 0.1	19.8 ± 0.1	12 ± 0.3	8.5 ± 0.3	8.5 ± 0.3	10.6 ± 0.2

the free atmosphere should be observed at 2400-200 hr, while the maximum of the observed variations occurs in daytime (800-1300 hr). Hence an increase in the role of the temperature effect should lead to a reduction in the amplitude of the observed variations and to a shift of the maximum towards a later time. This is in conflict with the experimental data shown in Table 2 and in the Figure.

Thus, the sharp change in the amplitude of the diurnal variations, δI_h, which occurs when the counters are transported to another location, is not of atmospheric origin but is due to the primary radiation.

It is also clear from the figure that the difference between the amplitude of the variations δI_h at Moscow and Yakutsk gradually decreased after 1956 and practically vanished in July-August 1957. The gradual disappearance of the difference in the diurnal variations δI_h at the above two stations may be ascribed to a gradual change in the longitude distribution of the geomagnetic field. However, this is contradicted by a comparison of the results obtained with two other instruments at Yakutsk (S-2 with an effective filter of 163 $\pm$ 6g/cm^2 and ASK-1 with an effective filter of 267 $\pm$ 4g/cm^2). It is also evident that the difference which is apparently associated with the difference in the screen cannot be due to a temperature effect in the hard cosmic-ray component. It follows that the change in the absorption of the diurnal variations is not of terrestrial nature and is apparently associated with a change in solar activity. 1953-1955 was characterized by minimum solar activity, while 1956-1957 was characterized by a sharp rise in the activity which reached a maximum at the end of 1957. This is clear from Fig. 1, which gives the relative number of sunspots during 1953-1959 (Curve 4).

If it is assumed that the diurnal variations are due to a particular source, then it must also be assumed that the properties of this source are very dependent on the level of solar activity. Moreover, the dependence is such that during the years of minimum activity the energy of the particles which participate in the solar diurnal variations is lower than during the year of maximum solar activity.

3. In fact, the mean diurnal variations δI_h in 1954-1955 changed by a factor of 2.3 when the thickness of the screen was altered by 94g/cm^2, while the corresponding change in the recorded radiation was 5—6%. Hence the radiation responsible for the diurnal variations in I underwent a change by a factor of 2.3 x 1.06 = 2.4. However, when the contribution due to the oscillations in the temperature of the free atmosphere to the diurnal effect in I is allowed for, it turns out that this factor must be reduced to 1.48. If this

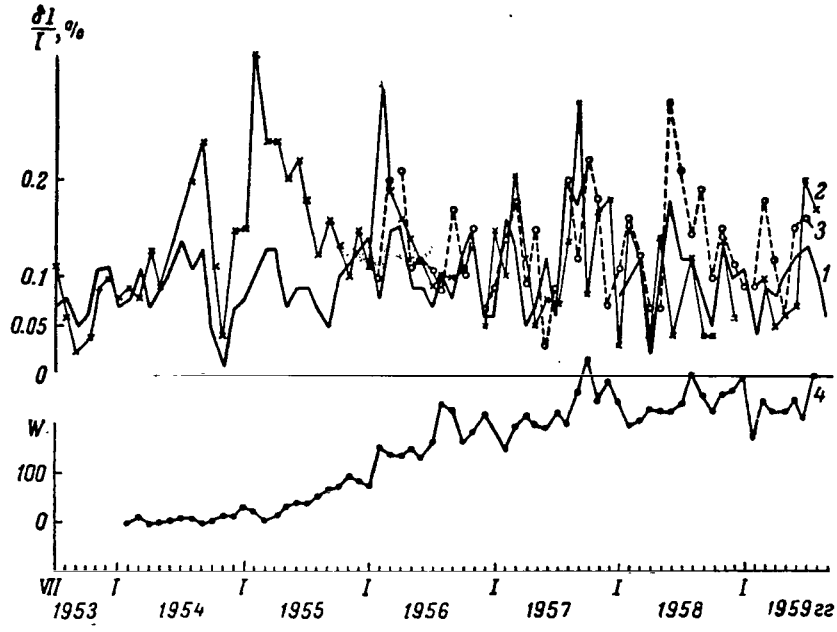

Mean monthly values of the amplitudes of solar diurnal variations in the intensity of the hard component of cosmic rays and the relative sunspot number:

1 - Diurnal variations measured at Yakutsk under a "thick" screen (ASK-1); 2 - Diurnal variations measured at Moscow under a "thin" screen (ASK-1); 3 - Diurnal variations measured at Yakutsk under a "thin" screen (S-2); 4 - Relative sunspot number.

radiation is absorbed in accordance with an exponential law of the form $I(x) = I_0 \exp(-\alpha x)$, then the absorption coefficient α turns out to be

$$\alpha = -\frac{100}{\Delta x} \ln \frac{I(x_1)}{I(x)} = \frac{100}{94} \ln 1.48 = 0.4\%\ \text{cm}^2/\text{g}.$$

This value of α is apparently rather low. The point is that the effective thickness of the screen was estimated for the intensity of the μ-meson component, while the radiation responsible for the diurnal variations is absorbed much more rapidly than the undisturbed flux of μ-mesons. Hence the effective thickness of the filter for the disturbed flux of μ-mesons, which is responsible for the diurnal variations, will be much nearer to the minimum thickness of the filter. The minimum thickness of the walls of the enclosure

at Yakutsk was 90g/cm^2, while the corresponding thickness for Moscow was 20g/cm^2. Under these conditions, the maximum estimated value of α is -0.57%cm^2/g. Combining the above two estimates of α we find that the absorption coefficient was $\alpha = -(0.5 \pm 0.1)\%\text{cm}^2/\text{g}$. A similar estimate for 1956-1958 gives $\alpha = -(0.23 \pm 0.05)\%\text{cm}^2/\text{g}$.

Thus, the μ-mesons which exhibited the diurnal variations during the years of minimum solar activity (1953-1955) had an absorption coefficient which was higher by a factor of 2 than the absorption coefficient for μ-mesons undergoing the same variations during the years of very high activity (1956-1958).

The sharp difference in the absorption coefficients for μ-meson undergoing diurnal variations during the periods of minimum and maximum solar activity may be due to the following effects.

Firstly, it is possible that during 1956-1958 the threshold energy for particles undergoing diurnal variations was increased so that there was a corresponding increase in the average energy. In order to explain the sharp difference in the absorption coefficient for the μ-mesons which were responsible for diurnal variations during 1953-1955 and 1956-1958, it is clearly sufficient to remove particles undergoing appreciable absorption in these additional 130g/cm^2. It is clear that these particles should have an energy between 0.3 and 0.5 BeV at the depth of observations. Hence the minimum energy of the primary particles ensuring the generation of μ-mesons having an energy of 0.3 BeV at sea level in 1953-1955 should have increased by 1956-1958 so as to ensure a flux of μ-mesons with minimum energy of 0.5 BeV at sea level. Accurate calculations of the change in the maximum primary energy are at present impossible. However, it appears that the change in the energy of the primary particles must have been of the order of 2—4 BeV.

Secondly, it is possible that the energy spectrum of the particles responsible for the diurnal variations in I during 1953-1955 was much softer than in 1956-1958. If this hypothesis is accepted, then in accordance with the dependence of the true absorption coefficient α on the exponent in the energy spectrum of the μ-mesons responsible for the diurnal variations, the exponent turns out to be approximately 5 for 1953-1955 and 3 for 1956-1958. An energy spectrum with an exponent equal to 3 is consistent with Dorman's theory [3] and is in agreement with the experimental determinations of the spectrum for 1957-1958. The spectrum with the exponent equal to 5 turns out to be much softer than that expected on the basis of a modulation of the primary beam by solar corpuscular streams carrying frozen-in magnetic fields, and approaches the exponent for particles from solar flares similar to that of February 23, 1956.

Thirdly, it is possible that both of the above factors were operating at the same time. In order to explain the sharp change in the μ-meson absorption coefficient during maximum and minimum solar activity, it is clearly necessary to introduce a much smaller change in the cut-off energy and a much smaller softening during the minimum. In either case there is no need to postulate a change in the mechanism responsible for the diurnal variations in I. In fact, the energy spectrum $\frac{\delta D(\varepsilon)}{D(\varepsilon)}$ of the diurnal variations in I may remain the same between the minimum and maximum solar activity.

In order to explain the difference in the absorption coefficients during these periods it is sufficient to assume that the energy spectrum of the undisturbed flux was much softer in 1953-1955 than in 1956-1958, i.e. $\frac{\delta N}{\delta \varepsilon} \sim \varepsilon^{-(3-4)}$ instead of $\frac{\delta N}{\delta \varepsilon} \sim \varepsilon^{-2}$. The absorption coefficient for diurnal variations in 1953-1955 will then be larger than the absorption coefficient for 1956-1958 by a factor of 2.5 if it is assumed that the mechanism of these variations, $\frac{\delta D(\varepsilon)}{D(\varepsilon)} \approx a\ \varepsilon^{-1}$, was the same in both cases. However, one would then expect a sharp increase in the absorption coefficient for the undisturbed μ-meson flux, and this is not observed. Thus, it may be concluded that the sharp change in the absorption coefficient for μ-mesons responsible for the diurnal variations between the minimum and maximum solar activity was due to either a change in the threshold energy, or a sharp change in the properties of the source of the diurnal variations. The former possibility has been suggested by a number of workers [4—6]. However, it is quite possible that both factors are present at the same time, and this will be discussed in detail in a subsequent paper.

REFERENCES

1. Shafer, Yu.G. Tr. YaFAN SSSR, ser. fizich., No. 2, 1, 1958.

2. Progress in cosmic ray physics. Vol. 1, ed. J.G. Wilson, IL, Moscow, 1954.

3. Dorman, L.I. Variatsii kosmicheskikh luchey (Cosmic ray variations). Gostekhizdat, Moscow, 1957.

4. Kuz'min, A.I. Tr. YaFAN SSSR, ser. fizich., No. 3, 99, 1960.

5. Skripin, G.V. Tr. Vsesoyuzn. konfer. po variatsiyam kosmicheskikh luchey (Proceedings of the 1960 All-Union Conference on Cosmic-Ray Variations). 1960.

6. Kuz'min, A.I. Tr. Mezhd. konfer. po kosmich. lucham (Proceedings of the International Conference on Cosmic Rays). Vol. IV, 258, 1960.

G. F. Krymskiy

LUNAR DIURNAL VARIATIONS IN COSMIC RAYS

A neutron monitor and an ionization chamber were used for the continuous recording of cosmic rays between September 1957 and August 1958. The data obtained were analyzed in order to establish the presence of a lunar diurnal variation. The two-hourly values of the intensities, corrected for the barometer effect, were used in the analysis. The solar diurnal variation was excluded by averaging the data over 30-day intervals. The resulting mean monthly values of the lunar diurnal variation were then subjected to a Fourier analysis and the results of this are shown in the table. The time is the lunar time, and the beginning of the day is taken to coincide with the upper culmination of the moon.

It was found that the amplitude of the lunar diurnal wave varies from month to month (cf. Table).

Amplitude and time of maximum of the first and second harmonics of the mean monthly variations of the lunar diurnal variation

Month	Neutrons				Ionization chamber ASK-1			
	t_{max_1}	A_1, %	t_{max_2}	A_2, %	t_{max_1}	A_1, %	t_{max_2}	A_2, %
1957								
IX	14.1	0.24	0.4	0.04	—2.7	0.063	7.4	0.012
X	—6.2	0.03	—1.4	0.10	—3.6	0.024	—1.9	0.017
XI	—3.5	0.09	—2.8	0.05	—2.0	0.048	—4.8	0.011
XII	—7.7	0.27	0.9	0.03	—6.1	0.089	5.6	0.009
1958								
I	—1.9	0.09	0.9	0.05	—7.7	0.042	—3.3	0.019
II	—11.8	0.15	1.1	0.11	—1.1	0.064	—0.9	0.007
III	—4.3	0.34	0.6	0.06	—3.1	0.116	—3.2	0.013
IV	5.8	0.08	0.7	0.05	—1.5	0.010	—5.4	0.006
V	—0.6	0.05	—0.4	0.06	—4.6	0.040	—3.3	0.025
VI	—7.1	0.26	—0.5	0.13	—8.9	0.068	—0.7	0.022
VII	7.7	0.15	1.0	0.02	7.0	0.108	—0.2	0.030
VIII	—12.4	0.25	0.5	0.06	—	—	—	—

The average amplitude for the neutron component is 0.17%, while the result for the hard component, which was deduced from the ionization, is 0.06%. The statistical errors in the mean monthly variation are respectively equal to 0.04% and 0.01%.

A semi-diurnal wave was established and was found to have an amplitude of 0.06% and 0.015% for the neutron and hard components respectively.

Figure 1 shows a vector plot of the lunar diurnal variation relative to the culmination of the moon. Each vector represents a mean monthly value of the amplitude and phase of the lunar diurnal wave. It is evident from Figure 1 that the phase of the diurnal wave varies from month to month, but tends to remain constant. The minimum intensity occurs on the average after 4-6 hours after the moon's culmination. Figure 2 shows an analogous diagram for the semi-diurnal wave.

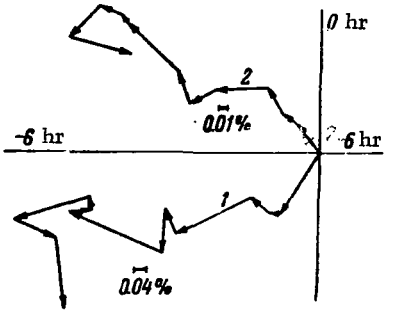

Fig. 1. Vector diagram of the first harmonics of the lunar diurnal variation:

1 — neutron component, 2 — hard component.

As can be seen from Figure 2, the semi-diurnal lunar variation [1] is more stable in phase than the diurnal wave. The maximum of the semi-diurnal wave for neutrons coincides with the culmination of the moon, while for the hard component it occurs three hours before the culmination.

The lunar tidal wave in the atmosphere [2] is apparently responsible for the appearance of the semi-diurnal variation. A dynamic effect, which gives rise to a systematic error in the barometer readings, is associated with the motion of the tidal wave. In order to explain the semi-diurnal wave indicated by the above results, it is necessary to have an effect giving an error in the pressure of 0.08-0.09 mb. The wave at the surface of the earth is approximately equal to 0.08 mb [2], which is in agreement with the above.

Bagge and Binder [3] have suggested three possible mechanisms for the lunar diurnal variations, namely, the shadow effect of the lunar mass, the shadow effect of the lunar magnetic field, and a lunar diurnal variation of the geomagnetic field.

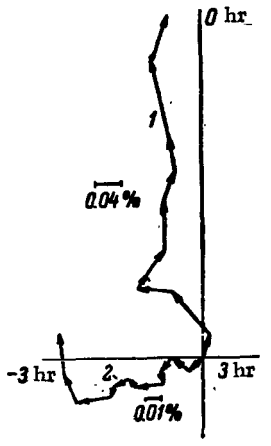

Fig. 2. Vector diagram of the second harmonics of the lunar diurnal variation (notations as in Fig. 1).

According to measurements carried out from the second Soviet space rocket, the moon has no magnetic field, while the shadow effect of the lunar mass is, according to [3], much smaller than is required for the explanation of the variation. Variations in the geomagnetic field affect the cut-off threshold for cosmic rays. If it is assumed that the geomagnetic variations amount to about 0.01%, then the variation in the cut-off threshold will be about 0.0001 BeV. Hence, the variation for neutrons is

$$\frac{\delta N}{N} = \delta E_{\min} W(E_{\min}, h_0) \sim 3 \cdot 10^{-4}\,\%.$$

For the ionization chamber, $\frac{\delta N}{N} \leqslant 10^{-4}\,\%$, which is much less than the observed value.

It is known that the solar diurnal variations are amplitude and phase modulated with a period of 27-29 days.

In order to estimate this effect, consider the following amplitude modulation

$$I(t) = A_0\left(1 + \sigma \cos \frac{2\pi}{T_{27}} t\right) \cos \frac{2\pi}{T_c} t,$$

where A_0 is the average amplitude of the solar variation; $0 \leqslant \sigma \leqslant 1$ is the depth of

modulation; T_{27} is the period of the modulation; and T_c is the period of the solar diurnal variation.

The modulated solar diurnal variation I(t) may be written as a sum of three simple harmonic variations:

$$I(t) = A_0 \cos \frac{2\pi}{T_c} t + \frac{A_0 \sigma}{2} \cos \frac{2\pi}{T_1} t + \frac{A_0 \sigma}{2} \cos \frac{2\pi}{T_2} t,$$

where

$$T_1 = \frac{T_c T_{27}}{T_c + T_{27}}; \quad T_2 = \frac{T_c T_{27}}{T_{27} - T_c} = 24^h 55'.$$

The period T_2 approaches the length of the lunar day ($24^h 50' 14''$) and the variation corresponding to this period may manifest itself as the lunar diurnal variation. Assuming that $A_0 = 0.3\%$ and $\sigma = 0.6$, the neutron variation amounts to 0.1%, which is of the same order of magnitude as the observed result.

It is to be expected that there is a correlation between the observed variation and the solar activity.

CONCLUSIONS

1. The neutron and hard components of cosmic rays exhibit variations with a period equal to one-half of the lunar day with amplitudes of 0.06% and 0.015% respectively. Lunar tides in the atmosphere may be responsible for these variations.

2. A variation has been established with a period equal to the lunar day and a tendency to a constant phase. The variation is apparently of solar origin and is associated with the 27-day modulation of the diurnal variation.

I should like to express my gratitude to G. V. Skripin for his help and valuable advice.

REFERENCES

1. Kuz'min, A.I. and Skripin, G.V. ZhETF, 28, 608, 1955.

2. Chapman, S.R. Met. Soc., 50, 165, 1924.

3. Bagge, E. and Binder, O. Proceedings of the International Conference on Cosmic Rays, IV, 273, 1960.

Yu. G. Shafer

"DAY-NIGHT" EFFECT IN THE COSMIC RAY INTENSITY FROM MEASUREMENTS IN THE STRATOSPHERE

It is commonly believed that the key to the discovery of the nature of diurnal variations lies in the careful study of the effect of solar corpuscular streams on the primary cosmic rays. However, the earlier hypotheses, among them the Janossy hypothesis [1] according to which the variations are due to the existence of a solar magnetic dipole, have not as yet been disproved either completely or partially. According to Janossy, the solar magnetic field can give rise to a diurnal variation as a result of the rotation of the earth relative to a "forbidden direction". This hypothesis is an outcome of Störmer's theory of the motion of charged particles in the field of a dipole.

According to this hypothesis, an additional influx of low-energy particles (less than 10 BeV) should be present on the night side of the earth; i.e., the source of these variations should lie left of the sun at an angle of $\sim 90°$ to the earth-sun line.

This hypothesis is attractive because it provides a simple explanation of the nature of the diurnal variations and allows one to calculate the magnitude of the solar magnetic moment from measurements on the day-night effect in the stratosphere.

Assuming the existence of a magnetic sun, Janossy has calculated the diurnal variations of low-energy particles for different dipole moments of the sun between 10^{34} and $0.4 \cdot 10^{34}$ oe/cm^3 and found that the amplitudes of these variations reached up to some tens of percent.

Dawton and Elliot [2] largely accepted the Janossy mechanism, but in addition allowed for the scattering of cosmic rays by the earth's magnetic field. This gave rise to a reduction in the amplitude of the diurnal effect down to 3-4% on the assumption that the equatorial solar field cannot be greater than 18 oe.

There are also other hypotheses on the nature of solar diurnal variations. Among them is the emission of an additional stream of cosmic rays by the sun (Cane and Sarabhai [3]), rotation of the sun about its axis (Brunberg and Dattner [4]), and so on. All these hypotheses suggest that the diurnal effect should increase with height.

So far, stratospheric measurements of the diurnal effect have not been extensively used in the study of diurnal variations. Only rarely have measurements of this kind been carried out, and these were of low accuracy.

Measurements of the diurnal effect in the stratosphere have been carried out by Korff [5] (two night and two day flights), Pomerantz [6], Pomerantz and McClure [7], Elliot and Dolbear [8] (three flights), Bergstrahl and Schroeder [9] (one night and one day flight), and finally by Dawton and Elliot [2]. The latter workers carried out eighteen flights both in daytime and at night.

The results of all these experiments are quantitatively contradictory: -1, 2, 1.5%. According to Dawton and Elliot, the day-night effect was +6.4, +1.7, +2.2, -0.9, -0.3, -6.1, +0.5% (+ indicates larger effect in daytime, -larger effect at night).

A common shortcoming of all these experiments is the large experimental error which in all cases was either equal to or greater than the day-night effect itself.

Dorman [10] has concluded from these results that the magnitude of the diurnal effect is practically independent of height. Hence, according to Dorman, particles which are responsible for the diurnal variations should be absorbed in the same way as the main part of cosmic rays, i.e., their average energy should be roughly 10 BeV or more.

We have thought it desirable to repeat these experiments with allowance for the fact that the cosmic-ray intensity varies irregularly from day to day and night to night owing to solar and geomagnetic activity. In order to obtain an accurate result, i.e., in order to ensure that the systematic difference between day and night intensities should not be masked by irregular variations, it is necessary to carry out a large number of such measurements near the maximum of Pfotzer's curve (100 mb).

We made more than 20 night and day flights in Yakutsk during 1958. The results of the experiments showed: if the results of all the day flights are averaged, it shows that the intensity of the night flights exceeds that of the day flights. The day-night effect is equal to 1% at a level of 500 mb and reaches 10% at the maximum of Pfotzer's curve. However, the experimental errors turned out to be very large:

$$I_{\text{day 500 mb}} = 17\% \quad I_{\text{night 500 mb}} = 18\%$$

$$I_{\text{day 100 mb}} = 11\% \quad I_{\text{night 100 mb}} = 9\%.$$

If one ignores the flights which were carried out during magnetic disturbances, then the day-night effect is limited to 2% and the experimental error is comparable with the effect itself.

All these results indicate that the diurnal effect in the intensity of cosmic rays in the stratosphere is very small, and support the corpuscular theory of variations, showing that the energy spectrum of the solar diurnal variations has a cut-off at low energies.

It is to be hoped that existing information about the mechanism of diurnal variations will be extended as the result of satellite and rocket studies of diurnal variations (day-night effect) and more careful and frequent stratospheric measurements during the minimum of solar activity, particularly at high latitudes.

REFERENCES

1. Janossy, L. Z. Phys., 104, 430, 1937.
2. Dawton, D. I. and Elliot, H. of Atm. and Terr. Phys., 3, 217, 1953.
3. Cane, R. P. and Sarabhai, V. Phys. Rev., 92, 415, 1953.
4. Brunberg, E. A. and Dattner, A. Tellus, 6, 73, 1954.
5. Korff, S. A. J. Franklin Inst., 229, 21, 1940.
6. Pomerantz, M. A. Phys. Rev., 77, 830, 1950.
7. Pomerantz, M. A. and McClure, G. W. Phys. Rev., 86, 536, 1952.
8. Dolbear, D. W. W. and Elliot, H. Nature, 159, 58, 1947.
9. Bergstralh, T. A. and Schroeder, C. A. Phys. Rev., 81, 244, 1951.
10. Dorman, L. I. Variatsii kosmicheskikh luchey (Cosmic-ray variations). p. 174, Gostekhizdat, Moscow, 1957.

A. I. Kuz'min and G. V. Skripin

ELECTROMAGNETIC CONDITIONS IN THE EARTH'S NEIGHBORHOOD ON MAY 10-24, 1959

A large number of papers relating various effects in the intensity of cosmic rays during magnetic storms with solar corpuscular streams have appeared in recent years [1—8]. In some of these papers [1, 5, 8] the main part of the effect, which is known as a Forbush decrease, is related to the effect of the induced electric field of such streams on the primary cosmic rays, while in other papers it is related to the scattering of primary particles by the elements of a turbulent magnetic field [2, 4], or the scattering of primary cosmic rays by regular frozen-in magnetic fields [3].

There are at the present time a number of experimental papers [9—13] from which it follows that preference should be given to the hypothesis advanced in [3] which relates Forbush decreases with the effect of the frozen-in regular magnetic field in the corpuscular streams. In accordance with this idea, an attempt was made [11] to determine the electromagnetic conditions in the earth's neighborhood between August 15 and September 15, 1957, using neutron and hard-component cosmic-ray data recorded at various stations all over the earth's surface.

It is difficult to correctly determine the spectrum of primary variations from ground level data only for the description of electromagnetic conditions, and it is even more difficult to obtain dependable information about the temporal changes of the variation spectrum. These difficulties are due to the fact that, firstly, the coefficients of coupling between the primary and the secondary components recorded at different points on the earth's surface in the energy range $\epsilon >$ 20 BeV are not sufficiently different. Secondly, the relative contribution of nuclei with $Z \geqslant 2$ to the various components of cosmic rays is apparently a function latitude, and therefore unless changes in the composition of the primary flux are taken into account, it is difficult to obtain reliable information from the measurements on the different components. Thirdly, the utilization of data from a large number of different stations is complicated by the difficulty of estimating, and correctly allowing for, meteorological changes in the earth's atmosphere.

An attempt is made in the present paper to describe the electromagnetic conditions in the earth's neighborhood between May 8 and May 22, 1959, on the basis of cosmic-ray meson measurements at ground level and at various depths underground.

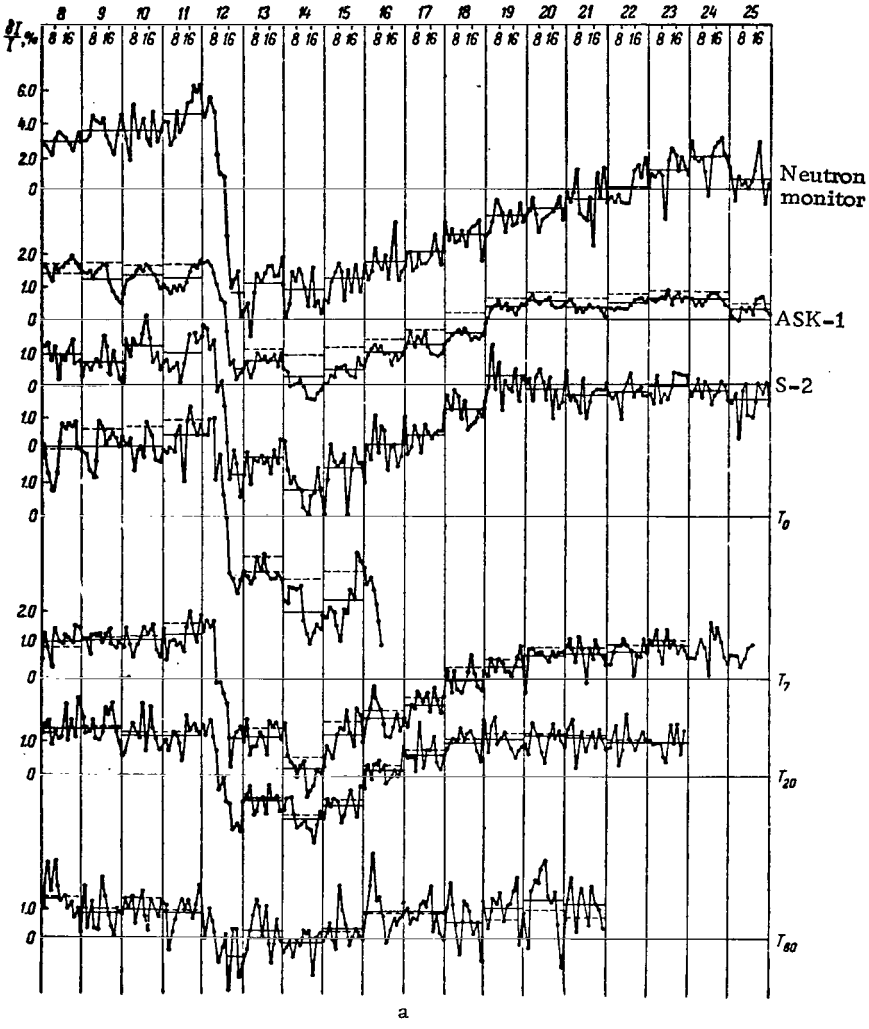

a

Two-hourly values of cosmic-ray intensity (corrected for barometer effect) during the major magnetic storm of May 11, 1959.

a - ground level data: neutron monitor, ionization chambers ASK-1, S-2, vertical counter telescope T_o and vertical counter telescopes at 7 (T_7), 20 (T_{20}) and 60 (T_{60}) m w.e.; b - counter telescope data at ground level and at depths of 7, 20 and 60 m w.e. for telescopes pointing south (S) and north (N) at 30° to the zenith. Continuous horizontal lines - daily mean values corrected for the barometer effect; broken horizontal lines - ditto, corrected for barometer and temperature effects. Local time.

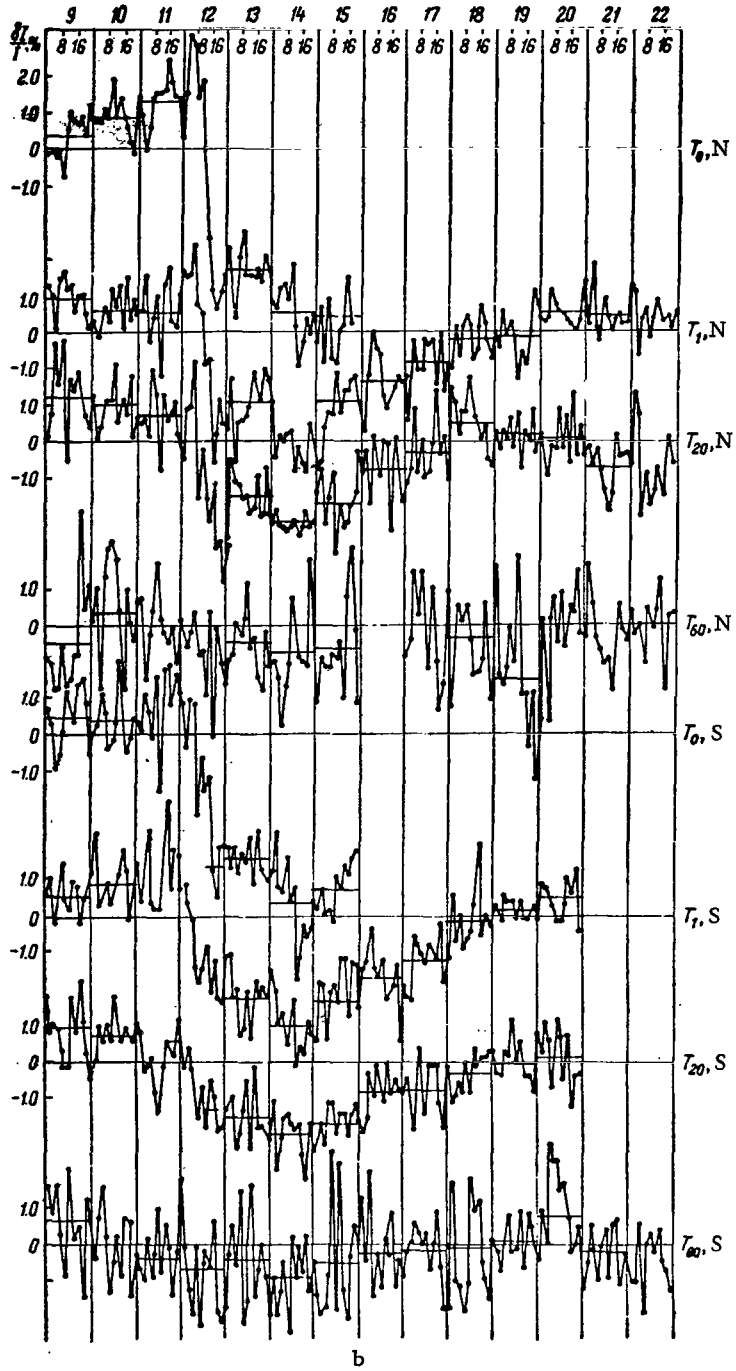
9 10 11 12 13 14 15 16 17 18 19 20 21 22
8 16
2.0
1.0
0
-1.0
T_0, N
T_1, N
T_{20}, N
T_{60}, N
T_0, S
T_1, S
T_{20}, S
T_{60}, S

b

1. EXPERIMENTAL DATA

According to IZMIRAN data [14], May 1959 was characterized by a number of geomagnetic and ionospheric disturbances due to certain geoactive regions on the sun. Two minor magnetic storms were noted up to May 11, but gave rise to no effects in the cosmic-ray intensity. At 0500 UT on May 11, a major magnetic storm with a non-sudden commencement was recorded. The beginning of the active period was at 2300 hr UT.

Ionospheric disturbances which were accompanied by radio fade-out were noted during this period. If this storm is related to the flare of importance 3 which passed through the first quadrant at the latitude of 19° and longitude of 50° at 2000 hr on May 10, then it is necessary to suppose that a stream having a width of not less than 100° was ejected at the same time. The expected duration of the storm on the earth would then be 6—8 days. Since the magnetic storm on the earth began after 9 hours, it is reasonable to suppose that the mean velocity of the stream was

$$V_{\text{к}} \frac{1.5 \cdot 10^{13}}{9 \cdot 3.6 \cdot 10^{3}} = 5 \cdot 10^{8} \text{ cm/sec}$$

The initial rate of entry of the earth into the stream was

$$V_{\text{E}} = \sqrt{V_{\text{к}}^2 + V_0} = 5 \cdot 10^{8} \text{ cm/sec}$$

since

$$V_0 = \frac{2\pi \cdot 1.5 \cdot 10^{13}}{27 \cdot 24 \cdot 3.6 \cdot 10^{3}} = 3 \cdot 10^{7} \text{ cm/sec}$$

It should be remembered that this is the lower limit for this velocity. A moderate storm began at 0800 hr on May 15 and terminated at 1100 hr on May 16. Thereafter, the magnetic field of the earth remained relatively quiet up to May 14, and no storm-type disturbances were recorded. A magnetic storm began on May 24, but was not accompanied by appreciable oscillations in the cosmic-ray intensity.

In order to investigate the electromagnetic conditions on May 10—25, we used, in addition to the above data, the continuous measurements of the hard component at Yakutsk, which were carried out with the composite apparatus described in [10, 15]. This apparatus measures the intensity at ground level and at depths of 7, 20 and 60 m water equivalent (m w.e.). The data were corrected for the barometer and temperature effects. Oscillations in the barometric pressure were taken into account with the aid of constant coefficients, namely, -0.13, -0.10, -0.08 and -0.04% mb for the four depths

0, 7, 20 and 60 m w.e. The temperature effect was allowed for with the aid of the temperature coefficient curve which was specially computed for our apparatus [10]. The variation in the intensity between May 8 and May 22, 1959, is indicated in the figure.

It is evident from the figure that the rapid decrease in the intensity recorded by vertical semi-cubic telescopes, and by the telescopes pointing north, occurred between 1900 and 2100 hr on May 11 and 0900—1100 hr on May 12. The decrease in the intensity recorded from the southern direction began 8—10 hours earlier. The reason for this discrepancy will be discussed below. The cosmic-ray intensity measured at all the levels and in all directions reached its minimum value at 0900—1100 hr on May 12, and then began to recover. This was interrupted by a new decrease which began at 2200 hr on May 13. The decrease reached the minimum value at 1600 hr on May 14, and was replaced by a gradual increase which was unaffected by magnetic storms between May 15 and 24. It was found that the normal intensity was reestablished more quickly at the larger depths. An appreciable increase in the amplitude of the solar diurnal variations was observed before and after the magnetic storm of May 11.

2. THE EFFECT IN THE COSMIC-RAY INTENSITY DURING THE MAGNETIC STORM

The amplitude of the main effect at all the depths and in all the directions was determined as the difference $I_0 - I_1$ between the intensities before and after the storm, where I_0 represents the mean diurnal intensity for May 10, and I_1 the mean diurnal intensity for May 12 between 0600 and 1600 hr. The errors in the main effect are determined by the errors in the above averages and by possible errors due to inadequate allowance for meteorological effects.

The values of the amplitude of the effect are given in the table, which also gives the times of the beginning of the decrease in the intensity, the duration of the decrease, and the duration of the recovery. These parameters were determined as follows. The beginning of the decrease was defined as the beginning of a systematic and stable (over a number of two-hourly intervals) negative value for the rate of change in the cosmic-ray intensity. This rate of change was determined from two-hourly values corrected for the barometer effect. It was considered that the use of data for shorter intervals of time could provide more accurate values owing to statistical fluctuations in the intensity at 20 and 60 m w.e.

Data on the cosmic-ray storm of May 11, 1959 (UT).

Depth, m w.e.	Direction of recording	Beginning of decrease of May 11, hr	Time of minimum of May 12, hr	Duration of decrease, hr	Duration of recovery, days	Magnitude of the first decrease, %	Magnitude of the 2nd decr., %
Ground level	Vertical	21—23	9—11	14	—	4.1±0.3	5.5±0.3
	South	9—13	11	22—24	—	4.0±0.4	5.9±0.4
	North	23	9	10—12	—	4.4±0.4	5.8±0.4
7	Vertical	21	7—9	10	8—9	3.0±0.4	4.2±0.4
	South	9—15	13	22—28	9	2.9±0.5	4.4±0.5
	North	23	7	8—10	9	3.2±0.5	3.8±0.5
20	Vertical	19—21	9—11	10—12	7—8	2.7±0.4	3.1±0.4
	South	15—17	13	20—22	7—8	2.0±0.5	3.0±0.5
	North	23	13	14	7—8	3.0±0.5	3.2±0.5
60	Vertical	19—21	7—9	12—16	4—5	1.0±0.6	1.0±0.6
	South	—	15	—	—	0.9±0.7	0.9±0.7
	North	23	7	—	4—5	1.0±0.7	1.3±0.7

The time of the recovery of the intensity, which is necessary for the determination of the duration of the recovery, was defined as the time of occurrence of stable zero values for the rate of change in the cosmic-ray intensity.

It is evident from the table that the duration of the decrease in the intensity, as measured by the vertical semi-cubic telescopes pointing north at 30° to the zenith, was roughly the same at ground level and at different depths underground, and varied between 700 and 1100 hours. At the same time, the duration of the decrease measured by telescopes pointing south at ground level and at various depths underground, varied between 1800 and 2400 hours. The increase in this time is associated with the fact that the beginning of the decrease in the southern direction occurred earlier by approximately 10 hours than in the vertical and northern directions. However, it should be noted that at the beginning of the decrease in the southern directions, all the telescopes pointing in the vertical and northern directions also recorded a decrease over a number of hours. This decrease was followed by a recovery which continued until 2100—2300 hr, and was then replaced by a rapid decrease. It may therefore be considered that a decrease in the intensity occurred simultaneously in all directions and at all depths of recording (3—5 hours after the onset of the storm.

The decrease in the intensity in the northern and vertical directions terminated for some reason at 1400—1600 hr, and a rapid decrease was observed again at 2000 hr. This second rapid decrease was simultaneous with the beginning of the first active period of the magnetic storm of May 11, which occurred at 2300 hr.

The magnitude of the general decrease in the intensity was the same in all directions at each depth and decreased with depth. The mean amplitude of the decrease in the intensity at 0, 7, 20 and 60 m w.e. was 4, 3, 2 and 1% respectively, for all directions.

It should be noted that the intensity reached its minimum value at approximately 0900— 1100 hr on May 12, and this time was independent of the depth or the direction of recording. From this time onward the intensity gradually increased and was then interrupted again by a new decrease. The mean amplitude of the new decrease at 0, 7, 20 and 60 m w.e. was 4.7, 3.9, 2.5 and 1.0% respectively. Beginning at 1800 hr on May 14, the intensity gradually recovered over a period of 4—12 days. The duration of the recovery was found to decrease with the depth of recording for all the directions. The longest duration of recovery was observed in the neutron component whose intensity remained below the normal level even after May 25.

The energy spectrum of the decrease was determined both with the aid of the coupling coefficients [3, 10, 13] and from the absorption of the μ-mesons [10]. It was found from the results of these analyses of the energy spectrum for the main effect of the decrease by the methods given in [10, 13], that the main effect may be described by a spectrum of the form:

$$\frac{\delta D(\varepsilon)}{D(\varepsilon)} = -f \begin{cases} 1, & \text{when } \varepsilon < \frac{\varepsilon_1}{4}, \\ \frac{1}{\pi} \sin^{-1}\left(\frac{\varepsilon_1}{2\varepsilon} - 1\right), & \text{when } \frac{\varepsilon_1}{4} < \varepsilon < \frac{\varepsilon_1}{2}, \\ \frac{1}{2}\left(\frac{\varepsilon_1}{2\varepsilon}\right)^{-\alpha}, & \text{when } \varepsilon > \frac{\varepsilon_1}{4} \end{cases} \qquad (1)$$

with $\epsilon_1 = 40$ Bev, $f = 0.2$ and $\alpha = +0.5$.

In this spectrum the first and second terms represent the effect of the frozen-in uniform magnetic field, while the third term represents either the effect of the electric field or the effect of some irregular magnetic field. It is easy to see that the contribution of the first and second terms is small for the underground counters, and that at the same time these terms can completely describe the effect observed at ground level. We shall use this spectrum below to describe the electromagnetic situation during the magnetic storm.

The energy spectrum of the second decrease is of the same form as (1), but with $\epsilon_1 = 60$ BeV, $f = 0.25$ and $\alpha = -0.5$. Hence, it is clear that the spectrum of the second decrease which occurred after the termination of the first major storm on May 11, and before the beginning of the moderate storm of May 15, was much harder than the spectrum of the first decrease.

During the recovery, the energy spectrum was found to soften systematically. Thus, the second term in the spectrum became negligible on the 5th

day after the onset of the magnetic storm on May 11, while the parameters of the first term in (1) were such that ϵ tended to decrease, while f remained practically constant.

3. INTERPRETATION OF THE RESULTS

Using the above parameters of the spectrum of the primary variations, and following Dorman's theory [3], let us first determine the strength of the frozen-in magnetic field, and then try to determine the velocity of the particles in the stream.

According to [3], particles with $\epsilon < \epsilon_1$ are scattered by a magnetic field whose strength is $H_1 = \frac{\epsilon_1/3}{300\, l_1}$ where $l_1 = U_E \tau_d$. Since the corpuscular stream captures the earth by its lateral surface, it follows that the velocity with which the earth enters the stream is $U_E \sim 3 \times 10^7$ cm/sec, the duration of the decrease τ_d is 22—24 hours, $l_1 = 2 \times 10^{12}$cm, and $H_1 \approx 2 \times 10^{-5}$ oe.

The increase in the intensity at 1300 hr on May 12 in the northern and vertical directions can then be explained by the fact that the magnetic field was so irregular that the particles recorded by these telescopes were not appreciably scattered. At the same time, this irregularity was not significant for particles recorded by the southern telescopes. The dimensions of the irregularity in the tangential direction can be characterized by $L \approx 3 \times 10^7 \times 1.5 \times 10^4 \approx 4.5 \times 10^{11}$cm.

The hypothesis of the lateral capture of the earth by the stream is in agreement with the fact that the amplitude of the diurnal variations both before the stream and after the storm was much greater than the variations during quiet days. Hence, it may be concluded that the direction of the frozen-in magnetic field in the stream was perpendicular to the plane of the ecliptic. A rapid change in the direction of this field was noted in a considerable part of the cloud, and this ensured the drift of low-energy particles which enabled them to be recorded by the northern and vertical telescopes but not by the southern telescopes. After passing through this region, the earth again entered a region with an almost regular field whose strength was apparently approximately the same as that calculated above.

After reaching the minimum, the earth gradually left the stream. The new decrease in the intensity which occurred prior to the storm of May 15 may

be explained as follows. The corpuscular stream responsible for the magnetic storm of May 15 penetrated a stream left of the earth, and compressed the magnetic field of the first stream which was ejected on May 10. The magnetic field increased from H_1 to $H_1' = H_1 \frac{\varepsilon_1'}{\varepsilon_1} \approx 1.5 H_1$. This stream captured the earth by its lateral surface, and was responsible for the storm of May 15, which did not affect the normal course of recovery in the intensity. The recovery can, in fact, be fully explained by the gradual departure of the earth from the first corpuscular stream.

The mean magnetic field strength in the rear part of the stream is

$$H_2 = \frac{\frac{\varepsilon_1}{3}}{300 l_2},$$

where

$$l_2 = U_E \tau_E \approx 1 \cdot 10^{13} \text{ cm/sec}$$

and since

$$H_2 l_2 = H_1 l_1,$$

it follows that

$$H_2 = \frac{H_1 l_1}{l_2} = 0.2 H_1.$$

Thus, the magnetic field strength at the rear of the stream should be smaller by roughly an order of magnitude than the field strength in the front part of the stream. This is in agreement with the suggestion that the front part of the stream is compressed by the interplanetary medium which gives rise to an increase in the magnetic field [11].

The mean radial velocity of the stream may be determined from a consideration of the diurnal variations. If the disturbed diurnal variations have a spectrum of the form

$$\frac{\delta D(\varepsilon)}{D(\varepsilon)} = \pm \frac{\Delta \varepsilon}{\varepsilon} \begin{cases} 1, & \text{when } \varepsilon < \frac{\varepsilon_1}{4}, \\ 1 - \frac{2}{\pi} \sin^{-1} \left(\frac{\varepsilon_1}{2\varepsilon} - 1 \right), & \text{when } \frac{\varepsilon_1}{4} < \varepsilon < \frac{\varepsilon_1}{2}, \\ 0, & \text{when } \varepsilon > \frac{\varepsilon_1}{2}, \end{cases}$$

then $U_\rho = \frac{\Delta \varepsilon}{300 Hl}$. Hence, knowing the amplitude of the disturbed diurnal variation and the magnitude of Hl, one can determine U_ρ. This procedure yields

$U_\rho\, l \approx 4 \times 10^8 - 6 \times 10^8$ cm/sec.

We consider that the magnetic field is not completely random, although the stream does include irregularities which do not, however, strongly disturb its uniform nature. We note that the corpuscular stream possibly transported cosmic-ray particles which were recorded as an intensity burst in the low-energy range. However, the upper energy limit of the transported particles should be less than 2 BeV, which follows from the absence of a burst in the neutron intensity at Yakutsk.

CONCLUSIONS

1. The analysis of cosmic-ray data obtained with the aid of identical installations at ground level and underground during the magnetic storm of May 11-12, leads to an agreement with the hypothesis [3] according to which the modulation of cosmic rays by the magnetic and electric fields of solar corpuscular streams is responsible for magnetic storms.

2. Cosmic-ray data obtained as a result of composite measurements at a given point can, in principle, provide a series of significant characteristics of solar corpuscular streams, such as the electric and magnetic field strengths, the stream velocity, the nature of the capture, and so on.

3. Cosmic-ray data are in agreement with the lateral capture of the earth by the stream at 0900—1300 hr on May 11. The stream carried a frozen-in magnetic field of the order of 10^{-5} oe. which had a radial velocity of 5×10^8 cm/sec. The stream included appreciable regions occupied by magnetic field irregularities.

REFERENCES

1. Alfvén, H. Cosmical electrodynamics. IL, Moscow, 1952.

2. Morrison, P. Phys. Rev., 101, 1397, 1956.

3. Dorman, L.I. Variatsii kosmicheskikh luchey (Cosmic ray variations). Gostekhizdat, Moscow, 1957.

4. Parker, E.N. Phys. Rev., 103, 1518, 1956.

5. Brunberg, E.A. and Dattner, A. Tellus, 6, 254, 1954.

6. Sekido, J. and Wada, M. Rep. Ionos. Res., Japan, 9, 174, 1955.

7. Nerurkar, N. W. Proc. of the Indian Acad. of Sci., XIV, 341, 1957.

8. Progress in cosmic ray physics. Vol. IV, ed. by J.G. Wilson, Moscow, 1957.

9. Kuz'min, A.I. and Skripin, G.V. Tr. YaFAN SSSR, ser. fizich., No. 3, 121, 1960.

10. Kuz'min, A.I. Dissertation, NIYaF MGU, Moscow, 1960.

11. Blokh, Ya.L., Glokova, Ye.S. and Dorman, L.I. Tr. MGG, No. 2, 2, 1959.

12. Kuz'min, A.I., Yefimov, N.N., Krasil'nikov, D.D., Skripin, G.V., Sokolov, V.D., Shafer, G.V. and Shafer, Yu. G. Tr. MGG, No. 3, 64, 1961.

13. Kuz'min, A.I. Tr. Mezhd. konfer. po kosmich. lucham (Proc. International Conference on Cosmic Rays). IV, 45, 1960.

14. Kosmicheskiye dannyye (Cosmic data). May, 1959.

15. Kuz'min, A.I. and Skripin, G.V. Tr. YaFAN SSSR, ser. fizich., No. 2, 195, 1958.

N. P. Chirkov, V. A. Filippov and G. V. Shafer

11-YEAR VARIATIONS IN THE INTENSITY OF COSMIC RAYS

The existence of 11-year variations in the intensity of cosmic rays has long attracted the attention of many workers.

Forbush [1] established a close reciprocal correlation between the mean annual cosmic-ray intensity and the Wolf numbers.

Other workers [2—5] showed that the 11-year variation is due to a modulating mechanism of solar origin.

Dorman [6] has suggested that the long-period variations and the decreases in the cosmic-ray intensity during magnetic storms (Forbush effects) may be due to the same mechanism. However, in a subsequent paper [7] Dorman maintained that these mechanisms should be different.

A study of experimental data on the neutron component for the last cycle of solar activity, which was carried out by Lockwood [8], led him to the conclusion that the decrease in the cosmic-ray intensity during the 11-year variations is due to rapid Forbush-type decreases and an incomplete return to the normal level.

In the present paper we investigate the 11-year variations in the cosmic-ray intensity between the 1954 solar activity minimum and the 1958-1959 maximum, using hard component intensity data, obtained with ionization chambers, and neutron intensity data, obtained with standard neutron monitors. The list of the stations and their coordinates, the recorded component, and the height above sea level are given in Table 1. The experimental data on the neutron component for Mt. Washington were taken from [8] and from the review given in [9].

All the data were corrected for pressure differences using the following barometer coefficients: $-0.11\%\ mb^{-1}$ for the ASK-1 chamber, $-0.14\%\ mb^{-1}$ for the S-2 (Yakutsk), ASK-1 (Moscow) and ASK-2 (Tiksi). The Yakutsk and Tiksi hard component data were also corrected for the temperature effect by the Feynberg-Dorman method, using the temperature distribution up to the 50 mb level. The data for Cheltenham and Moscow (corrected for the temperature) were taken from [10].

Table 1

List of stations, coordinates, and heights above sea level.

№	Station	Component	Geographic coordinates		Geomagnetic coordinates		Height above sea level
			Latitude	Longitude	Latitude	Longitude	
1	Tiksi	Hard,	71.6°N	128.9 E	60.6°	191.3°	Sea level
2	Yakutsk	Hard,neut.	62.0°N	129.7 E	51.0	193.8	» »
3	Moscow	Hard	55.7°N	37.6 E	58.0	120.5	» »
4	Cheltenham	"	38.7°N	76.8 W	50.1	350.4	» »
5	Mt. Washington .	Neutron	44.2°N	71.0 W	55.6	356.0	1917 м
6	Huancayo	Hard	12.0° S	75.2 W	—0.6	353.8	3350 м

1. When the temperature corrections are introduced into the seasonal variations in the hard component in accordance with the Feynberg-Dorman scheme, an inverse wave with an amplitude of 1.0—1.5% is obtained for Yakutsk (Fig. 1).

It was shown in [11] that the temperature coefficients calculated with $\gamma_{eff} = 0.5$ are too high (γ_{eff} is the exponent in the differential π-meson production spectrum).

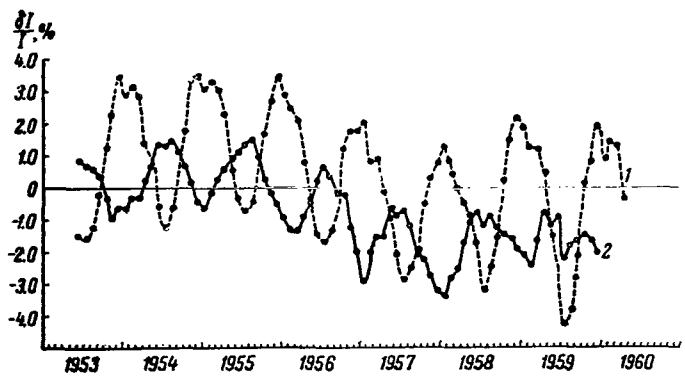

Fig. 1. Seasonal variations in the intensity of the hard component:

1 - with correction for pressure, using the ASK-1 ionization chamber data for Yakutsk; 2 - with correction for pressure and the temperature effect (the temperature coefficients were calculated for $\gamma_{eff} = 0.5$).

The seasonal variations in the S-2 chamber data were excluded by means of temperature coefficients calculated for $\gamma_{eff} = -0.2$. These coefficients (corrected for the additional screen) were used to calculate new temperature corrections for the ASK-1 instrument.

Moreover, in order to allow for the temperature effect we have also adopted a somewhat artificial procedure. We calculated the regression coefficient ($\beta = 0.72$) between the temperature corrections calculated for $\gamma_{eff} = 0.5$ with allowance for the screen, and the experimental seasonal variations with correction for the secular variation. After multiplying the temperature coefficient by 0.72, we obtained coefficients which were equal to those calculated for $\gamma_{eff} = -0.2$ with allowance for the additional screen above the ASK-1 chamber. Seasonal variations were excluded with the aid of these new temperature coefficients. This is clear from Fig. 2 which also shows the cosmic-ray intensity corrected for pressure and temperature at Moscow, Cheltenham and Tiksi, and the neutron component intensity at Mt. Washington and Yakutsk.

The resulting irregular variations are global in character since they are observed at all stations and are correlated with the neutron data, and the relative sunspot numbers (the correlation coefficient with the sunspot numbers at Yakutsk is -0.83). It is clear from Fig. 2 that the cosmic-ray intensity maximum is delayed relative to the solar activity minimum at Yakutsk by about 5 months, while the delay for Moscow is 15 months and for Cheltenham about one month, if it is assumed that the solar activity minimum occurred in June 1954. The new cycle of solar activity began in August, in view of the recorded appearance of the coronal line $\lambda = 5303$ Å in the active region at high solar latitudes, while at the equator the line was already absent [12].

The maximum number of sunspots was observed in October 1957 and the largest decrease in the cosmic-ray intensity during this period, as recorded by the ASK-1 chamber at Yakutsk, occurred in December and January 1958 and amounted to 3.2% of the 1954 intensity maximum. The decrease in the intensity which was observed in July 1959 was even greater and amounted to 3.9%. This decrease was due to a series of major storm decreases (between April and July), none of which was followed by a recovery.

The intensity of the neutron cosmic-ray component on Mt. Washington fell 25% by March 1958 and 27.5% by July 1959, as compared with July 1954.

2. Regular seasonal variations can also be excluded by averaging the mean monthly values of the cosmic-ray intensity (corrected for the pressure) by the method of sliding averages over 12 subsequent months. Fig. 3 shows the results obtained in this way between 1953-1959.

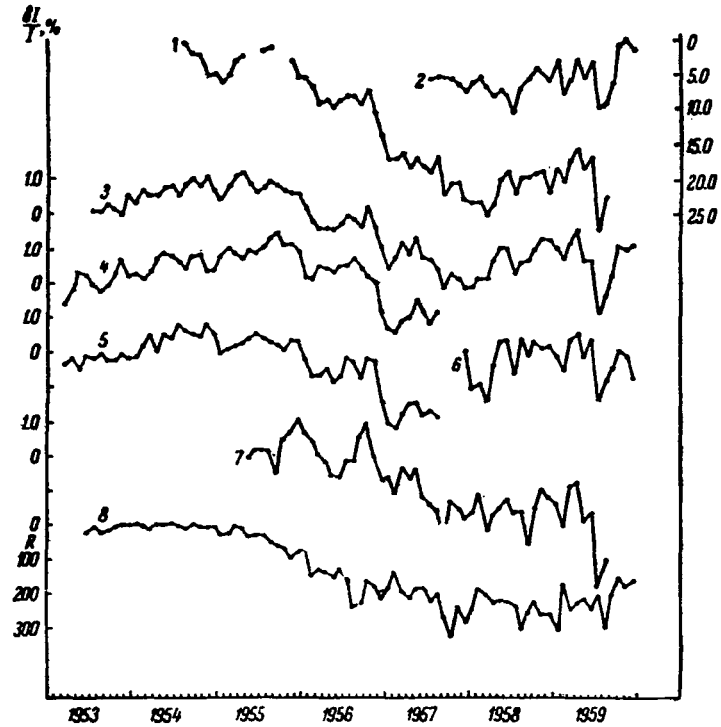

Fig. 2. Secular variation in the cosmic-ray intensity:

1 - neutron monitor on Mt. Washington [8-9]; 2 - neutron monitor at Yakutsk; 3 - ASK-1 ionization chamber at Yakutsk; 4 - ditto at Moscow [10]; 5 - ditto at Cheltenham [10]; 6 - ASK-2 ionization chamber, Tiksi; 7 - S-2 ionization chamber at Yakutsk; 8 - Solar activity in Wolf numbers (R).

It is clear from Fig. 3 that the cosmic-ray intensity maximum is delayed relative to the solar activity maximum at Yakutsk by 9—11 months. The delay at Moscow, Cheltenham and Huancayo is 10—11, 7—9 and 7—8 months respectively. The solar activity minimum indicated by the smoothed Wolf-number curve obtained by the method of sliding averages occurs in May 1954. After this, the solar activity increases and the decrease in the intensity of cosmic rays occurs in proportion to the solar activity. The general decrease in the cosmic-ray intensity during this time was as follows: Yakutsk (ASK-1) 2.4%, Moscow 3.0%, Cheltenham 2.6% and Huancayo 3.0%. If the instrumental effect at Huancayo is corrected for [6, p.274], the final figure becomes 2.0%.

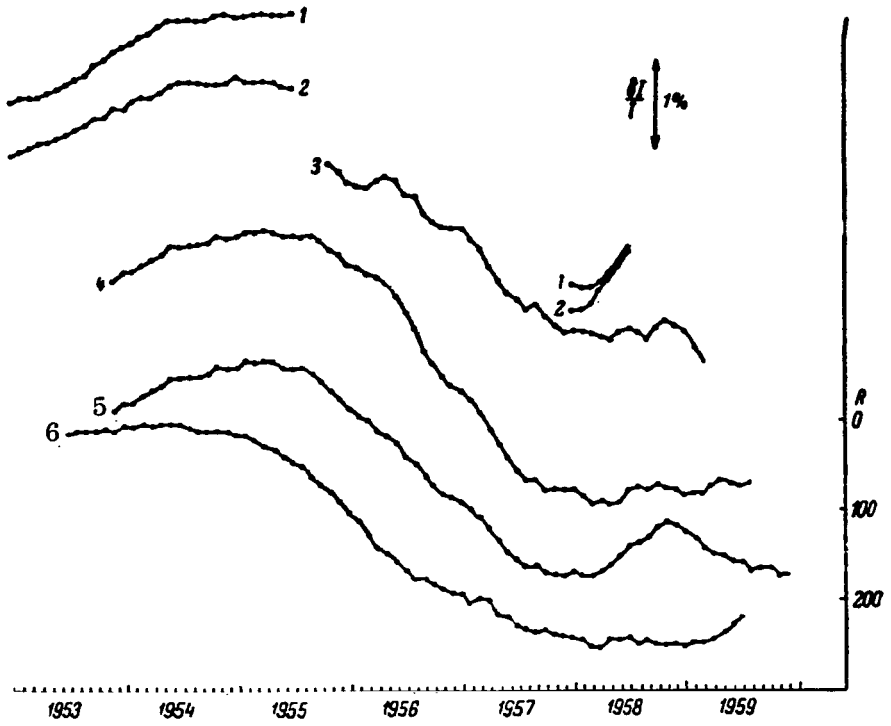

Fig. 3. Mean monthly values of the cosmic-ray intensity:

1 - ionization chamber at Huancayo; 2 - ditto at Cheltenham; 3 - S-2 ionization chamber at Yakutsk; 4 - ASK-1 ionization chamber at Moscow; 5 - ditto at Yakutsk; 6 - relative sunspot number.

Comparison with the data for Cheltenham indicates the presence of a latitude effect in the secular variation in the cosmic-ray intensity. The appreciable difference between the decreases in the cosmic-ray intensity at Moscow and at Yakutsk and Cheltenham can apparently be explained by an instrumental effect at Moscow. The small difference between the decreases at Yakutsk and Cheltenham can largely be explained by differences in the screening of the two instruments.

If the above method is used to smooth out the mean monthly cosmic-ray intensities corrected for temperature, then the reduction in the intensity for Yakutsk between 1954 and 1958 becomes equal to 2.6%, which differs by 0.2% from the result given earlier. This is explained by the fact that the temperature corrections also exhibit a secular variation which amounts to 0.2% during the period 1954-1958. The existence of this variation suggests a cooling of the atmosphere during this period by about 1.5°C (if it is assumed

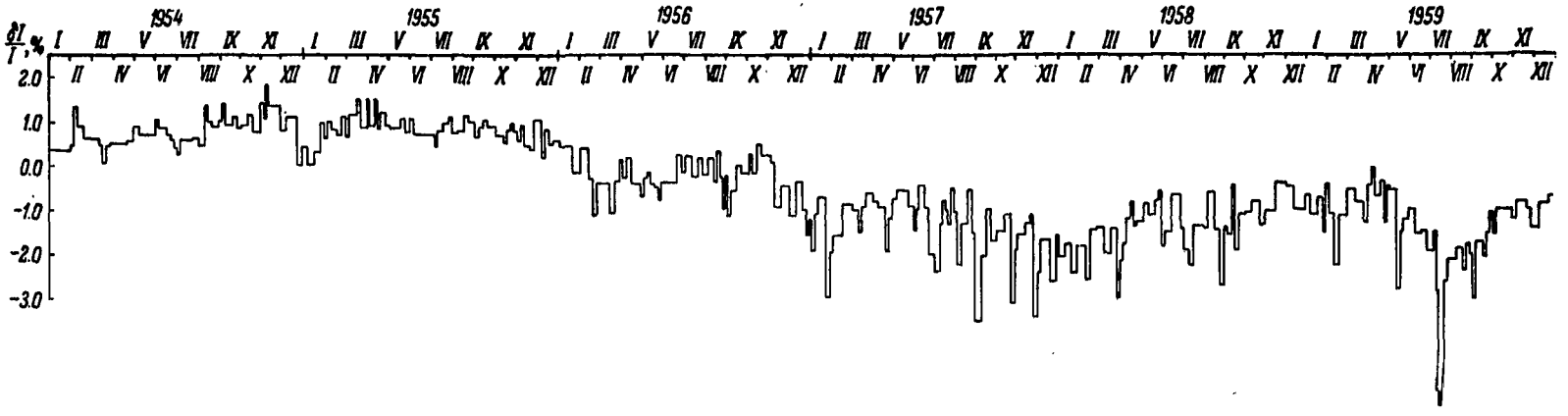

Fig. 4. Intensity of the hard component of cosmic rays between 1954 and 1959 (ASK-1 ionization chamber data for Yakutsk).

that the temperature coefficient is 0.15% per °C). Subsequent secular variation suggests that the entire atmosphere became warmer by approximately the same amount in 1959.

In view of the above discussion, the reduction in the intensity of cosmic rays at Cheltenham between 1954 and 1958 turns out to be 2.8%, while the result for Huancayo is 2.2%.

It is also clear from Fig. 3 that after the maximum at the beginning of 1958 had been reached, the solar activity did not fall off but remained constant throughout the year.

A slight maximum in the cosmic-ray intensity was observed at the end of 1958 at all the Soviet stations and also at American stations.

The absence of bi-annual variations during the period under investigation is also noticeable.

3. We have used the method given by Dorman in [7] to determine the role of short-period sharp decreases in the intensity of the hard component of cosmic rays. To do this, we averaged the experimental results obtained with the ASK-1 chamber at Yakutsk and corrected for the barometer and temperature effects when the mean diurnal values of the intensity varied by not more than 0.2—0.4% from the mean, except for the July magnetic storms of 1959 when the departure from the mean was 0.6—1.5%. The average values for these periods are plotted in Fig. 4. It is clear from this figure that in 1954, at the solar activity minimum, the cosmic-ray intensities did not vanish altogether, but amounted to 0.5—1.0%. Thus, in February and June 1954, a slow reduction was observed in the cosmic-ray intensity over the period of a month or more. Between August and December 1954, the cosmic-ray intensity remained roughly constant though higher than during the first half of that year. In November it began to fall off and decreased rapidly in the middle of December and the beginning of January. The total decrease was 1% as compared with September 1954. During February—March 1955, the cosmic-ray intensity recovered to the November 1954 value and then remained at practically a constant level. In December 1955 there were sharp decreases after which the intensity did not recover. Beginning with the second half 1956, a small recovery in the cosmic-ray intensity was observed up to October. After the series of sharp decreases without recovery in the winter of 1956-1957, the intensity fell by 4% at the end of January 1957, as compared with 1955. During the following months the intensity rose somewhat. New sharp decreases without recovery were then observed in August 1957 and continued until February 1958. During the following period (February 1958—April 1959), the intensity began to recover. The cosmic-ray intensity in May 1959 was higher by 1.5% as compared with the beginning of February 1958.

New rapid decreases in the cosmic-ray intensity without recovery to the previous level were observed in May, June, and particularly in July, 1959.

At the end of 1959 the intensity practically returned to the level of May 1959.

Thus, during the period 1954-1959 there were five characteristic active periods as regards the decrease in the intensity: December 1954—January 1955, December 1955—March 1956, November 1956—January 1957, August 1957—January 1958 and April—July 1959. It is precisely during these periods that the reduction in the intensity, which is associated with the 11-year cycle of solar activity, occurs. Thus, the reduction in the intensity between 1954 and 1959 occurred not gradually but by sharp periodic decreases after which the intensity tended to recover. However, each subsequent period reduced the intensity still further. These periods are characterized by the fact that in most cases of Forbush-type decreases the intensity did not tend to recover to the normal level. The duration of decreases during such periods amounted to 2—5 months, after which a small recovery was observed over a period of 2—4 months. The intervals between the above five decreases amounted to 11—17 months.

If all the peaks in Fig. 4 are joined together, the resulting curve resembles the magnetic storm effect in cosmic rays, with the gradual onset and the lack of recovery. Apparently, this is not a spurious effect and may suggest that these variations have a common mechanism. In order to resolve this problem it is necessary to calculate the spectrum of the 11-year variations in the intensity of cosmic rays.

According to [6] the relation between the primary and secondary variations is of the form

$$\frac{\delta N_\lambda^i(h_0)}{N_\lambda^i(h_0)} = \int_{\varepsilon_\lambda^{\min}}^{\varepsilon_1} W_\lambda^i(\varepsilon,\ h_0)\frac{\delta D(\varepsilon)}{D(\varepsilon)}\,d\varepsilon.$$

In the calculations we have used data from Washington, Yakutsk, Cheltenham (Yakutsk and Cheltenham were combined) and Huancayo. We thus have the neutron and the hard components at the geomagnetic latitude of $\lambda \cong 50°$N and the hard component at the equator. It follows that our estimates will be rather approximate. By assuming a definite form for the spectrum, for example, $a\varepsilon^0$, $a\varepsilon^{-1}$, . . . and so on, it is possible to select an energy ε_1 for which the above equation will be satisfied. As can be seen from Table 2, the ratio of the experimental amplitudes of the neutron and hard components at $\lambda \cong 50°$, and the ratios of the amplitudes of the hard component at $\lambda = 50°$ and $0°$ are in good agreement when $\frac{\delta D(\varepsilon)}{D(\varepsilon)} \sim \text{const}$ with the upper limit $\varepsilon_1 \approx 14$—15 BeV. The spectrum of the form $a\varepsilon^{-1}$ is not in agreement with the experimental data. Our final result for the spectrum of the 11-year variations is

$$\frac{\delta D(\varepsilon)}{D(\varepsilon)} = a \begin{cases} -1, & \text{when } \varepsilon \leqslant \varepsilon_1, \\ 0, & \text{when } \varepsilon \geqslant \varepsilon_1, \end{cases}$$

where $a = 0.38 \pm 0.05$. This spectrum was determined from the mean monthly values of the cosmic-ray intensity smoothed with a 12-monthly sliding mean over 1954—1958 and corrected for the secular variations in the temperature for Cheltenham and Yakutsk. A correction was also made for the instrumental effect at Huancayo, and the intensity was reduced to sea level (by a factor of 2.15). Assuming that the absorption occurs in accordance with the exponential law $I = I_0 \exp(-h/L)$, where $h \cong 260 g/cm^2$, it is found that $L = 340 g/cm^2$.

Table 2

Expected and experimental ratios of the amplitudes of the neutron and hard components for a spectrum of the form $\frac{\delta D(\varepsilon)}{D(\varepsilon)} = a\varepsilon^{\circ}$

ε_1, BeV	$\frac{\delta N}{N} : \frac{\delta I^{\infty}}{I^{\infty}}$	$\frac{\delta I^{\infty}}{I^{\infty}} : \frac{\delta I^{\circ}}{I^{\circ}}$
11	11.4	∞
13	8.4	3.6
15	6.6	2.2
17	5.5	1.8
Experiment . .	$(22 \pm 0.2) : (2.7 \pm \pm 0.2) = 8.1 \pm 04$	$(2.7 \pm 0.2) : (0.9 \pm \pm 01) = 2.9 \pm 0.3$

Assuming that $\frac{\delta D(\varepsilon)}{D(\varepsilon)} \sim$ const between 1954 and 1959 (this was also obtained in [13] for the period between February 1958 and April 1959), we can determine the cut-off energy during the above period of time. Using the data shown in Fig. 2, we have carried out the appropriate calculations and the results are given in Table 3. It is clear from this table that between the solar activity minimum and maximum (1954—1958), the cut-off energies tend to become smaller, i.e. the mechanism becomes more and more effective for low energies. The strength of the source of the 11-year variations [6] tends to increase. This is followed by a depression in the solar activity, and the cosmic-ray intensity increases, reaching a maximum in April 1959.

It is clear from Table 3 that during this period the source strength decreased and the mechanism was effective largely at low energies ($\leqslant$ 12 BeV). It is also evident from Table 3 that between April and July 1959, the strength of the source increased again and the mechanism became effective for particles with higher energies.

Table 3

Changes in the cut-off energy in the spectrum, and the characteristics of the source of the 11-year variation in the cosmic-ray intensity

	1954—V 1956	1954—I 1957	1954—I 1958	1954—IV 1959	1954—VII 1959
Washington, $\frac{\delta N}{N}$, %	9.5±0.2	17.0±0.2	23.5±0.2	16.0±0.2	27.5±0.2
Yakutsk, $\frac{\delta I}{I}$, % . .	1.6±0.1	2.6±0.1	3.2±0.1	1.6±0.1	3.9±0.1
$\frac{\delta N}{N} : \frac{\delta I}{I}$	6.0±0.4	6.5±0.4	7.35±0.4	10.0±0.6	7.1±0.4
ε_1 BeV	16±0.5	15±0.5	14±0.5	12±0.5	14±0.5
a	0.15±0.03	0.30±0.04	0.40±0.04	0.25±0.03	0.45±0.04
$l \cdot 10^{11}$, см	37 (11)	17 (5)	12 (4)	21 (6)	10 (3)
$H \cdot 10^{-5}$, oe	1.4 (4.8)	2.9 (10.0)	3.9 (11.7)	1.9 (6.7)	4.7 (15.5)

A number of theories exist at the present time for the interpretation of the 11-year variations in the intensity of cosmic rays. They have been critically reviewed by Dorman in [6-7]. The most attractive is the solar wind hypothesis due to Parker [2], which was verified in [7] on the basis of experimental data. According to the latter paper, Parker's hypothesis can be made to fit the experimental data in a somewhat modified form. Thus, it may be considered that the irregularities have different dimensions, which are effective for different energies, and that the solar wind velocity given by Parker ($u = 10^8$ cm/sec) is somewhat too high. The length of the free path for scattering λ should depend on the energy. According to our calculations

$$\frac{\delta D(\varepsilon)}{D(\varepsilon)} \sim \text{const};$$

in the modified Parker model this corresponds to $\lambda = l$, where l is a typical linear dimension of the irregularity.

Using equation (11) of [6] for the latter case, it is possible to determine l provided the experimental spectrum is known. Such calculations have been carried out and the results are shown in Table 3 for $u = 10^8$ cm/sec. The figures in brackets are for $u = 3 \times 10^7$ cm/sec. For example, for the period 1954—1958, the theoretical and experimental data agree for $l = 12 \times 10^{11}$ cm ($u = 10^8$ cm/sec) and $l = 4 \times 10^{11}$ cm ($u = 3 \times 10^7$ cm/sec). Knowing ϵ_1 and l it is possible to determine the magnetic field H of the irregularities which will scatter particles with energies $\leqslant \epsilon_1$. These values of H are shown in the last line of Table 3.

The following conclusions may be drawn from an analysis of Table 3.

With increasing solar activity there is an increase in the strength of the source of the 11-year variations, owing to the increase in the number of corpuscular streams emitted by the sun [6, p. 317]. With increasing number of these streams, the linear dimensions, l, of the irregularities decrease, while the magnetic field H increases if it is assumed that the dimensions of the layer in which the solar wind prevails remain constant. However, these dimensions should apparently increase with increasing solar activity, so that the values of l may be even smaller.

As was noted above, an increase in the cosmic-ray intensity was observed between February 1958 and April 1959. It follows from Table 3 that this was due to a reduction in the number of corpuscular streams with weak magnetic fields. Thus, the mechanism which was operative during this period was most effective at low energies. Its effect on particles with energy $\leqslant 15$ BeV was weakened. This explains the relatively large increase in the hard component during this period as compared with the netron component. An increase in the intensity was also observed at Huancayo (Fig. 3). In fact, this increase was due to particles with energies $\leqslant 15$ BeV or somewhat less. Hence the lower limit $\epsilon_1 = 10$ BeV reported in [13] is apparently too low.

During the next period, April—July 1959, the number of corpuscular streams with high magnetic fields increased and the source strength became larger. Thus, with increasing solar activity, the mechanism of the 11-year variations in the cosmic-ray intensity became more effective at low energies (a few BeV), right down to the cut-off, which was also noted in [14].

Summarizing the above discussion, we may draw the following conclusions:

1. Seasonal variations in the intensity of the hard component can be eliminated by means of temperature coefficients calculated for $\gamma_{eff} = -0.2$ in

the differential π-meson production spectrum (a somewhat different conclusion is reached in [10] in which temperature corrections were employed which were themselves corrected for the screen above the instrument).

2. A secular cooling of the earth's atmosphere, amounting to 2° between 1954—1958, was observed together with a comparable increase in the temperature toward 1960.

3. The cosmic-ray intensity recorded at Yakutsk with the ASK-1 chamber, fell by 3.2% ± 0.1% between 1954 and 1958.

4. The intensity maximum in the hard component of cosmic rays was delayed by 5—8 months relative to the solar activity minimum in 1954.

5. The neutron component minimum was delayed by 5 months and the hard component by 2-3 months relative to the solar activity maximum in October, 1957.

6. The delay of the change in the cosmic ray intensity relative to the solar activity suggests that the irregularities which scatter cosmic rays have a relatively long lifetime (a few months).

7. The large delay of the hard-component maximum (5—8 months) relative to the solar activity minimum, as compared with the delay of the cosmic-ray intensity minimum after the solar activity maximum had been reached, and the large delay of the neutron component minimum, can apparently be explained by the longer lifetime of small-scale irregularities which are effective for low-energy particles. This is also associated with the decay of large irregularities into smaller formations.

8. Since the spectrum of the 11-year variations and Forbush-type effects [6] is of the same form, namely,

$$\frac{\delta D(\varepsilon)}{D(\varepsilon)} \sim \text{const},$$

it follows that these variations have a common solar origin and apparently a common mechanism, except that the mechanism is more effective for low-energy particles in the 11-year variations than in the Forbush-effects, and may be stronger in the former case.

This can be understood if it is assumed that corpuscular streams which initially carry regular frozen-in magnetic fields [6] subsequently become turbulent and decay into smaller and longer-lived irregularities. The accumulation of such fine-scale irregularities leads to an increase in the strength of the source of the 11-year variations which is most effective for low-energy particles.

REFERENCES

1. Forbush, S.E. J. Geophys. Res., 59, 529, 1954.

2. Parker, E.N. Phys. Rev., 110, No. 6, 1958.

3. Davis, L.J. Phys. Rev., 110, 1440, 1955.

4. Morrison, P. Phys. Rev., 101, 1397, 1956.

5. Singer, S.F. Nuovo Cimento, Suppl., 8, No. 2, 334, 1958.

6. Dorman, L.I. Variatsii kosmicheskikh luchey (Cosmic ray variations). Gostekhizdat, Moscow, 1957.

7. Dorman, L.J. Proc. of the Moscow Cosmic-Ray Conference, IV, 320, 1960.

8. Lockwood, J.A. Phys. Rev., 112, 1750, 1958.

9. Cosmic Ray Intensity during the International Geophysical Year, No. 1, Tokyo, 1959.

10. Glokova, Ye.S. Tr. YaFAN SSSR, ser. fizich., No. 3, 84, 1959.

11. Danilov, A.A., Krymskiy, G. F. and Filippov, V.A. Tr. YaFAN SSSR, ser. fizich., No. 4, 41, 1961.

12. Astronomicheskiy kalendar' za 1957 (Astronomical calendar for 1957). GITTL, Moscow, 1956.

13. Shafer, J.G. Proc. of the Moscow Cosmic Ray Conference, IV, 74, 1960.

14. Meyer, P. and Simpson, J.A. Phys. Rev., 106, 568, 1957.

A.I. Kuz'min, G.V. Kuklin, A.V. Sergeyev, G.V. Skripin, N.P. Chirkov and G.V. Shafer

COSMIC-RAY INTENSITY BURST OF MAY 4, 1960

A considerable increase in the cosmic-ray intensity was recorded by standard neutron monitors on May 4, 1960, at Irkutsk (geomagnetic coordinates $\varphi = 40.8°$, $\lambda = 174.5°$, h = 433 m above sea level, $\epsilon_\lambda^{min} = 3.2$ BeV) and at Yakutsk ($\varphi = 51°$, $\lambda = 193.8°$, h = 105 m, $\epsilon_\lambda^{min} = 1.25$ BeV). An analogous effect was observed at many other stations in the world network. In particular, this is reported in [1-4] which we have used to determine the energy spectrum of the variations and to obtain a more accurate determination of the onset and maximum of the burst. As can be seen from Figures 1 and 2, which show the 15-minute values of the cosmic-ray intensity, the increase began approximately at 1015-1030 UT and reached a maximum at approximately 1045 UT. The time of the maximum will be given more precisely below. The reduction in the intensity of the neutron component continued for 1.5-2 hours. The temporal and amplitude characteristics of this phenomenon cannot be determined with great accuracy owing to considerable statistical fluctuations in the 15-minute values of the intensity. A simultaneous determination of the intensities of the hard component was made at the above stations by counter telescopes (triple coincidences) and ionization chambers (type ASK), and of the general component (counter telescope, double coincidences). A description of the instrumentation and the experimental conditions is given in [5-6]. Figures 1 and 2 also show the results of underground observations at Yakutsk on May 4, 1960, which were carried out with the aid of semi-cubic telescopes at the depths of 7, 20 and 60 m water equivalent in the vertical, southern and northern directions; the data obtained with a standard neutron monitor at Tbilisi ($\varphi = 36.3°$, $\lambda = 122.0°$, sea level, $\epsilon_\lambda^{min} = 5.7$ BeV); and the ionization chamber data (ASK-2) for Murmansk ($\varphi = 68°55'$, $\lambda = 33°10'$, sea level, $\epsilon_\lambda^{min} = 0.54$ BeV). Meteorological effects were excluded by the introduction of appropriate corrections into the original data.

Comparison of all these data and the data obtained at other stations (Fig. 3) led to the following conclusions.

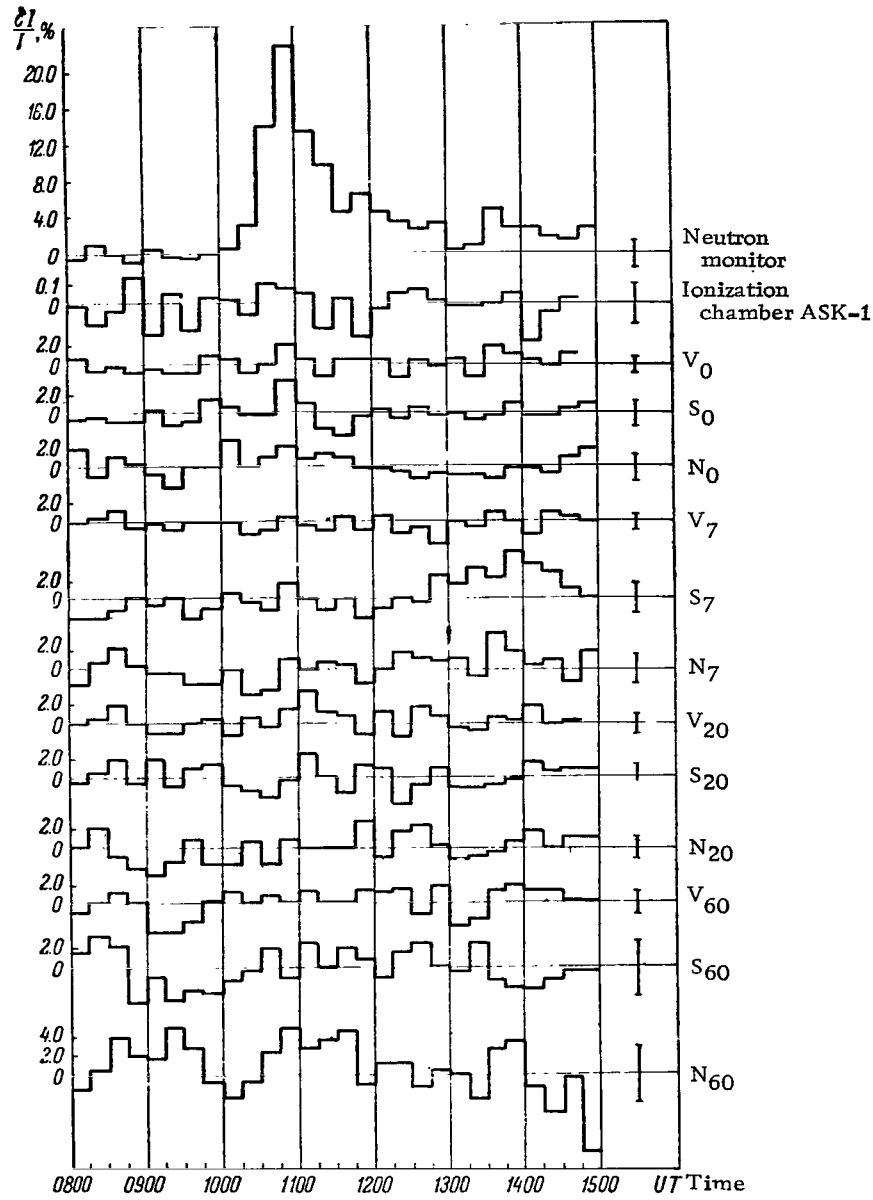

Fig. 1. Fifteen-minute values of the cosmic-ray intensity on May 4, 1960, at Yakutsk.

The triple coincidence counter telescopes were pointing in the vertical (V), southern (S) and northern (N) directions at the angle of 30° to the zenith. The subscripts 0, 7, 20 and 60 represent the depth of the instrument below ground level in m water equivalent. The statistical error is indicated by the length of the vertical lines on the right.

1. The increase in the cosmic-ray intensity could be reliably followed in the Northern Hemisphere between $\varphi = 41°$ (Irkutsk) and $\varphi = 83°$ (Resolute Bay).

2. The effect in the hard component was only observed at the American stations. At other stations its magnitude lay within the statistical accuracy of the measurements, except for the ground level south telescope at Yakutsk which recorded an increase of the order of $4.0 \pm 1.3\%$.

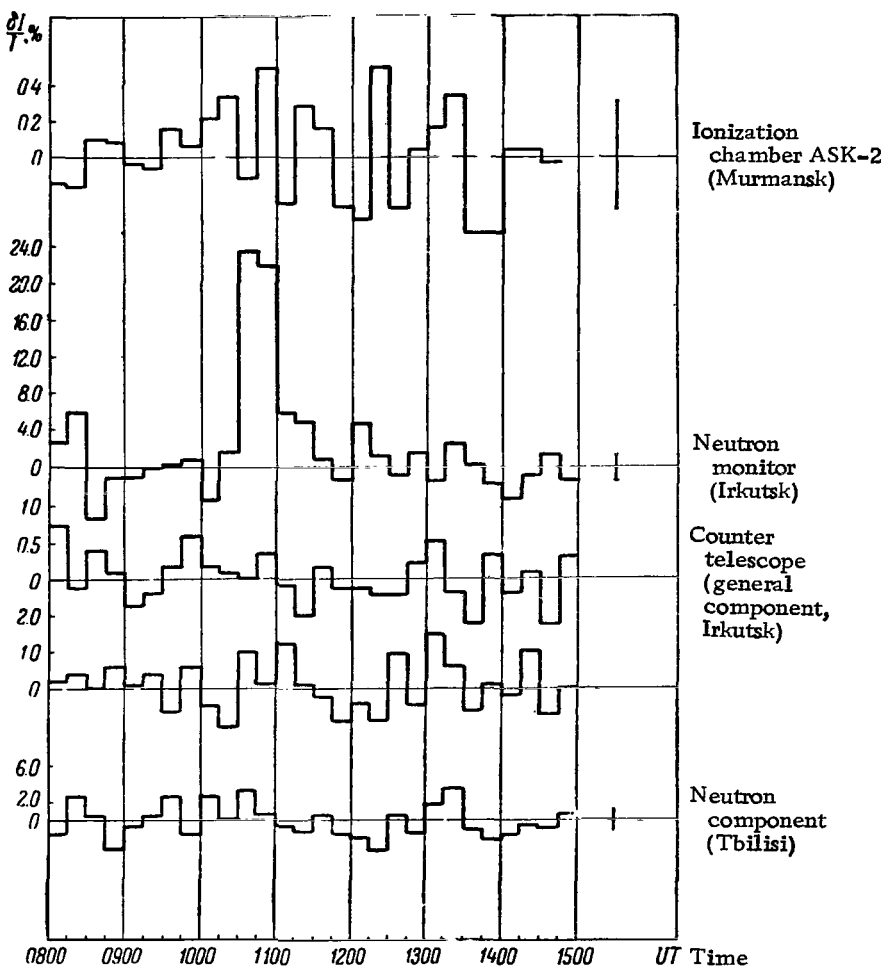

Fig. 2. Fifteen-minute values of the cosmic-ray intensity on May 4, 1960 at Murmansk, Irkutsk and Tbilisi. The lengths of the vertical lines on the right represent the statistical errors.

3. Clearly defined zones of incidence were observed for the cosmic rays (Fig. 3). The most clearly defined were the 9 and 4 hour zones. However, a

small effect was also observed in the background zone which can apparently be traced over the entire globe (in the latitude range ~25-60°).

4. The absence of appreciable changes in the underground intensity at the depth of 60 m water equivalent during the burst shows that there were no large changes in the temperature of the upper atmosphere during this period.

The above results may be used to find the energy spectrum of primary cosmic-ray variations. According to [7, pp. 74-92] the relation between the primary and secondary variations is of the form

$$\frac{\delta N_\lambda^i(h_0)}{N_\lambda^i(h_0)} = \int_{\varepsilon_\lambda^{min}}^{\infty} \frac{\delta D(\varepsilon)}{D(\varepsilon)} W_\lambda^i(\varepsilon, h_0)\, d\varepsilon.$$

In the case under consideration, the spectrum cannot be found from the latitude distribution of the effect in view of the considerable anisotropy of the particles. By measuring the different components at a given point it is possible to determine the energy spectrum of the variations. Calculations for Irkutsk and Yakutsk showed that at the intensity maximum the spectrum was of the form $\frac{\delta D(\varepsilon)}{D(\varepsilon)} \sim \varepsilon^{-5\pm2}$. An analogous result was obtained from the neutron and meson data for the North American stations.

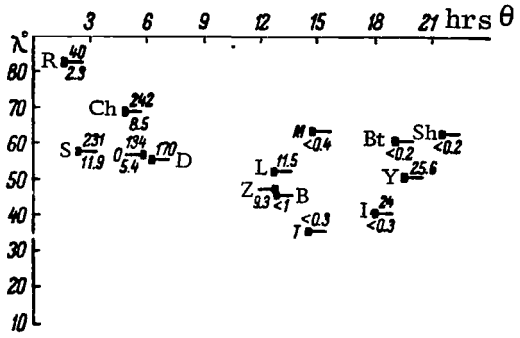

Fig. 3. Distribution of the cosmic-ray burst effect at the maximum over the Northern Hemisphere on May 4, 1960.

The geomagnetic time (θ) is plotted along the abscissa axis; the geomagnetic latitude φ is plotted along the ordinate axis. The numerators represent the neutron component, the denominators the meson component as measured by the counter telescopes and the ionization chanbers; R - Resolute Bay, Ch - Fort Churchill, S - Sulphur, O - Ottawa, D - Deep River, L - Lide, Z - Zugspitse, B - Bologna, M - Murmansk, T - Tbilisi, I - Irkutsk, Y - Yakutsk, BT - Bay of Tiksi, Sh - Cape Shmidt.

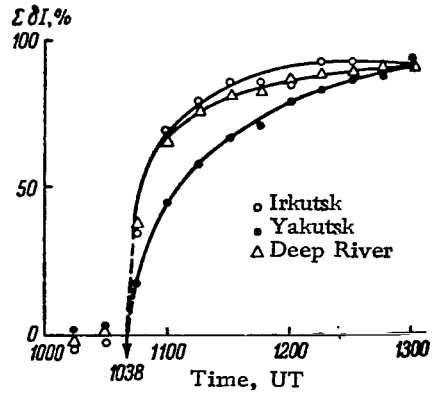

Fig. 4. Integral curves for the determination of the time of maximum of the cosmic ray burst on May 4, 1960.

Consider now the general nature of the reduction in the intensity of the burst at different stations. Since the burst occupied a short period of time, the fluctuations in the 15-minute data which we have used are considerable and have an appreciable effect on the amplitude and the time of maximum of the burst. This can be removed to a considerable extent by using the integral-curve method put forward by A.V. Sergeyev to calculate the times of the maximum and the complete return to normal level. In the case under consideration, an error of the order of 2 minutes is admissible. Figure 4 shows three integral curves based on the 15-minute data for Irkutsk, Yakutsk and Deep River. The point of intersection of the background line occurs at 1038 UT at all stations and this is in agreement with the result in [3]. It is possible that the coincidence of the maxima does not hold for all the stations in the world network. This must be verified by the method proposed in this paper or by some other method. The integral curves may be used to follow the general nature of the decrease very accurately. Thus, assuming that the change in the intensity may be described by $\delta I = \beta t^{\gamma}$ [7], it is easy to show that the integral curve should be of the form

$$S = \alpha + \frac{\beta}{\gamma + 1} t^{\gamma+1}.$$

The parameters α, β and γ may be found by the method of least squares. The table shows the values obtained for γ using the Deep River, Irkutsk and Yakutsk results.

Thus, beginning with 1038 UT, the decrease in the intensity of the neutron component was of the form $\frac{\delta I}{I} \sim t^{-(1.6 \pm 0.6)}$. The observed difference in the general nature of the decrease may be explained by a variable fraction of low-energy particles which can reach a given point on the earth's surface. It may, therefore, be concluded that the fraction of low-energy particles in the general spectrum during the decrease of the burst was higher at Yakutsk than at Irkutsk and Deep River.

Moreover, as can be seen from Figures 1 and 2, the increase in the intensity of the neutron component at Irkutsk occurred 3-5 minutes earlier (at 1028 UT) than at Yakutsk. The return to the normal level was also faster. Similar effects were also observed at the Deep River station (the burst began at 1028 UT).

Values of γ at different stations

Station	γ
Deep River	$-(1.7\pm0.4)$
Irkutsk	$-(2.2\pm0.4)$
Yakutsk	$-(0.8\pm0.2)$
Mean	$-(1.6\pm0.6)$

The cosmic-ray burst was preceded [1] by a solar flare which began at 1020 UT on May 4, in the neighborhood of the sunspot group 90° west of the central solar meridian.

According to [8], the appearance and the rapid development of loop prominences was observed on the western limb of the sun. An intensive development of the first loop was recorded at 1016 UT. Ionospheric disturbances (fading, phase anomalies, atmospherics) were observed at the same time. A rapid development of the second loop was observed at 1040 UT. These phenomena occurred in the coronal region above a developing and very variable sunspot group ($\varphi = +15°$) which passed through the central meridian on April 27, 1960. It is suggested in [8] that the rapid development of loop prominences is a source of ionizing short-wave radiation.

All this suggests that the sun was in fact the source of the cosmic-ray burst. The relatively short lifetime of this burst can apparently be explained by the fact that the source was located on the western limb of the solar disc.

The following conclusions may be drawn from the above discussion.

1. The source of the burst should lie in the plane of the ecliptic since the ground level south telescope at Yakutsk which was at an angle of 30° to the zenith showed an appreciable effect ($4.0 \pm 1.3\%$) as compared with other instruments recording the μ-meson component.

2. The existence of zones of incidence indicates that the effect was due to positive particles of solar origin.

3. During the burst there were apparently no scattering centers for the particles. This follows both from (a) the anisotropy of the flux during the maximum

and the decrease, (b) the very rapid approach to the maximum of the burst (~7 minutes) as compared with other bursts [1], and (c) from the absence of variation in the electromagnetic field of the earth.

4. The delay in the onset of the burst (~1028 UT) relative to the ionospheric disturbance (1016 UT) is explained by the arrival at the earth of, first, the shortwave radiation, and, somewhat later, the particle stream.

5. The variation spectrum ($\frac{\delta D(\varepsilon)}{(D)} - \varepsilon^{-5}$) which was derived above is in agreement with the spectrum of previous bursts [7]. The mechanism responsible for all these bursts should, therefore, be the same.

REFERENCES

1-2. McCracken, K.G. and Palmeira, R.A.R. The production of cosmic radiation on the sun during July 1959 and May 1960.

3. Rose, D.C. The sudden increase in cosmic-ray intensity of May 4, 1960.

4. Ehmert, A., Erbe, H., Kirsch, E. and Pfotzer, G. Solar cosmic rays at Lindau on May 4, 1960.

5. Kopylov, Yu.M. Sovetskiye stantsii kosmicheskikh luchey (Soviet cosmic ray stations). Izd. AN SSSR, Moscow, 1960.

6. Kuz'min, A.I. Dissertation, YaFAN MGU, Moscow, 1959.

7. Dorman, L.I. Variatsii kosmicheskikh luchey (Cosmic-ray variations). Moscow, 1957.

8. Kletzek, J. and Krivcky, L. Bull. of the Astron. Inst. of Czechoslovakia, 4, 165, 1960.

Yu. G. Shafer and V. D. Sokolov

EFFECT OF MAGNETIC STORMS IN THE INTENSITY OF COSMIC RAYS ACCORDING TO MEASUREMENTS IN THE STRATOSPHERE

The present note reports the results of a preliminary analysis of experimental data on the intensity of cosmic rays in the stratosphere during intense and very intense magnetic storms.

The cosmic-ray intensity in the stratosphere was measured with the aid of the counter telescope described in [1].

During 1959 the measurements of the cosmic-ray intensity in the stratosphere coincided in six cases with effective magnetic storms. The table shows some data relating to these storms. The stratospheric data on the cosmic-ray intensity refer to the 100 mb level.

Magnetic storm data and the corresponding effects in the intensity of cosmic rays according to stratospheric (S), neutron monitor (N) and ionization chamber (I) measurements in 1959.

№	Time of storm	Characteristic of storm	Beginning of flight to the stratosphere	Time of maximum effect in cosmic rays	Effect of storm, % (decrease)		
					S	N	I
1	March 26^d09^h—31^d24^h	V.P.S., sudden start	$27^d05^h30'$	27^d13^h—14^h	5.5±1.5	4.2±1.5	1.5±0.3
2	May 11^d05^h—13^d00^h—15^d08^h—16^d00^h	P.S., sudden start	14 04 22	14 09 —10	11.0±1.5	7.5±1.5	3.0±0.3
3	July 15^d08^h—16^d20^h	V.P.S., sudden start	16 02 24	15 18 —20	12.0±2.0	16.0±2.0	4.5±0.3
4	July 17^d16^h—19^d20^h	V.P.S., sudden start	18 00 34	18 06 —0.8	17.0±2.0	17.8±2.0	5.3±0.3
5	September 08^d22^h—16^d12^h	P.S., sudden start	04 06 50	4 05 —10	16.0±1.5	3.0±1.5	2.3±0.3
6	September 20^d02^h—22^d21^h	P.S.	22 06 30	19 21 —24	5.0±1.5	1.5±1.5	0.7±0.3

Note: V.P.S.—Very powerful storm; P.S.—Powerful storm.

In order to compare the effect of a magnetic storm in the stratosphere with the effect at the earth's surface we have used neutron monitor data corrected for the barometric pressure and the intensity of the hard component of cosmic rays (ionization chamber, ASK-1) corrected for cosmic-ray bursts and barometric pressure.

The effect of a magnetic storm on the cosmic-ray intensity in the stratosphere was determined as the difference between the data obtained in a flight during a storm, and the neighboring period with undisturbed cosmic-ray intensity.

It is clear from the table that effective magnetic storms were accompanied by a considerable reduction in the cosmic-ray intensity in the stratosphere.

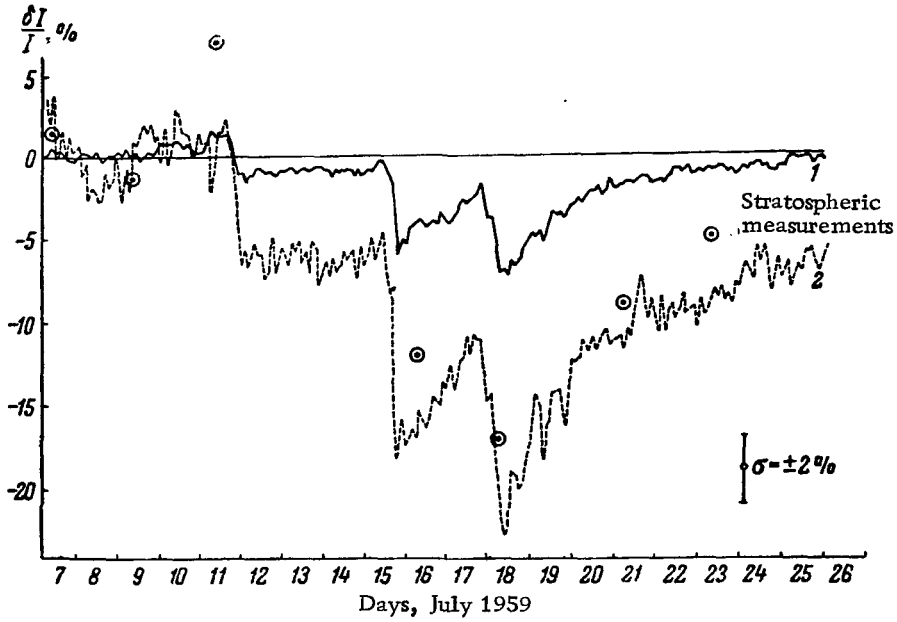

Fig. 1. Effect of magnetic storms on the intensity of cosmic rays in July 1959.
1 - Hard component; 2 - Neutron component.

The three successive magnetic storms in July 1959 are of particular interest. These storms occurred between July 7 and July 23. Seven flights into the stratosphere were carried out during this period, and reliable data on the cosmic-ray intensity up to the 100 mb level and above were obtained. Figure 1 shows the results obtained during these flights, and the corresponding measurements of the cosmic-ray intensity at ground level.

Since the flights did not exactly coincide with the times of maximum storm effects in cosmic rays, and since we have no more detailed data on the cosmic ray intensity in the stratosphere at different phases of the magnetic storm, it is

difficult to estimate the energy characteristics of the particles which experienced the effect of the magnetic storms. Comparison of the effect of magnetic storms on the intensity of cosmic rays in the stratosphere and at ground level leads to the very preliminary conclusion that the particles which were affected by the July magnetic storms were primary particles with energies up to 20-30 BeV.

Inspection of the table and of Figure 1 will show that the effect of a magnetic storm in the stratosphere is apparently much greater than the corresponding effect in the neutron and hard component of cosmic rays at the earth's surface.

A further interesting fact connected with the July storms should be noted. The first of these successive storms began on July 11 at about 1600 hrs. Approximately 12 hours before the beginning of this storm we carried out a flight into the stratosphere. The altitude variation in the intensity of the cosmic rays which was obtained during this flight is shown in Figure 2. For comparison, this figure also shows the average altitude variation of the cosmic-ray intensity for two other flights (July 7 and 9, 1959) when there were no special changes in the cosmic-ray intensity. As can be seen, on July 11 the cosmic-ray intensity increased at 300 mb and above, the changes being 10% at 100 mb and 20% at 50 mb. The flight of July 11 began at 0200 hrs UT. The 300 mb level was reached in approximately 40 minutes, and the ascent continued for another 60 minutes.

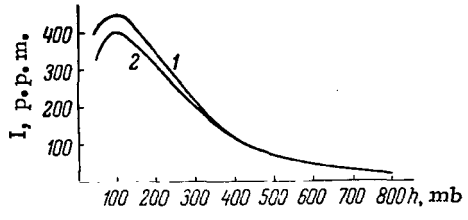

Fig. 2. Altitude variation of cosmic-ray intensity.

1 — July 11, 1959, 2 — average for July 7 and 9, 1959.

According to ionospheric observations at Yakutsk during the period corresponding to this flight, there were no particular ionospheric changes. Exactly 24 hours before that (on July 10 between 0200 and 0415 hrs UT), a very strong ionospheric disturbance was observed and was characterized by total absorption in the lower layers and a rapid oscillation in the critical frequencies of F2. These ionospheric disturbances were due to the strong chromospheric flare on July 10.

Several difficulties were encountered in attempts to interpret the increase in the intensity of cosmic rays on July 11. Here, we shall briefly discuss two interpretations.

1. It is possible to assume that the increase in the intensity of the cosmic-rays in the stratosphere which occurred on July 11 was due to the influx of additional radiation.

It is known from the theory of geomagnetic effects that at the latitude of 51°, the minimum energy of particles which will reach this point in the vertical direction is about 2 BeV. It follows that on July 11 the geomagnetic field was modified so that particles with energies less than 2 BeV could reach the earth.

The neutron component of cosmic rays at sea level, which is an indicator of changes in the intensity of low-energy particles in cosmic radiation [2], should react to this additional radiation. However, as can be seen from Figure 1, during the flight of the instruments on July 11, there was no appreciable change in the intensity of the neutron component at the earth's surface. On the other hand, the increase in the intensity of cosmic rays during the flight at 300 mb and above, shows that the suggested additional radiation included particles with energies of at least up to 0.5-0.6 BeV. Summarizing, it may be said that on July 11 at the latitude of 51° there was an additional flux of radiation amounting to at least 20% of the normal cosmic ray background. This additional flux consisted mainly of low-energy particles with energies of 0.5-0.6 BeV and less. It is difficult to imagine the conditions which would allow such low-energy particles to reach the earth at the latitude of 51°, and also the mechanism and the conditions of production of this additional radiation.

2. Winckler has reported [3] that balloon measurements on cosmic rays during the IGY revealed two cases when radioactive layers appeared in the atmosphere. In both of them the radioactive layer was encountered at 300-350 mb and was recorded only when the instruments passed through it. Below and above the layer, the cosmic-ray intensity had its usual value. Analysis of these two cases led Winckler to the conclusion that the increase in the intensity was due to the presence in the layer of radioactive matter emitting γ-rays (decay products) with energies of about 1 MeV.

If the increase in the cosmic-ray intensity in the stratosphere which was observed on July 11 was due to this type of radioactive cloud, then the thickness of the cloud was of the order of 15-20 km, and the cloud was localized above 300-350 mb.

Analysis of the data obtained as a result of other flights has not so far led to the discovery of an analogous effect, and it is therefore difficult to decide which of the above two interpretations is to be preferred.

REFERENCES

1. Belomestnykh, V.A. and Shafer, Yu.G. Tr. TaFAN SSSR, ser. fizich., No. 2, 47, 1958.

2. Simpson, J.A. Phys. Rev., 73, 1389, 1948; 81, 895, 1951.

3. Winckler, J.R. Balloon study of high altitude radiations during the International Geophysical Year. University of Minnesota, March, 1960.

COMPOSITE GEOPHYSICAL OBSERVATIONS AT YAKUTSK DURING JULY, 1959*

A.I. Kuz'min, G.V. Shafer, Yu.G. Shafer,
D.D. Krasil'nikov, G.F. Krymskiy, A.P. Mamrukov,
N.S. Smirnov, and V.I. Yarin

1. INTRODUCTION

New important information about the correlation between various geophysical factors and solar activity was obtained during the IGY. It is currently believed that the sun emits corpuscular streams which are responsible for disturbances in the geomagnetic field and the ionosphere, for the appearance of auroras, and for certain characteristic variations in cosmic-ray intensity. The study of cosmic-ray variations provides information on the electromagnetic properties of the corpuscular streams [1]. However, these properties depend on the model of the stream, and it is not always possible to obtain an agreement with experimental data [2].

Three successive magnetic storms with sudden commencement, which gave rise to three successive decreases in the cosmic-ray intensity, were noted in July 1959. The study of these events is of interest from the point of view of the sun-earth interaction.

The present paper reports the results of processing and analysis of composite experimental studies of geomagnetism, the ionosphere, auroras, cosmic-rays and aerology, which were carried out at Yakutsk in July 1959.

2. PRIMARY DATA PROCESSING

General Description of the Data

The Yakutsk Laboratory of Physical Problems has been engaged in measurements of the components of the geomagnetic field, the state of the ionosphere, the properties of auroras, and the intensities of the various cosmic-ray components in a wide primary energy range [3]. Aerological

*An abridged version was published in the materials of the Symposium on events in July 1959.

soundings of the atmosphere above the point of observation were obtained by the Yakutsk Hydrological and Meteorological Service.

This set of composite geophysical data appears to be unique. This is particularly so in the case of the cosmic-ray data. The utilization of these composite data obviates a number of serious difficulties [3] which are encountered in studies of the electromagnetic properties of the earth-sun neighborhood, the state of the upper atmosphere, the time transformation of the primary cosmic-ray energy spectrum, and the role of the geomagnetic field.

Geomagnetic Data

The primary data are in the form of records of variations in the H, D and Z components of the geomagnetic field obtained with Eschenhagen variometers. In this paper, use will be made of:

a) magnetic storm records;
b) mean hourly absolute values of H and Z (in gammas) and the magnetic declination (in minutes); and
c) hourly amplitudes of the horizontal component (in gammas).

The intensity of the geomagnetic storms was estimated from the nature of the disturbances and the maximum amplitudes of the magnetic elements during the storms (Table 1). Two disturbed periods (July 4—5 and 24—27) and three magnetic storms (July 11—12, 15—16 and 17—19) were noted during the month.

The character of the variations in the magnetic elements, the amplitude and the duration of continuous disturbances during the disturbed periods, suggest that they cannot be regarded as magnetic storms.

Table 1

Maximum amplitudes of magnetic elements during a storm.

Type of storm	*D* (in gammas)	*H* (in gammas)	*Z* (in gammas)
Low intensity . .	130—179	110—170	100—180
Moderate intensity	180—310	171—280	181—300
High intensity .	311—400	281—510	301—480
Very high intensity . . .	> 401	> 511	> 481

Table 2 gives for comparison the diurnal sums of the hourly visual characteristics $\Sigma n_1 + 2n_2$ and the sums of the K-indices for a) five quiet days, b) the disturbed periods, and c) days corresponding to magnetic storms.

All the three magnetic storms have clearly defined sudden commencements which are characterized by a sharp increase resembling a positive pulse in the horizontal component, and an equally sharp, though smaller, reduction in the Z component.

The storm of July 11 which began at 1625 UT and continued for 18 hours had the lowest intensity. In spite of the absence of sharp instantaneous and sufficiently large changes in the field components, which are characteristic for intense storms with sudden commencement, the average variation in the H component exhibits features which are characteristic for this class of storms, namely, the presence of a considerable initial phase (enhanced field intensity) and a depression (reduction in the mean field during the principal phase).

Table 2

Daily sums of the hourly visual characteristics ($\Sigma n_1 + 2n_2$) and sums of K-indices.

Characteristic	Quiet days					Disturbed days						Days with magnetic storms						
	1 VII	3 VII	10 VII	29 VII	30 VII	4 VII	5 VII	24 VII	25 VII	26 VII	27 VII	11 VII	12 VII	15 VII	16 VII	17 VII	18 VII	19 VII
Σ_K	5	2	11	7	5	12	14	20	25	26	20	24	18	52	25	30	36	24
$\Sigma n_1 + 2n_2$	—	—	—	3	—	7	11	17	19	19	10	8	4	36	16	16	34	6

The characteristic features of this storm were as follows:

a) Large first positive peak in the H curve, although it was a low-intensity storm ($\Delta H = 159\ \gamma$).

b) Weak development of the initial phase (there was a decrease in the field immediately after the first peak).

c) The absence of sharp changes in the magnetic elements and short-period pulsations which are characteristic for storms with sudden commencement.


γ
58600
58400
58200
Z γ
15000
14700
14400
H γ
400
200
0
r γ H
20°00'
19°40'
19°20'
D

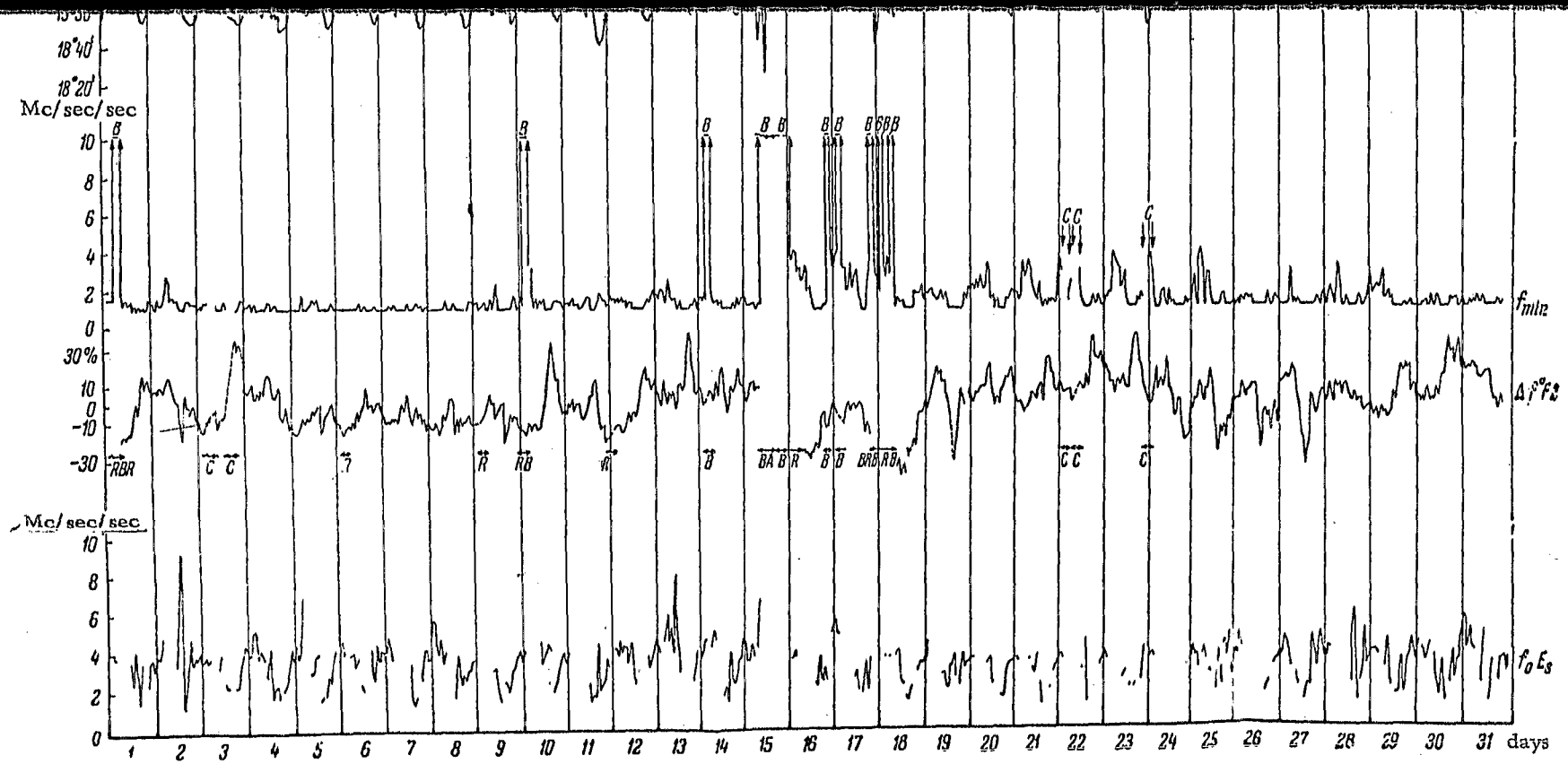

Fig. 1. The magnetic field, the state of the ionosphere, and the auroras at Yakutsk in July, 1959: Z^{γ}—vertical component of the geomagnetic field (in gammas), H^{γ}—horizontal component (in gammas), r_H^{γ}—amplitudes of the horizontal component (in gammas), D—declination (in minutes), f_{min}—minimum reflection frequency (in Mc/sec), $\Delta f^{o}F2$—departure of the critical frequencies of the F2 layer (in %), f_oE_s—critical frequency of the sporadic E (in Mc/sec).

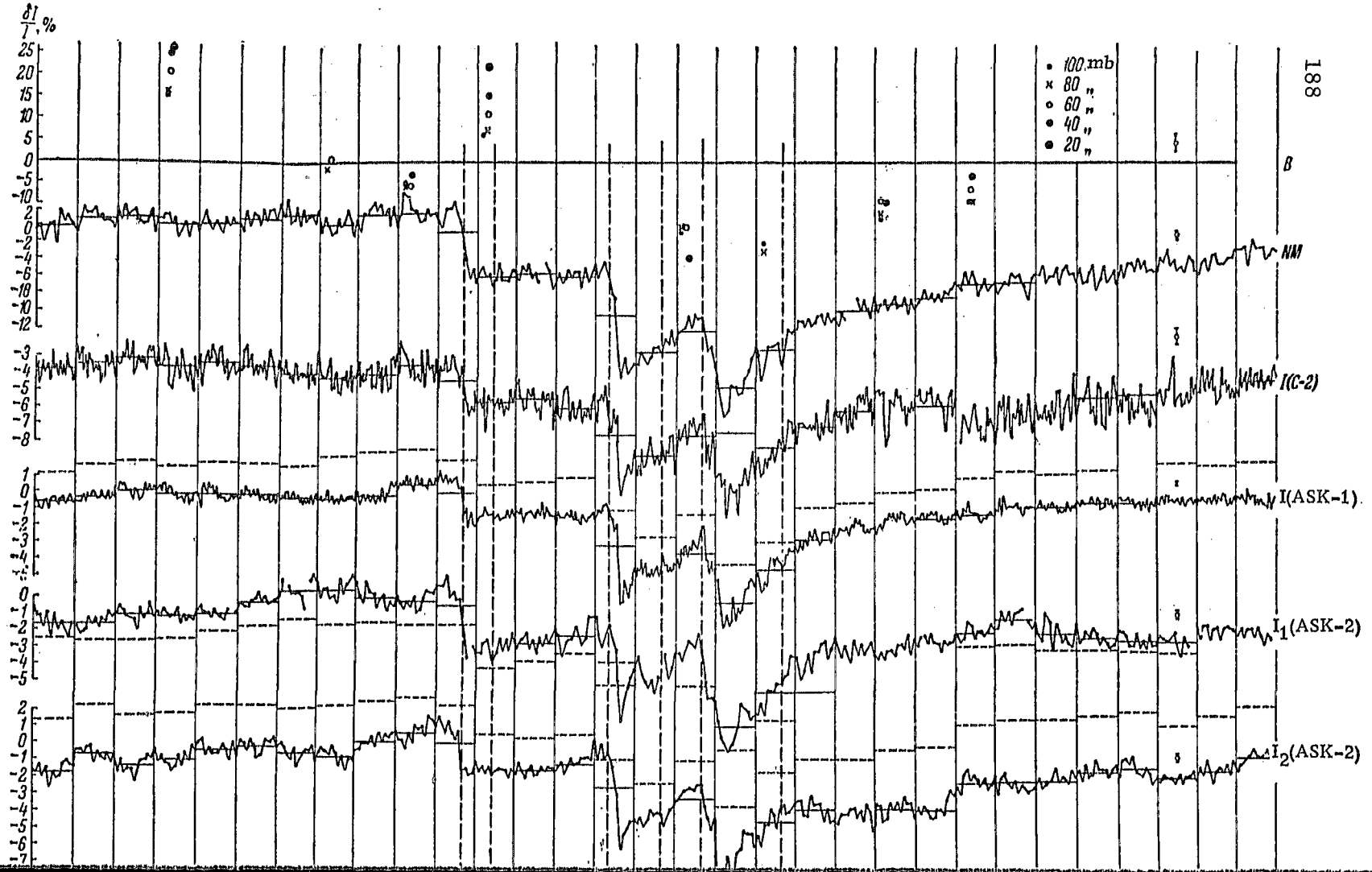
δI/I, %
• 100 mb
× 80 „
○ 60 „
● 40 „
● 20 „
B
NM
I(C-2)
I(ASK-1)
I1(ASK-2)
I2(ASK-2)

$T_0^0(Z)$
$UT_7^0(Z)$
$UT_{20}^0(Z)$
$UT_{60}^0(Z)$
$T_0^{30}(S)$
$UT_7^{30}(S)$

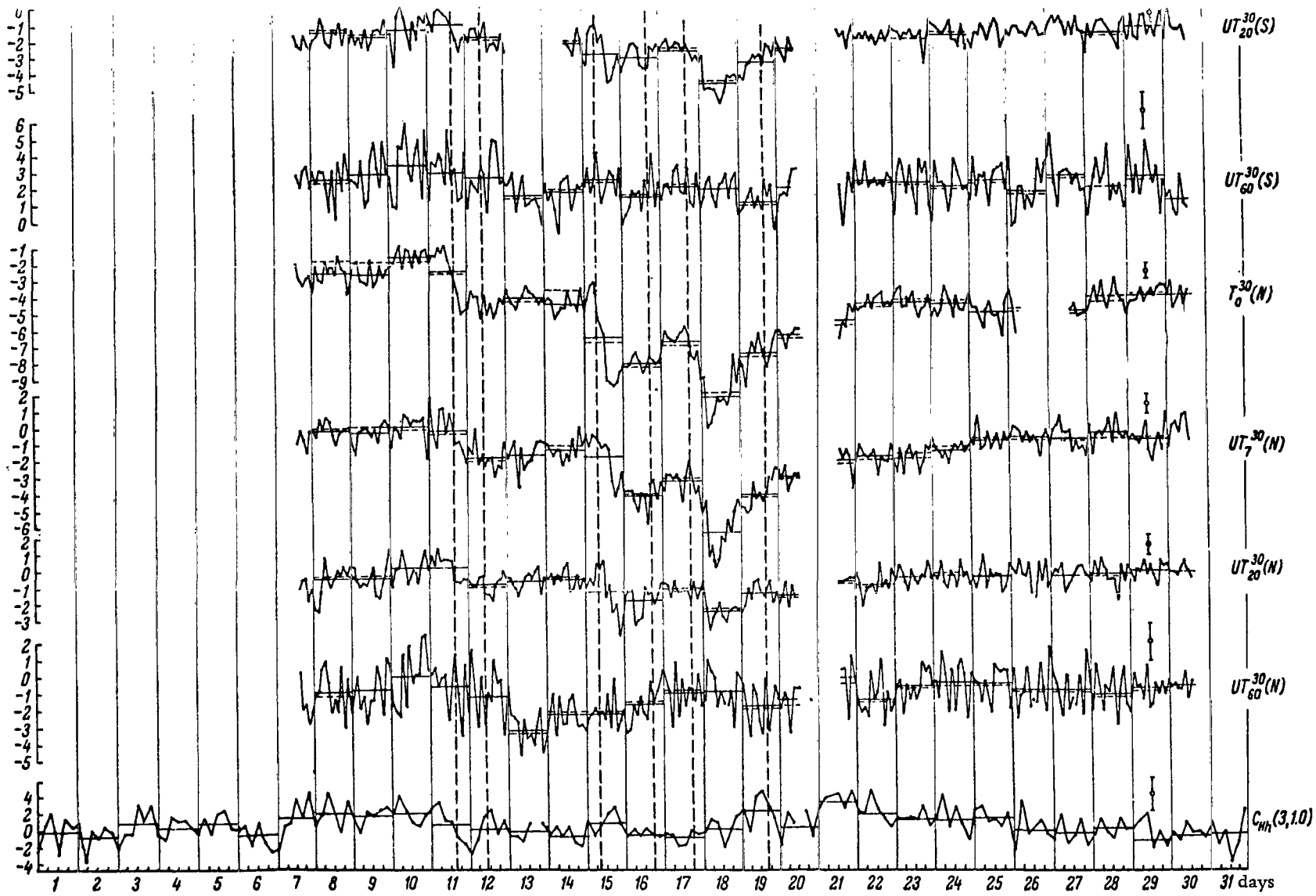

Fig. 2. Variations in the cosmic-ray intensity in July, 1959 (corrected for the barometer effect):

B—stratospheric data, NM—neutron monitor, I(S-2)—the S-2 ionization chamber, I(ASK-1)—ionization chamber ASK-1, $I_{1,2}$(ASK-2)—ionization chambers ASK-2 in the Bay of Tiksi and on Cape Shmidt; $T_0^0(Z)$, $T_0^{30}(S)$, $T_0^{30}(N)$—ground level telescope at 0° and 30° to the zenith, south and north; $UT_7^0(Z)$, $UT_7^{30}(S)$, $UT_7^{30}(N)$, $UT_{20}^0(Z)$, $UT_{20}^{30}(S)$, $UT_{20}^{30}(N)$, $UT_{60}^0(Z)$, $UT_{60}^{30}(S)$, $UT_{60}^{30}(N)$ same telescopes at depths of 7, 20 and 60 m w.e; $C_{Hh}(3, 1.0)$—extensive air shower installation recording triple coincidences between banks of $1\,m^2$ in area (mean EAS frequency over four identical installations is reproduced).

d) The maximum amplitude of H was several times larger than the maximum amplitude of Z ($A_{H\ max} = 358\ \gamma$; $A_{Z\ max} = 78\gamma$).

The storm which began on July 15 at 0802 UT and continued for 32 hours, belongs to the class of great storms. This storm clearly exhibited the characteristic features of storms with sudden commencement, namely, considerable mobility of the magnetic elements during the principal phase and superposition of short-period pulsations.

The storm began with a positive peak equal to 142 γ in the H component, which was followed by a highly developed (both in time and in depth) initial phase. The enhanced intensity of the field continued for over 6 hours, reaching a maximum at 1236 UT, i.e. 4.6 hours after the beginning of the storm. The maximum intensity in the initial phase exceeded the undisturbed field by 780 γ. A rapid reduction in the mean level of the field (relative to the undisturbed field), with large instantaneous amplitudes and superposition of pulsations, began at 1440 UT. This reduction and the increased variability coincided with the beginning of radio echoes from auroras.

The maximum reduction in the field strength occurred on July 15 at 1854 UT and was equal to 900 γ. During the storm $A_{H\ max}$ and $A_{Z\ max}$ were respectively equal to 1677 and 771 γ.

The particular features of this storm were:

a) Rapid development of the initial phase in spite of the relatively small first positive peak (during the minor storm of July 11 this peak amounted to 159 γ, while during the great storm of July 15 it was 142 γ).

b) Intensive development of the principal phase with an instantaneous maximum depression of 900 γ.

On July 17 at 1636 UT, i. e. the day after the end of the storm, a new very intense storm began with a sudden positive peak equal to 142 γ. This storm continued for 48 hours but was less intense than the storm of July 15 (the maximum amplitudes of H and Z during this storm were 770 and 695 γ). The initial phase of both this storm and the storm of July 11 exhibited an exceptionally weak development (the increase in the intensity continued for less than two hours). Moreover, the sudden commencement peak occurred only just in the maximum, and the development of the principal phase began as early as 1830 UT on July 17 in the form of a sharp reduction in the field with superimposed large short-period pulsations.

At 0300 UT on July 18, the field became nearly the same as the undisturbed field, the variations became gradual and continuous, and the storm developed a phase similar to the initial phase of July 15 (0400—1000 UT, July 18).

Comparison of the variations in the Z, H and D elements with the variation in the amplitude of the horizontal component r_H illustrated in Fig. 2 shows that the same phases of the storms of July 15 and 17 occurred at the same hours GMT but at different time intervals within the storms. The initial phase of the storm of July 17 was so underdeveloped that it gave the impression that the storm began (after the sudden pulse) immediately with the principal phase, which was then followed by a phase similar to the initial phase of the storm of July 15.

The field of the magnetic storm consisted of S_D, D_{st} and D_i variations while S_D variation in the H and Z components at Yakutsk had a summer maximum at 0700—1000 UT.

Ionospheric Data

The ionospheric data shown in Fig. 1 were obtained by vertical radio sounding with the aid of an automatic panoramic station which carried a transmitter giving 2.5 kW per pulse. The sensitivity of the receiver was better than 10 μV. The observations were carried out at 15-minute intervals in the frequency range 1—18 Mc/sec.

The criteria which were taken as indicating the presence of ionospheric disturbances were as follows:

1) Five-hour persistence of a 20%, or greater, deviation of the critical frequency of F2 from the sliding median calculated for each hour of the day over 30 days ($\Delta f^{\circ}F2 \geqslant 20\%$).

2) Complete or enhanced absorption characterized by $f_{min} \geqslant 3$ Mc/sec.

3) The presence, in the E region, of stable screening layers with critical frequencies greater than 4 Mc/sec ($f^{\circ}E_s > 4$ Mc/sec).

An example of an exceptionally disturbed ionosphere is illustrated in July in Fig. 2. From the point of view of the above estimates of the state of the ionosphere, it is possible to distinguish the following active periods:

July 1, 0400—0645 UT - complete absorption (B) in the lower ionosphere (60—100 km); no disturbance in the upper layers.

July 3, 1800—2300 UT - positive disturbance in F2·$\Delta F^{\circ}F2$, reaching 25—30% and accompanied by a type-C sporadic E_s.

July 10, 0200—0415 UT - very strong disturbances characterized by complete absorption in the lower layers and sharp oscillations in the critical frequency of F2. During this period there was complete radio fadeout over the territory of the Yakutsk ASSR.

July 14, 0345—0515 UT - sudden increase in the absorption leading to complete absorption.

July 15, 0900 UT - July 16, 0130 UT - complete absorption; between 0130 and 1500 UT on July 16, f_{min} gradually decreased and absorption returned to normal; a strong reduction in the critical frequency of F2 (up to about 40%) was observed simultaneously with the disturbance in the lower layers.

July 16, 2130—2230 UT - total absorption in the lower ionosphere; considerably increased absorption until July 17, 1400 UT; quiet upper ionosphere.

July 17, 1700 UT - July 18, 2000 UT - disturbances in the entire ionosphere, $\Delta f^{\circ}F2$ reaching about 40%, and the absorption in the lower layers at times practically complete.

July 22—30, rapid oscillations in $\Delta f^{\circ}F2$ and f_{min}; ionosphere unstable, large disturbances absent.

The disturbances of July 1, 10, 14 and (to a lesser extent) July 16 have much in common. The main feature in all these cases is the rapid increase in the ionization density at 60—100 km (D and E regions). At the same time, the F1 and F2 layers did not undergo any changes. A further common feature was that these disturbances developed close to local midday and occupied a time interval of 2—3 hours. They were not accompanied by (i.e. were not simultaneous with) strong magnetic disturbances, although according to solar data, chromospheric flares were observed on the sun. Hence, solar ultraviolet radiation may have been responsible for these disturbances. The disturbances of July 15—17 are quite different. Their main features were as follows:

1) The disturbances occurred throughout the ionosphere and the ionization density in the lower layers (D and E) increased (this is suggested by the increase in f_{min} and B), while in the upper layers, particularly in the F2 layer, the intensity decreased considerably.

2) The disturbances continued for a long interval of time and were simultaneous with disturbances in the earth's magnetic field.

3) The disturbances of July 15 were preceded by the chromospheric flare of July 14, and therefore a corpuscular stream of solar origin may have been responsible for them.

Cosmic-Ray Data

The Yakutsk Laboratory has been engaged in measurements of the intensity of the neutron component at sea level with a standard neutron monitor

[4], the cosmic-ray intensity in the stratosphere using double-coincidence telescopes [5], and the hard component at ground level and different depths underground. Measurements of the hard component are being carried out with the aid of ionization chambers under different amounts of absorbing matter, and with the aid of triple-coincidence telescopes at ground level and at depths of 7, 20, and 60 meters water equivalent (m w.e.) [6]. The vertical telescopes have a large acceptance angle ($\omega \cong \pi$), while the south and north telescopes, which are at 30° to the zenith, have a small acceptance angle ($\omega = 0.2\,\pi$). Moreover, measurements are being made on the extensive air showers corresponding to different mean energies of the primary particles [7].

In the present work, use is also made of cosmic-ray data obtained with ionization chambers at stations in the Bay of Tiksi and at Cape Shmidt.

Figure 2 shows the two-hourly values of the intensity of the various cosmic-ray components for July 1959. The EAS data are in the form of four-hourly values.

The statistical accuracy and the changes of meteorological conditions were taken into account in the processing and analysis of the data about the components [I - ionization chamber; $T_K^i(n)$ - semi-cubic telescope, at a depth of K m w.e. at an angle i equal to 0 and 30° to the zenith where n = S (south), n = N (north) and n = Z (vertical) directions; NM - neutron monitor; C - the EAS Station]. Changes in the barometric pressure were allowed for by means of constant barometric coefficients of $\beta = -0.68$ (neutron component), -0.12 (hard component at ground level), and -0.10, -0.08 and -0.04% g^{-1} cm^{-2} at 7, 20 and 60 m w.e. respectively. The temperature effect was excluded with the aid of the temperature-coefficient density function calculated with allowance for changes in the effective exponent in the differential π-meson production spectrum for different depths of recording [2] and the atmospheric temperature profile.

Three sharp decreases in the intensity occurred in July 1959 (July 11, 15, and 17).

A small increase in the intensity was observed prior to the sharp decrease on July 11. Between July 12 and 14, the intensity of all the cosmic-ray components did not exhibit any appreciable changes and remained approximately constant up to July 15 when a new sudden decrease occurred in connection with the magnetic storm of July 15. This decrease was followed by a gradual increase in the intensity, which was interrupted by the next rapid decrease on July 17 which was due to the magnetic storm on that day. The intensity gradually returned to the normal level between July 17 and 21.

It should also be noted that, firstly, there was some increase in the intensity in the course of the normal recovery before the principal rapid decreases on July 15 and 17. Secondly, the general decrease in July does not exhibit any appreciable dependence on the direction of incidence of the

recorded radiation, and thirdly, the amplitude of all the variations decreases with increasing mean energy of the recorded particles.

General Description of Solar Phenomena

Four active regions which were characterized by extensive facular fields and a small number of spots and flares were observed between July 1 and 9. Between July 11 and 20, four active regions passed through the central meridian and one of these regions was associated with a large sunspot group. Intense chromospheric flares were observed in this region between July 10—14 [8].

3. ENERGY CHARACTERISTICS OF COSMIC-RAY VARIATIONS

Determination of Primary Variations from Variations in the Secondary Components

The variations in the i-th secondary component of cosmic-rays at a depth h are related to the primary variations by

$$\frac{\delta N_i(h)}{N_i(h)} = \int_{\varepsilon_{min}}^{\infty} W_i(h, \varepsilon) \frac{\delta D(\varepsilon)}{D(\varepsilon)} d\varepsilon; \tag{1}$$

where $W_i(h, \varepsilon)$ are the coefficients of coupling between the i-th component at the depth h and the primary component at the top of the atmosphere [1]; $\frac{\delta D(\varepsilon)}{D(\varepsilon)}$ represents the variations in the primary beam. If the variation amplitude of a number of secondary components is known, then it is possible to determine the spectrum of the primary variations.

Since the amplitude of the variations during the July events in 1959 decreased with increasing mean energy of the recorded particles, it follows that the primary variations $\frac{\delta D(\varepsilon)}{D(\varepsilon)}$ may either be of the form

$$\frac{\delta D(\varepsilon)}{D(\varepsilon)} = -f \begin{cases} \text{const}, & \text{when } \varepsilon < \varepsilon_1, \\ 0, & \text{when } \varepsilon > \varepsilon_1, \end{cases} \tag{2}$$

or of the form

$$\frac{\delta D(\varepsilon)}{D(\varepsilon)} = - \begin{cases} b, & \text{when } \varepsilon < \varepsilon_1 \\ a\varepsilon^{-\alpha}, & \text{when } \varepsilon > \varepsilon_1. \end{cases} \tag{3}$$

We shall now use our composite cosmic-ray data, which cover practically the entire range of primary energies, to determine ϵ_1, and f.

We note that the calculation will be carried out with the aid of two coupling coefficients namely W' [1] and W'' [2]. However, since the final results are not very sensitive to different W' and W'' for the spectra given by (2) and (3), the parameters given below were determined with W' only.

Main Decrease in the Intensity and the Energy Spectrum of the Variations on July 11, 1959

The decrease in the cosmic-ray intensity began on July 11 at 1100—1200 UT and was detected by all the Yakutsk instruments. The intensity continued to decrease for 8—9 hours, and reached its minimum value at 2000 hours on July 11. The decrease was estimated as follows: the mean value for July 9 and 10, corrected for the barometer and temperature effects, was adopted as the normal level and all the subsequent effects were estimated relative to it. The minimum intensity was estimated as a mean over the interval between 1800 and 2400 hours on July 11, when the intensity recorded by most of the instruments reached the minimum. The amplitude of the effect is therefore equal to the difference between the normal level and the value at the minimum.

Table 3 shows the values of the amplitudes of the main decrease in the intensity during the magnetic storm of July 11, 1959.

The mean rate of decrease in the cosmic-ray intensity determined from the hard component at ground level was 0.25—0.30%/hr. Errors in the amplitude of effect were made up by the mean statistical errors and the errors due to the diurnal variations. Table 4 gives the values of the errors in the amplitude of the main effect of the storm for each instrument.

The energy spectrum of the variations is of major importance for the elucidation of the mechanism responsible for the reduction in the cosmic-ray intensity during the magnetic storm. Calculations show that the observed variations are in disagreement with the spectrum given by (2) which corresponds to scattering of the cosmic-rays by uniform magnetic fields of corpuscular streams. For small ϵ_1 the disagreement occurs at high energies, while for large ϵ_1 it occurs at low energies. The observed spectrum of the decrease is also in disagreement at high energies with the spectrum predicted by Piddington [9]. The amplitude of the decreases at 20 and 60 m w.e. is much smaller than the value predicted by the reflection of the cosmic-ray particles by the wall of the perfect magnetic cone considered by Piddington.

The best agreement between the observed and calculated variations is obtained for the following spectrum

$$\frac{\delta D(\varepsilon)}{D(\varepsilon)} = -a \begin{cases} \left(\frac{\varepsilon}{\varepsilon_1}\right)^{-\alpha}, & \text{when } \varepsilon > \varepsilon_1, \\ 1, & \text{when } \varepsilon < \varepsilon_1, \end{cases} \qquad (3a)$$

where

$$\varepsilon_1 = (8 \pm 3)\ \text{BeV}, a = 0.13 \pm 0.03;\ \alpha = 1 \pm 0.2.$$

Characteristics of the Recovery in the Intensity and the Spectrum at the Beginning of the Decrease on July 15, 1959

After rapid decrease during the magnetic storm of July 11, the cosmic-ray intensity remained practically constant during the subsequent days (July 12—14). The spectrum before the beginning of the decrease of July 15 was estimated from the mean daily values of the cosmic-ray intensity for July 14,

Table 3

Amplitudes of the main decrease in the intensity during the magnetic storm of July 11, 1959

Station	Instrument	Amplitude	
		A_i %	$\frac{A_i}{A\,T_0^0(Z)}$
Yakutsk	Neutron monitor	6.8	2.38
Cape Shmidt	ASK-2	2.0	0.72
Bay of Tiksi	ASK-2	3.2	1.12
Yakutsk	S-2	2.4	0.83
»	ASK-1	1.8	0.65
»	Vertical telescope		
	Ground level	2.8	1.00
	7 m w.e.	2.0	0.72
	20 m w.e.	0.9	0.32
	60 m w.e.	0.4	0.12
»	North telescope		
	Ground level	2.7	0.95
	7 m w.e.	1.5	0.53
	20 m w.e.	0.5	0.18
	60 m w.e.	1.3	0.46
»	South telescope		
	Ground level	2.6	0.91
	7 m w.e.	2.8	0.98
	20 m w.e.	0.6	0.21
	60 m w.e.	1.2	0.42

Table 4

Errors in the determination of the amplitude of the main effect of the storm.

Instrument	Error, %
Neutron monitor	0.30
ASK-2	0.19
S-2	0.28
ASK-1	0.17
Vertical telescope	
Ground level	0.19
7 m w.e.	0.19
20 m w.e.	0.20
60 m w.e.	0.24
North and south telescopes	
Ground level	0.28
7 m w.e.	0.31
20 m w.e.	0.31
60 m w.e.	0.51

and was found to be the same as immediately after the decrease on July 11.

Main Decrease in the Cosmic-Ray Intensity and the Energy Spectrum of the Variations on July 15, 1959.

The next major decrease in the intensity of cosmic-rays began at 0800 on July 15 and was also detected by all the instruments. The beginning of the decrease coincided with the onset of a very intense magnetic storm. The intensity continued to decrease after about ten hours, and reached a minimum at 1700—1800 on July 15. The minimum intensity was estimated as the mean of the values between 1600 and 2100 on July 15. Table 5 gives the amplitudes of the decrease on July 15 as recorded by the various instruments at Yakutsk.

The errors in the amplitudes are given in Table 2.

The mean rate of decrease for the hard component at ground level was about 0.6%/hr. The observed effect (Table 5) is in agreement with spectrum (3a) with $\epsilon_1 = 10 \pm 2$ Bev, $a = 0.30 \pm 0.10$ and $\alpha = 1.0 \pm 0.2$.

Table 5

Amplitude of the decrease in the cosmic-ray intensity during the magnetic storm of July 15, 1959.

Station	Instrument	Amplitude, %	$\frac{A_i}{A_{T_0^0}(Z)}$
Yakutsk	Neutron monitor	18.2	2.21
Cape Shmidt	ASK-2	5.8	0.70
Bay of Tiksi	ASK-2	6.3	0.76
Yakutsk	S-2	5.6	0.68
»	ASK-1	6.0	0.73
»	Vertical telescope		
	Ground level	8.2	1.0
	7 m w.e.	6.0	0.72
	20 m w.e.	3.3	0.40
	60 m w.e.	1.2	0.15
»	North telescope		
	Ground level	7.5	0.91
	7 m w.e.	3.7	0.45
	20 m w.e.	2.8	0.34
	60 m w.e.	2.6	0.32
»	South telescope		
	Ground level	8.7	1.06
	7 m w.e.	6.0	0.73
	20 m w.e.	2.8	0.34
	60 m w.e.	1.8	0.22

Characteristics of the Recovery and the Spectrum at the Beginning of the Decrease on July 17, 1959

The rate of recovery in the cosmic-ray intensity during the first 10 hours after the decrease of July 15 was about 0.15%/hr for the hard component, and was subsequently slightly lower. The spectrum of the variations at the end of July 16 was of the form of (3a) with $\epsilon_1 = 6 \pm 2$ BeV, $a = 0.33 \pm 0.10$ and $\alpha = 1 \pm 0.2$.

Main Decrease on July 17 and its Spectrum

A very intense magnetic storm with sudden commencement, which was accompanied by a sharp decrease in the cosmic-ray intensity and was recorded by all the instruments, began at 1636 UT on July 17. The decrease in the intensity continued for about 15 hours. The recovery began after the minimum

was reached on July 18 at 0800—0900 hours. The minimum intensity was estimated as the mean for the period 0600—1100 on July 18. The amplitudes of the decrease are given in Table 6.

Table 6

Amplitude of the decrease in the cosmic-ray intensity on July 17, 1959.

Station	Instrument	Amplitude, %	$\frac{A_i}{A_{T_0^\circ(Z)}}$
Yakutsk	Neutron monitor	22.4	2.52
Cape Shmidt	ASK-2	7.8	0.89
Bay of Tiksi	ASK-2	8.7	0.98
Yakutsk	S-2	7.6	0.85
»	ASK-1	7.6	0.85
	Vertical telescope		
	Ground level	8.8	1.0
	7 m w.e.	7.6	0.86
	20 m w.e.	5.1	0.58
	60 m w.e.	0.8	0.10
»	North telescope		
	Ground level	9.5	1.07
	7 m w.e.	8.0	0.90
	20 m w.e.	1.7	0.19
	60 m w.e.	1.0	0.11
»	South telescope		
	Ground level	9.0	1.02
	7 m w.e.	6.6	0.75
	20 m w.e.	3.6	0.4
	60 m w.e.	1.6	0.18

The mean rate of decrease in the intensity of the hard component at ground level was 0.53%/hr. The amplitudes given in Table 6 are in agreement with spectrum (3a) with $\epsilon_1 = 6 \pm 2$ BeV, $a = 0.50 \pm 0.15$ and $\alpha = 1 \pm 0.2$.

Characteristics of the Recovery in the Intensity and Time Variations in the Spectrum

The rate of recovery of the intensity of the hard component as measured by the ASK-1 ionization chamber during the first 15 hours after the minimum

was 0.17%/hr. During the subsequent time, the rate of recovery gradually decreased and became equal to 0.007%/hr on July 23. The spectrum became softer in the course of the recovery. The decrease of July 23 is in agreement with the spectrum given by (3a) with $\epsilon_1 = 4 \pm 2$ BeV, $\alpha = 1.3 \pm 0.2$ and $a = 0.35 \pm 0.10$.

4. DISCUSSION OF THE RESULTS AND THEIR INTERPRETATION

General Remarks on the Connection between Magnetic Ionospheric Disturbances and Cosmic-Ray Variations with Solar Phenomena

We have seen that the magnetic storms of July 11, 15 and 17 were accompanied by considerable disturbances in the ionosphere, by characteristic changes in the intensity of cosmic rays in a broad energy range, and by the appearance of auroras.

A notable feature was the fact that about 24 hours before the sudden commencement of the magnetic storms, a short-period total absorption of radio waves was observed in the lower layers of the ionosphere. Thus, ionospheric absorption bursts were observed on July 10 at 0215 UT. A large chromospheric flare, which was accompanied by strong ultraviolet emission, occurred at approximately the same time.

The geomagnetic storm of July 11, began at 1625 UT with a sudden-commencement amplitude of 149 γ. Hence, if it is considered that a corpuscular stream was ejected on July 10 at 0215 UT in the neighborhood of the chromospheric flare, and having reached the earth was responsible for the geomagnetic storm, then the mean velocity of the corpuscular stream turns out to be

$$V_{st} = \frac{1.5 \cdot 10^{13}}{3.8 \cdot 3.6 \cdot 10^{-4}} = 1 \cdot 10^{8} \text{ cm/sec}$$

A similar analysis for the streams responsible for the storms of July 15 and 17 yielded velocities of 1.5×10^8 and 2.2×10^8 cm/sec respectively.

A lower limit for the width of the corpuscular stream may be obtained from the duration of the geomagnetic storms. It may be assumed that, at the distance of the earth's orbit or less, the corpuscular stream still retains the angular velocity of the sun. In that case the velocity of the earth relative to the axis of the stream will be of the order of 10^7—4×10^7 cm/sec, depending on the dynamic coupling between the stream and the sun after a determined time from the onset of the flare. Since the duration

of the visible flare is usually not more than 3—5 hours, it follows that the minimum distance from the sun at which the stream loses its "contact" with the sun is not less than $2 \times (3—5) \times 3.6 \times 10^3 \times V_{mean} \approx 2 \times 10^{12}—4 \times 10^{12}$ cm. It follows that if the duration of the storm is denoted by t, then the lower limit for the width of the stream is $2\pi(2—4) \times 10^{12} t/27 \times 24 \times 3.6 \times 1000$. In particular, for the storm of July 11, $l_*' = 5 \times 10^{11}$ cm, while the result for the storms of July 15 and July 17 is 10^{12} and 1.5×10^{12} cm respectively. If it is assumed that the stream is still coupled to the sun at the distance of the earth's orbit, then the stream widths for the storms of July 11, 15 and 17 turn out to be $\sim 2 \times 10^{12}$, $\sim 4 \times 10^{12}$ and $\sim 6 \times 10^{12}$ cm respectively.

The Parameters of a Corpuscular Stream Deduced from Cosmic-Ray Data

Since definite changes in the cosmic-ray intensity were observed during the magnetic storms of July 11, 15 and 17, 1959, it may be considered that these effects are associated with the ejection of magnetized corpuscular streams from the sun.

The effect of corpuscular streams on the intensity of cosmic rays has been considered by a number of workers [1, 9, 10]. Two models are being discussed at the present time, namely, the model involving a uniform corpuscular stream [1], the magnetic cone [9], and various modifications of these two models [11, 12].

a) Uniform corpuscular stream. According to this model, corpuscular streams carry frozen-in uniform magnetic fields. When the earth enters a stream head-on, the event is accompanied by a magnetic storm with sudden commencement. Lateral entry into the stream is associated with non-sudden commencement storms. At the same time, the cosmic-ray intensity undergoes variations of the form

$$\frac{\delta D(\varepsilon)}{D(\varepsilon)} = -f \begin{cases} 1, & \text{when } \varepsilon < \frac{\varepsilon_1}{4}; \\ \frac{2}{\pi} \sin^{-1}\left(\frac{\varepsilon_1}{2\varepsilon} - 1\right), & \text{when } \frac{\varepsilon_1}{4} < \varepsilon < \frac{\varepsilon_1}{2}, \\ 0, & \text{when } \varepsilon > \frac{\varepsilon_1}{2}. \end{cases}$$

The form of the variations may be used for rough estimates of the nature of the entry of the earth into the stream. This mechanism has been verified

experimentally on the basis of continuous measurements of the various cosmic-ray components at ground level [13]. The considerable duration of cosmic-ray disturbances as compared with geomagnetic disturbances is explained by the leakage of the magnetic field to distances exceeding 2—3 times the width of the corpuscular stream.

However, this model cannot be made to agree with underground data [2, 3, 14]. In order to remove this discrepancy in the spectrum of the variations, it has been suggested [11] that the uniform model should be generalized by taking into account the interaction of the stream with the interplanetary medium. Thus, it has been suggested that the corpuscular stream and the magnetic field originating from it sweep up various magnetized clouds in space. These irregularities are such that low and moderate energy particles are scattered by them and diffuse through the general field behind the stream, but are reflected by the field of the stream itself. High-energy particles are not affected by these irregularities and are scattered appreciably only by the extensive external field of the stream. Magnetized clouds may become oriented in the general field of the stream and may amplify the external field [14].

We have already seen that experimental data supplied by our composite apparatus are not in agreement with the expected spectrum of the uniform model. Therefore, the stream parameters given below were derived with allowance for the complicated structure of the interplanetary space.

In order to determine these parameters, it may be assumed that the experimental spectrum (3a) is, in fact, a superposition of two spectra of the form

$$\frac{\delta D(\varepsilon)}{D(\varepsilon)} = -\begin{cases} f_1 = \text{const}, & \text{when } \varepsilon < \varepsilon_1, \\ 0, & \text{when } \varepsilon > \varepsilon_1, \\ f_2, & \text{when } \varepsilon_2 < \varepsilon < \varepsilon_3, \\ 0, & \text{when } \varepsilon > \varepsilon_3. \end{cases} \tag{4}$$

The parameters of this spectrum may be determined from the readings of instruments located at ground level and underground at depths of 7, 20 and 60 m w.e. It may be shown on the basis of these assumptions, that the minimum value of the frozen-in magnetic field, $H = \epsilon_1/300\, l$, for the storms of July 11, 15 and 17, 1959, was approximately equal to 4×10^{-5}, 7×10^{-5} and 10×10^{-4} oe respectively.

The field strength of magnetized clouds during storms is 10^{-4}—10^{-5} oe and the effective linear dimensions are $R \sim 10^{10}$ cm. Clouds of this type should fill space to 3—5%.

The main difficulty of the uniform model of a uniform corpuscular stream is the change in the source of the variations at a practically unaltered spectrum.

b) The magnetic sack model. On this model, corpuscular streams are identified with a magnetic sack. The walls of the sack cannot be penetrated by particles with certain energies. When the earth enters the sack a geomagnetic storm and a decrease in the cosmic-ray intensity are observed. The recovery in the cosmic-ray intensity depends on the disintegration of the sack or the exit of the earth from it.

A perfect magnetic sack gives a spectrum of the form [12]

$$\frac{\delta D(\varepsilon)}{D(\varepsilon)} = \begin{cases} 1, & \text{when } P < \frac{P_0}{2}, \\ \cos^{-1}\left(1 - \frac{P_0}{P}\right), & \text{when } P > \frac{P_0}{2}. \end{cases} \tag{5}$$

Experimental data on cosmic-ray variations, which were obtained with our apparatus, are not in agreement with this model, However, agreement may be achieved if it is assumed that the sack is partially filled when the earth enters it. The variation spectrum will then differ from (5) by a factor of the form [15]

$$f(\varepsilon) = \exp\left[-\frac{3c\beta t}{2R}\left(1 - \frac{\delta D(\varepsilon)}{D(\varepsilon)}\right)\right],$$

where R is the radius of the sack, β is the probability of a collision between a cosmic-ray particle and an irregularity inside the sack, and t is the time between the formation of the sack and the capture of the earth by it. The collision probability is $\beta = 4R/3L$ where L is the mean free path. For a qualitative agreement with experiment it is necessary that $L \approx ct$. The July events may be understood on the basis of this model, if it is assumed that the degree of filling of the sack by cosmic rays increased from storm to storm. This means, in fact, that in certain directions the sack was bounded by walls having a thickness of the order of the linear dimensions of the sack itself, and this brings the model close to the uniform corpuscular stream, or else it is necessary to assume that the walls of the sack include cavities (holes) through which the filling-up takes place, or again, that the sack is ejected from a sufficiently large region ($R \sim 10^{10}$ cm) and subsequently expands only slightly (not more than by a factor of 2).

The main difficulty of this model is the strictly defined relations between the parameters ($L \approx ct$).

Interpretation of the July Events

We have seen that none of the above models is in really satisfactory agreement with all the events which we have observed. Nevertheless, it is

possible to trace out the following very approximate picture.

On July 10, 1959, a corpuscular stream was ejected from the sun and reached the earth at 1600 hr on July 11. This stream carried a magnetic field in one way or another. Since no appreciable changes in the diurnal variations of cosmic rays were observed during the magnetic storm, the magnetic field lay along the direction of propagation of the stream, and therefore the field leaking from the stream extended to considerable distances, which were of the order of $10^4 \times 4 \times 10^7 \times 1.8 \times 3.6 \times 10^3 \approx 10^{14}$ cm.

This large penetration range of the field explains the presence of a plateau in the recovery of the intensity between July 11 and July 15. The fact that there was a reduction in the cosmic-ray intensity on July 11, prior to the magnetic storm, suggests that the magnetic field of the stream travelled in advance of its leading front. This also confirms the conclusion that the magnetic field of the stream was longitudinal.

A new stream was ejected on July 14. It entered the field of the preceding stream and gave rise to a new storm and a new decrease in the cosmic-ray intensity. This stream carried a frozen-in magnetic field which was characterized by the same $H\ell$ as the storm of July 11, but the field strength in the stream was considerably higher. Owing to the high velocity and density of the particles in this stream, the latter gave rise to an extraordinary magnetic storm. In such cases the recovery in the cosmic-ray intensity should be much more rapid as compared with the period after the storm of July 11, and this was, in fact, observed.

A new stream was ejected on July 16, and gave rise to a very intense storm on July 17. The stream carried a very strong magnetic field, but the affective value of $H\ell$ was approximately the same as for the storms of July 11 and July 15.

Since the first stream, which gave rise to the storm of July 11, was very wide, the regular magnetic field which was frozen into it was appreciably non-uniform, and this led to a drift of the cosmic-ray particles in the stream and a reduction in the strength of the source of the variations.

The streams which were responsible for the storms of July 15 and 17 penetrated into the stream ejected earlier. This led to a contraction of the matter in the streams and to an enhancement of the field frozen into them.

As the result of contraction, the frozen-in magnetic field became more uniform and the strength of the source of the decrease in the cosmic-ray intensity was increased.

Since the $H\ell$ for the three streams remained approximately constant, the spectrum of the cosmic-ray variations during the three storms should have remained constant.

There was a recovery in the cosmic-ray intensity as the earth left the stream and its field. On July 23, the earth was captured by an old stream which gave rise to a minor storm with non-sudden commencement and total duration of 6—7 days. The stream consisted of a system of irregularities which were responsible for the drift of low-energy particles and a sharp recovery in the neutron component of cosmic rays, thus upsetting the normal softening of the variation spectrum.

This rough scheme is sufficient for the understanding of our data, although there are, apparently, certain features which do not fit into it. As regards a tendency to a 2% variation in the EAS frequency between July 7 and 22, it seems to us that this indicates that a considerable proportion of the primary EAS particles are heavy nuclei, and that during this period the upper atmosphere (above 50 mb) experienced considerable changes.

In conclusion, the authors wish to thank V.P. Razin and G.A. Akisheva of the Yakutsk Laboratory for their collaboration in this work.

REFERENCES

1. Dorman, L.I. Variatsii kosmicheskikh luchey (Cosmic ray variations). Gostekhizdat, Moscow, 1957.

2. Kuz'min, A.I. Dissertation, NIYaF MGU, Moscow, 1959.

3. ---, Yefimov, N.N., Krasil'nikov, D.D., Sokolov, V.D., Skripin, G.V., Shafer, Yu.G. and Shafer, G.V. Tr. MGG, No. 3, 64, 1961.

4. Kopylov, Yu.M. Sovetskiye stantsii kosmicheskikh luchey (Soviet cosmic ray stations). Izd. AN SSSR, Moscow, 1960.

5. Belomestnykh, V.A. and Shafer, Yu.G. Tr. YaFAN, ser. fizich., No. 2, 47, 1958.

6. Kuz'min, A.I., Skripin, G.V. and Yarygin, A.V. Tr. YaFAN, ser. fizich., No. 2, 34, 1958.

7. Krasil'nikov, D.D. Tr. YaFAN, ser. fizich., No. 3, 22, 1960.

8. Kosmicheskiye dannyye (Cosmic data). (A monthly review), No. 7, July 1959, Moscow, 1959.

9. Piddington, J.H. Phys. Rev., 112, 589, 1958.

10. Dorman, L.I. and Feynberg, Ye.L. In the book: Variatsii kosmicheskikh luchey pod zemley, na urovne morya i v stratosfere (Cosmic ray variations underground, at sea level and in the stratosphere). Izd. AN SSSR, Moscow, 1959.

11. ---, Kuz'min, A.I. and Skripin, G.V. Tr. XII assamblei MGGS (Proceedings of IGYC), 1960.

12. Stepanyan, A.V. Konfer. po variatsiyam kosmicheskikh luchey (Proceedings of a Conference on Cosmic Ray Variations). IZMIRAN, 1960.

13. Blokh, Ya.L., Glokova, Ye.S. and Dorman, L.I. In the book: Variatsii kosmicheskikh luchey pod zemley, na urovne morya i v stratosfere (Cosmic ray variations underground, at sea level and in the stratosphere). Izd. AN SSSR, Moscow, 1959.

14. Kuz'min, A.I., Danilov, A.A., Krymskiy, G.F. and Skripin, G.V. Tr. Confer. po variatsiyam kosmicheskikh luchey (Proceedings of a Conference on Cosmic Ray Variations). IZMIRAN, 1960.

15. Dorman, L.I. Tr. konfer. po variatsiyam kosmicheskikh luchey (Proceedings of a Conference on Cosmic Ray Variations). IZMIRAN, 1960.

S. V. Makarov

ON THE THEORY OF SEQUENCES

In some problems of mathematical statistics it is of interest to determine the distribution of a series of identical outcomes in a sequence of trials (cf. for example [1], which should also be consulted for the definition of a sequence).

Consider the simple example of a part of a sequence of independent trials with two equally probable outcomes. In order to be specific, we shall consider a series of outcomes of a given type, for example, a series of successes.

Let k be the number of trials ($k \geqslant 0$), m the number of sequences of given length ($m \geqslant 0$), and l the length of the sequence ($l \geqslant 1$).

P(k, m, l) is the probability that as a result of k trials precisely m sequences of length l will be encountered. Clearly, P(k, m, l) can be written in the form

$$P(k, m, l) = \frac{A(k, m, l)}{2^k},$$

where A(k, m, l) can only assume integral values. It is easy to show that the quantities A(k, m, l) are related by the following expressions

$$\left.\begin{aligned} A(k, 0, 1) &= A(k-1, 0, 1) + A(k-2, 0, 1) + A(k-4, 0, 1), \\ A(k, 1, 1) &= A(k-1, 1, 1) + A(k-2, 0, 1) + \sum_{i=1}^{k-3} A(i, 1, 1), \\ &\cdots\cdots\cdots\cdots\cdots\cdots\cdots\cdots\cdots\cdots \\ A(k, m, 1) &= A(k-1, m, 1) + A(k-2, m-1, 1) + \sum_{i=1}^{k-3} A(i, m, 1), \end{aligned}\right\} \quad (1)$$

$$\begin{aligned} A(k, m, l) = {} & 2A(k-1, m, l) - A(k-l-1, m, l) + \\ & + A(k-l-2, m, l) + A(k-l-1, m-1, l) - \\ & - A(k-l-2, m-1, l). \end{aligned} \quad (2)$$

where

$$A(k, -1, l) = 2,$$
$$A(0, m, l) = 0.$$

Moreover,

$$M(k,\ l)=\frac{k-l+3}{2^{l+2}}, \tag{3}$$

where M(k, l) is the mathematical expectation of the number of sequences of length l for k trials.

REFERENCES

1. Dunin-Barkovskiy, I.V. and Smirnov, N.V. Teoriya veroyatnostey i matematicheskaya statistika v tekhnike (obshchaya chast') (Theory of probability and mathematical statistics in technology), Chapter 6, Section 5, Moscow, 1955.

G.V. Skripin and G.V. Shafer

SOME DECREASES IN COSMIC-RAY INTENSITY

The extensive data accumulated during the International Geophysical Year reveal new and interesting facts on the behavior of the cosmic-ray intensity. A number of decreases in the cosmic-ray intensities prior to magnetic storms have been reported [1, 2]. Such decreases are of short duration and are most frequently recorded by instruments west of the earth-sun line. Detailed studies of these and similar events enlarge our knowledge of the relation between helio- and geo-physical phenomena.

Below, we report cosmic-ray intensity decreases which preceded the storms of October 21, 1957 and July 8, 1958. Moreover, a description is given of an event on May 9-10, 1958, when all the stations in the world network observed a cosmic-ray intensity decrease 2—3 days prior to the onset of the magnetic storm. The analysis covered μ-meson and neutron cosmic-ray data obtained at various stations at sea level, and also the composite ground-level and underground cosmic-ray measurements which have been carried out at Yakutsk.

THE EVENT OF OCTOBER 21, 1957

Figure 1 shows the two-hourly values of the cosmic-ray intensity, corrected for the barometer effect, for the period between October 19 and October 26, 1957.

It is clear from Fig. 1 that all the instruments at Yakutsk recorded a large Forbush-type decrease in the cosmic-ray intensity. The beginning of the decrease was simultaneous with the sudden commencement of a minor storm at 2240 hr on October 21. This well-known typical phenomenon was preceded by an event recorded at southern stations [1]. The phenomenon took the form of a short-lived decrease in the cosmic-ray intensity, and was clearly recorded only by stations located on east longitudes in excess of 140°. The decrease began before the magnetic storm and continued for 8—10 hours. The minimum was reached at 2000 hr UT on October 21. At Yakutsk, this effect was not as clearly defined, since it was simultaneous with the principal Forbush decrease.

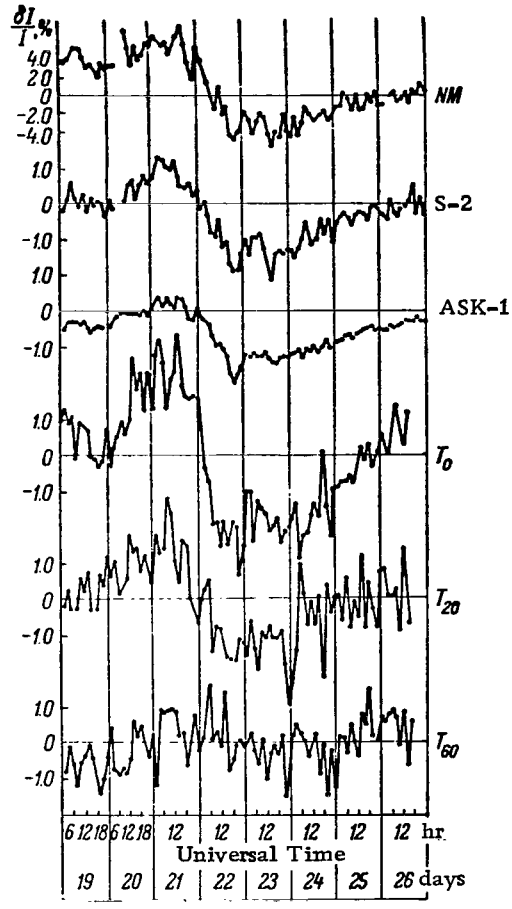

Fig. 1. Two-hourly values of cosmic-ray intensity, corrected for the barometer effect, for the period between October 19 and October 26, 1957, according to measurements at Yakutsk.

NM - neutron monitor; S-2, ASK-1 - ionization chambers; T_0, T_{20}, T_{60} - vertical counter telescopes at ground level and at 20 and 60 m w.e.

Nevertheless, it may be considered that the ground-level and underground telescopes down to 20 m water equivalent (m w.e.) did definitely record the effect. This was not so at 60 m w.e., owing to the large statistical errors in the

recording of the cosmic-ray intensity. At European stations the effect was not detected at all.

Thus, our data confirm the conclusions of [1] that between 1600 and 2400 UT on October 21, 1957, a mechanism appeared right of the earth-sun line in the 6—12 hr quadrant, which reduced the intensity of cosmic rays by a few per cent before the principal Forbush-type event. Moreover, it should be noted that primary particles with energies of at least up to 100 BeV took part in the phenomenon. This is indicated by the presence of the effect at the depth of 20 m w.e.

THE EVENT OF JULY 8, 1958

This case is interesting in that the cosmic-ray intensity exhibited unusual and considerable variations both before and after the onset of the storm. In distinction from all other known similar events, this event was characterized by the fact that high-energy particles up to 400 BeV exhibited considerable variations.

Figure 2 shows the two-hourly values of the cosmic-ray intensity recorded at various points by different detectors. The major storm with sudden commencement at 0749 UT on July 8, 1958, was simultaneous with the beginning of a Forbush decrease in the cosmic-ray intensity. The decrease was clearly seen at 60 m w.e., and therefore particles with energies up to the figure indicated above took part in the phenomenon. As in the above case, the onset of the storm was preceded at Yakutsk, and other stations at similar longitudes, by a decrease in the cosmic-ray intensity with a minimum at 1500—1900 UT on July 7, which was then replaced by a considerable increase in the intensity. At the European stations (Leeds, Amsterdam, Halle, Weissenau and others), these events were somewhat smaller in magnitude and were delayed by 4—8 hours relative to Yakutsk.

This considerable decrease, which was replaced after 8—10 hours by an increase in the intensity, may be regarded as an anomalous diurnal variation prior to a magnetic storm. It is of particular interest to consider this event separately before the storm, using the Yakutsk counter telescope data. The table gives the magnitude of the decrease and the increase from the mean for July 7, 1958, and the amplitude of the diurnal variation prior to the storm.

It is clear from Fig. 2 that particles with energies up to 400—500 BeV (mean energy) participated in the pre-storm effect, since the variation is not attenuated even at 60 m w.e.

The constancy of the magnitude of the diurnal variation prior to the storm at all the levels, immediately suggests that up to about 400 BeV, the

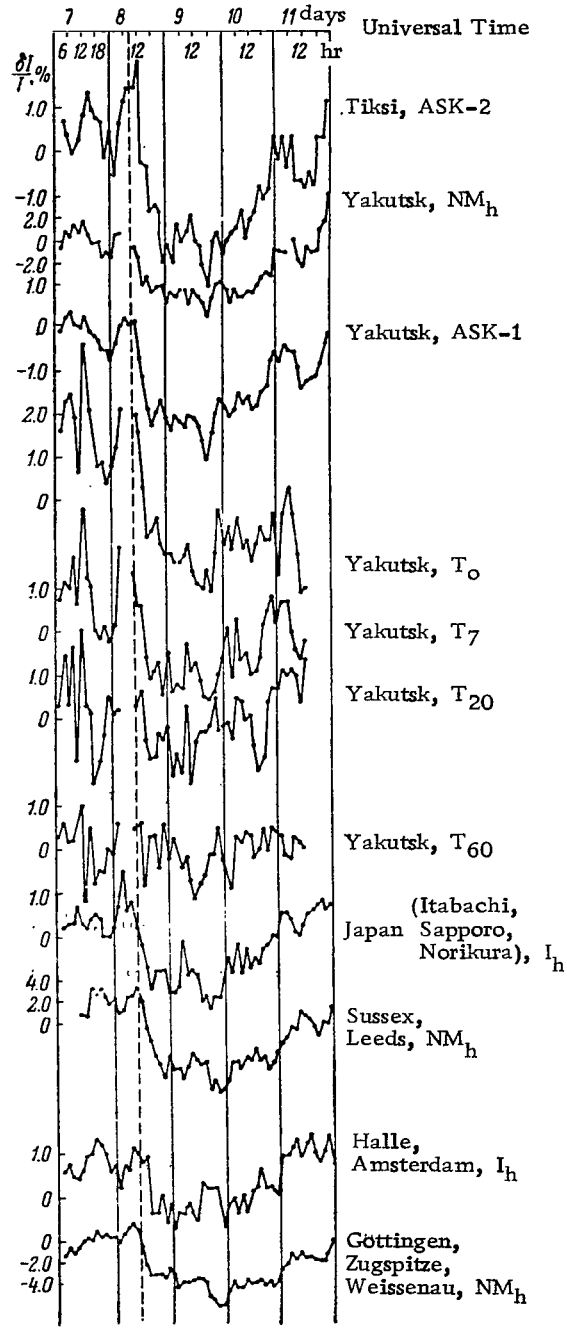

Fig. 2. Two-hourly values of the cosmic-ray intensity, corrected for the barometer effect, between July 7 and July 11, 1958. According to data of Yakutsk complex and stations of the world network. I_h - ionization chamber; NM_h - neutron monitor. T_0, T_7, T_{20}, T_{60} - same as in Fig. 1

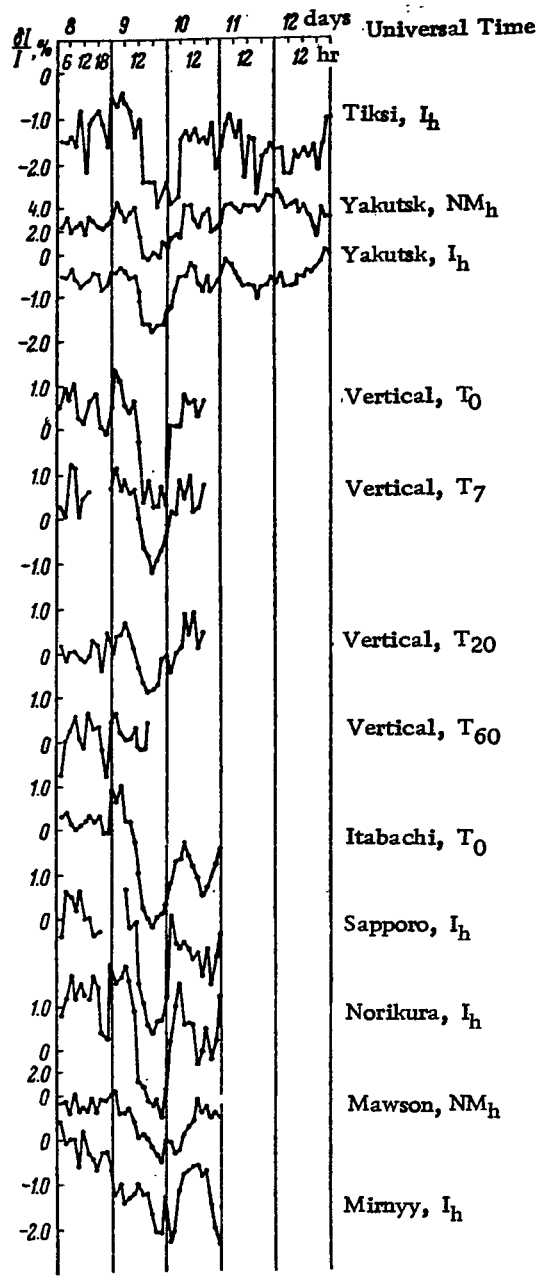

Fig. 3. Two-hourly values of the cosmic-ray intensity, corrected for pressure, for the period May 8—12, 1958.
According to data of Yakutsk complex and stations of the world network.

(Notation as in Figs. 1 and 2).

spectrum of the particles responsible for the effect was of the form

$$\frac{\delta D(\varepsilon)}{D(\varepsilon)} = 0.010.$$

Size of the decrease and increase in the cosmic-ray intensity prior to the storm of July 8, 1958, as measured by the system of counter telescopes at Yakutsk at 0, 7, 20 and 60 m w.e.

Instrument	Minimum primary energy ε, BeV	Magnitude of the pre-storm decrease, %	Magnitude of the pre-storm increase, %	Amplitude of the diurnal variation of July 8, 1958	Time of maximum, hr
T_0	26	1.2±0.1	0.2	0.8	16.2
T_7	40	1.1±0.2	0.6	1.0	16.9
T_{20}	80	1.7±0.3	0.5	1.0	16.6
T_{60}	180	0.7±0.4	0.7	0.8	17.7

An effect in which particles with this kind of spectrum participate may be due to a mechanism whose influence on the primary cosmic rays does not depend on the energy of these particles, at least up to 400 BeV. At the present time, a mechanism of this kind is difficult to visualize.

Thus, we can distinguish the following common features of the above two events. Both effects occurred before the Forbush decreases, their duration was less than a day, and the minimum occurred at the same time (4—8 hr local time). Primary particles of relatively high energy, up to 100—400 BeV, participated in the formation of these effects. Moreover, it is noticeable that as the more energetic particles begin to participate in the formation of these effects, there is a tendency to a more clearly defined diurnal variation in them.

THE EVENT OF MAY 8—9, 1958

A very interesting and rare cosmic-ray phenomenon occurred on May 8—9, 1958. All the stations in the world network recorded a rapid decrease in the cosmic-ray intensity at 0900—1200 hr on May 9. The decrease reached the minimum at 2000 hr, and recovered to the normal level at 0500—0600 UT on May 10. This decrease was in the form of a symmetric "well", and the minimum values of the neutron and μ-meson components at ground level were

respectively 4 and 2.0%. This phenomenon was not accompanied, as is usually the case, by any appreciable geophysical disturbances. A magnetic storm was recorded three days later, on May 12, while ionospheric disturbances were also found to occur later, namely, on May 11, 12, 14 and 15. This phenomenon was apparently related to an active region on the sun which passed through the central meridian on May 8—10. The region lay in the northern hemisphere, and consisted of intense hydrogen and calcium flocculi, a facular field, and a sunspot group. A single flare was noted in the region of the group.

Figure 3 shows the two-hourly values of the intensity of the cosmic-ray components at ground level at various points on the earth's surface, and also the Yakutsk surface and underground data. It is evident from this figure that there was a worldwide intensity decrease which cannot be explained by a spatial anisotropy. Primary particles with energies up to 80—150 BeV were subject to the effect, since the intensity decrease was clearly defined at 20 m w.e., where the decrease was $\sim 1\%$. The composite underground data obtained at Yakutsk may be used to determine the energy spectrum of the effect using the method and tables given in [3]. The spectrum is of the form

$$\frac{\delta D(\varepsilon)}{D(\varepsilon)} = \begin{cases} -0.2\varepsilon^{-0.7} & \text{when } \varepsilon_1 > 10\text{—}15 \text{ BeV}, \\ -0.1 & \text{when } \varepsilon_1 < 10\text{—}15 \text{ BeV}. \end{cases}$$

Comparison with the results given in [3] leads to the conclusion that the decrease in the cosmic-ray intensity on May 7, 1958, which was unaccompanied by appreciable geophysical phenomena, has the same energy spectrum as ordinary Forbush decreases during magnetic storms. It follows that the nature of these effects is the same. Following the interpretation given in [3], it may be considered that the reason for the decrease of May 7, 1958, was a solar corpuscular stream which carried frozen-in magnetic fields with irregularities at the edges. Moreover, in distinction to normal streams, the velocity and density of the particles in the stream were relatively low.

REFERENCES

1. McCracken, K.G. and Parsons, N.R. Phys. Rev., 112, No. 4, 1958.

2. Fenton, A.G., McCracken, K.G., Rose, D.C. and Wilson, B.G. Canad. J. Phys., 27, 970, 1950.

3. Kuz'min, A.I. and Skripin, G.V. Tr. YaFAN SSSR, ser. fizich., No. 4, 67, 1961.

"The aeronautical and space activities of the United States shall be conducted so as to contribute . . . to the expansion of human knowledge of phenomena in the atmosphere and space. The Administration shall provide for the widest practicable and appropriate dissemination of information concerning its activities and the results thereof."

—NATIONAL AERONAUTICS AND SPACE ACT OF 1958

NASA SCIENTIFIC AND TECHNICAL PUBLICATIONS

TECHNICAL REPORTS: Scientific and technical information considered important, complete, and a lasting contribution to existing knowledge.

TECHNICAL NOTES: Information less broad in scope but nevertheless of importance as a contribution to existing knowledge.

TECHNICAL MEMORANDUMS: Information receiving limited distribution because of preliminary data, security classification, or other reasons.

CONTRACTOR REPORTS: Technical information generated in connection with a NASA contract or grant and released under NASA auspices.

TECHNICAL TRANSLATIONS: Information published in a foreign language considered to merit NASA distribution in English.

SPECIAL PUBLICATIONS: Information derived from or of value to NASA activities. Publications include conference proceedings, monographs, data compilations, handbooks, sourcebooks, and special bibliographies.

TECHNOLOGY UTILIZATION PUBLICATIONS: Information on technology used by NASA that may be of particular interest in commercial and other nonaerospace applications. Publications include Tech Briefs; Technology Utilization Reports and Notes; and Technology Surveys.

Details on the availability of these publications may be obtained from:

SCIENTIFIC AND TECHNICAL INFORMATION DIVISION

NATIONAL AERONAUTICS AND SPACE ADMINISTRATION

Washington, D.C. 20546